

Translating Discharge into Local Hydraulic Conditions on the Sabie River: An Assessment of Channel Flow Resistance

**LJ Broadhurst • GL Heritage • AW van Niekerk
CS James • KH Rogers**

**Report to the Water Research Commission
by the
Centre for Water in the Environment
University of the Witwatersrand**

WRC Report No 474/2/97



Disclaimer

This report emanates from a project financed by the Water Research Commission (WRC) and is approved for publication. Approval does not signify that the contents necessarily reflect the views and policies of the WRC or the members of the project steering committee, nor does mention of trade names or commercial products constitute endorsement or recommendation for use.

Vrywaring

Hierdie verslag spruit voort uit 'n navorsingsprojek wat deur die Waternavorsingskommissie (WVK) gefinansier is en goedgekeur is vir publikasie. Goedkeuring beteken nie noodwendig dat die inhoud die siening en beleid van die WVK of die lede van die projek-loodskomitee weerspieël nie, of dat melding van handelsname of -ware deur die WVK vir gebruik goedgekeur of aanbeveel word nie.

**TRANSLATING DISCHARGE INTO LOCAL HYDRAULIC
CONDITIONS ON THE SABIE RIVER: AN ASSESSMENT OF
CHANNEL FLOW RESISTANCE**

by

**L.J. BROADHURST, G.L. HERITAGE, A.W. VAN NIEKERK, C.S. JAMES, K.H.
ROGERS.**

**Centre for Water in the Environment
University of the Witwatersrand
Johannesburg, Private Bag 3, WITS 2050, South Africa.**

**Report to the Water Research Commission on the project "The geomorphological
response to changing flow regimes of the Sabie and Letaba River systems. "**

Project Leaders : Prof. C.S. James and Prof. K.H. Rogers

WRC Report No. 474/2/97

ISBN 1 86845 207 7

EXECUTIVE SUMMARY

INTRODUCTION

The need for an understanding of the links between local hydraulic conditions, channel morphology and riverine ecosystem structure in the Kruger National Park was first recognised by Rogers *et al.* (1992), as part of an integrative holistic research programme, with the overall aim of quantifying the water demand of the environment. Local hydraulics and channel morphology are the primary determinants of the physical habitat, which controls ecosystem functioning. Therefore, it is essential to understand the mechanisms controlling local hydraulic parameters to predict the effect of altering the flow and sediment regime on a river. Hydrological data in the form of a simulated, daily discharge regime must be translated into point discharge values, and further, into local hydraulic conditions such as flow depth, width, velocity and bed shear stress, in order to assess the impact the discharge regime would have on the form of the existing river. Progress in this research area for many South African rivers is limited at present, particularly for bedrock influenced channels (van Niekerk *et al.* 1995). Current research is primarily concerned with riverine geomorphological classification (Wadson and Rowntree 1995 and van Niekerk *et al.* 1995) and pioneering investigation of bedrock channel dynamics (van Niekerk and Heritage 1993, Heritage *et al.* 1994 and Moon *et al.* 1995).

It is the flow resistance and geometry of a channel that determines the local hydraulic conditions (Richards 1982). Therefore, it is essential to evaluate the local flow resistance characteristics to provide a predictive capacity for a variety of users. Total flow resistance represents a sum of several, individual flow resistance components, which must be identified. Such a methodology will provide a link between water resource managers, geomorphologists and biologists, by relating a specific discharge regime to local physical parameters. The impact on channel morphology, hence riverine ecology, can then be evaluated. Additionally, the flow resistance values obtained must be transferable to similar channel types, allowing prediction of hydraulic conditions at unstudied sites.

Most research concerning channel flow resistance has concentrated on temperate, perennial rivers and much of this work is based on flume studies (Bathurst 1985a). Consequently, translation of discharge into local hydraulic variables, in natural channels, is often highly inaccurate, even on simple channels. It is thus necessary to critically evaluate and, if appropriate, modify methods currently used to determine flow resistance in open channels for use in semi-arid, bedrock influenced channels, commonly encountered in southern Africa.

The morphological diversity of many South African rivers, especially the Sabie River, provides further complications by creating complex cross sections, where different morphologies and associated vegetation communities, sediment sizes and presence or absence of bedrock, create high variability in boundary roughness through a cross section. A study to identify and evaluate the influence of the various flow resistance components is required.

PROJECT AIMS

The overall aim of this project was to identify and quantify the flow resistance components on the Sabie River and to predict their effects on local hydraulic variables under different flow conditions. This information is vital for predicting channel change and consequent habitat change. The steps necessary to achieve this aim are summarised below.

a) Identification of the flow resistance components along the Sabie River.

Representative reaches on the Sabie River were identified from objective classification of the geomorphology. The term 'reach' can be used flexibly in the Sabie River. It can be viewed in context of the hierarchical geomorphological classification (van Niekerk *et al.* 1995) and by the physical, spatial extent of an individual resistance component, namely, at a channel type, at a morphological unit, at a cross section or at a distributary channel level. There are a variety of factors controlling flow resistance, such as the type of vegetation community found, the channel geometry of the river and the sedimentary or lithological characteristics of the channel bed and banks. A comprehensive geomorphological, sedimentological and vegetational survey was undertaken for each channel type that characterises the Sabie River, to identify all these flow resistance components over the range of 'reach' scales.

b) Evaluation of different methods for assessing flow resistance.

A literature review identified flow resistance estimation methods which were most appropriate for the Sabie River. Where necessary, new models were proposed to enable flow resistance calculation in the environments found in the Sabie River.

c) Establishment of hydraulic monitoring networks.

Hydraulic data were collected at five 'representative' reaches, covering the range of channel types found on the Sabie River, over a range of discharges, for use in quantifying flow resistance.

d) Quantification of flow resistance.

The data obtained from field investigations were used to extend knowledge of flow resistance characteristics and to provide predictive models for determining hydraulic parameters from local channel characteristics and hydrological records for the channel types found on the Sabie River. Results quantified on a reach level were successfully transferred to other unstudied, but similar environments to independently test and validate the flow resistance results.

e) Guideline compilation.

Guidelines of appropriate methodology for use over different channel types and scales of investigation were compiled.

ASSESSMENT OF CHANNEL FLOW RESISTANCE: APPROPRIATE METHODOLOGIES

There are several forms of flow resistance in natural open channel flow which all contribute to the total resistance. These are: skin resistance, channel form resistance, vegetational resistance and free surface resistance. With few exceptions, models developed to quantify the individual types of flow resistance rely on empirical calibration. This leads to the models being highly specific to the conditions the equations were developed in and of limited relevance to the unstudied riverine environments on the Sabie River. The complex interaction of the different flow resistance components and the inappropriate nature of existing empirical models precluded quantitative isolation of individual component effects, and only total flow resistance was quantified.

Following the geomorphological hierarchy outlined by van Niekerk *et al.* (1995) and the physical, spatial extent of flow resistance components, it was possible to characterise the Sabie River at a variety of relevant physical scales, namely at a channel type, at a morphological unit, at a cross section or at an individual distributary. Therefore, several cross sections, defining a reach (channel type) or sub-reach (morphological unit) must be analyzed, in addition to single cross sections. A representative value of total flow resistance for a multiple section reach, over a variety of reach scales, at a given discharge can be obtained by the method developed by Barnes (1967).

CONCEPTUAL MODELLING

All of the channel types studied, with the exception of the single thread channel, had multiple channels active at low or medium flows. In alluvial sections, where there is good water connectivity through the sediments, the water level in multiple channels was found to be the same and a single stage-discharge relationship characterises the whole section. However, in bedrock dominated sections the water level in one channel is dependent on the upstream conditions in that channel, so that a cross section may contain channels with different water surface elevations.

'Horizontal' model

Where the water level across a cross section is horizontal, conventional methods for calculating hydraulic and channel geometry parameters apply and a single rating relationship can be used.

'Non-Horizontal' model

Bedrock influences in a reach produce a laterally non-horizontal water surface in multiple active distributaries over a cross section. Therefore, a 'Non-Horizontal' model was developed to predict hydraulic and channel geometry variables in multi-distributary cross sections with non-horizontal water surfaces. At low discharges, the water levels in the distributary channels differ but their rate of change with increasing discharge are similar when a channel fills to

capacity, it overflows into an adjacent channel. Its level then remains constant while it contributes its share of the increase in discharge to the adjacent channel until the water levels are equal.

QUANTIFICATION OF TOTAL FLOW RESISTANCE

Following the Barnes (1967) methodology, which allows multiple cross section reach quantification of flow resistance, and using the hydraulic and channel geometry parameters derived from either the 'Horizontal' or 'Non-Horizontal' model in bedrock influenced sections, reach and morphological unit flow resistance was quantified for the five channel types.

CONCLUSIONS

Flow resistance investigation of the channel types found on the Sabie River in the Kruger National Park has produced some unique, extreme channel flow resistance values for bedrock influenced channel types at low flows, and has confirmed other authors' estimates for different (alluvial) channel environments. The magnitude of the flow resistance coefficient depends strongly on the physical scale of analysis as reach estimates average several different local environments. The previously unstudied bedrock anastomosing channel type yielded the highest flow resistance magnitude, with low flow reach estimates for the Darcy-Weisbach friction factor of 480; local bedrock tributary values were in excess of 3700 at very low flows. The values obtained in this study are greater than those reported in any study of extreme channel flow resistance. These high flow resistance values reflect energy dissipation due to hydraulic jumps and internal distortions resulting from major flow disturbances and suggest that flow resistance equations such as Darcy-Weisbach, Manning and Chezy are inappropriate for use in such conditions.

High discharge flow resistance values were quantified at three of the channel types. The flow resistance magnitudes found under these rare, high flows are highly influenced by a component of vegetation flow resistance, producing Darcy-Weisbach friction factors of between 0.1 and 0.4.

The discharge:flow resistance relationships varied between the channel types, with a distinct difference in flow resistance magnitudes at low flows between alluvial and bedrock influenced channels. This suggests a need to model the channel types independently. Modelling the hydraulic conditions in bedrock influenced channels is complicated by a non-horizontal water surface at a cross section, making the concept of a single 'stage' misleading. Therefore, in non-alluvial reaches, such as those found in mixed and bedrock anastomosing channel types, conventional techniques for modelling flow resistance and stage-discharge relationships are inappropriate. Large discrepancies in geometric and hydraulic parameters result if the 'Non-Horizontal' model is not used to account for the difference in water elevation between active channels and a horizontal water surface is assumed. Under these conditions use of the 'Non-Horizontal' model is recommended as it is physically more realistic than the conventionally used 'Horizontal' model and has been shown to predict actual average velocity and maximum depth far more accurately.

Independent testing of the reach flow resistance values, to assess the applicability and generality of the flow resistance estimates on similar morphologic cross sections has produced mixed results. Synthesis of rating curves at the alluvial sections, where the 'Horizontal' model could reasonably be applied, reproduced close fits to actual rating curves. However, misuse of the 'Horizontal' model, due to lack of data at the bedrock-influenced sections precluding application of the 'Non-Horizontal' model, particularly in mixed anastomosing areas, has introduced errors between actual and synthesised rating curves at several test sections. This confirms the need to account for a non-horizontal water surface. The deviation from actual stage:discharge relationship may be compounded by the use of 'regional' water surface slopes to approximate friction slope. Local water surface slope surveys over a range of discharges would improve the accuracy the independent testing procedure.

ACHIEVEMENT OF STATED AIMS

With reference to the project aims:

- a) All the factors controlling the different components of flow resistance were identified by detailed geomorphological, sedimentological, vegetational and cross sectional shape surveys. The system of cross sections surveyed, within five 'representative' channel type reaches, enabled analysis of flow resistance over a variety of scales.
- b) An extensive literature review of channel flow resistance theory concluded that most resistance models are based on empirical calibration and are therefore not appropriate for use on the Sabie River, which contains previously unstudied riverine environments.
- c) Hydraulic monitoring networks were established at numerous cross sections within five study reaches. Due to reliance on natural floods to furnish a range of discharge data, the actual range of hydraulic conditions sampled during this study covered low and medium magnitude flows only. High discharge data at three of the reaches were available from a previous study and were used to provide a useful but less accurate quantification of high discharge flow resistance.
- d) Total channel flow resistance was quantified at five reaches representating the riverine environments encountered on the Sabie River over a range of discharges. The inapplicability of existing models for predicting specific flow resistance components on the Sabie River, where many components interact in a complex manner, precluded quantitative isolation of individual flow resistance components. A qualitative estimation of the effect of specific components of flow resistance was possible at certain sections, for example large scale roughness was the solitary flow resistance effect in low flows within the bedrock distributaries.
- e) Guidelines for computation of channel geometric and hydraulic parameters between alluvial and bedrock cross sections, for use in flow resistance quantification, have been devised. Representative flow resistance values are presented at a reach level for

the five principal channel types and at a subreach, cross section or individual distributary scale for morphological units.

GUIDELINES FOR USING THE PRODUCTS OF THIS RESEARCH

Knowledge arising from this project, has led to the following guidelines, which are suggested as an appropriate methodology for quantifying flow resistance in environments similar to those found on the Sabie River.

- 1) Use the 'Horizontal' model to predict hydraulic and channel geometry parameters in alluvial sections.
- 2) Use the 'Non-Horizontal' model to predict hydraulic and channel geometry parameters in bedrock influenced sections.
- 3) Apply Barnes (1967) methodology to quantify multi-section reach flow resistance over a variety of scales.
- 4) The reach or channel type flow resistance values reported in this project can be reliably transferred to similar channel environments. However, the bedrock morphological unit resistance values need to be treated with caution, as the flow resistance values obtained represent major energy dissipation due to hydraulic jumps and other flow disturbances. Under such conditions conventional definitions of hydraulic and channel geometry parameters may not be applicable and equations to quantify flow resistance may be invalid.

RECOMMENDATIONS FOR FUTURE RESEARCH

This report provides the first intensive study of the hydraulics of mixed and bedrock anastomosing channel types. In these channel types, conventionally defined hydraulic and channel geometry parameters are not applicable and new methods for quantifying these parameters have been developed, in the form of the 'Non-Horizontal' model. Direct calibration of this model at flows other than a single low flow have been limited for this report, as measurement of high stage levels in every active channel across a cross section of the Sabie River during a flood flow is a dangerous and difficult task. However, acquiring this information is essential if the 'Non-Horizontal' model's accuracy is to be tested over a range of discharges. Prioritising monitoring of flow levels at all distributaries within a study reach is a recommendation for further research.

Further independent testing of the reliability of the flow resistance values quoted in this study, on rivers other than the Sabie that display similar channel environments, is needed.

TABLE OF CONTENTS

EXECUTIVE SUMMARY	i
ACKNOWLEDGEMENTS	xvi
GLOSSARY	xviii
CHAPTER 1: INTRODUCTION	1
1.1 Background	1
1.2 Aims	4
CHAPTER 2: FLOW RESISTANCE	8
2.1 Total channel flow resistance	8
2.2 Components of flow resistance	11
2.2.1 Skin resistance	11
Boundary layer theory	11
Semiempirical equations based on boundary resistance	11
2.2.2 Large scale roughness	12
2.2.3 Channel form flow resistance	15
2.2.4 Vegetational flow resistance	19
Flow over submerged vegetation	20
Flow through vegetation	24
2.2.5 Free surface resistance	28
CHAPTER 3: CHARACTERISTICS OF THE SABIE RIVER	29
3.1 Catchment characteristics	29
3.2 Riparian geomorphological hierarchy	29
3.3 Channel types	34

3.3.1 Bedrock anastomosing	34
3.3.2 Single thread	34
3.3.3 Pool-rapid	34
3.3.4 Braided	35
3.3.5 Mixed anastomosing	35
CHAPTER 4: ASSESSMENT OF CHANNEL FLOW RESISTANCE: APPROPRIATE METHODOLOGIES	42
4.1 Visual comparison method	42
4.2 Reach flow resistance quantification	42
CHAPTER 5: IDENTIFYING THE VARIETY OF FLOW RESISTANCE COMPONENTS ENCOUNTERED ON THE SABIE RIVER AND HYDRAULIC MONITORING	46
5.1 Criteria for reach selection	46
5.2 Identifying flow resistance components within the study reach	51
5.3 Measurement of local stage	51
5.4 Discharge gauging	52
CHAPTER 6: CONCEPTUAL MODELLING	59
6.1 Physical Scales of analysis	59
6.2 Approaches to modelling channel geometry in alluvial and bedrock multi- channel cross sections	59
6.2.1 'Horizontal' model	59
6.2.2 'Non-Horizontal' model	59
CHAPTER 7: CHANNEL FLOW RESISTANCE QUANTIFICATION	70
7.1 Quantification of hydraulic and channel geometry parameters	70

7.2 Quantification of channel type or 'reach' flow resistance	71
7.3 Quantification of morphological unit or 'sub-reach' flow resistance	76
7.4 Comparison with flow resistance values reported in similar natural channel environments and quantification of components of flow resistance	83
7.5 Transfer of the flow resistance values to independent sections	87
CHAPTER 8: CONCLUSIONS AND RECOMMENDATIONS	98
8.1 Uses of the products of this research	99
8.2 Recommendations for further research	99
8.3 Guidelines	99
REFERENCES	101
NOTATION	107
APPENDIX 1: LOCATION OF BENCHMARKS AND FLOW MONITORING STATIONS FOR THE CHANNEL FLOW RESISTANCE INVESTIGATION	
APPENDIX 2: CROSS SECTION SURVEY DATA	
APPENDIX 3: STAGE-DISCHARGE RATING CURVES	
APPENDIX 4: SEDIMENTOLOGICAL DATA	
APPENDIX 5: MORPHOLOGICAL UNIT GLOSSARY, WITH CODES	
APPENDIX 6: PHYSICAL CHARACTERISTICS OF VEGETATION ACROSS CROSS SECTIONS, RELATED TO MORPHOLOGICAL UNITS	

LIST OF TABLES

Table 1: Vegetation characteristics that affect flow resistance.	19
Table 2: Quantification of vegetation flow resistance coefficients <i>i</i> and <i>j</i> (after Kouwen and Li 1980).	22
Table 3: Stiffness values for various grasses from experimental data (after Kouwen and Li 1980).	23
Table 4: Description of morphological units found on the Sabie River (after Moon <i>et al.</i> in press).	31
Table 5: Combinations of channel types found on the Sabie River (after Moon <i>et al.</i> in press).	32
Table 6: Components of flow resistance found in the different channel types.	33
Table 7: Methodology for high discharge flow resistance quantification	71
Table 8: Description of active distributary channels used in morphological unit flow resistance quantification.	76
Table 9: Flow resistance coefficients for a variety of channel conditions	84
Table 10: Inundation pattern of morphological units at cross section 20 with increasing discharge	86
Table 11: Summary of flow resistance coefficients calculated at a reach and at a morphological unit scale.	88

LIST OF FIGURES

Figure 1: Relationships between riparian biota, local hydraulics and channel morphology (after Rogers <i>et al.</i> 1992).	2
Figure 2: Links between local hydraulics, resource managers and geomorphologists.	3
Figure 3: Use of flow resistance in determination of channel dynamics.	4
Figure 4: Research programme for the channel flow resistance project.	7
Figure 5: Components of flow resistance relevant to the Sabie River.	9
Figure 6: Definition of cross section channel geometry and hydraulic parameters, where A is channel area, W is width, P is wetted perimeter, d is hydraulic mean depth, d_m is maximum depth, R is hydraulic radius, Q is discharge and V is velocity.	10
Figure 7: Location of study reaches and gauging weirs in the Sabie River catchment.	30
Figure 8: Hierarchical river classification system for the Sabie River, Kruger National Park (after van Niekerk <i>et al.</i> 1995).	32
Figure 9: Longsection water surface and bed profiles through the study reaches.	36
Figure 10: Idealised cross sections through the five channel types and two morphological units found on the Sabie River.	37
Figure 11: Schematic representation of possible flow paths through the bedrock anastomosing study reach and the corresponding, actual plan form.	38
Figure 12: Definition of channel geometry and hydraulic parameters for use in calculating flow resistance in a multi-section reach (modified after Barnes 1967).	43
Figure 13: Plan view of reach 1, a single thread channel type, showing cross section locations. Sections upstream of 1.0 are not represented in the aerial photographic record. The flow direction is from right to left.	46
Figure 14: Plan view of reach 4, a bedrock anastomosing channel type, showing cross section locations. Flow direction is from top to bottom.	47
Figure 15: Plan view of reach 14, a braided channel type, showing cross section locations. Flow direction is from top to bottom.	48

Figure 16: Plan view of reach 15, a pool-rapid channel type, showing cross section locations. Flow direction is from top to bottom.	49
Figure 17: Plan view of reach 21, a mixed anastomosing channel type, showing cross section locations. Flow direction is from top to bottom.	50
Figure 18: Calculation of stage at a study site, between two gauging weirs, during a flood event.	53
Figure 19: Conventional velocity-area method for calculation of subarea discharge.	54
Figure 20: Typical velocity profiles in a bedrock distributary.	55
Figure 21: Three-dimensional representation of velocity isovels at a cross section, produced from SURFER software.	56
Figure 22: Difference between SURFER and velocity-area analyzed gauging data.	57
Figure 23: Error between weir discharge and that obtained from SURFER and velocity-area analyzed gauging data at three cross sections.	58
Figure 24: Scales of analysis used in the calculation of flow resistance.	60
Figure 25: Horizontal water surface characteristic of alluvial sections compared to the 'stepped' non-horizontal water surface observed for bedrock influenced sections.	61
Figure 26: Errors in average velocity calculation at discharge $1\text{m}^3\text{s}^{-1}$, between the 'Horizontal' and the actual 'Non-Horizontal' models.	62
Figure 27: Conceptual diagram of the 'Non-Horizontal' model, for use in bedrock influenced sections, to define flow depth:cross section discharge relationships for individual distributaries.	64
Figure 28: Similarity between bedrock anastomosing rating curves, reduced to a common initial elevation at discharge $1\text{m}^3\text{s}^{-1}$	65
Figure 29: Definition of 'Non-Horizontal' and 'Horizontal' model errors.	67
Figure 30: Error between observed and 'Non-Horizontal' and 'Horizontal' model predicted maximum depth, over a range of low and medium discharges for five seasonal distributaries.	68
Figure 31: Distributary channel area error between observed and 'Non-Horizontal' model predicted over a range of low and medium discharges for five seasonal distributaries.	69

Figure 32: Hydraulic and channel geometry parameter definitions in a bedrock influenced section with a non-horizontal water surface elevation, where W is width, V is velocity, A is area, h is height above datum and P is wetted perimeter.	70
Figure 33: Summary of procedure for calculating flow resistance in alluvial and bedrock sections.	72
Figure 34: Darcy-Weisbach friction factor, f quantification over the five channel type reaches.	73
Figure 35: Manning's n quantification over the five channel type reaches.	74
Figure 36: Chezy C quantification over the five channel type reaches.	75
Figure 37: Darcy-Weisbach friction factor, f quantification for a variety of morphological units.	77
Figure 38: Manning's n quantification for a variety of morphological units.	78
Figure 39: Chezy C quantification for a variety of morphological units.	79
Figure 40: Darcy-Weisbach friction factor, f quantification for bedrock distributaries. Numbers refer to individual distributaries.	80
Figure 41: Manning's n quantification for bedrock distributaries. Numbers refer to individual distributaries.	81
Figure 42: Chezy C quantification for bedrock distributaries. Numbers refer to individual distributaries.	82
Figure 43: Manning's n :hydraulic radius relationship, for use in synthesising independent rating curves.	90
Figure 44: Synthesised rating curves (SYN) for the Narina study site, a braided cross section. The SYN $R:n$ curve was synthesised using a hydraulic radius to flow resistance relationship; the SYN $Q:n$ curve was synthesised using a discharge to flow resistance relationship.	91
Figure 45: Synthesised rating curves (SYN) for Section 11, a bedrock anastomosing cross section. The SYN $R:n$ curve was synthesised using a hydraulic radius to flow resistance relationship; the SYN $Q:n$ curve was synthesised using a discharge to flow resistance relationship.	92
Figure 46: Synthesised rating curves (SYN) for Section 16, a pool-rapid cross section. The SYN $R:n$ curve was synthesised using a hydraulic radius to flow resistance relationship; the SYN $Q:n$ curve was synthesised using a discharge to flow resistance relationship.	93

Figure 47: Synthesised rating curves (SYN) for Section 27, a mixed anastomosing cross section. The SYN R:n curve was synthesised using a hydraulic radius to flow resistance relationship; the SYN Q:n curve was synthesised using a discharge to flow resistance relationship.	94
Figure 48: Synthesised rating curves (SYN) for Section 29, a mixed anastomosing cross section. The SYN R:n curve was synthesised using a hydraulic radius to flow resistance relationship; the SYN Q:n curve was synthesised using a discharge to flow resistance relationship.	95
Figure 49: Synthesised rating curves (SYN) for Section 30, a mixed anastomosing cross section. The SYN R:n curve was synthesised using a hydraulic radius to flow resistance relationship; the SYN Q:n curve was synthesised using a discharge to flow resistance relationship.	96

LIST OF PLATES

Plate 1: Typical morphological and vegetational characteristics of bedrock anastomosing channel types, with High Level Flow Recorder.	39
Plate 2: Typical morphological and vegetational characteristics of single thread channel types.	39
Plate 3: Typical morphological and vegetational characteristics of pool-rapid channel types.	40
Plate 4: Typical morphological and vegetational characteristics of braided channel types.	40
Plate 5: Typical morphological and vegetational characteristics of mixed anastomosing channel types.	41

ACKNOWLEDGEMENTS

The research in this report emanated from a project funded by the Water Research Commission, entitled:

"The geomorphological response to changing flow regime of the Sabie and Letaba river systems"

The Steering Committee responsible for this project, consisted of the following persons:

Dr P C M Reid	Water Research Commission (Chairman 1991-1994)
Dr S Mitchell	Water Research Commission (Chairman 1995)
Mr D Huyser	Water Research Commission (Secretary)
Mr F van Zyl	Department of Water Affairs and Forestry
Dr C Bruwer	Department of Water Affairs and Forestry
Dr B P Moon	University of the Witwatersrand
Prof. K H Rogers	University of the Witwatersrand
Dr F Venter	National Parks Board
Prof. B R Davies	University of Cape Town
Dr M Chutter	AFRIDEV
Dr K M Rowntree	Rhodes University
Prof. J H O'Keeffe	Rhodes University
Prof. D Stephenson	University of the Witwatersrand
Mr D S van der Merwe	Water Research Commission

The financing of the project by the Water Research Commission and the contribution of the members of the Steering Committee is acknowledged gratefully.

This project was only possible with the co-operation of many individuals, institutions and companies. The authors therefore wish to record their sincere thanks to the following:

Department of Water Affairs and Forestry, Potchefstroom Division, in particular Mr N. Smith, Mr Tobie Roux, Mr Jaco con Radie and Mr Coenie van der Berg, Mr Joseph Khwitsidi and Mr Stephans Mathyse for field survey data collection assistance and reduction.

National Parks Board, Kruger National Park, in particular Mr Gerhard Strydom, Dr Freek Venter, Dr Andrew Deacon, Mr George Maluleke, Mr Philemon Ndlovo, Mr Samuel Nkuna, Mr Judas Makakula and Mr Alfred Nkuna for logistical support.

Undergraduate exchange students **Mr Peter Frost, Mr Krishan Kapur and Ms Louise Peel**, King's College, London University, England, for field data collection assistance and data reduction.

Mr Andrew Birkhead, University of the Witwatersrand, Department of Civil Engineering, for field data collection assistance and computing advice.

Mrs Wendy Midgley, Centre for Water in the Environment, University of the Witwatersrand, for invaluable administrative assistance.

Ms Rachel Spencer, University of Western Australia, Perth, for field data collection assistance.

Mr Philip Clegg and Ms Clare Fielden of the University of East Anglia, England, for field data collection assistance.

Mazda Wildlife Fund for financial support in the form of 4WD vehicle use.

GLOSSARY

Active morphological units

Perennially flowing bedrock, mixed or alluvial channels or other associated morphological units within the **macro-channel**.

Channel geometry parameters

These parameters are two dimensional cross section and three dimensional long profile shape parameters, namely, channel width, cross sectional area, maximum depth, wetted perimeter and reach length. Further parameters can be derived from the above, these include: hydraulic radius and mean depth (Figure 6).

Channel types

Distinct **channel types** are generated by associations of specific, smaller **morphological units**. Five principal **channel types** have been observed on the Sabie River (van Niekerk *et al.* 1995).

Horizontal model

Conventional methods for defining channel geometry and hydraulic parameters, where the water surface elevation across either a single channel or multiple distributary cross section, is horizontal, are described as '**Horizontal**' in this report.

Hydraulic jump

A **hydraulic jump** occurs as flow changes its state from subcritical to supercritical flow. The jump represents a large decrease in the average velocity of flow and a loss of energy. Open channel examples include white water in the vicinity of boulders, rapids and flow constrictions.

Hydraulic parameters

Parameters relating to hydraulic properties, such as friction slope, velocity, shear stress or discharge are referred to as **hydraulic parameters** in this report.

Macro-channel

The **macro-channel** is a large over-wide channel, incised into bedrock, within which all fluvial processes are contained.

Morphological unit

A hierarchical classification of the Sabie River (van Niekerk *et al.* 1995), has identified **morphological units** which are produced and/or maintained as a result of specific processes. Each **morphological unit** has a distinctive substrate characteristic or microhabitat. The Sabie River flows over an incised bedrock base, with varying degrees of sedimentation cover,

Each **morphological unit** has a distinctive substrate characteristic or microhabitat. The Sabie River flows over an incised bedrock base, with varying degrees of sedimentation cover, creating a 'floodplain' or **macro-channel**, as opposed to the perennially flowing active distributaries or **seasonally flooded** features within it's confines.

Non-Horizontal model

A new method for defining and generating channel geometry and hydraulic parameters, where the water surface elevation across multiple distributaries at a cross section, are not horizontal, is described as '**Non-Horizontal**' in this report.

Reach

For the purposes of this study, a **reach** is composed of five or more cross sections, within one channel type environment.

Representative reach

Objective river classification has enabled categorisation of the Sabie River into similar **channel types**, based on associations of **morphological units**. Single examples of each type have been chosen as **representative reaches**.

Roughness component

Total roughness represents the sum of a variety of individual **roughness components**. On the Sabie River, the **roughness components** encountered are: skin, vegetation, large scale, free surface and channel form roughness (defined in more detail in Chapter 2).

Seasonal morphological units

These **morphological units** are influenced by elevated annual flows.

Sub-reach

For the purposes of this study, a **sub-reach** comprises two or three cross sections, encompassing one morphological unit, within a **reach**.

CHAPTER 1: INTRODUCTION

1.1 Background

The need for an understanding of the links between local hydraulic conditions, channel morphology and riverine ecosystem structure in the Kruger National Park was first recognised by Rogers *et al.* (1992) (Figure 1), as part of an integrative holistic research programme, with the overall aim of quantifying the water demand of the environment. Local hydraulics and channel morphology are the primary determinants of the physical habitat, which controls ecosystem functioning (Figure 1), however, both animals and vegetation exert reciprocal, feedback, forces on the hydraulics and morphology. Therefore, it is essential to understand the mechanisms controlling local hydraulic parameters to predict the effect of altering the flow and sediment regime on a river. Hydrological data, in the form of a simulated, daily discharge regime must be translated into point discharge values, and further, into local hydraulic conditions, namely flow depth, width, velocity and bed shear stress, in order to assess the impact such a discharge regime would have on the form of an existing river. Progress in this research area for many South African rivers is limited at present.

It is the flow resistance of a channel that determines the local hydraulic conditions (Richards 1982). Therefore, it is essential to evaluate the local flow resistance characteristics to provide a predictive capacity for a variety of users (Figure 2). Total flow resistance represents a sum of several, individual flow resistance components. Individual components must be identified and quantified, for use in derivation of local hydraulic conditions for various flow scenarios. Such a methodology will provide a link between water resource managers, geomorphologists and biologists, by relating a specific discharge regime to local physical parameters, for example habitats, geomorphology or hydraulics (Figure 2). The impact on channel morphology, hence riverine ecology, can then be evaluated. Consequently, quantification of "local hydraulic conditions" has been identified as a necessary link in the Kruger National Park Rivers Research Programme (Figure 1). Additionally, the flow resistance values obtained are transferable to similar channel types, allowing prediction of hydraulic conditions at unstudied sites.

Most research concerning channel flow resistance has concentrated on temperate, perennial rivers and much of this work is based on flume studies (Bathurst 1985a). Consequently, translation of discharge into local hydraulic variables, in natural channels, is often highly inaccurate, even on simple channels. It is thus necessary to critically evaluate and, if appropriate, modify methods currently used to determine flow resistance in open channels for use in semi-arid, bedrock influenced channels, commonly encountered in southern Africa.

The morphological diversity of many South African rivers, especially the Sabie River, provides further complications by creating compound cross sections, where different morphologies and associated vegetation communities, sediment sizes and presence or absence of bedrock, create changes in boundary roughness through a cross section. A study to identify and evaluate the influence of the various flow resistance components is required, to link hydrological data to hydraulic variables. This was identified as a research need in two major research projects being undertaken through Water Research Commission contracts, as part of the Kruger National Park Rivers Research Programme (Birkhead *et al.* 1996 and

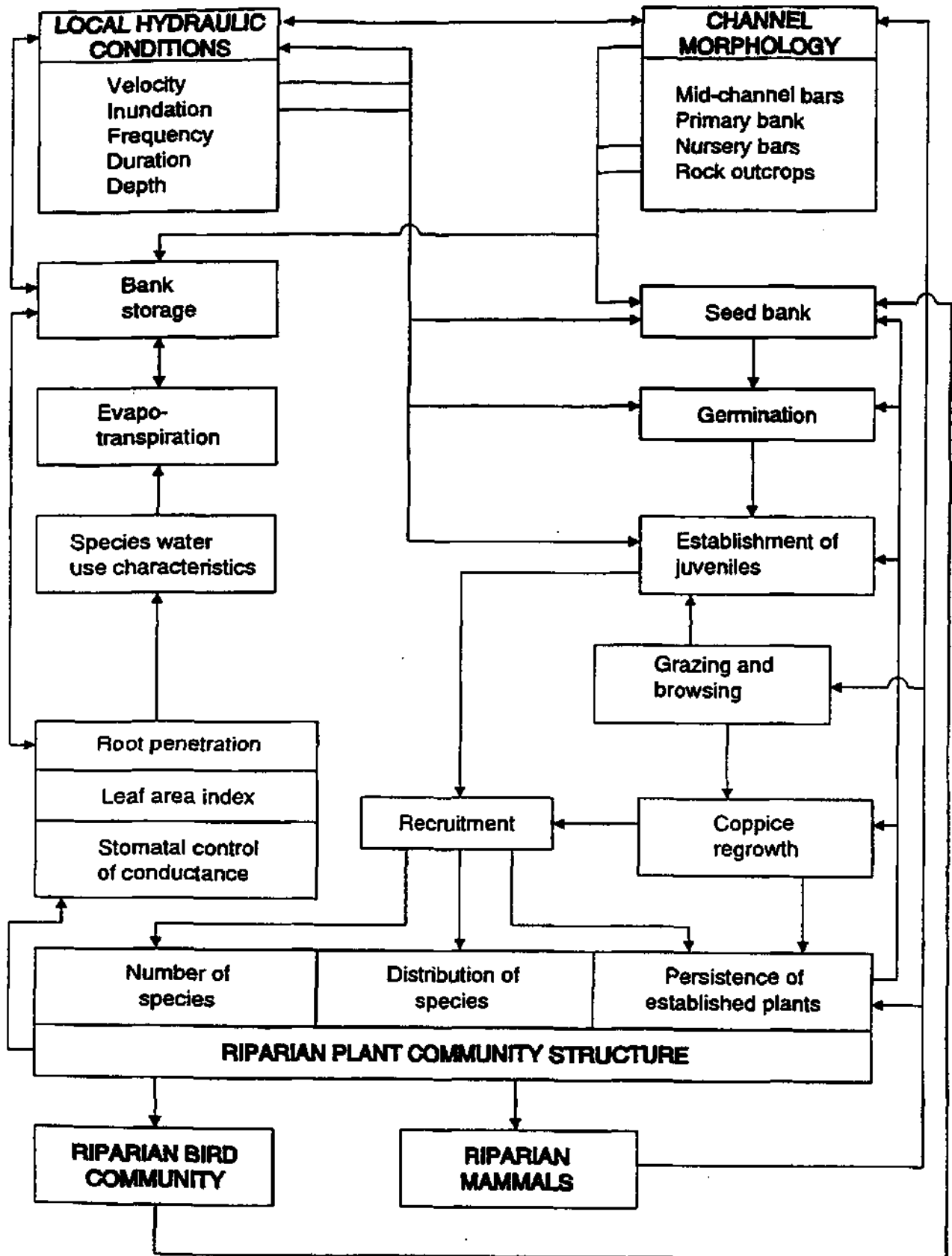


Figure 1: Relationships between riparian biota, local hydraulics and channel morphology (after Rogers *et al.* 1992).

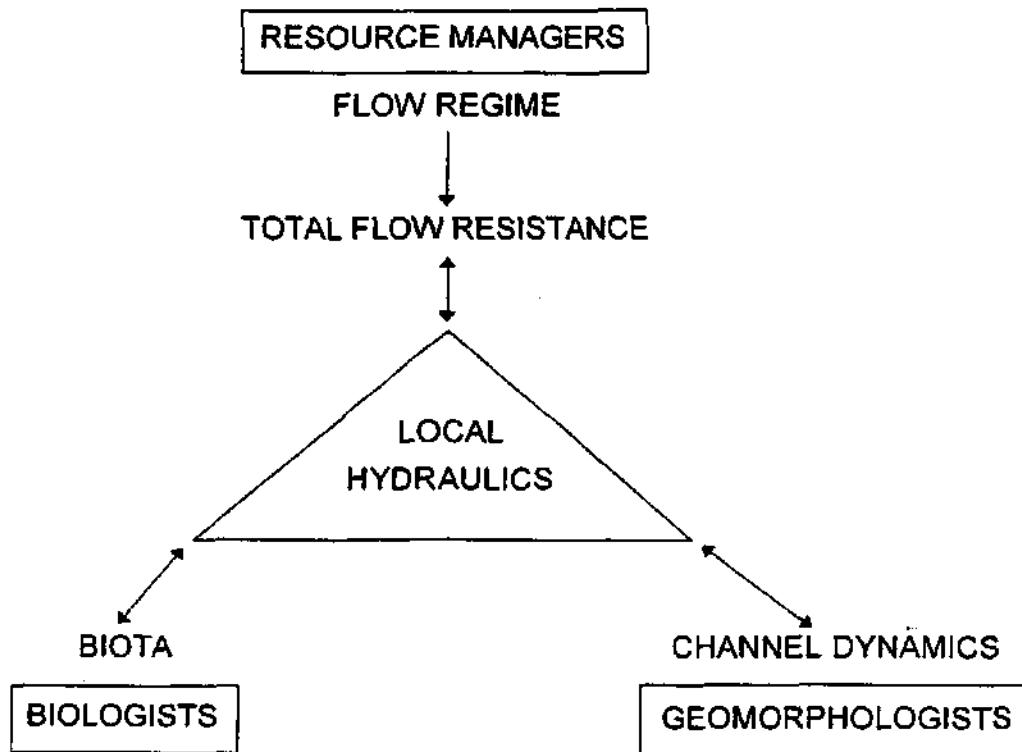


Figure 2: Links between local hydraulics; resource managers and geomorphologists.

Heritage *et al.* 1996). In addition to providing an independent study of channel flow resistance, output from this investigation has been utilised by these two projects in the following ways: quantification of channel flow resistance has enabled synthesis of stage-discharge relationships in independent, but similar reaches and the generation of a variety of hydrodynamic parameters, such as shear velocity, sediment transport rates and stream power (Heritage *et al.* 1996, Birkhead *et al.* 1996). Calculation of these parameters are essential for assessing channel dynamics and consequent biotic change (Figure 3).

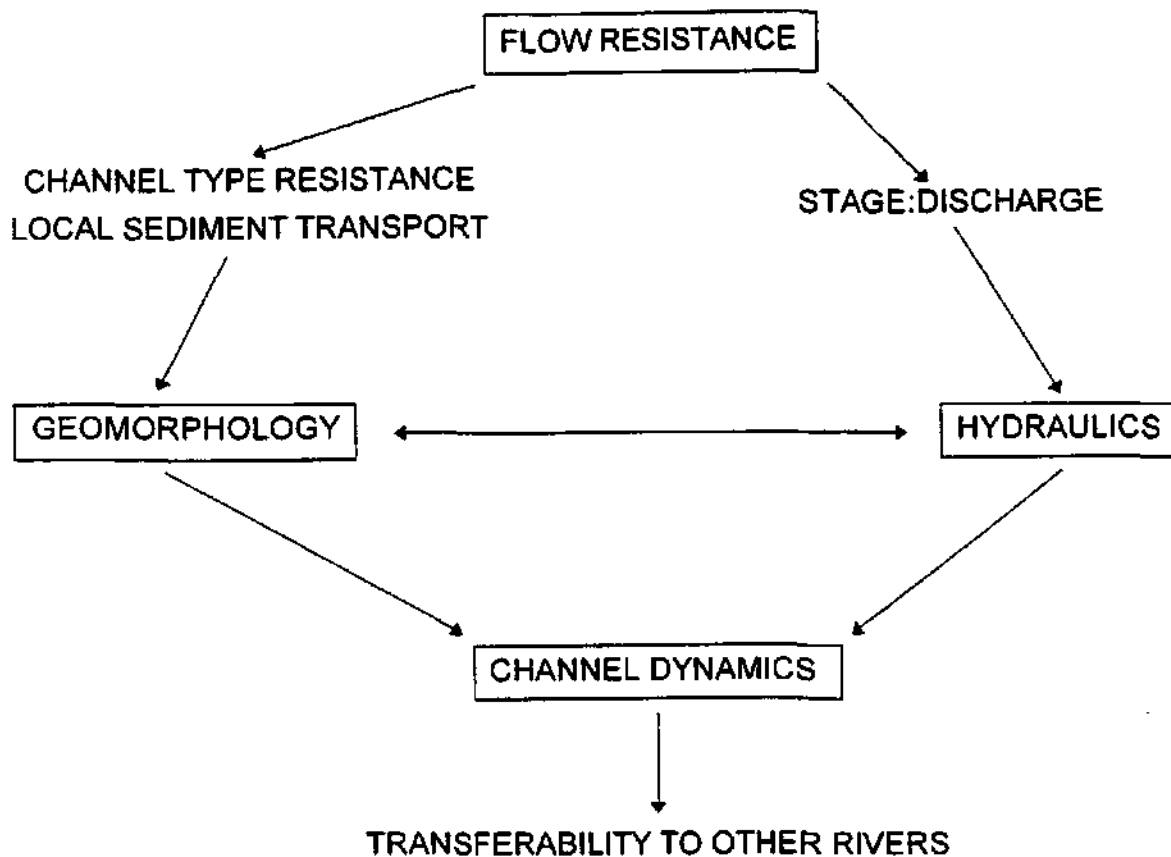


Figure 3: Use of flow resistance in determination of channel dynamics.

The following section outlines the rationale for building on the pilot flow resistance study of Birkhead *et al.* (1996), to explicitly define and quantify the flow resistance components on the Sabie River.

1.2 Aims

The overall aim of this project was to identify and quantify the flow resistance components on the Sabie River and to predict their effects on local hydraulic variables under different flow conditions. Such data are vital in predicting channel change and consequent habitat change. The steps necessary to achieve this aim are summarised below.

- a) Identification of the flow resistance components along the Sabie River.
- b) Evaluation of different methods for assessing flow resistance.
- c) Establishment of hydraulic monitoring networks.
- d) Quantification of flow resistance.
- e) Guideline compilation.

These aims were linked to form a research programme (Figure 4), in several stages, which is described in more detail below.

- a) Identification of the flow resistance components along the Sabie River.

Representative reaches on the Sabie River were determined from objective classification of the geomorphology (Stages 1 and 2, Figure 4). The term 'reach' can be used flexibly in the Sabie River. It can be viewed in context of the hierarchical geomorphological classification (van Niekerk *et al.* 1995)(Stages 3 and 4, Figure 4) and by the physical, spatial extent of an individual resistance component, namely, at a channel type, at a morphological unit, at a cross section or at a distributary channel level (Stage 4, Figure 4)(Section 6.1). There are a variety of factors controlling flow resistance, such as the type of vegetation community found, the channel geometry of the river and the sedimentary or lithological characteristics of the channel bed and banks (Chapter 2). A comprehensive geomorphological, sedimentological and vegetational survey was undertaken for each channel type that characterises the Sabie River, to identify all these flow resistance components over the range of 'reach' scales (Stage 5, Figure 4)(Section 5.2).

- b) Evaluation of different methods for assessing flow resistance.

A literature review identified flow resistance estimation methods which were most appropriate for the Sabie River (Chapters 2 and 4). Where necessary, new models were proposed to enable flow resistance calculation in the environments found in the Sabie River (Chapter 6).

- c) Establishment of hydraulic monitoring networks.

Hydraulic data were collected at five 'representative' reaches, covering the range of channel types found on the Sabie River, over a range of discharges, for use in quantifying flow resistance (Stage 5, Figure 4)(Section 5.3).

- d) Quantification of flow resistance.

The data obtained from field investigations were used to extend knowledge of flow resistance characteristics (Stage 7, Figure 4) and to provide predictive models for determining hydraulic parameters from local channel characteristics and hydrological records for the channel types found on the Sabie River (Stage 6, Figure 4)(Chapter 7). Results quantified on reach level,

transferred to other, unstudied but similar environments to successfully independently test and validate the flow resistance results (Stages 8 and 9, Figure 4).

e) Guideline compilation.

Guidelines of appropriate methodology for use over different channel types and scales of investigation were compiled (Chapter 8).

STAGE

1

HIERARCHICAL CLASSIFICATION OF THE GEOMORPHOLOGY OF THE SABIE RIVER IN THE KRUGER NATIONAL PARK

2

REPRESENTATIVE REACHES TO BE STUDIED

3

DEFINITION OF PHYSICAL SCALES FOR ROUGHNESS CALCULATION

4

REACH SUB-REACH CROSS SECTION SINGLE DISTRIBUTARY

5

IDENTIFICATION OF ROUGHNESS COMPONENTS WITHIN REPRESENTATIVE REACHES

HYDRAULIC MONITORING WITHIN REPRESENTATIVE REACHES

6

MODELS TO DEFINE CHANNEL GEOMETRY IN ALLUVIAL AND BEDROCK SECTIONS

7

QUANTIFICATION OF TOTAL ROUGHNESS AND ISOLATION OF ROUGHNESS COMPONENTS

8

VALIDATION

9

TRANSFER OF KNOWLEDGE TO SIMILAR, UNSTUDIED CHANNEL ENVIRONMENTS

Figure 4: Research programme for the channel flow resistance project.

CHAPTER 2: FLOW RESISTANCE

This chapter provides an extensive review of the resistance to flow in open channels. It includes reviews of models to predict flow resistance in all channel types, including temperate alluvial rivers. Relevance of these models to the channel environments encountered on the Sabie River is assessed. Methods to quantify total flow resistance are outlined initially, with details of the individual flow resistance components discussed later in the chapter.

2.1 Total channel flow resistance

There are several forms of flow resistance in natural open channels which all contribute to the total resistance. These are: skin resistance, large scale resistance, channel form resistance, vegetation resistance (Figure 5) and free surface resistance (Bathurst 1985a).

Three standard equations have been used by engineers for at least a century, to calculate discharge, Q , in a channel, using the premise that it is proportional to a power of the friction slope, S_f (often approximated by the water surface slope), the hydraulic radius, R , and the cross sectional area, A (as defined by Figure 6).

These equations are:

Chezy:

$$Q = A C (R S_f)^{\frac{1}{2}} \quad (1)$$

Manning:

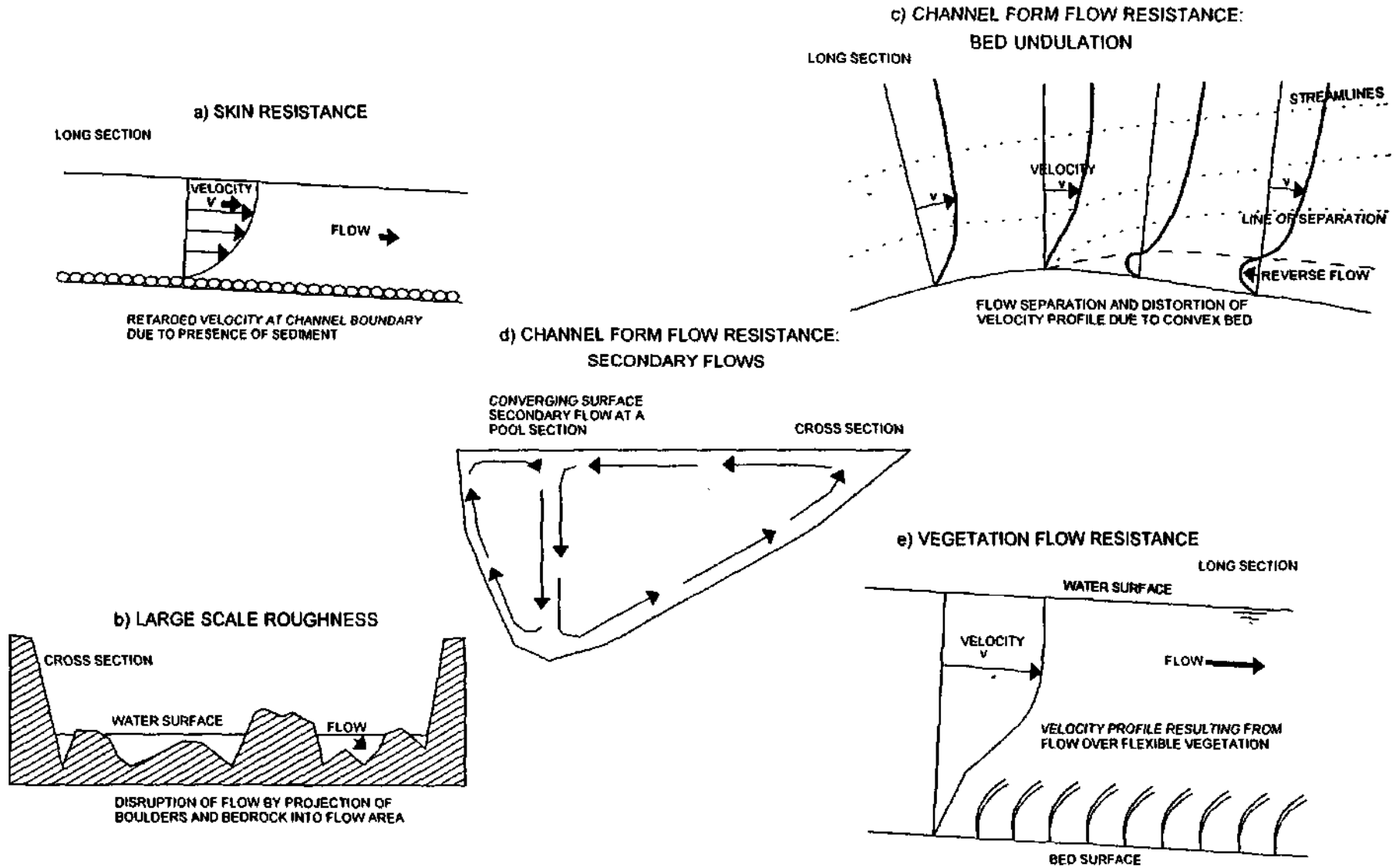
$$Q = \frac{A R^{\frac{2}{3}} S_f^{\frac{1}{2}}}{n} \quad (2)$$

Darcy-Weisbach:

$$Q = A \left(\frac{8 g R S_f}{f} \right)^{\frac{1}{2}} \quad (3)$$

where g is the acceleration due to gravity.

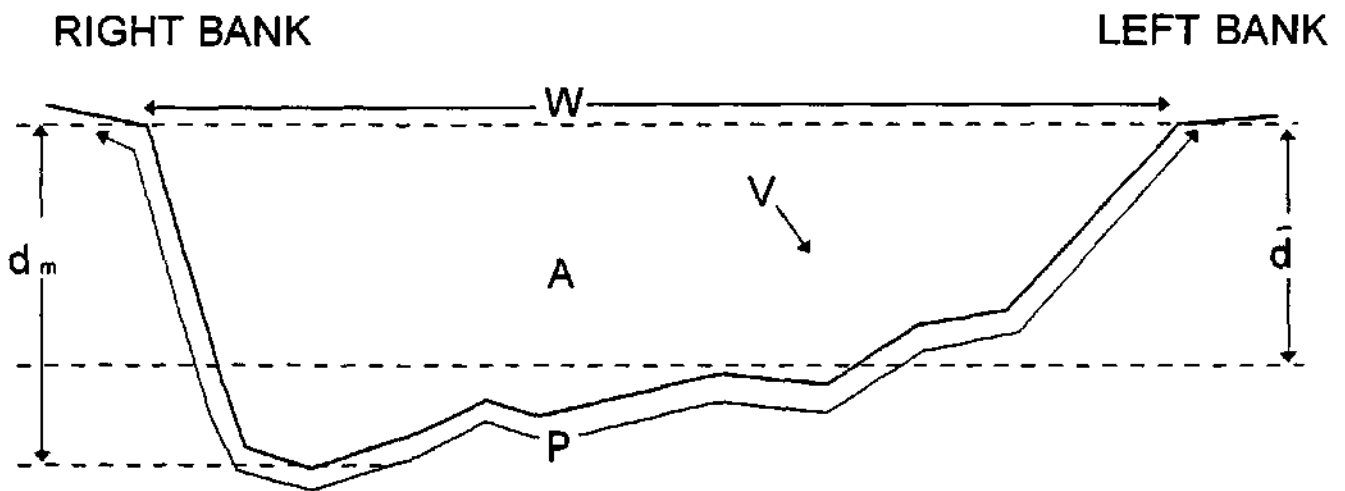
Figure 5: Components of flow resistance relevant to the Sabie River.



The evaluation of the coefficients, namely C , n and f in the above equations, gives a quantification of total flow resistance. These coefficients are interrelated, in the following way:

$$C = \frac{R^{\frac{1}{6}}}{n}; \quad f = \frac{8 g n^2}{R^{\frac{1}{3}}}; \quad f^{\frac{1}{2}} = \frac{(8 g)^{\frac{1}{2}}}{C} \quad (4)$$

Equation 3 gives a dimensionless friction coefficient which is based on boundary layer and pipe flow theory and its use is recommended by The American Society of Civil Engineers Task Force (1963). The advantage of this equation is that it is related to the processes of fluid mechanics which actually determines the flow resistance. However, all three equations are still widely used in channel design, therefore, results from all three flow resistance equations will be presented in this report.



$$R = \frac{A}{P} \quad Q = W \bar{d} V = A V \quad \bar{d} = \frac{A}{W}$$

Figure 6: Definition of cross section channel geometry and hydraulic parameters, where A is channel area, W is width, P is wetted perimeter, \bar{d} is hydraulic mean depth, d_m is maximum depth, R is hydraulic radius, Q is discharge and V is velocity.

The components of total flow resistance will be reviewed below.

2.2 Components of flow resistance

2.2.1 Skin resistance

The interaction between the flow and the channel boundary is named skin resistance and most equations describing this interaction are based on turbulent boundary layer theory. This theory can not be applied to the effects of large scale roughness, where the water depth is of the same order of magnitude as the bed material height. Under such conditions, for example boulder bed channels, a more empirical approach is used (Section 2.2.2).

Boundary layer theory

The boundary layer is the flow depth, measured from the boundary, where velocity, V , changes with depth due to the friction of the boundary surface. Therefore, for a given depth, the velocity falls from an undisturbed free stream value remote from the bed, to zero at that surface, as a result of the diminishing retardation effect of the boundary with distance from it (Figure 5a). In natural channels, the boundary layer extends to the water surface (Richards 1982). The velocity profile thus created can be described by well known laws, using the theories of Prandtl (1952) and von Karman (1930). These theories state that in a boundary layer over a rough surface the velocity is influenced by boundary effects, which vary with distance, y , from the boundary.

$$\frac{V}{V_*} = \frac{2.303}{\kappa} \log \left(\frac{y}{k_s} \right) + B \quad (5)$$

where κ is von Karman's universal constant and V_* is shear velocity. Strictly, this 'law of the wall' theory applies only to the inner 10 to 15% of the boundary layer, and relies on adequate prediction of boundary characteristics, B , and boundary roughness, k_s (Richards 1982, Bathurst 1985a). This latter term has often been referred to as the equivalent uniform sand roughness height (Nikuradse 1933), but this is unpractical to determine for most natural channels (Bathurst 1985a). Therefore, coefficients such as k_s are evaluated empirically from experimental or field data, creating semiempirical flow resistance equations, which are reviewed below.

Semiempirical equations based on boundary resistance

Several authors have developed flow resistance equations based on the Prandtl-Von Karman theory (for example Limerinos 1970, Burckham and Dawdy 1976, Bray 1979 and Hey 1979). Generally these take the form:

$$\frac{1}{f^{\frac{1}{2}}} = C_o + 2.03 \log \frac{R}{k_s} \quad (6)$$

These 'Keulegan type' equations are dependent on compliance with specific flow conditions, namely, fully developed turbulence in uniform channels with rough, fixed boundaries, where the water surface slope, bed slope and energy slope are equal.

It is the value of the coefficient C_o and the determination of the roughness height that varies between equations. The boundary roughness will be dependent on bed material size range, nonuniformity of grain shape and packing configuration or orientation. Grain packing is not easily determined for natural rivers (Bathurst 1985a), so bed roughness is more often quantified using a specific percentile (eg. D_{50} or D_{n4} , where $n\%$ of the sediment sample is less than or equivalent to D_n) from the size distribution of the intermediate axis of the bed material. The sediment sampling procedure most often used is that proposed by Wolman (1954), the grid sample by number frequency distribution. Bathurst (1982) has shown that for natural alluvial channels a single, surface, bed material size is acceptable to characterise bed roughness as sediment size distribution, shape and orientation or spacing differences are sufficiently small.

As not all the factors influencing skin resistance are accounted for by the above equations, their application is limited to specific conditions; essentially they can only give adequate estimations of skin resistance in straight, uniform reaches with fully developed turbulence and fixed rough boundaries, which are rare on the Sabie River. In alluvial reaches of the Sabie River, at low flow, these conditions may be satisfied, but many reaches are non-uniform in cross sectional and plan form, with bedrock and boulders disrupting the flow, creating other forms of flow resistance.

2.2.2 Large scale roughness

Where the flow depth is of the same order of magnitude as the bed material height, the projection of individual roughness elements into the flow (Figure 5b) disrupts the velocity profile described by equation 5. The resulting resistance is more accurately represented by the sum of the drag on each element and is primarily dependent on the roughness geometry. At relative roughnesses of $k_s/d > 0.3$, in which k_s is the height of the roughness, the flow resistance is considered to be large scale (Bathurst 1985b). Studies of large scale roughness show that the velocity profile deviates from the semilogarithmic pattern, with velocities tending to be higher and rate of change of the resistance with discharge underestimated, resulting in a 'S' shaped velocity profile, compared to predictions using equation 5 (Bathurst 1985a, Bathurst 1985b).

Three equations specifically intended for large scale roughness situations have been developed to predict the friction factor from the channel shape and bed material characteristics. These are:

Bathurst 1978

$$\frac{V}{(g R S_f)^{\frac{1}{2}}} = \left(\frac{8}{f}\right)^{\frac{1}{2}} = \left(\frac{R}{0.365 D_{84}}\right)^{2.34} \left(\frac{W}{d}\right)^{7(\lambda_E - 0.08)} \quad (7)$$

in which, W is the water surface width, d is the flow depth and λ_E is the roughness concentration of the exposed roughness elements, described by:

$$\lambda_E = \frac{\Sigma A_F}{A_{Bed}} \quad (8)$$

Here, ΣA_F is the total wetted frontal area of boulders protruding through the free surface in an area of bed, A_{Bed} .

In practical terms, field measurement of the frontal area of protruding boulders is difficult, so Bathurst developed an empirical equation using field data from the River Tees, England, to link the roughness concentration to the relative roughness (equation 8):

$$\lambda_E = 0.039 - 0.139 \log \left(\frac{R}{D_{84}}\right) \quad (9)$$

An alternative model developed from boulder bed channels in New Zealand was proposed by Thompson and Campbell (1979):

$$\left(\frac{8}{f}\right)^{\frac{1}{2}} = 5.62 \left[1 - \left(0.1 \frac{k_s}{R}\right) \log \left(12 \frac{R}{k_s}\right) \right] \quad (10)$$

where, k_s is the characteristic roughness size of the bed material. For the boulders sampled this was found to be:

$$k_s = 4.5 D_{50} \quad (11)$$

in which D_{50} is the median boulder size.

To overcome the limitations of the above, semiempirical, equations (equations 7 to 11), Bathurst, Li and Simons (1981) identified each of the sources of flow resistance in mountain streams and presented them in the following functional relationship:

$$\left(\frac{8}{f}\right)^{\frac{1}{2}} = fn_1(R_E) \times fn_2(F_R) \times fn_3(\lambda_E) \times fn_4\left(\frac{A_F}{W d'}\right) \quad (12)$$

where R_E is the Reynolds number; F_R is the Froude number; λ_E is the effective roughness concentration; A_F is the total wetted frontal area of roughness elements at a section and d' is the average depth defined by the actual cross sectional area of the flow, excluding roughness element frontal area, divided by the water surface width.

The authors quantified this theoretical relationship using data from a steep stream flume. Flow resistance was found to be:

$$f = \left[1.175 \left(\frac{Y_{50}}{W} \right)^{0.557} \left(\frac{d}{S_{50}} \right) \right]^{0.648\sigma - 0.134} \quad (13)$$

where Y_{50} is the median cross stream axis of the boulders; S_{50} is the median vertical axis and σ is a factor representing the standard deviation of the bed material size distribution (Bathurst 1978, Bathurst, Li and Simons 1981) and is defined by:

$$\sigma = \log \left(\frac{D_{84}}{D_{50}} \right) \quad (14)$$

To aid field measurement, an approximation of the last term in equation 12 is given by:

$$\frac{A_F}{W d'} = \left(\frac{W}{d} \right)^{-f} \quad (15)$$

This model has a strong base in theory, unlike equations 7 and 10 which are largely empirical. However, Thorne and Zevenbergen (1985) found that all three equations (7, 10 and 13) produced errors of up to 30%, overestimating mean velocity when tested on their data from a Colorado mountain river. They identified sampling error in the determination of bed material size as a major contributor to the observed discrepancy between predicted and observed velocity, but discounted boulder shape as an important parameter. The errors arising from the use of these models demonstrate the need for further research into process based flow resistance models for mountain rivers and other river types with large scale bed roughness, such as that found in several channel environments on the Sabie River. The errors identified by Thorne and Zevenbergen (1985) also highlight the problem with empirical approaches, that they are highly specific to the conditions the equations were developed in.

Consequently, they may be of limited use in the unstudied environments encountered on the Sabie River.

2.2.3 Channel form flow resistance

In a channel free of vegetation, the channel form resistance component can be significant, particularly at low flows (Allen 1939, Leopold *et al.* 1960, Parker and Peterson 1980, Bathurst 1981 and Hey 1988). A channel's form resistance to flow is composed of two elements: firstly, the channel bed geometry and secondly, the plan form of the river. The additional resistance imparted to the flow by channel form can not be modelled consistently by any single value of relative roughness, k/D (Church *et al.* 1990), as grain resistance can, so alternative relationships have been sought.

In natural channels, irregular bed topography in the form of pools and riffles or rapids and cascades and channel curvature, create additional components of resistance (Figure 5c). The velocity profile along a reach with a concave downwards boundary, such as the entrance to a pool in natural channels is altered as the velocity decelerates. This creates increased turbulence, encouraging separation of the flow from the boundary (ven te Chow 1959) and inducing a reverse flow to maintain discharge continuity at a section.

Meandering plan form induces secondary circulation (Figure 5d) in the flow and this constitutes an energy loss from the primary flow and an addition to flow resistance (Bagnold 1960 and Leopold *et al.* 1960). Additional energy losses may be caused by turbulence in eddies associated with flow separation at sharp bends. Most authors assume that this separation does not normally occur at realistic ratios of radius of curvature to channel width (Leopold *et al.* 1960). The degree of sinuosity on the Sabie River is generally low, except in braided channels at low flows, so the effect of channel curvature and consequent secondary circulation, flow separation and velocity redistribution will be minimal. Therefore, the effect of channel curvature has been neglected for this report.

In sand bed channels, which are prevalent on the Sabie River, bedform development is common as ripples and larger dune features. Several studies to predict flow resistance in sand bed channels exist, (for example Einstein and Barbarossa 1952, Alam *et al.* 1965, Brownlie 1983). These models generally split the total Darcy-Weisbach friction factor into components relating to a flat bed skin resistance, f^1 and that due to bedform formation, f^2 , with the total resistance being the sum of the two components. The study of the effect of dune and ripple formation in alluvial reaches of the Sabie River, was prohibited, due to the detail of data that would be required to model this aspect of channel form flow resistance. Therefore, only channel form flow resistance resulting from non-uniform bed topography is considered in this study.

A variety of models have been proposed to calculate channel form flow resistance due to irregular bed topography; a selection are reviewed below.

Hey 1979

Hey modified the Colebrook-White 'Keulegan type' equation to include the effect of cross sectional shape, a , on flow resistance, to give:

$$\frac{1}{f^2} = 2.03 \log \left(\frac{a R}{D} \right) \quad (16)$$

The coefficient, a , varies between 11.1 and 13.46 depending on the hydraulic shape of the cross section, R/y , where y is the perpendicular distance from the perimeter to the point of maximum velocity. This can be assumed to be the maximum depth, d_m , for most channels. A value for a can be established using the approximation

$$a = 11.1 \left(\frac{R}{d_m} \right)^{-0.314} \quad (17)$$

Equation 16, which accounts for shape and nonuniform sediment size at a cross section, was shown to predict actual flow resistance to $\pm 12.7\%$ for uniform flow, riffle, sections. However, non-uniform reach influences, which are common on the Sabie River, were not considered.

Miller and Wenzel 1985

The processes by which bar resistance is generated was addressed by Miller and Wenzel (1985). They developed equations which accounted for the energy losses due to the local accelerations and decelerations of flow between pools and riffles. Their model used the friction slope, S_f , which was assumed to be the linear sum of the losses due to form resistance, S_{FM} , and local losses, S_L , due to flow contraction and expansion. They suggested that the majority of energy losses at riffles would be due to grain resistance, while pools would be influenced by expansions and contractions which significantly affect total energy loss. The Darcy-Weisbach equation (equation 3) was used to compute flow resistance losses:

$$S_{FM} = \frac{f V'^2}{8 g R'} \quad (18)$$

where the superscript $'$ refers to subreach parameters.

Local losses are related to a local expansion and contraction coefficient, C_E , by:

$$S_L = C_E \frac{V^2}{2 g L} \quad (19)$$

where L is the distance between cross sections and V is the entrance velocity in expanding sections and exit velocity in contracting sections.

The choice of value for C_E depends on channel geometry and head and velocity differences over the subreach. The criteria for evaluation of this coefficient are ill defined and it exists primarily as a 'correction' factor. Values for friction factor, f , were calculated using various logarithmic or power form flow resistance equations, (see Section 2.2.1). These equations apply strictly to uniform flow conditions. Therefore, although predicted (from Darcy-Weisbach) and actual (from Keulegan-type) values corresponded well at riffle sites, as would be expected, the claim that the discrepancy between the two values at pool sites is due to the energy losses associated with flow divergence or convergence, is erroneous.

Bathurst 1981

Bathurst (1981) presented a mechanistic approach to the quantification of bar form resistance. The Bathurst 1981 model considered that bars increase flow resistance by two main processes: ponding of the reach by the topographic high points, the riffles, and large scale roughness due to the low flow depths over the riffle. This latter process's effect on flow resistance would be magnified by the coarser sediments found at riffles. In low flows, the ponding effect will be dominant, but both processes diminish with increasing discharge (because the ratio of the residual depth to the actual depth decreases with increasing discharge). Therefore, it was proposed that the residual depth, I_0 , (that remaining when the discharge is zero) which is a measure of ponding, should account for the major portion of bar resistance. It was assumed that flow resistance in the absence of bars (presumably in a straight channel) consists mainly of grain resistance. Therefore, the hypothetical values of the discharge resulting from this condition, Q_G , were calculated using the following:

$$Q_G = 5.62 A (g I S_f)^{\frac{1}{2}} \log \left(\frac{a I}{3.5 D_{84}} \right) \quad (20)$$

where a is Hey's 1979 channel shape parameter (equation 17) and I is the flow depth.

This predicted discharge was compared to the actual, measured, discharge and the ratio $Q:Q_G$ was used as an (inverse) measure of the effect of bar resistance. If bar resistance does depend largely on the residual depth then the magnitude of the resistance should be an inverse of the ratio: $(I - I_0)/I$. Bathurst (1981) provided limited field data to support this hypothesis. This approach provided a good insight into some of the processes responsible for channel form resistance.

Hey 1988

Hey's 1988 model further developed the ideas proposed by Bathurst (1981), by recognising that the riffle sections, where flow is locally uniform, control the velocity and depth of flow in the reach (Hey 1979), whereas reach average conditions are also dependent on pool geometry. He assumed that the channel form resistance is the linear difference between reach

resistance and skin resistance, as determined at the riffle. The skin resistance can be determined using Darcy Weisbach (equation 21) and Colebrook White (equation 22) friction factor equations:

$$f_r = \frac{8 g R_r S_r}{V_r^2} \quad (21)$$

$$\frac{1}{f_r^{\frac{1}{2}}} = 2.03 \log \left(\frac{a_r R_r}{D_s} \right) \quad (22)$$

where the subscript _r denotes riffle data; other data is reach average.

Assuming $D_b = D_t - D_s$:

$$D_b = a d \left(\frac{D_s}{a_r d_r} \right)^{\left(\frac{f_r}{f} \right)^{\frac{1}{2}}} - D_s \quad (23)$$

where D_b is bar form roughness height, D_s is grain roughness height and D_t is total roughness height.

This solution indicates that both reach average and riffle data contribute to total flow resistance via flow expansions and contractions. However, this solution fails to recognise that the bed material size (hence skin resistance) varies between pools and riffles.

The channel form flow resistance models reviewed above, have dealt specifically with longitudinal changes of bed topography and the associated flow resistance. However, most were developed for use in gravel bed rivers, where flow is through pools and riffles. The extreme non-uniformity of the water surface slope over bedrock influenced channel types, creating pools and rapids, which are common morphological units on the Sabie River, means that these models are not applicable to large sections of the Sabie River. The irregular water surface slope profile, controlled by local changes in the lithology, will introduce significant flow resistance, particularly at low flows. A few studies have been made of 'pool/fall' streams (Beven *et al.* 1979 and Whittaker and Jaeggi 1982) similar to channel environments found in bedrock reaches on the Sabie River. They show that flow resistance at low flows is extremely high as a result of ponding of the flow in the pools and hydraulic jumps over 'falls' or rapids, yet propose no mechanistic solution. Bathurst (1985a) and Hey (1988) noted that there is no generally accepted flow resistance equation for use in such channels and since publication of these reviews there has been little progress in modelling channel form flow resistance.

2.2.4 Vegetational flow resistance

Riparian and aquatic vegetation is important for a variety of economic, environmental, aesthetic and hydraulic reasons. Therefore, the maintenance of this vegetation is integral to the conservation of riparian ecosystems. Vegetation growth stabilises channel bed and banks by inhibiting scour; the presence of certain species is a good indicator of water quality and vegetation growth alters the local hydraulic conditions by physically reducing a channel's capacity via reduction of the cross sectional area and introducing a resistance to flow or roughness. The positive aspects of riparian and aquatic vegetation mean that vegetated channels are desirable and therefore common. This necessitates the understanding of the effect vegetation has on channel hydraulics.

The presence of vegetation in a channel will physically increase the wetted perimeter, P , (and consequently the hydraulic radius) due to its bulk volume, and will retard the flow by introducing frictional resistance (Figure 5e). A variety of plant characteristics determine the response of hydraulic variables, such as water depth, friction slope and velocity, to aquatic and riparian plant presence (Table 1). The 'hydraulic' characteristics affect the resistance of the vegetation to flow, whereas the 'biological' parameters also present a blockage to the channel capacity by virtue of their volume and biomass. Klaassen and van der Zwaard (1974) found that even the presence of organic trash trapped in hedges and trees contributed significantly to an increase in flow resistance in overbank flood conditions. The response of the vegetation to a given flow will depend on its hydraulic characteristics.

Table 1: Vegetation characteristics that affect flow resistance.

Biological	Hydraulic
Stem/trunk height	Density of plant material
Cross sectional shape of stem/trunk and foliage	Flexibility/stiffness of stem /trunk
Stem/trunk diameter	Spatial arrangement of individual vegetal elements.
Complexity of form (single stem/branched/coppiced; presence of canopy)	
Spatial arrangement and density of vegetal elements	

The retarding effect of vegetation on velocity has long been recognised (Cook and Campbell 1939) and models to predict river behaviour in the presence of vegetation have been developed. The models fall into two major groups: those concerned with flow over submerged vegetation (primarily aquatic weeds and grasses) and those addressing emergent vegetation (such as wetland or floodplain grasses, crops, shrubs and trees). This division of models according to depth of flow is important, as flow over vegetation differs substantially from flow through dense vegetation (Hydraulics Research 1985). At low discharges flow will

pass around and between stems and foliage without bending them. As the discharge increases, the volume of vegetation in the flow path increases and so does the resistance to flow, reaching a maximum when the vegetation is partly bent over and is oscillating in the flow (Maheshwari 1992). Examples of vegetation flow resistance models are reviewed below.

Flow over submerged vegetation

Much of the early work on vegetational flow resistance was concerned with flow over submerged grass surfaces, as grass occurs naturally and is planted deliberately on floodplains and channel banks (Hydraulics Research 1985, 1992). Consequently, there is limited information available for non-grass vegetation.

The Manning equation

Estimation of a coefficient of hydraulic resistance, such as Manning's n in equation 24, is the most commonly used solution to quantifying the retarding effect of vegetation on flow.

$$V = \left(\frac{1}{n}\right) R^{\frac{2}{3}} S_f^{\frac{1}{2}} \quad (24)$$

Cowan (1956) outlined a procedure for estimating n in which adjustments are made to a basic value, determined from an equivalent straight, uniform, smooth channel, after allowing for additional factors, such as sinuosity, irregular bed or banks or vegetation presence. Ven te Chow (1959) and Barnes (1967) provided an analysis of the factors affecting flow resistance in open channels and gave photographs with related n values for 'base' cases and correction factors for natural streams. Therefore, the 'base' value can be assigned by visual, photographic, comparison or from empirical equations. The principle inadequacy of these approaches are that they do not provide information on the change in Manning's n value with increase in flow depth or discharge (Jarrett 1984). A reliable procedure would account for factors such as height of vegetation in relation to depth of flow, the type of vegetation, the degree to which the cross section is occupied by vegetation and the transverse and longitudinal distribution of stems, as well as any changes in the character of the vegetation with age or season, because these factors will generate a range of Manning's n values with varied flows. However, the Manning equation (equation 24) remains the most widely used in hydraulic resistance problems and the experience gained from this use gives this method an advantage.

Empirical studies

The US Soil Conservation Service (USDA 1954) derived empirical relationships between the flow resistance coefficient, Manning's n , and the product of the average velocity and hydraulic radius. The n -VR relationship was represented as a family of curves for different physical characteristics of grass cover, namely, height, density and uniformity.

Despite the fact that the n -VR type curves are not derived from principles of fluid mechanics, they do represent the resistance coefficient for grass channels in terms of physical biological

parameters. Several authors have provided both laboratory and field evidence to support the relationship between n and VR (Kouwen and Li 1980, Kouwen *et al.* 1981, Larsen *et al.* 1990, Kouwen 1992), however, the validity of this method has also been questioned (Strelkoff and Fangmeier 1974, Turner *et al.* 1978, Turner and Chanmeesri 1984, Smith *et al.* 1990, Abdelsalam *et al.* 1992). The Manning equation (equation 24) was developed for flow in defined courses, where the roughness elements do not intrude through the water stream. It is therefore not suited to natural, vegetated, channels. The major criticism of the n - VR model is that it can not generate a unique n value, as the same VR product can be obtained from different V and R values. The definition of R in a vegetation choked channel is questionable, as the plant surface area should ideally be accounted for in the wetted perimeter calculation. An additional problem is that if the density of vegetation is high, the flow cross section character through the vegetation will resemble a porous media, not open channel flow (Turner and Chanmeesri 1984). The n - VR method also assumes that the relationship is independent of water surface slope, but Eastgate (1969) has proved that the curves will vary with changing slope. Consequently, other methods of vegetation flow resistance quantification have been developed.

The relative roughness approach

Kouwen, along with several co-authors, (Kouwen, Unny and Hill 1969, Kouwen and Unny 1973, Kouwen and Li 1980) presented a quasi-theoretical analysis which developed the functional relationship between n and VR , to incorporate hydraulic vegetational parameters as a relative roughness term in the semi-logarithmic equations that describe rigid boundary flow resistance, as originally developed by Keulegan (1938).

The relative roughness concept recognises that grass tends to deform under an imposed fluid drag, thus smoothing the vegetation boundary roughness with increased flow. The response of the vegetation to flow depends on the characteristics of the vegetation itself (Table 1) and the flow conditions imposed on it. For prone roughness, such as tall grass submerged under a deep flow, the flow boundary in effect becomes a smooth wavy surface, which is a function of the Reynolds number, R_E .

Kouwen and Li (1980) report the relative roughness models as:

$$\frac{1}{\sqrt{f}} = i + j \log \left(\frac{d}{k_s} \right) \quad (25)$$

where: i and j are coefficients dependant on the extent to which the vegetation is bent and k_s is the height of the roughness, as determined by equation 26, where the roughness height varies as a function of the drag exerted by the flow and is calculated from:

$$k_s = 0.14p \left[\frac{\left[\frac{MEI}{\tau_0} \right]^{0.23}}{p} \right]^{1.59} \quad (26)$$

here, p is the length of the vegetation, M reflects the stem density and EI reflects the flexural rigidity of the stem.

The total boundary shear, τ_0 , is given by:

$$\tau_0 = \gamma R S_f \quad (27)$$

where γ is the unit weight of water.

The coefficients i and j in equation 25 are based on a classification of shear stress to a critical shear velocity, v^*_{crit} for each vegetation, where:

$$v^*_{crit} = \text{minimum of } (0.028 + 6.33 MEI^2, 0.23 MEI^{0.106}) \quad (28)$$

Table 2 lists the values of i and j as a function of v^*/v^*_{crit} .

Table 2: Quantification of vegetation flow resistance coefficients i and j (after Kouwen and Li 1980).

Classification	Criteria	Parameter i	Parameter j
Erect	$(v^*/v^*_{crit}) \leq 1.0$	0.15	1.85
Prone	$1.0 < (v^*/v^*_{crit}) \leq 1.5$	0.2	2.7
Prone	$1.5 < (v^*/v^*_{crit}) \leq 2.5$	0.28	3.08
Prone	$2.5 < (v^*/v^*_{crit})$	0.29	3.5

A dimensional analysis, given by Kouwen and Unny (1973), of uniform flow through uniformly dense, randomly distributed vegetation, demonstrates the importance of biomechanical flexural rigidity terms:

$$f = \phi_1 \left[\frac{p}{\left(\frac{MEI}{\tau_0} \right)^{0.25}}, \frac{k_s}{p}, \frac{k_s}{d} \right] \quad (29)$$

The use of such a term combines both the biological and hydraulic characteristics of vegetation. Kouwen and Li (1980) give MEI values for limited vegetation types, calculated from field data (Table 3).

Table 3: Stiffness values for various grasses from experimental data (after Kouwen and Li 1980).

Grass type	Bed slope	Stem density	Stem length	MEI
Alfalfa; green; uncut	0.021	1087	0.33	6.22
Alfalfa; green; uncut	0.039	1388	0.24	2.89
Bermuda grass; long; green	0.2	1592	0.38	16.7
Bermuda grass; long; dormant	0.2	1592	0.38	116
Kikuyu; short; green	0.04	1184	0.107	0.144
Kikuyu; long; green	0.04	1334	0.42	35
Kikuyu; short; green	0.04	1184	0.107	0.144
African star; long; green	0.07	1506	0.29	5.74
Mixture; short	0.03	-	0.12	0.074
Mixture; long	0.03	-	0.63	1.83

Empirical relationships between MEI and p were shown by Kouwen (1988) to be:

$$\text{Green grass: } MEI = 319 p^{3.3} \quad (30)$$

$$\text{Dormant grass: } MEI = 24.5 p^{2.26} \quad (31)$$

These relationships reflect the fact that the longer the grass, the more biomass is present in the vegetation, so it resists compression. Two field methods to evaluate biomechanical properties of vegetative channel linings are given by Kouwen (1988). The first is a "board

test", where a hinged board is dropped onto the vegetated lining. The final board position will be a reflection of the density, stiffness and length of the grass and the ability of the grass to resist bending. The second method to evaluate MEI is by the use of a statistical empirical relationship between vegetation length and stiffness (equations 30 and 31). Clearly, these field estimation techniques are only applicable to grass-like vegetation and a reliable determination of flexural rigidity for complex stands of vegetation is not possible. Kouwen *et al.* (1969) suggest, as a more practicable field solution, the use of the ratio of cross sectional area to the area blocked by vegetation, as the relative roughness term. This approach has also been recommended by Hydraulics Research (1992), Bakry *et al.* (1992) and Abdelsalam *et al.* (1992).

As already noted, the velocity distribution above the vegetal lining differs from that within the vegetation (Figure 5e). Kouwen, Unny and Hill (1969) and El-Hakim and Salama (1992) found the velocity distribution within deflected vegetation elements to be uniform and a function of the drag forces on vegetal elements. Kouwen *et al.* (1969) and Kouwen and Unny (1973) described the velocity distribution above the flexible roughness elements as logarithmic. This form of the profile was confirmed by Kadlec (1990), in his study of flow through wetland vegetation. However, El-Hakim and Salama (1992) suggest a three zone velocity profile, with a transition zone of constant shear separating the flow within the roughness elements and that unaffected by the elements. Analysis of laboratory data revealed that equations describing flow over a smooth plate (equation 32) or a power law relationship (equation 33) provided the best fit to their data.

$$\frac{V}{V_*} = -2.662 + 0.959 \ln \left[\frac{(y-p)V_*}{\nu} \right] \quad (32)$$

$$\frac{V}{V_{\max}} = 1.13 \left[\frac{(y-p)}{(d-p)} \right]^{0.312} \quad (33)$$

where, V_{\max} is maximum velocity and ν is kinematic viscosity.

Although models of flow over submerged vegetation have been developed that successfully account for a variety of biological and hydraulic vegetation parameters, these parameters are known for only a few species of commercial crops (Table 3) or for laboratory simulations of vegetation. Without exception, the models at least partially, rely on empirical calibration, which leads to difficulties in transferring the models to unstudied environments such as bedrock influenced reaches of the Sabie River.

Flow through vegetation

Much of the past research on estimation of hydraulic resistance due to vegetation has been devoted to flows in open channels and rivers, where vegetation is generally submerged (Maheshwari 1992). Recently models have been developed that deal with shallow flow through vegetation, such as that found in overland flow, surface irrigation and on floodplains.

The effect of dense, emergent, vegetation on flow through it has often been accommodated by assigning a high value to the Manning's n (Jadhav and Buchberger 1994), for example, Petryk and Bosmajjian (1975):

$$n = n_b \sqrt{1 + \frac{C_D \sum A_i}{2gAL} \left(\frac{\lambda}{n_b}\right)^2} R^{\frac{4}{3}} \quad (34)$$

This model predicts the Manning's n value in terms of vegetation density, $C_D \sum A_i / (2gAL)$, the hydraulic radius and the Manning's n value in the absence of vegetation, n_b . The vegetation density variable contains a vegetation drag coefficient term, C_D and the exposed vegetation area, A_i to the flow of cross sectional area, A and reach length L . The correction factor of 1.0 or 1.49 for S.I. units or imperial units is given by λ . The limitations to this model require that the velocity is low enough to prevent vegetation bending, that it is uniformly distributed and that the vegetal density is constant laterally.

Hall and Freeman's (1994) flume investigation revealed values for Manning's n through dense bulrush stands that varied from 0.27 to 0.7, depending on the stem density and flow conditions. These values are between 2 and 5.4 times larger than the equivalent number obtained from USGS vegetated channel flow resistance guidelines and clearly suggest care should be employed when using Manning's n to quantify vegetation flow resistance.

The inadequacies of the Manning equation have already been discussed and these will be particularly pertinent when the flow is through vegetation. Therefore, in addition to the limiting assumptions behind it, there is little justification in making alterations or 'improvements' to the Manning equation, such as that in equation 34. When the flow is through a dense network of stems and leaves, it is generally slow and therefore viscous shear, rather than turbulent shear predominates. Under these conditions the porosity, or proportion of the cross sectional area not blocked by vegetation to the total cross sectional area of the channel must be considered in calculations of velocity. For example, Hammer and Kadlec (1986) report porosities of 80% in densely vegetated wetlands. Flow through dense vegetation results in channelisation of the flow. Ree *et al.* (1977) have termed these flows "subdivided" and suggest that the average flow velocity is relatively independent of discharge. Turner *et al.* (1978) recommend the use of a discharge-depth equation, rather than the more commonly used Manning equation, as an appropriate empirical approach when considering flow through vegetation. This form of vegetation flow resistance is reviewed below.

Discharge-depth equations

The discharge-depth equation for shallow overland flow given by Turner *et al.* (1978) is:

$$Q = k_e d^r \quad (35)$$

or

$$Q = G^{-1} d^t S_f^{0.5} \quad (36)$$

The coefficient k_s describes the geometry of the surface, t is an exponent that reflects the degree of mixing in the flow and G is a coefficient of flow resistance independent of slope. Work by Turner and co-workers (Turner *et al.* 1978 and Turner and Chanmeesri 1984) validated the equations for a wide range of simulated and real vegetation types (including different sowing patterns, stem densities and stages of plant growth), but for limited, low, flow depths and discharges.

Smith *et al.* (1990) analyzed a wider range of data, incorporating deeper, more rapid flows over emergent and submerged vegetation. They suggest a more general form of the discharge-depth equation, containing an friction slope term, S_f :

$$Q = \theta S_f^\epsilon d^\omega \quad (37)$$

Where θ , ϵ and ω are fitted parameters and were found to be constant for any particular grass or crop.

A major drawback, however, of the use of this generalised, discharge-depth equation (equation 37), is that the parameter values are empirically derived and therefore specific to individual vegetation type, channel geometry and flow conditions (Smith *et al.* 1990).

Momentum concept and drag around isolated stems

An alternative method for assessing vegetation flow resistance is the consideration of drag around individual vegetal elements. Li and Shen (1973) presented an analytical study of the mechanics of flow in channels with tall, emergent, vegetation by applying the momentum concept to determine the effect of the arrangement of vegetal elements on drag. Their model predicts the drag on individual stems (in their study, uniform cylinders) and uses superposition of the wakes produced to predict the velocity profile across the channel. They concluded that staggered patterns of vegetation are more effective in retarding the flow than any other configuration.

Thompson and Roberson (1976) present a summary of calculations of frictional drag around cylinders:

$$F = C_{DG} A_N \left(\frac{\rho \bar{v}^2}{2} \right) \quad (38)$$

The drag force, F , is a product of the drag coefficient, C_{DG} , the projected area normal to the flow, A_N (equivalent to the stem diameter, D_s , multiplied by the submerged stem height, p), and a local velocity, v and density, ρ terms.

Drag coefficients are calculated as functions of the stem Reynolds number, R_D (Kadlec 1990):

$$R_D = \frac{D_s \rho \bar{v}}{M} \quad (39)$$

Results presented by Kadlec (1990) show that overland flow in wetlands is controlled by drag around vegetation which results in flows in the transition region between laminar and turbulent.

Kadlec (1990) derived a local resistance coefficient, J , which combined the drag coefficient and the vegetation frontal area per unit volume, a_i (replacing the MD_s , equivalent in the cylinder array models), for wetland flow conditions:

$$S_f = C_{DG} a_i \frac{\bar{v}^2}{2g} = J \frac{\bar{v}^2}{2g} \quad (40)$$

Analysis of field and laboratory data from a variety of authors, confirmed that measured values of J provided reasonable predictions of flow rates (Kadlec 1990). However, use of the resistance coefficient, J , is restricted as it is depth dependant and is not independent of velocity in the laminar flow regime. Kadlec proposed that the appropriate friction rule under conditions of flow through dense vegetation is a power law for velocity, in terms of depth and friction slope (equation 41).

$$\frac{Q}{W} = K d^\phi S_f^{\Psi} = V_0 \bar{d} \quad (41)$$

Where, V_0 is the average superficial velocity and \bar{d} is the average depth of free water (the surface water volume divided by the inundated area of wetland). The exponent, ϕ , reflects both a vertical stem density gradient and Ψ represents a bottom elevation distribution.

This model represents a reliable discharge estimation technique for emergent vegetated wetlands with vertical variation in vegetation density. Vegetation surveys are required but there is no need for detailed hydrological data.

As the preceding review of vegetation flow resistance demonstrates, most models have empirical components calibrated from either laboratory approximations to vegetation or relate to studies conducted on a limited number of commercial crops (Table 3). Flow through

vegetation under low flow conditions complicates flow resistance computation, as flow is dominated by viscous shear and will act more like flow through a porous medium than open channel flow (Kadlec 1990). Under shallow overland flow conditions a power law depth-discharge equation may be more appropriate than the commonly used Manning's n or Darcy-Weisbach f approaches (Turner *et al.* 1978, Turner and Chanmeesri 1984, Smith *et al.* 1990). These authors' equations rely on empirical calibration for specific vegetation types, channel geometry and flow conditions. Therefore, there remains no universally applicable vegetation flow resistance equation and modelling the effects of the assemblages of vegetation species or communities found on the Sabie River would be extremely difficult using present techniques.

2.2.5 Free surface resistance

Free surface resistance represents the distortion of the free surface and the effect of the free surface on the turbulence structure. Most natural channels are too small for significant wind generated waves to develop, therefore their effect on the free surface is negligible. Roll waves caused by supercritical flow are an ephemeral phenomena in the majority of natural channels, however, in steep gradient bedrock channels, such as those found on the Sabie River, hydraulic jumps over rapids are locally common. Therefore, the effects of large scale roughness elements protruding through the free surface and of supercritical flow over rapids causes substantial free surface resistance in some environments on the Sabie River. Bathurst (1985a) has concluded that the effect of disruptions to the free surface can only be described in general terms. Therefore, for this study, the free surface resistance component will be combined with the large scale roughness component, where the channel boundary affects the free surface and into the channel form flow resistance component when irregular bed profiles, such as pool-rapids, cause supercritical flow.

CHAPTER 3: CHARACTERISTICS OF THE SABIE RIVER

3.1 Catchment characteristics

The Sabie River drains a 7096 km² catchment in the Mpumalanga Province, South Africa and Mozambique (Figure 7). It rises in the Drakensberg Mountains to the west (1600masl), descending rapidly onto the flat lowveld (400masl) and Lebombo zones (200masl) in the east. Rainfall is greater in the highland areas (2000mm.a⁻¹) and declines rapidly towards the border of South Africa with Mozambique (450mm.a⁻¹) and is concentrated in the summer months, from November to March. Evaporation varies from 1700mm in the east, to 1400mm in the west, with summer values 60% higher than winter ones in the lowveld. Winter base flows are supplied by the dolomitic aquifers in the mountainous areas to the west. Discharge patterns for the Sabie River reflect the variability of the rainfall and human influence, but the flow remains perennial at present.

The Sabie River is underlain by a wide variety of bedrock lithologies, comprising sedimentary, intrusive and extrusive igneous and metamorphic rocks. Lithological differences in the geology control the longitudinal slope profile of the Sabie River and consequently the geomorphological form (van Niekerk *et al.* 1995 and Cheshire 1996).

3.2 Riparian geomorphological hierarchy

The Mpumalanga region has been subject to uplift in the recent geological past (10Ka to 100Ka), resulting in incision into bedrock. This has generated a channel that has a 'floodplain' restricted by the width of incision into bedrock. This incised feature has been termed the macro-channel (van Niekerk *et al.* 1995), as opposed to the smaller, active, perennially flowing channels and seasonally flooded features within its confines. The Sabie is a physically diverse river system that displays marked changes in channel type as the distribution of sediment over bedrock alters. Van Niekerk *et al.* (1995) have identified morphological units on the Sabie River (described in Table 4), which form associations with each other to generate channel types (Heritage *et al.* 1995).

A hierarchical river classification system has been given by van Niekerk *et al.* (1995), based on observations of the Sabie River (Figure 8). The channel types listed in Figure 8 represent a stage in a continuum, as a length of channel may display a mixture of features as it develops from one channel type to another (Heritage *et al.* 1995). Therefore, the hierarchical classification can be extended to include alluvial, mixed or bedrock anastomosing channel types, for example. The combinations of channel types found on the Sabie River are indicated by a * in Table 5. Of the seven possible channel types (Table 5), five principal channel types are representative of those found on the Sabie River, in the Kruger National Park (Heritage *et al.* 1995).

The flow resistance components (Chapter 2) that are associated with specific morphological units and hence channel types, are listed in Table 6.

Figure 7: Location of study reaches and gauging weirs in the Sabie River catchment.

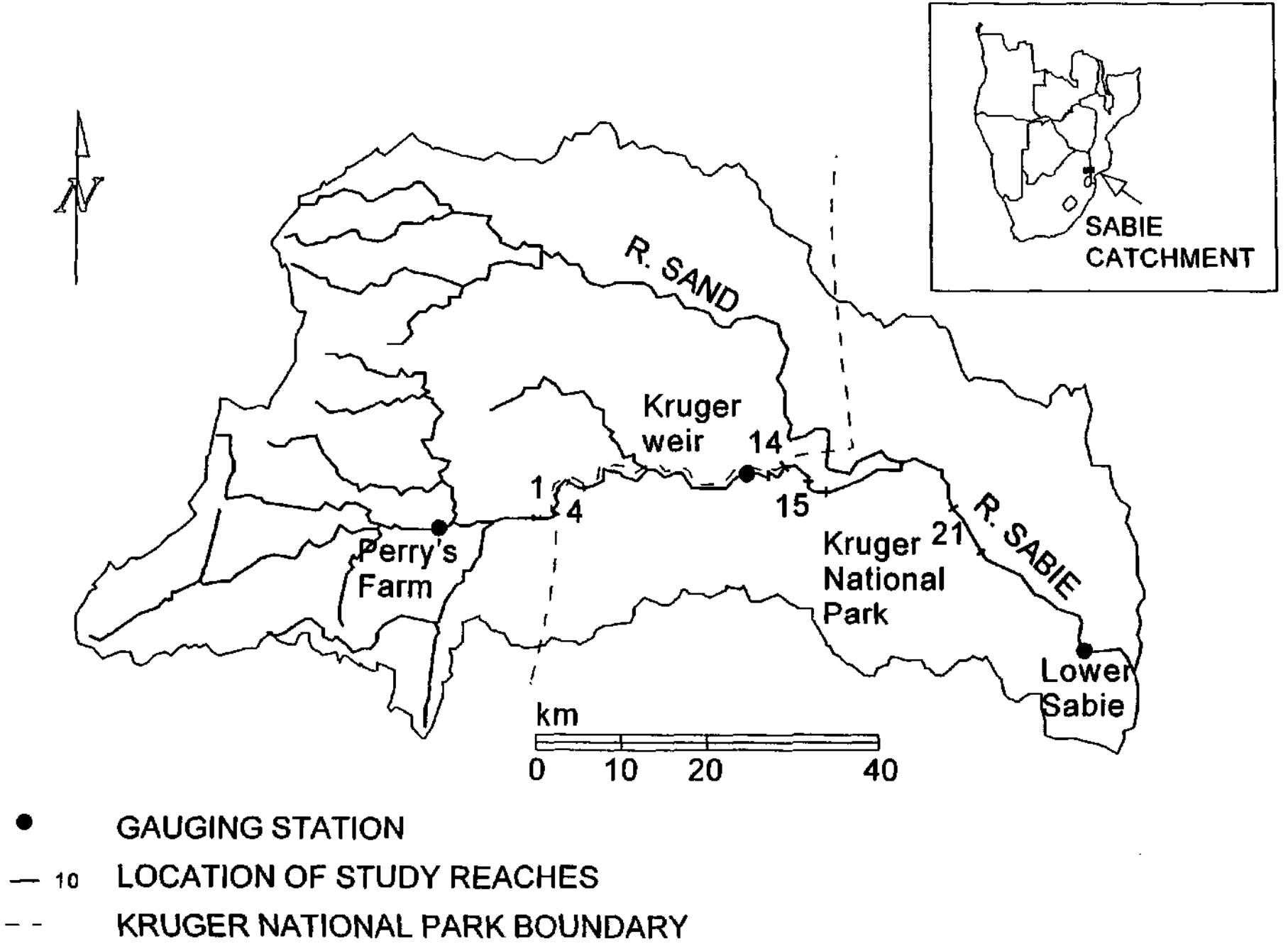


Table 4: Description of morphological units found on the Sabie River (after Moon *et al.* in press).

Morphological Unit	Description
Cataract	Step-like successions of small waterfalls, seldom drowned out at high discharges.
Rapid	Steep bedrock sections, high velocity, concentrated flow.
Waterfall	Abrupt vertical discontinuity in channel slope.
Bedrock pool	Deeper low velocity area upstream of a bedrock control.
Riffle	Accumulation of coarser sediment as a topographic high point as part of a pool-riffle sequence.
Pool	Topographic low point characterised by finer sediments, as part of a pool-riffle sequence.
Braid bar	Accumulation of sediment in mid-channel causing the flow to diverge over a scale that approximates to the channel width.
Lateral bar	Accumulation of sediment attached to the side of the channel, may occur sequentially downstream as alternate bars.
Point bar	Accumulation of sediment on the inside of a meander bend.
Bedrock core bar	Accumulation of finer sediment on top of bedrock in bedrock anastomosing areas.
Lee bar	Accumulation of sediment in the lee of flow obstructions.
Bedrock backwater	Stationary or near stationary bodies of water in bedrock, adjacent to the active channel.
Alluvial backwater	Stationary or near stationary bodies of water in alluvium, adjacent to the active channel.
River cliff	Vertical or near vertical alluvial erosion face.
Apical pool	Deep section of channel located on the outer bend of a meander, associated with point bars.
Rip channel	High flow distributary channel on the inside of point and lateral bars.
Boulder bed	Accumulation of locally derived material exceeding 0.25m.
Alluvial distributary	Individual active channel in an alluvial braided or anastomosing system.
Bedrock distributary	Individual active channel in a bedrock anastomosing system.
Island	Large mid channel sediment accumulation that is rarely inundated.
Terrace	Relic floodplain or valley floor deposits above the present river level.

Table 5: Combinations of channel types found on the Sabie River (after Moon *et al.* in press).

	Anastomosing	Pool-Rapid	Single thread	Braided
Bedrock	*	*	-	-
Mixed	*	*	*	-
Alluvial	-	-	*	*

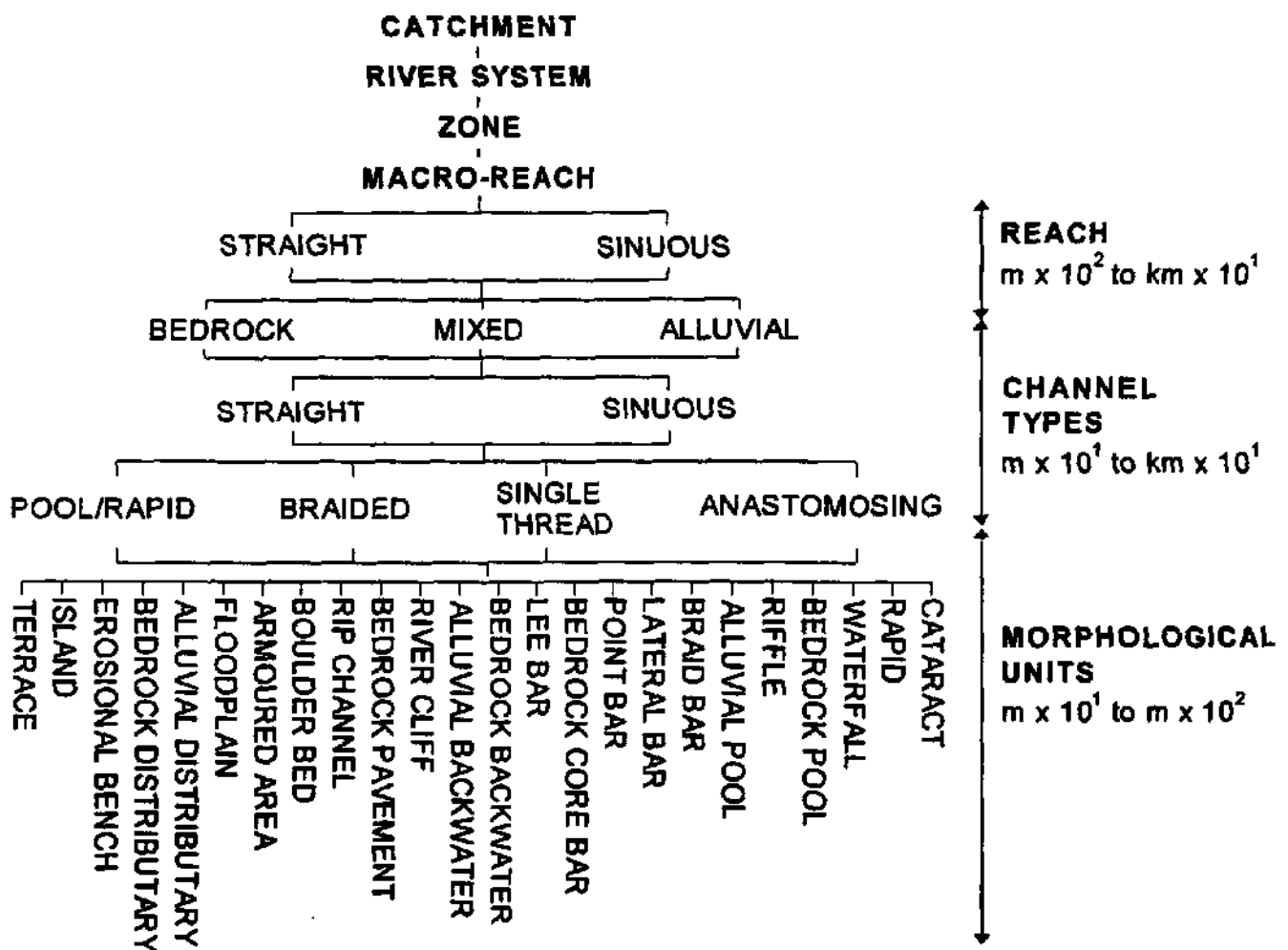


Figure 8: Hierarchical river classification system for the Sabie River, Kruger National Park (after van Niekerk *et al.* 1995).

Table 6: Components of flow resistance found in the different channel types.

Channel type	Principle flow resistance components associated with morphological units identified
Bedrock anastomosing	Skin: NEGLIGIBLE
	Channel form: ACBD, ACR, ACP
	Veg: ACBCB, SBCB, MCBCB, MCB
	Large scale: ACBD, ACR, SBD, SR, SBP
Mixed anastomosing	Skin: ACMD, ACAD, ACSS, SSS, SAD, SMD
	Channel form: ACMD, ACR, ACP
	Veg: ACBCB, SBCB, SAAB, SAD, MCB
	Large scale: ACBD, ACR, SBD, SR, SBP
Pool-Rapid	Skin: ACP, ACBB, ACLB, SLB
	Channel form: ACR, ACP
	Veg: ACBCB, ACLB, SLB, MCLB, MCB
	Large scale: ACR, SR
Braided	Skin: ACAD, ACBB, ACLB
	Channel form: ACAD
	Veg: SLB, SAD, MCLB, MCB
	Large scale: NONE
Single thread	Skin: ACAD
	Channel form: ACAD
	Veg: ACRC, MCLB, MCT
	Large scale: NONE
ACLB = Active channel lateral bar, ACBB = Active channel braid bar, ACRC = Active channel river cliff, ACBCB = Active channel bedrock core bar, ACAD = Active channel alluvial distributary, ACMD = Active channel mixed distributary, ACBD = Active channel bedrock distributary, ACSS = Active channel sand sheet, ACR = Active channel rapid, ACP = Active channel pool, SLB = Seasonal lateral bar, SAAB = Seasonal alluvial anastomosing bar, SAD = Seasonal alluvial distributary, SMD = Seasonal mixed distributary, SBP = Seasonal bedrock pavement, SSS = Seasonal sand sheet, SBCB = Seasonal bedrock core bar, SR = Seasonal rapid, SBD = Seasonal bedrock distributary, MCB = Macro channel bank, MCLB = Macro channel lateral bar, MCT = Macro channel terrace, MCBCB = Macro channel bedrock core bar	

The channel types that have been identified on the Sabie River are described in more detail below, with specific reference to characteristic geomorphology, geology and vegetation cover.

3.3 Channel types

3.3.1 Bedrock anastomosing

Chemical differences in the bedrock have generated resistant areas where the river is less able to erode vertically (Cheshire 1996). The macro-channel is widened to a width of three to four times the average width, for a distance of several kilometres downstream, but is variable as the size of the feature is a function of the local geology. A large number of steep gradient active bedrock channels exist within the macro channel. The longitudinal slope through a representative reach is steep, at 0.0165 (Reach 4 in Figure 9). A typical cross section is given in Figure 10a and an idealised map of the tortuous network of bedrock distributaries found in an actual bedrock anastomosing reach, is given by Figure 11. Each cross section, except the entry cross section (4.1), has multiple distributaries active at low flow, labelled A, B etc. in the schematic distributary diagram. These correspond to the actual distributaries shown in the planform of the bedrock anastomosing reach. The possible flow routes are shown as lines in the schematic diagram, where flow from cross section 4.1 can proceed to any of the distributaries A, B, C, D, E, F, G or H in cross section 4.2.

The planform of these active channels is fixed, being defined by the less resistant pathways in the bedrock (Cheshire 1996). Sediment accumulation is restricted to lee bar deposits downstream of bedrock obstructions, soft sediment in low energy areas and bedrock core bars on areas of elevated outcrops. A riparian tree, *Breonadia salicina* that establishes in bedrock cracks is commonly found in association with this channel type, encouraging sedimentation on the bedrock core bars and along with the commonly found *Diospyros mespiliformis*, creates a dense canopy tree layer (van Collier *et al.* Submitted).

Typical morphological and vegetational characteristics of bedrock anastomosing channel types are shown in Plate 1.

3.3.2 Single thread

Single thread channels have developed in alluvial sections of the Sabie River, where the only limitation to planform is the width of the macro-channel. They are characterised by a single channel flowing between lateral bars and/or terrace features and have a range of sinuities and associated alluvial single thread morphologies. The lateral bars are usually well vegetated, established features with dense spacing of trees, including the large sycamore fig, *Ficus sycomorus* and other open canopy riparian trees (Figure 10b). The long profile through a representative single thread section (Reach 1 in Figure 9), shows the low water surface slopes encountered.

Typical morphological and vegetational characteristics of single thread channel types are shown in Plate 2.

3.3.3 Pool-rapid

The flow in a pool-rapid channel reach is controlled by bedrock outcrops, which are the result of differential erosion potential of the underlying bedrock. The resistance of the bedrock is a function of differences in lithology, in addition to chemical differences that have

helped shape bedrock anastomosing sections. Resistant outcrops create steep gradient rapid units separated by lower energy pool units (Reach 15 in Figure 9). Deposition is favoured in the pools as a result of the low water surface slope, hence low energy, with higher energy rapids generally free of in-channel sediment and with bedrock outcrops protruding into the flow. A cross section through a typical pool and rapid unit is given in Figures 10c and 10d. The active pool-rapid channel(s) typically occupy only a portion of the macro-channel, with sediment derived from rare high magnitude floods covering the remainder of the incised channel. Rapid sections tend to be sparsely vegetated, whereas *Phragmites mauritianus* is common on pool site alluvial braid bars. Often a dense shrub cover, for example *Ziziphus mucronata* and *Dichrostachys cinerea*, is found on the macro-channel banks beneath an open canopy tree layer (van Coller *et al.* Submitted).

Typical morphological and vegetational characteristics of pool-rapid channel types are shown in Plate 3.

3.3.4 Braided

The definition of braided channels followed here is that used by van Niekerk *et al.* (1995): alluvial systems that exhibit channel splitting and rejoining over a distance of a few active channel widths. The degree of braiding in the Sabie River is low and appears to be restricted to the deposition of mid-channel and lateral bars within the active channel (Heritage *et al.* 1995). Lateral bar vegetation communities are dominated by a reed species, *P. mauritianus* (Figure 10e). Van Coller *et al.* characterise the braided vegetation type as being predominantly comprised of open canopy tree species *F. sycomorus* and *Combretum erythrophyllum*, with an understorey shrub layer characterised by *Maytenus senegalensis* and *Lantana camara*. Braided reaches are characterised by low water surface slope (Reach 14 in Figure 9).

Typical morphological and vegetational characteristics of braided channel types are shown in Plate 4.

3.3.5 Mixed anastomosing

Mixed bedrock and alluvial distributary channels divide and rejoin over a distance much greater than the distributary width within an alluvium covered macro-channel in this channel type (Heritage *et al.* 1995). Water surface slopes are fairly steep, characteristically at 0.002 (Reach 21 in Figure 9). Reed (*P. mauritianus*), tree (*B. salicina*) and shrub (*Nuxia oppositifolia*, *Phyllanthus reticulatus*, *Securinega virosa*, *M. senegalensis*) growth on bars can be locally dense (van Coller *et al.* Submitted) (Figure 10f), however, this channel type has a generally sparse vegetation cover, with numerous dead trees, indicating recent drought stress (van Coller pers. com.).

Typical morphological and vegetational characteristics of mixed anastomosing channel types are shown in Plate 5.

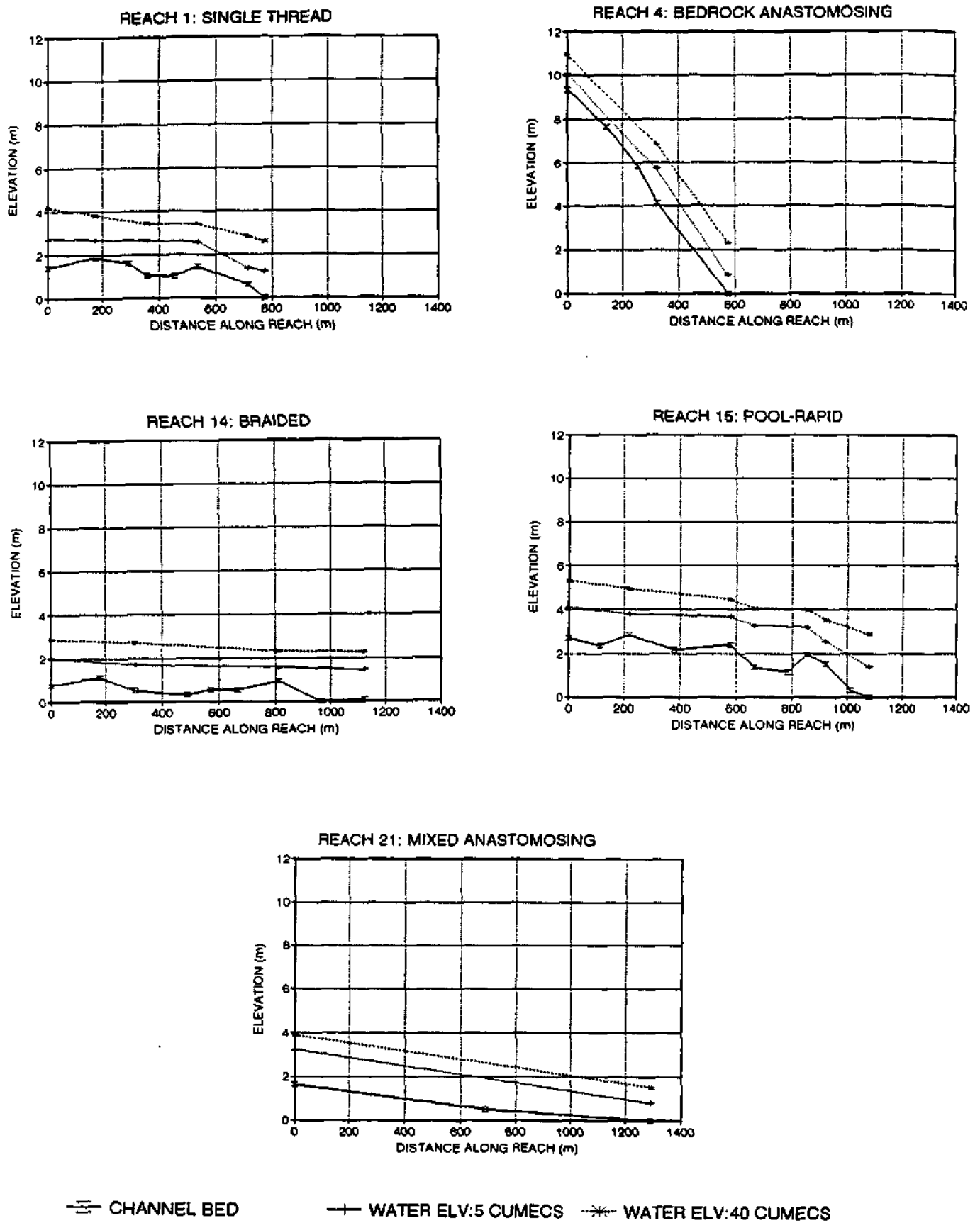


Figure 9: Longsection water surface and bed profiles through the study reaches.

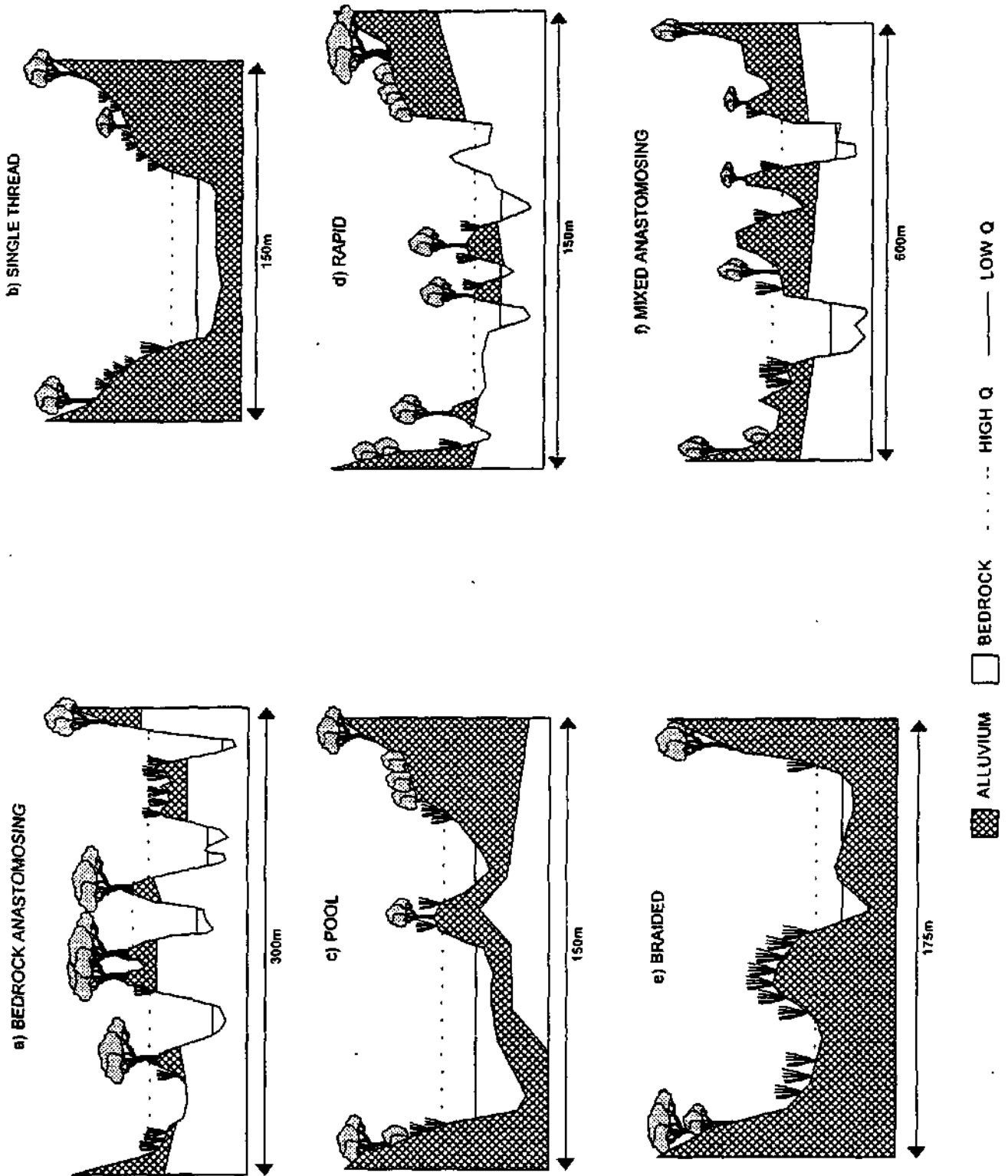


Figure 10: Idealised cross sections through the five channel types and two morphological units found on the Sabie River.

BEDROCK ANASTOMOSING REACH

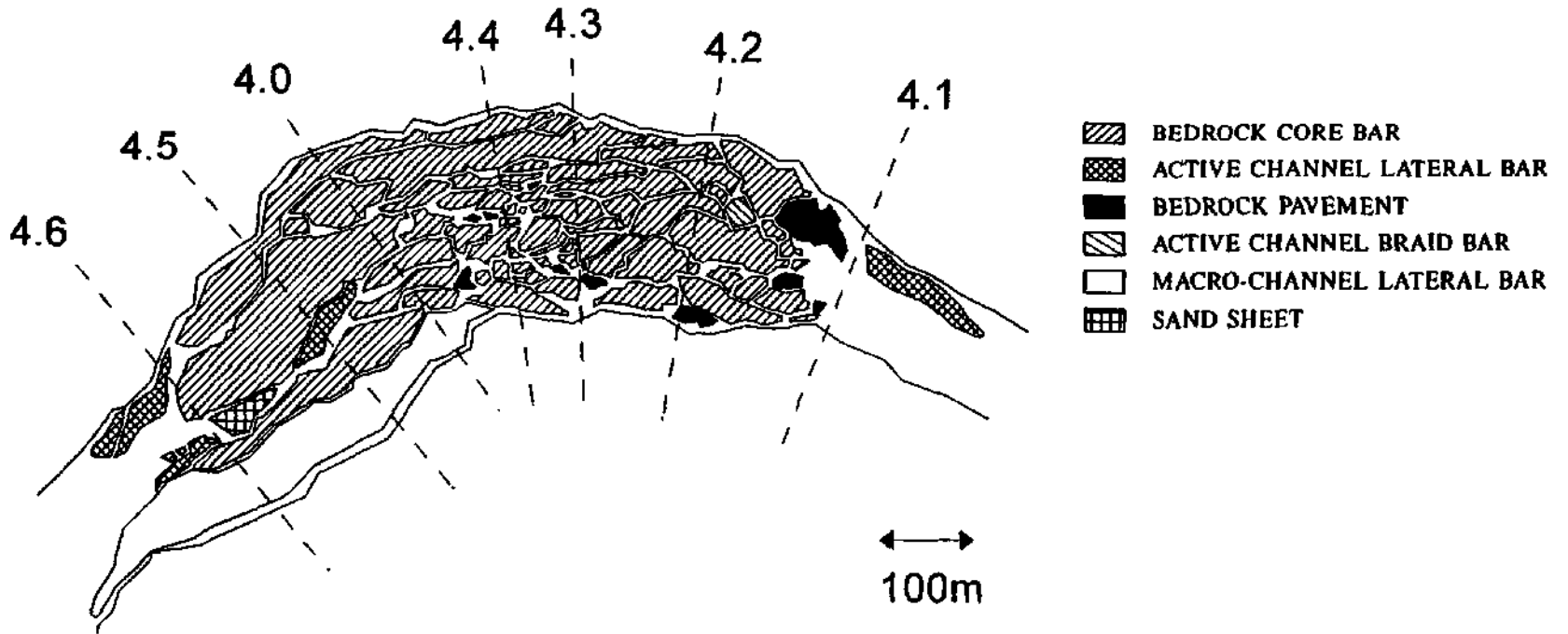
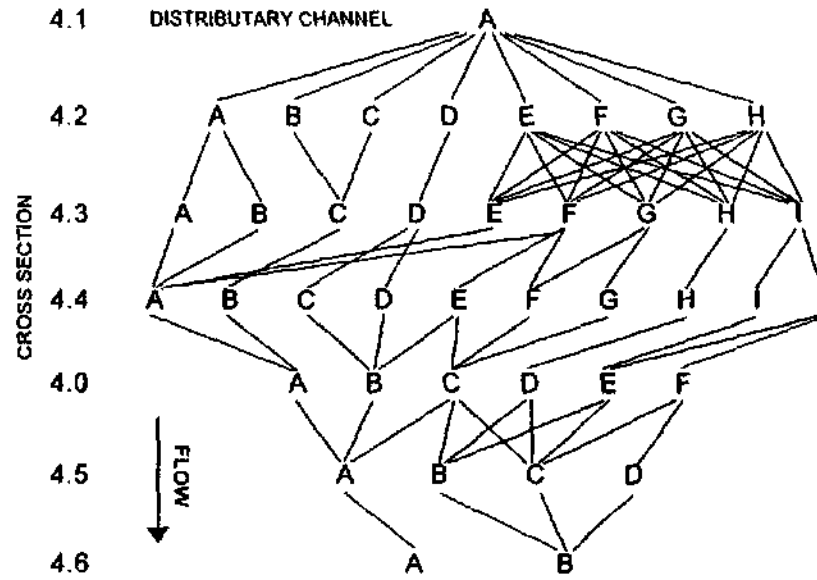


Figure 11: Schematic representation of possible flow paths through the bedrock anastomosing study reach and the corresponding, actual plan form.



Plate 1: Typical morphological and vegetational characteristics of bedrock anastomosing channel types, with High Level Flow Recorder.



Plate 2: Typical morphological and vegetational characteristics of single thread channel types.



Plate 3: Typical morphological and vegetational characteristics of pool-rapid channel types.

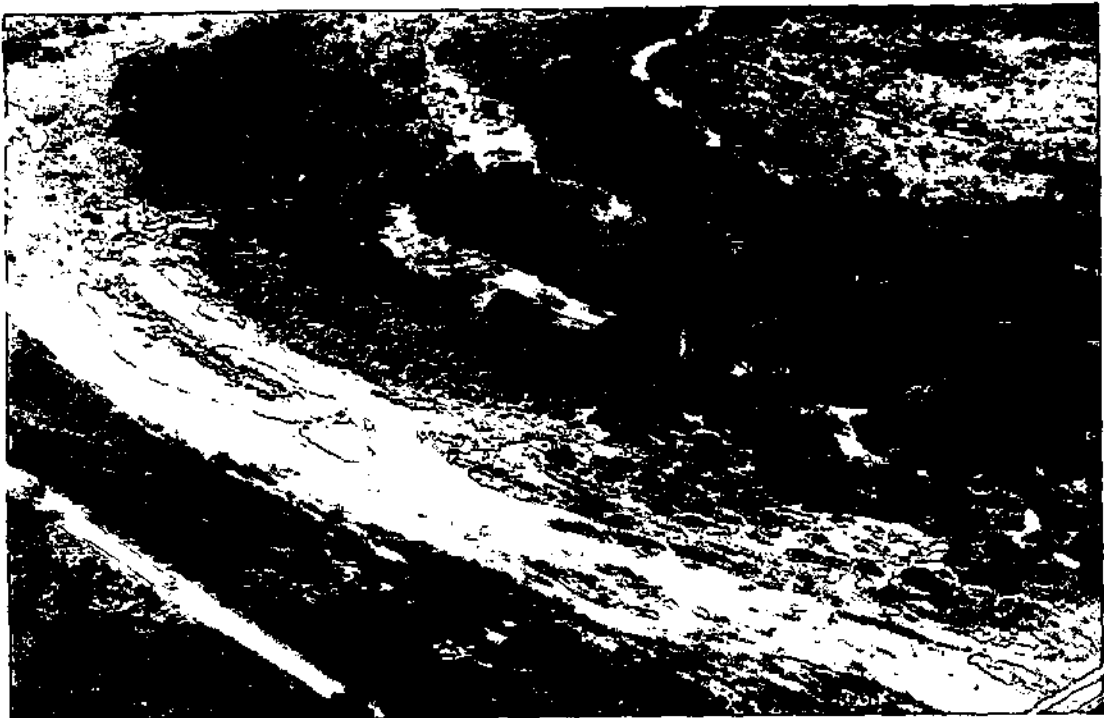


Plate 4: Typical morphological and vegetational characteristics of braided channel types.



Plate 5: Typical morphological and vegetational characteristics of mixed anastomosing channel types.

CHAPTER 4: ASSESSMENT OF CHANNEL FLOW RESISTANCE: APPROPRIATE METHODOLOGIES

The variety of channel type and morphological environments, along with associated vegetation species, described in Chapter 3, creates a complex interaction of different flow resistance components on the Sabie River. In addition, most models to quantitatively isolate individual flow resistance components are not appropriate for use on the Sabie River (Chapter 2). Consequently, it was impossible to quantitatively isolate individual flow resistance components, except at a few specific sites (for example a uniformly reeded lateral bar). Therefore, it was decided to quantify total flow resistance, as given by the Manning, Chezy and Darcy-Weisbach equations (equations 1 to 3).

Following the geomorphological hierarchy outlined above, it is possible to characterise the Sabie River at a variety of relevant physical scales, namely at the channel type, at the morphological unit scale or at a cross section. Therefore, several cross sections, comprising a reach (channel type) or sub-reach (morphological unit) must be analyzed. Several methods are commonly used to estimate total flow resistance and these are listed below.

4.1 Visual comparison method

A standard reference for estimating flow resistance coefficients by the "visual comparison" approach is that by Ven te Chow (1959) and Barnes (1967). Each author presented photographs of typical channels and their corresponding flow resistance values. Barnes (1967) featured a larger variety of natural channels than Ven te Chow (1959), but rarely presented more than a single flow resistance value per section. Thus, the change in flow resistance with increasing discharge is not accounted for.

Although mountain stream environments, with steep water surface slopes and a large bed material size, are included in the illustrations, multi-distributary bedrock sections, such as those found in bedrock or mixed anastomosing channel types on the Sabie River are not represented. Therefore, only the alluvial channels on the Sabie River are covered in the "visual comparison" literature and then only for low discharges.

4.2 Reach flow resistance quantification

A value of the friction slope, S_f , to be used in total resistance equations, Manning's n , Chezy C or Darcy-Weisbach f (equations 1 to 3) is only available between sections, as it is defined by:

$$S_f = \frac{h_f}{L} = \frac{\Delta h + \Delta h_v - k(\Delta h_v)}{L} \quad (42)$$

where h_f is the friction head loss, L is reach length, Δh is the change in elevation of the water surface between the upstream and downstream cross sections, Δh_v is the change in velocity head between the upstream and downstream cross sections and $k(\Delta h_v)$ approximates

the energy loss due to acceleration or deceleration in a contracting or expanding reach (Figure 12). Following convention, k is assumed to equal zero for contracting reaches and 0.5 for expanding reaches (ven te Chow 1959). The velocity head, h_v , at a cross section is equal to $\alpha V^2/2g$, where α is the velocity head coefficient, which indicates the uniformity of velocity across the section.

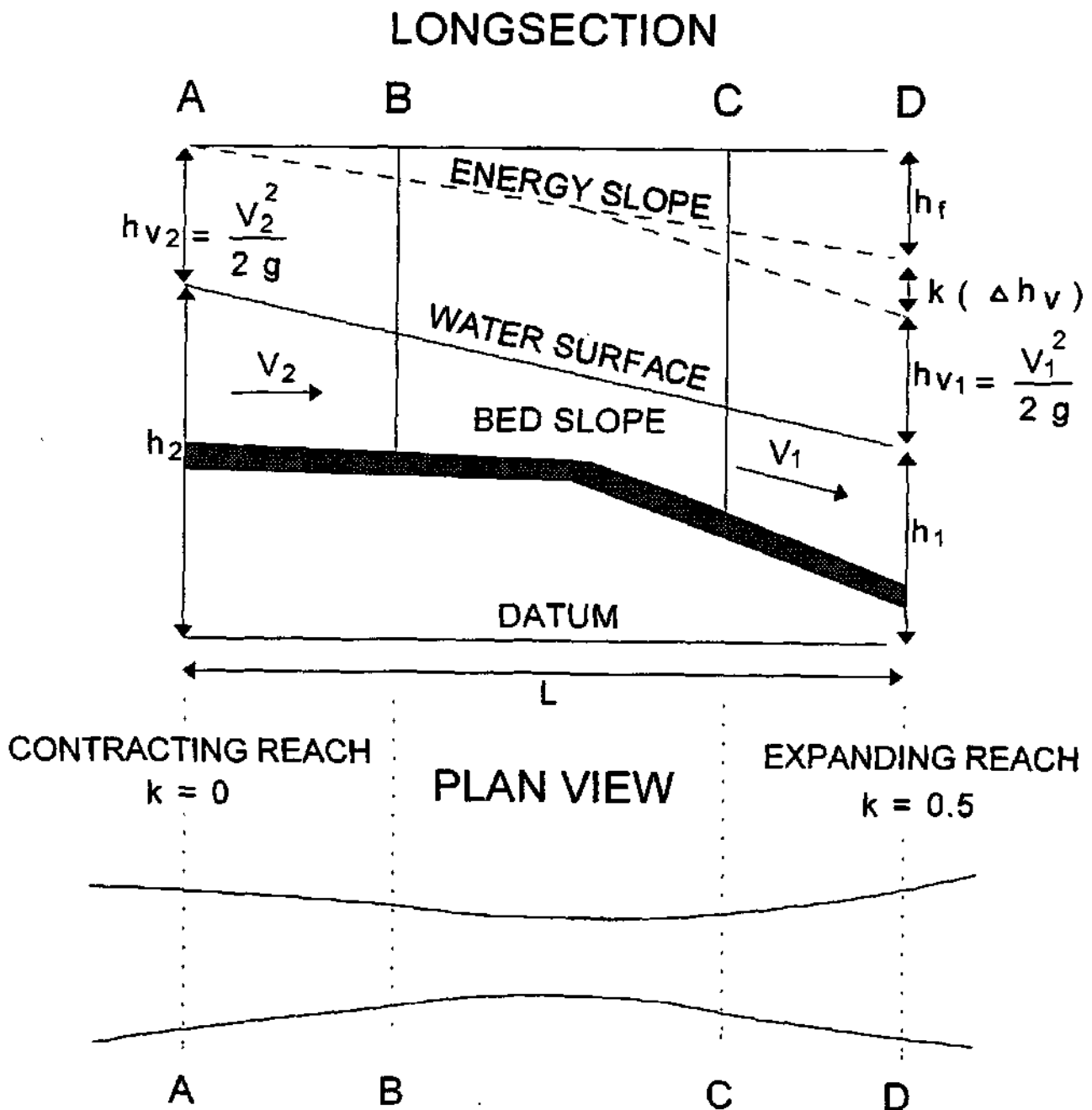


Figure 12: Definition of channel geometry and hydraulic parameters for use in calculating flow resistance in a multi-section reach (modified after Barnes 1967).

As no detailed knowledge of the change in velocity across the sections under investigation is known, it has been assumed for the purpose of this study that α equals 1. This follows a precedent set by ven te Chow 1959 and followed by others calculating flow resistance coefficients (Barnes 1967, Jarrett 1984, Hicks and Mason 1991). However, several studies have shown that values for α can far exceed unity, with values of greater than two attributed to expanding sections displaying flow separation (Streeter 1942), which is a phenomenon commonly found on the Sabie River.

A representative value of flow resistance for a multiple section reach at a given discharge can be obtained by equating the friction head loss calculated from the friction slope (equations 1 to 3) with the friction head loss given by equation 42. This uses the method adopted by Barnes (1967) and followed by Jarrett (1984) and Hicks and Mason (1991), (Figure 12). Therefore,

$$h_f = h_{f_{1,2}} + h_{f_{2,3}} + \dots h_{f_{(m-1),m}} \quad (43)$$

and from the Manning's equation (equation 2) and the continuity equation $Q=AV$:

$$h_f = n^2 Q^2 \left(\frac{L_{1,2}}{Z_1 Z_2} + \frac{L_{2,3}}{Z_2 Z_3} + \dots \frac{L_{(m-1),m}}{Z_{(m-1),m} Z_m} \right) \quad (44)$$

where m is the number of cross sections (with the m th cross section being furthest upstream), $m-1.m$ represents the difference in value of the parameter in question between cross section $m-1$ and cross section m , $Z = AR^{2/3}$, and a representative value of Z , following the convention given by Barnes (1967) for the reach between two adjacent cross sections is given by the average $(Z_1 Z_2)^{1/2}$.

From equation 42 and 43:

$$h_f = (h_m - h_1) + (h_{v_m} - h_{v_1}) - (k_{1,2} \Delta h_{v_{1,2}} + k_{2,3} \Delta h_{v_{2,3}} + \dots k_{(m-1),m} \Delta h_{v_{(m-1),m}}) \quad (45)$$

and therefore, from equation 44:

$$n = \frac{1}{Q} \left(\frac{(h_m - h_1) + (h_{v_m} - h_{v_1}) - (k_{1,2} \Delta h_{v_{1,2}} + k_{2,3} \Delta h_{v_{2,3}} + \dots k_{(m-1),m} \Delta h_{v_{(m-1),m}})}{\frac{L_{1,2}}{Z_1 Z_2} + \frac{L_{2,3}}{Z_2 Z_3} + \dots \frac{L_{(m-1),m}}{Z_{(m-1),m} Z_m}} \right)^{\frac{1}{2}} \quad (46)$$

In a similar fashion, Hicks and Mason (1991) derived a representative value of Chezy C from:

$$C = Q \left(\frac{\frac{L_{1,2}}{X_1 X_2} + \frac{L_{2,3}}{X_2 X_3} + \dots + \frac{L_{(m-1),m}}{X_{(m-1)} X_m}}{(h_m - h_1) + (h_{v_m} - h_{v_1}) - (k_{1,2} \Delta h_{v_{1,2}} + k_{2,3} \Delta h_{v_{2,3}} + \dots + k_{(m-1),m} \Delta h_{v_{(m-1),m}})} \right)^{\frac{1}{2}} \quad (47)$$

where $X = AR^{1/2}$

An equivalent expression for Darcy-Weisbach friction factor has been derived for use in this study:

$$f = \frac{8g}{Q^2} \left(\frac{(h_m - h_1) + (h_{v_m} - h_{v_1}) - (k_{1,2} \Delta h_{v_{1,2}} + k_{2,3} \Delta h_{v_{2,3}} + \dots + k_{(m-1),m} \Delta h_{v_{(m-1),m}})}{\frac{L_{1,2}}{(Y_1 Y_2)^2} + \frac{L_{2,3}}{(Y_2 Y_3)^2} + \dots + \frac{L_{(m-1),m}}{(Y_{(m-1)} Y_m)^2}} \right) \quad (48)$$

where $Y = A^2 R$

Using equations 46, 47 and 48, total flow resistance coefficients can be quantified over a variety of scales, from a two section 'sub-reach', which could encompass a morphological unit, to a numerous section channel type 'reach' (Figure 24).

Therefore, although the quantitative isolation of individual components of flow resistance is precluded by the complex interaction of these components in the highly variable riverine environments on the Sabie River, total flow resistance can be quantified at a variety of reach scales by using the Barnes (1967) methodology. Thus, channel type or morphological unit scale flow resistance can be estimated.

CHAPTER 5: IDENTIFYING THE VARIETY OF FLOW RESISTANCE COMPONENTS ENCOUNTERED ON THE SABIE RIVER AND HYDRAULIC MONITORING

The geomorphological hierarchy (van Niekerk *et al.* 1995) generates five principal channel types, each of which are composed of specific morphological units, with associated flow resistance components (Table 6). Representative reaches that cover all the channel types, were selected and flow resistance components identified to correlate with measured resistance (Section 5.2).

5.1 Criteria for reach selection

Five representative reaches of the Sabie River were chosen to represent the variety of channel types found on the Sabie River within the Kruger National Park boundaries. The channel types covered were: bedrock anastomosing (Reach 4), braided (Reach 14), single thread (Reach 1), pool-rapid (Reach 15) and mixed anastomosing (Reach 21). The locations for these reaches are shown on Figure 7 and Figures 13 to 17. Detailed location descriptions are given in Appendix 1.



Figure 13: Plan view of reach 1, a single thread channel type, showing cross section locations. Sections upstream of 1.0 are not represented in the aerial photographic record. The flow direction is from right to left.



Figure 14: Plan view of reach 4, a bedrock anastomosing channel type, showing cross section locations. Flow direction is from top to bottom.



Figure 15: Plan view of reach 14, a braided channel type, showing cross section locations. Flow direction is from top to bottom.

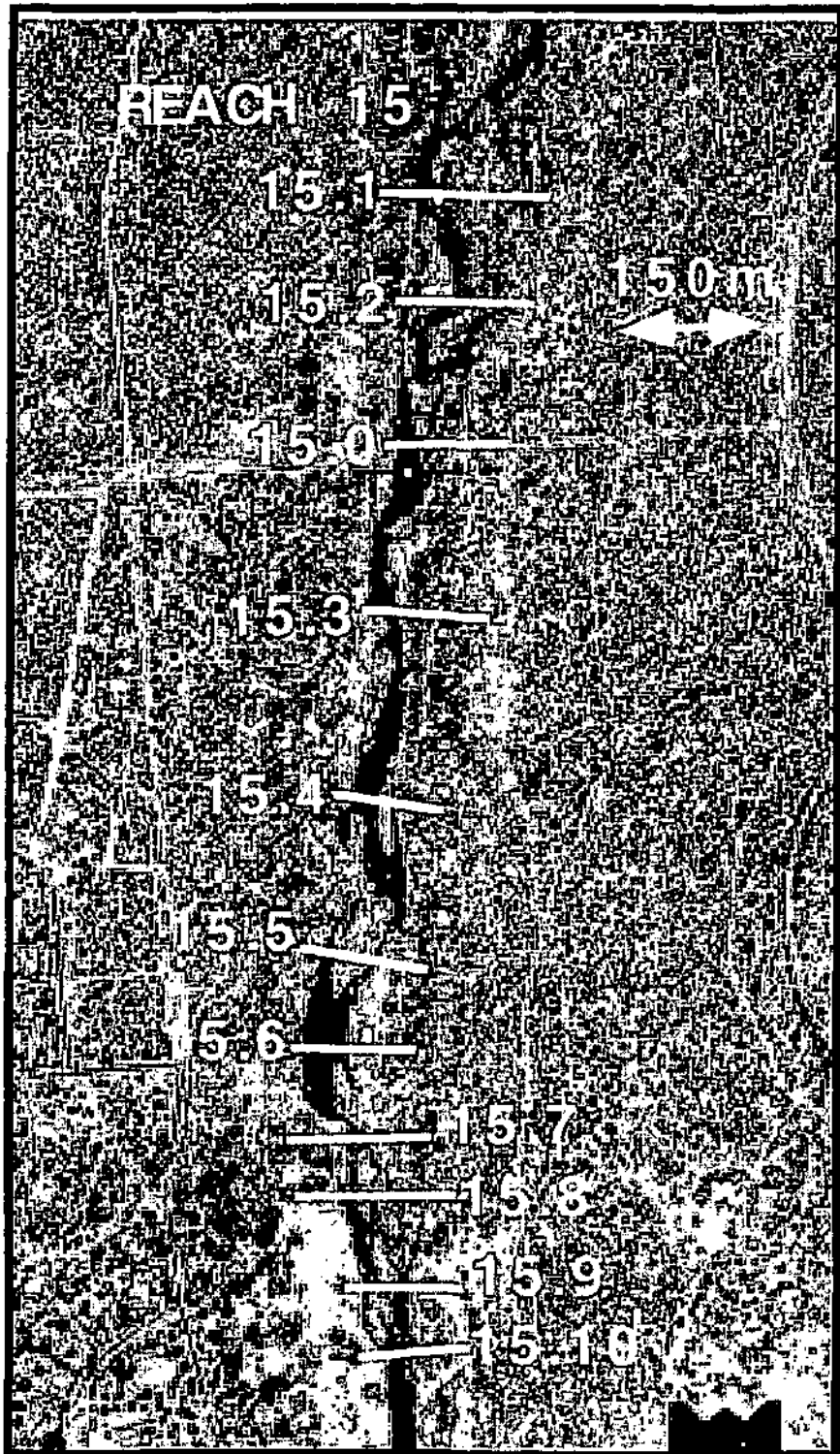


Figure 16: Plan view of reach 15, a pool-rapid channel type, showing cross section locations. Flow direction is from top to bottom.

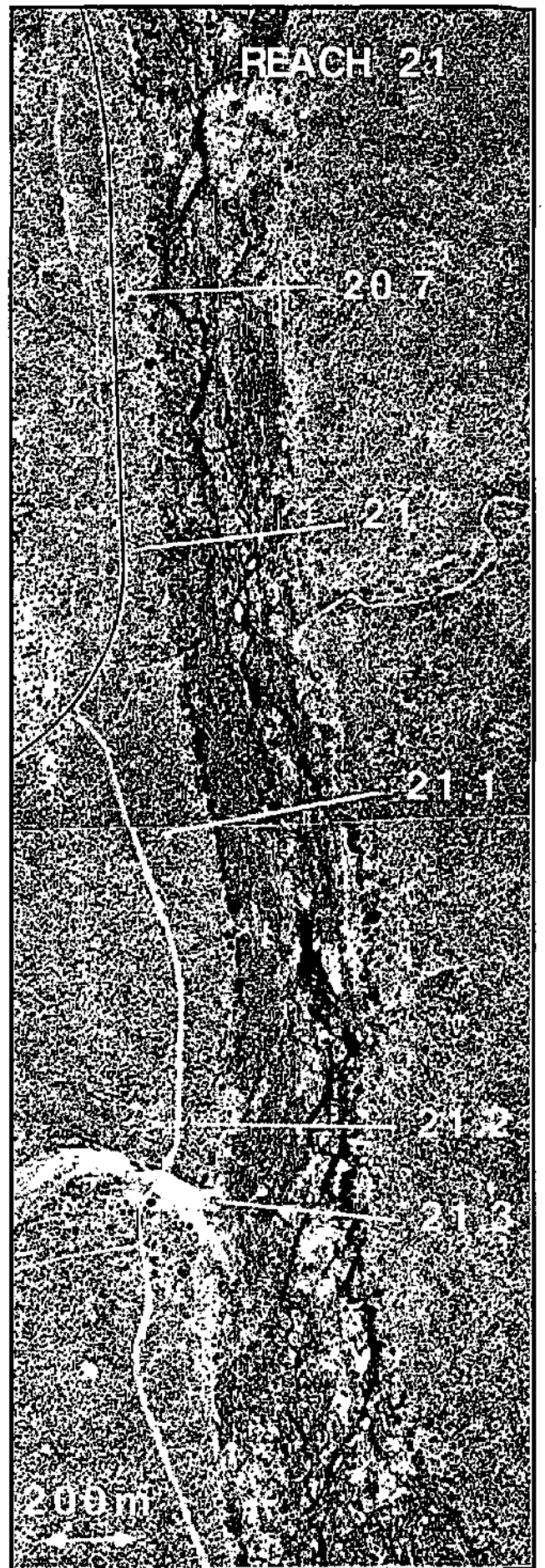
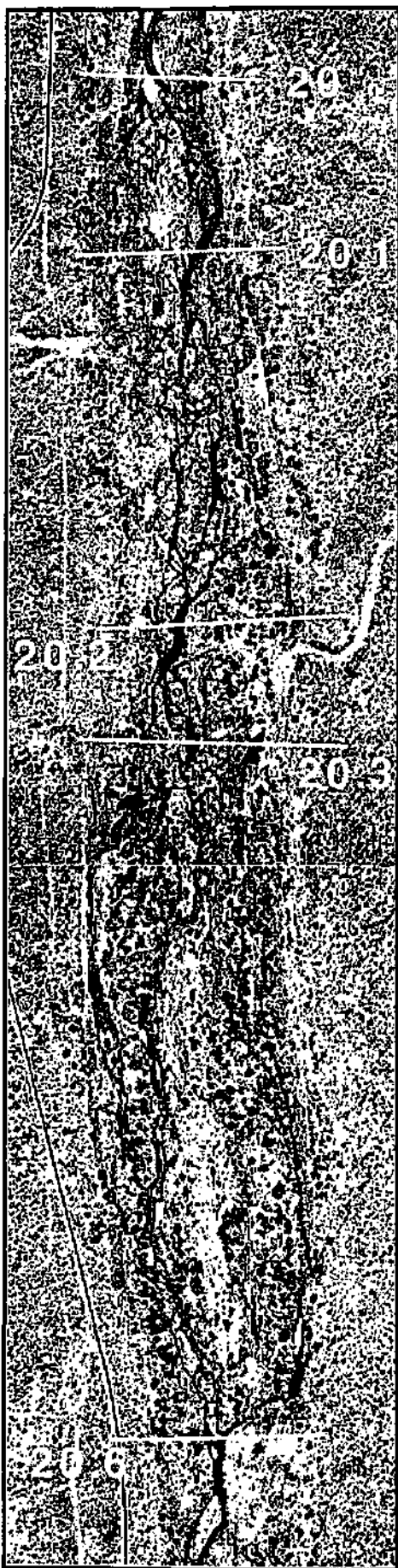


Figure 17: Plan view of reach 21, a mixed anastomosing channel type, showing cross section locations. Flow direction is from top to bottom.

5.2 Identifying flow resistance components within the study reach

To identify all the flow resistance components at each channel type and to correlate their occurrence to observed local hydraulic conditions, eight to ten cross sections per channel type were surveyed and flow resistance components were mapped. The longitudinal spacing of the cross sections was designed to incorporate the presence of low flow hydraulic 'controls' that cause energy loss, and thus to define accurately water surface slope along a reach. These 'controls' included bedrock outcrops, major alluvial bars or tributary confluences and major channel features, such as mid channel braid bars, meander apexes or changes in the vegetation community. In addition to the cross sectional shape survey, vegetational, sedimentological and morphological data, described below, were collected for each cross section.

Vegetational resistance to flow is dependent upon the physical character of the flora (the density, height, stem or trunk diameter and flexibility of the grass, shrub or tree (Kouwen and Unny 1973)) and whether the plant is submerged or emergent relative to the water surface (El-Hakim and Salama 1992). The vegetation communities found on the Sabie River vary between channel types (van Coller *et al.* 1995). These communities comprise differing assemblages of species, with differing flow resistance characteristics. The physical and hydraulic characteristics of the vegetation, as defined in Section 2.2.4, were recorded for the groundcover, understorey or shrub layer and the tree canopy across a cross section.

The skin resistance to flow is derived from bed material characteristics. These include: presence and size of boulders, sediment size and size distribution, particle shape, packing configuration and orientation; although the latter 3 effects are small for natural channels (Bathurst 1985a) and negligible in sand bed channels, so were ignored in this study. For every morphological unit or other change in sediment grade, a sediment sample was taken. This allowed determination of the bulk by weight size distribution by sieving. Plots of grain size frequency enabled determination of the grain size percentiles. The presence of boulders or bedrock, which are common in several morphological environments found in the Sabie River, complicates the flow resistance computation, by introducing large scale roughness. Areas of bedrock outcrops and individual boulders were accurately surveyed, to define cross sectional area and mean depth, as well as to consider their effect on boundary resistance. Cross section survey, vegetational, sedimentological and morphological data are presented in Appendix 2.

Hydraulic monitoring within representative reaches was required to facilitate quantification of flow resistance using the Barnes (1967) model (Chapter 4). This involved measurement of local stage over a range of discharges.

5.3 Measurement of local stage

Flow stage for a range of low and medium discharges was recorded at several hydraulically relevant points along each study reach, so as to define the water surface slope along the reach. Water surface slopes for a low and medium flow level and bed profiles, derived from 'thalweg' bed elevation, for the five study reaches are given in Figure 9.

Low flow levels were surveyed directly, whereas high flows were recorded using a system of graduated poles known as High Level Flow Recorders (HLFR). These were covered in water soluble paint and were stepped up the macro channel bank to cover a range of elevated flows. The paint washoff line corresponded to the level of the highest flood stage since resetting the paint and could be correlated to local debris strand lines. This indirectly recorded stage was related to the peak discharge recorded by the nearest gauging structure: Kruger Weir (reaches 1, 4, 14 and 15) or Lower Sabie Weir (reach 21) (Figure 7). It was assumed that the discharge recorded at these weirs was applicable to the study sites, as no major tributaries contribute to the Sabie between the weirs and reaches in question during low and intermediate flows. However, it is realised that attenuation, resulting from potential losses to groundwater are not accounted for, although in bedrock areas this will not be a problem. Instantaneous stage measurement was linked to discharge by lagging the flow record by a flood travel time, T_x , that corresponded to the proportion of the distance of the stage sample site from the total distance between the two weirs used (Figure 18), as equation 49 calculates:

$$T_x = T_1 + \left[(T_2 - T_1) \times \frac{(W_1 - S_1)}{(W_1 - W_2)} \right] \quad (49)$$

where T_1 and T_2 are the times at which the flood peak passes weirs 1 and 2 respectively, W_1 and W_2 are the chainages of weirs 1 and 2 respectively and S_1 is the chainage of the study site.

Therefore, stage-discharge relationships for each monitored site were generated using both directly and indirectly measured stage and the corresponding weir derived discharge.

Flow levels for one flood event, estimated at $650 \text{ m}^3\text{s}^{-1}$ (Kruger Weir) and $1000 \text{ m}^3\text{s}^{-1}$ (Lower Sabie Weir), were recorded at several sites within and adjacent to the channel flow resistance investigation reaches, prior to the initiation of this study. These recorded high flow levels were used to extend the rating curves for three of the five study reaches, to increase the range of flows to be used to estimate flow resistance.

5.4 Discharge gauging

In order to ascertain the proportion of total cross sectional discharge flowing in individual distributary channels at multi-channel bedrock sections, a low flow was gauged using a VALEPORT VEM003 electro-magnetic (EM) current meter, at three bedrock anastomosing cross sections. Here, an electromotive force, proportional to velocity is induced when the flow traverses the EM meter head. The EM meter head was mounted on a graduated staff, with a clamping mechanism to position the head at a known distance from the channel bed. A display unit converts current from the EM head directly into velocity. The velocity-area technique described in any standard fluvial hydraulics text (for example, Richards 1982), was employed to calculate discharge. Velocity and depth, d , were measured at equally spaced verticals across the section, approximately every 0.5m (Figure 19) and the contributing discharge, q_i of each segment was calculated (equation 50). Where the flow depth was greater than 0.15m, multiple point velocities were recorded at each vertical, as the flow was often

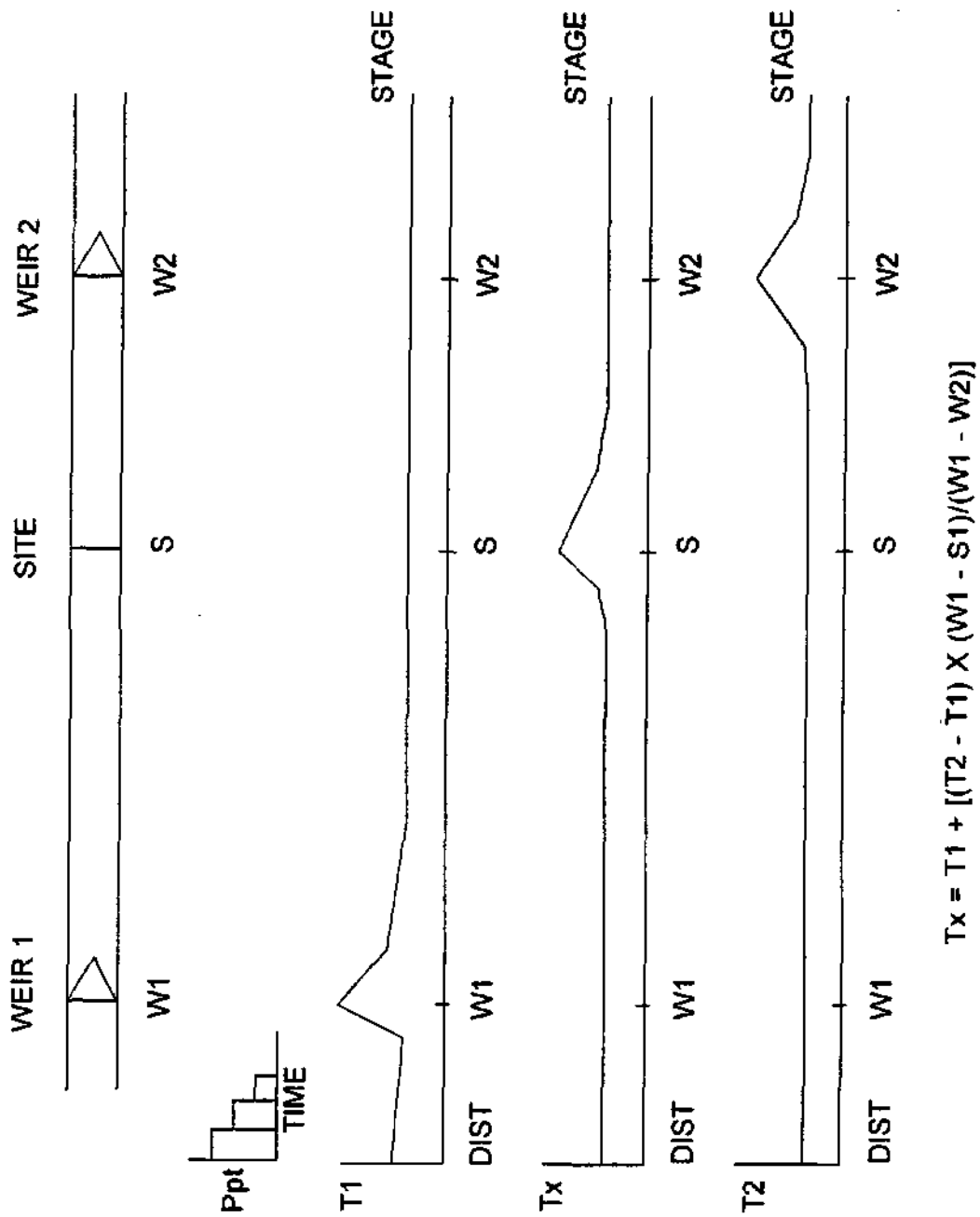


Figure 18: Calculation of stage at a study site, between two gauging weirs, during a flood event.

highly turbulent and non-uniform and a single velocity reading would not have been representative for the whole sub-section as velocity profiles were highly irregular (Figure 20). In verticals of depth greater than 0.15m, readings were taken every 0.1m from the bed, to the water surface.

The subarea discharge, associated with a specific velocity measurement, can be calculated from:

$$q_i = v_i \left[w_i \left(\frac{d_{i+1} + d_i}{2} - \frac{d_i + d_{i-1}}{2} \right) \right] \quad (50)$$

and the total cross section discharge is then given by

$$Q = \sum q_i \quad (51)$$

where q_i , w_i and v_i are the discharge, width and velocity of a subarea respectively and Q is the total cross section discharge.

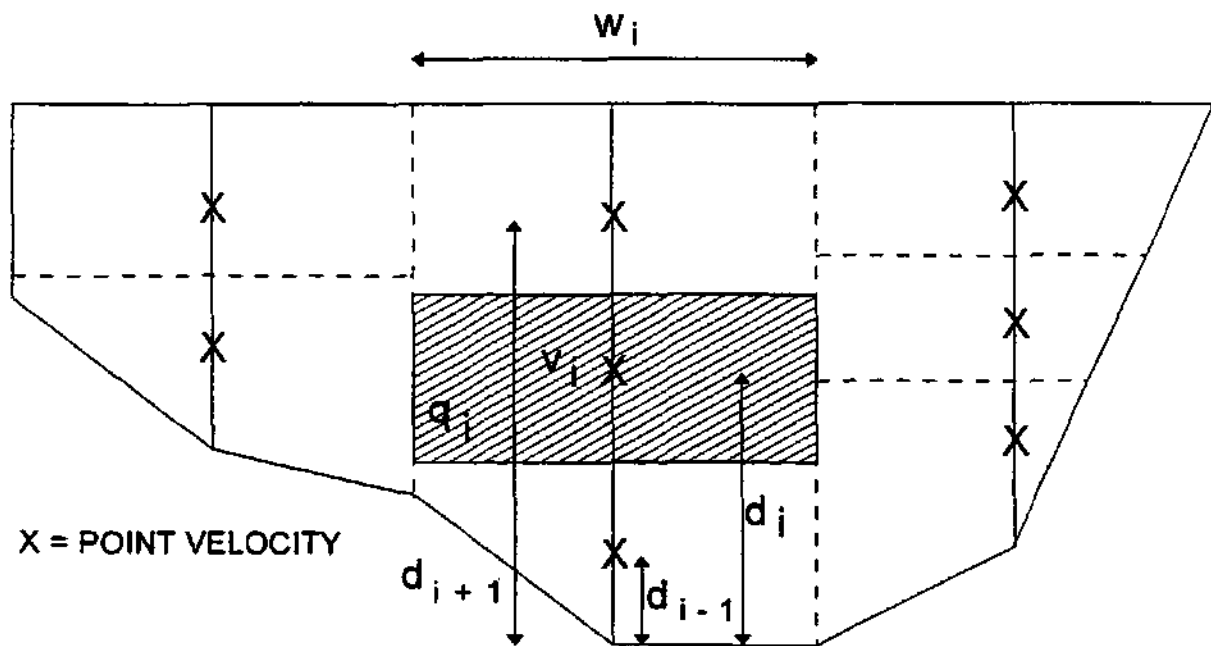


Figure 19: Conventional velocity-area method for calculation of subarea discharge.

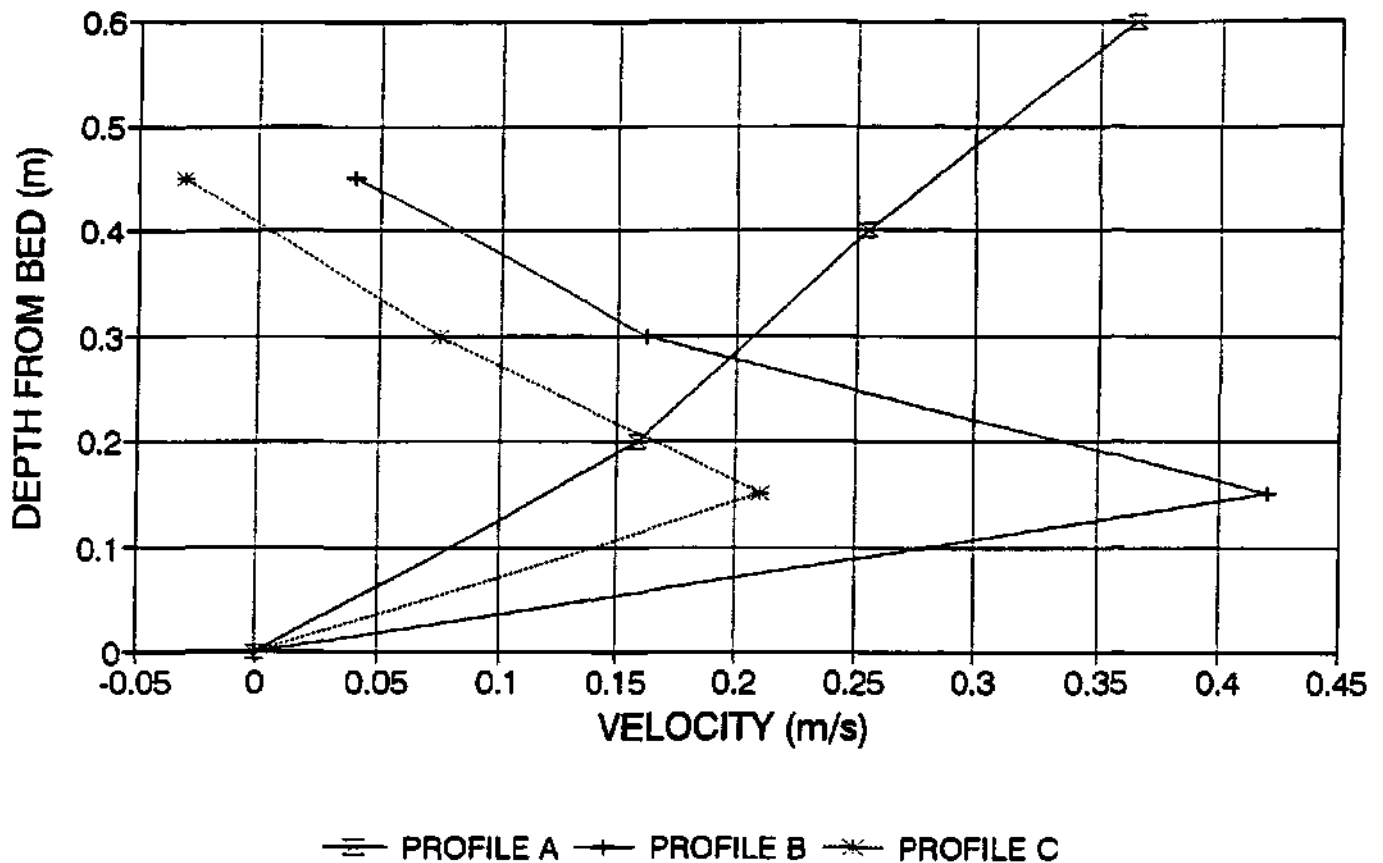


Figure 20: Typical velocity profiles in a bedrock distributary.

The discharge was also calculated from the volume under a three dimensional plot of isovels at a cross section (Figure 21). The computer package SURFER was used to calculate this volume, after using Kriging interpolation techniques to transform the measured velocity grid to isovels at a cross section. Coordinates denoting the cross section bed and banks formed the boundary. This analysis uses curvilinear interpolation techniques, as opposed to the mid-point velocity area method.

Calculation of the discharge was complicated by the fact that several subsections of cross sections displayed reverse flows or negative discharge. The definition of 'effective' discharge used in this case was the downstream, positive discharge minus the upstream, reverse discharge. This recognises that negative and positive areas provide opposing discharge values and it follows the procedure adopted by Bathurst *et al.* (1979) and others.

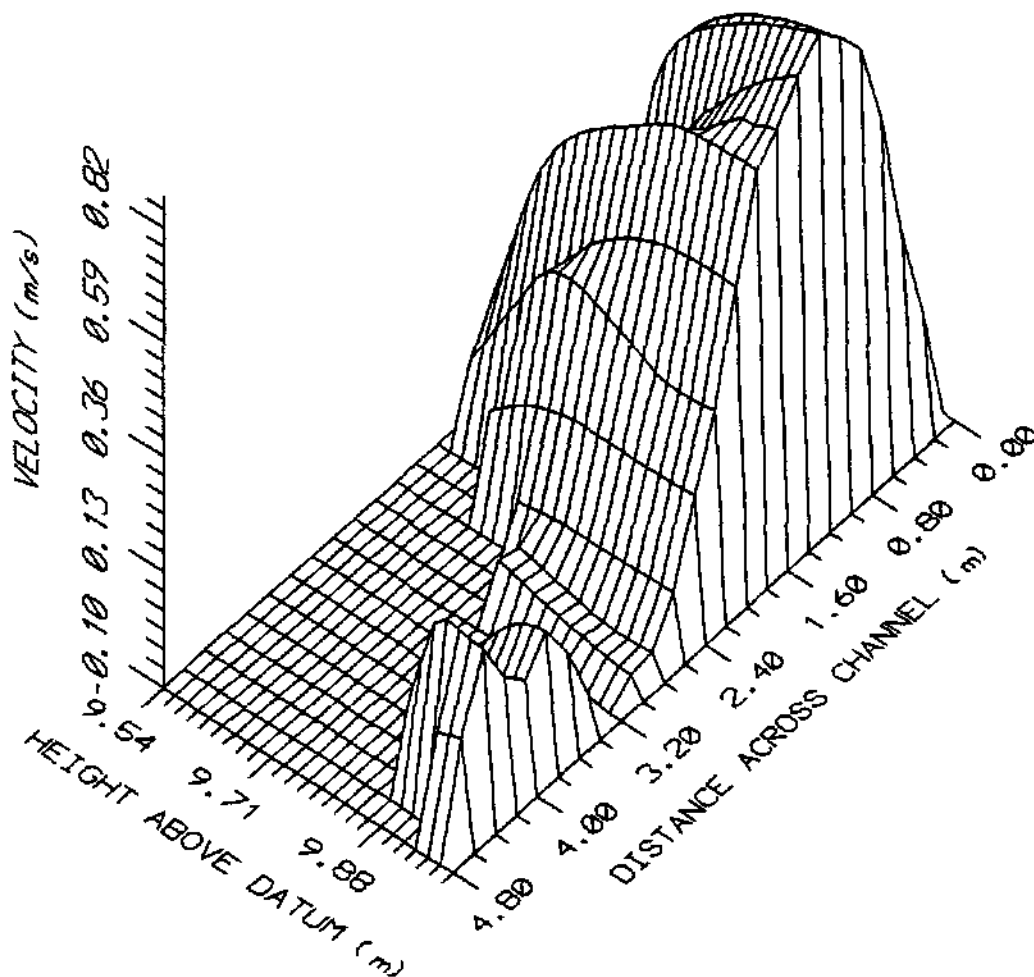


Figure 21: Three-dimensional representation of velocity isovels at a cross section, produced from SURFER software.

Comparison between the distributary channel discharge estimates from the velocity-area and SURFER analysis methods showed a systematic overestimation of discharge by the velocity-area method, when compared to the SURFER analysis (Figure 22). The gauged discharge in each active distributary at a cross section was summed to give the total discharge at each of the three cross sections gauged. These total cross sectional discharge estimates, from both the velocity-area and SURFER analyses, for the gauged distributaries were compared to actual, weir derived values (Figure 23). The velocity-area method overestimates actual, weir discharge by up to 174%, whereas the SURFER discharge analysis method estimates discharge to between 88% and 108% of actual, weir discharge. The construction of curvilinear isovels by the SURFER software was considered to be physically realistic, as opposed to the 'mid-point' subarea method (Figures 22 and 23), so was used in this study.

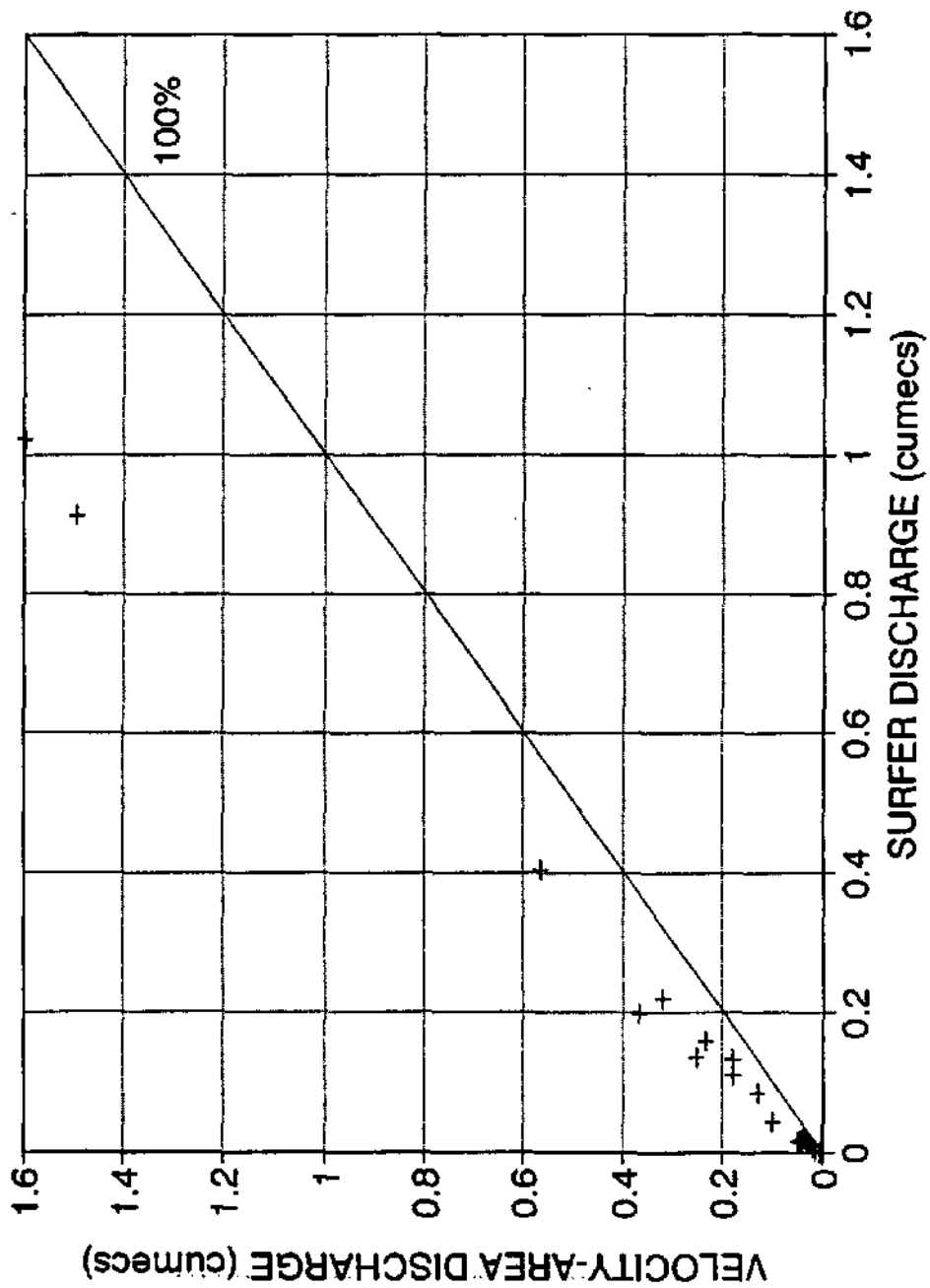


Figure 22: Difference between SURFER and velocity-area analyzed gauging data.

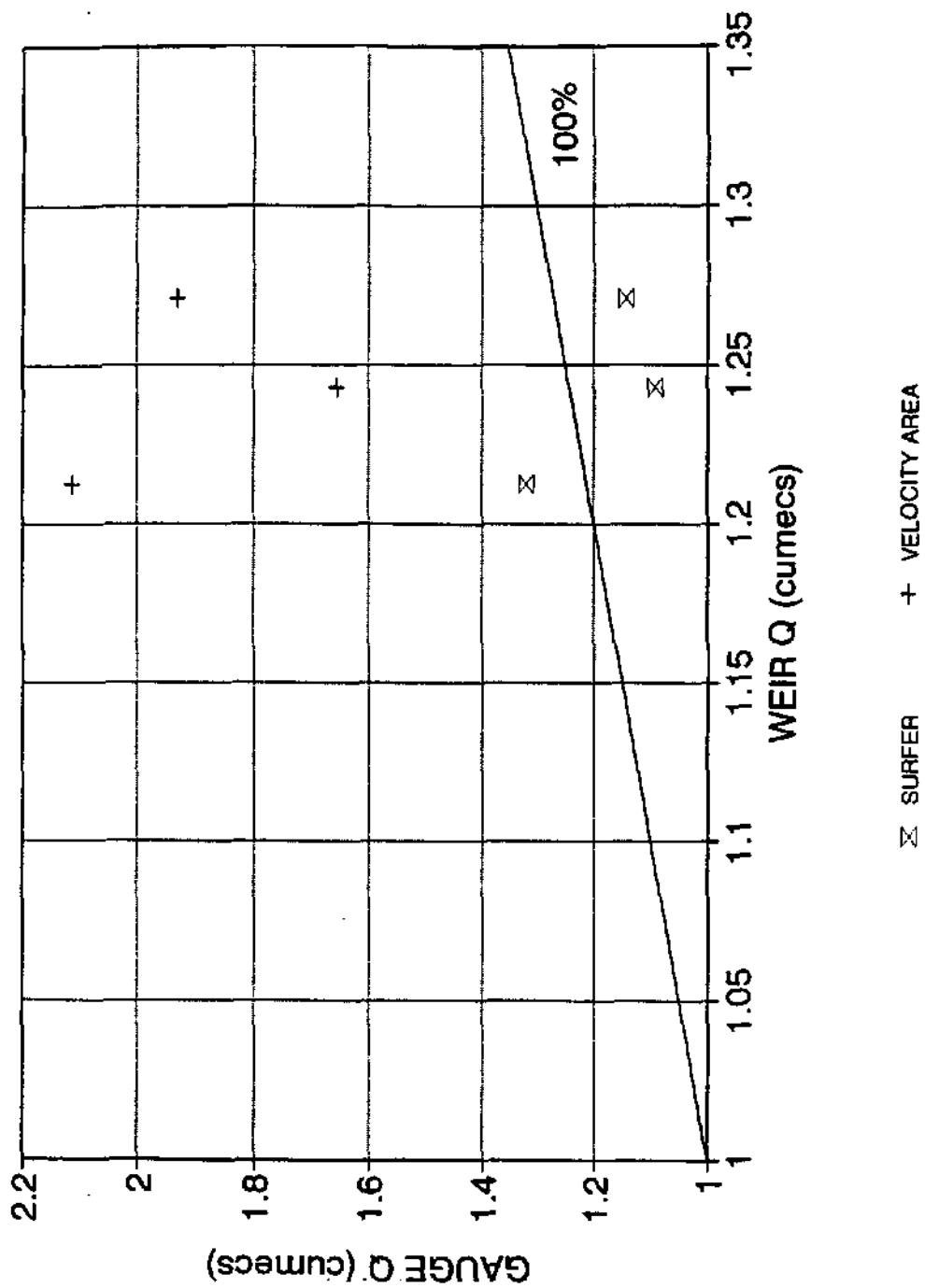


Figure 23: Error between weir discharge and that obtained from SURFER and velocity-area analyzed gauging data at three cross sections.

CHAPTER 6: CONCEPTUAL MODELLING

6.1 Physical Scales of analysis

The number of cross sections surveyed per reach and hydraulic data collection stations enables flow resistance to be quantified over a range of physical spatial scales. The variety of scales for flow resistance analysis for two of the channel types studied is shown in Figure 24. The bedrock anastomosing channel type allows flow resistance calculation over a whole channel type reach, consisting of several cross sections; at a multiple distributary cross section (A to B); or for an individual bedrock distributary (Z). The pool-rapid channel type can also be analyzed as a whole reach, as a morphological unit sub-reach (Q to R), or at a cross section (Y to Z). The Barnes (1967) methodology (equations 46 to 48) averages flow resistance for a multi-cross section reach and was used to quantify flow resistance for the reach and sub-reach scales described above. Total flow resistance at a cross section or at an individual distributary was calculated from equations 1 to 3, with local water surface slope used to approximate friction slope.

6.2 Approaches to modelling channel geometry in alluvial and bedrock multi-channel cross sections

All of the channel types studied, with the exception of the single thread channel, had multiple channels active at low or medium flows. In alluvial sections, where there is good water connectivity through the sediments, the water level in multiple channels was found to be the same and a single stage-discharge relationship, $A+B$, characterises the whole section (Figure 25). However, in bedrock dominated sections the water level in one channel is dependent on the upstream conditions in that channel, so that a cross section may contain channels with different water surface elevations (Figure 25). This leads to different flow depth:discharge relationships for each distributary channel (C and D in Figure 25).

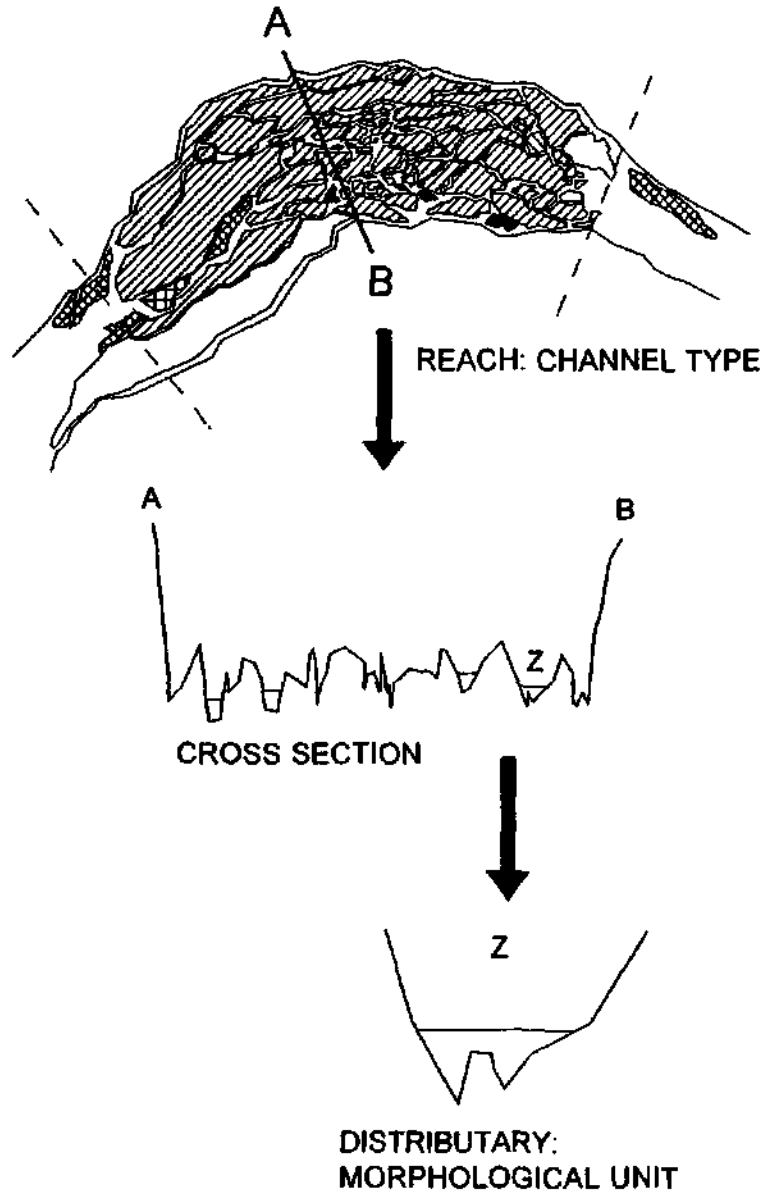
6.2.1 'Horizontal' model

Where the water level across a cross section is horizontal, conventional methods for calculating hydraulic and channel geometry parameters apply (Figure 6) and a single rating relationship can be used. This method is referred to as the 'Horizontal' model in this report. A computer program was used to calculate hydraulic and channel geometry parameters for each cross section, namely water surface width, W ; hydraulic mean depth, d ; wetted perimeter P ; hydraulic radius, R ; cross sectional area, A and cross section average velocity, V . A spreadsheet used the cross section parameters to quantify flow resistance, using the Barnes (1967) model.

6.2.2 'Non-Horizontal' model

Bedrock influenced reaches produce a non-horizontal water surface in multiple active distributaries across a cross section (Figure 25). This is particularly pertinent for the bedrock and mixed anastomosing reaches, where the low flow water surface elevation differed by up to 1.5m in separate channels. Therefore, the assumption of a horizontal water surface elevation for a cross section is not realistic. Errors in the calculation of average velocity

BEDROCK ANASTOMOSING



POOL/RAPID

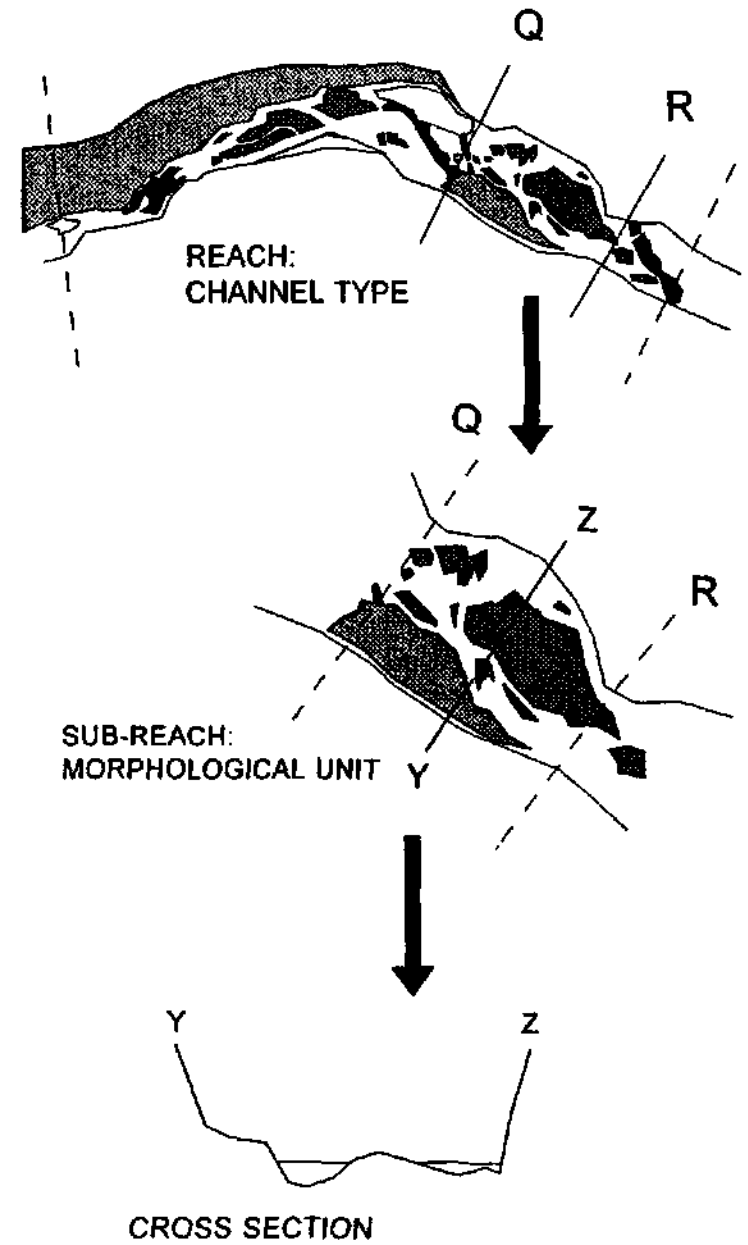


Figure 24: Scales of analysis used in the calculation of flow resistance.

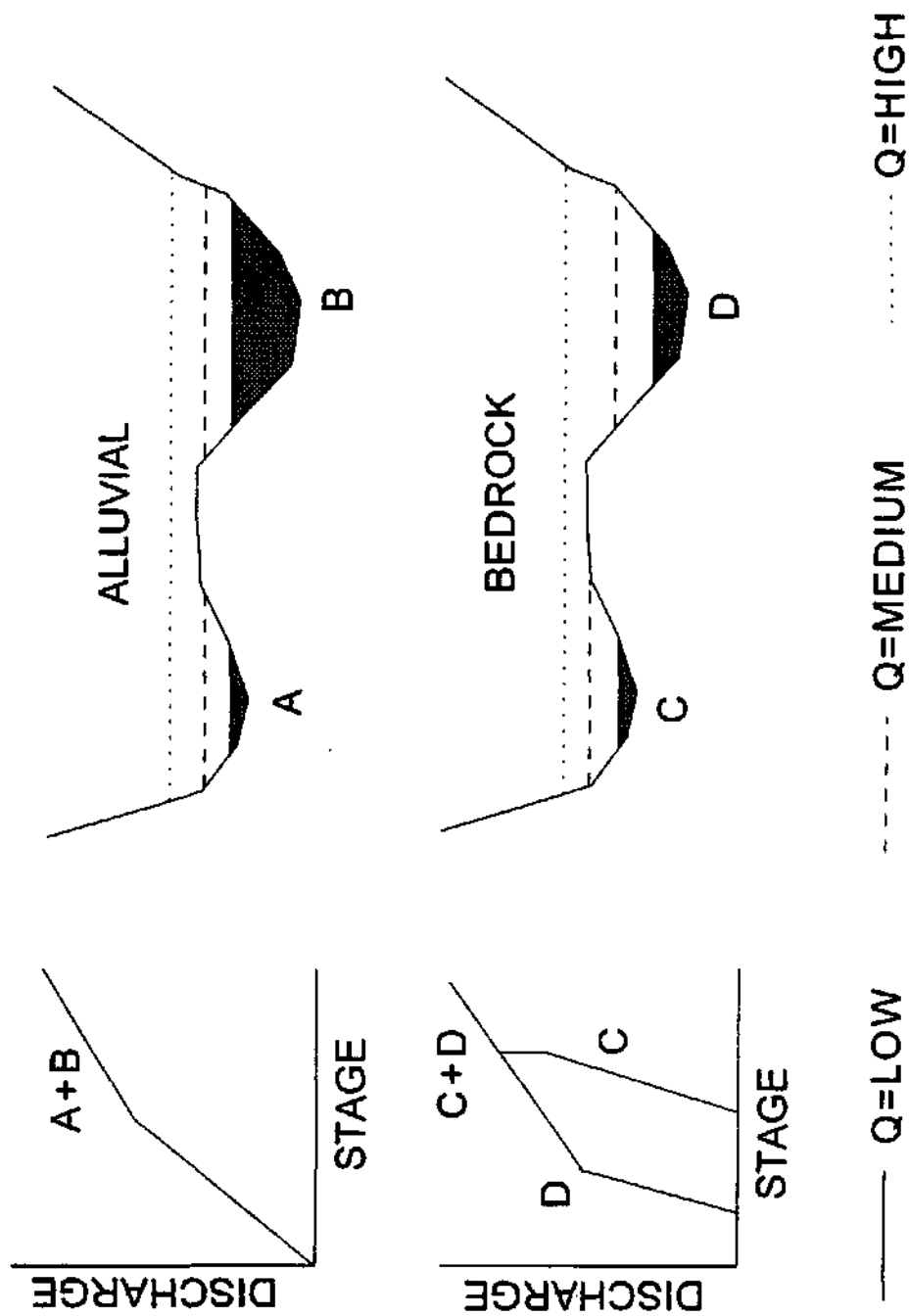


Figure 25: Horizontal water surface characteristic of alluvial sections compared to the 'stepped' non-horizontal water surface observed for bedrock influenced sections.

when using the 'Horizontal' model instead of the 'Non-Horizontal' model, were large. The 'Horizontal' model predicts velocity at between 30% and 2500% of the actual, 'Non-Horizontal' velocity, at a low discharge (Figure 26). To calculate this error, actual, measured elevations of the water surface in each active distributary were used to determine cross sectional area and hence velocity, for a known discharge. This represents average velocity according to the 'Non-Horizontal' model. The 'Horizontal' model assumes the water surface elevation in the active distributary nearest to the macro-channel bank represents the whole cross section. Therefore, an overestimation of velocity when using the 'Horizontal' model arises when the water surface elevation in the channel nearest to the macro-channel bank is lower than the actual water surface elevations in the remaining active distributaries.

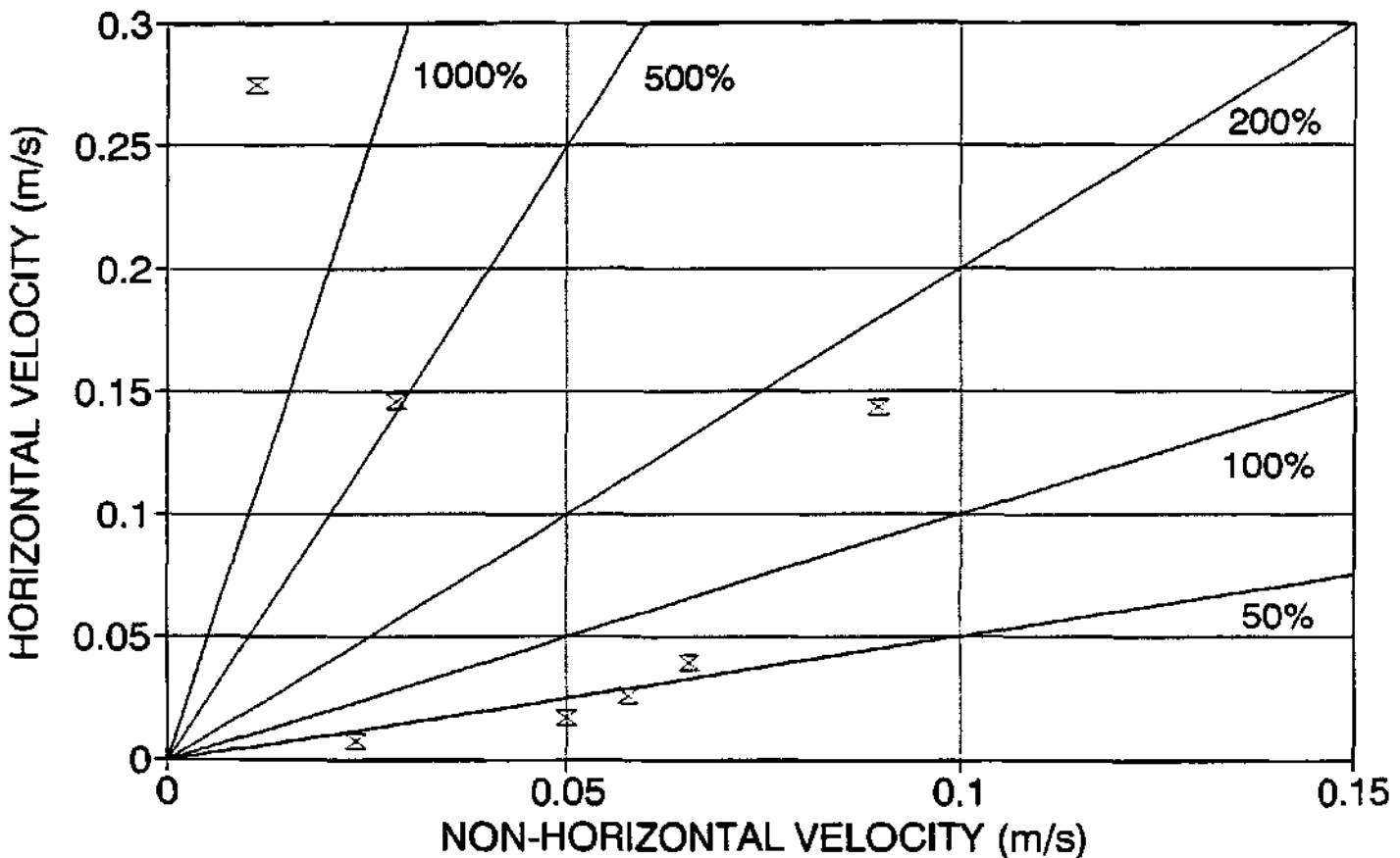


Figure 26: Errors in average velocity calculation at discharge $1\text{m}^3\text{s}^{-1}$, between the 'Horizontal' and the actual 'Non-Horizontal' models.

Measurement of flood flow levels at each channel was not feasible due to inaccessibility of a large proportion of the macro channel area in the wet season. Therefore, a stage discharge relationship was obtained only for the active and seasonal channels nearest to the accessible macro channel bank. To overcome this problem a multiple channel non-horizontal water surface overflow model ('Non-Horizontal') was devised, for use in bedrock influenced reaches. Where the water surface elevation varies in each channel of a multi-channel cross section, the concept of a single 'stage' becomes misleading. Individual channels will have different flow depth to total cross section discharge relationships (Figure 27).

The water level in each active channel was surveyed at low, dry season flow and the gradient of the flow depth-total cross section discharge relationship(s) obtained for the accessible channels at that cross section were applied to all of the remaining channels in that section, from the initial, measured elevation. Therefore, all the channels in a cross section have depth-total cross section discharge curves of the same gradient, so that the same increase in discharge results in the same increase in stage, but the curves start at different elevations. The assumption that the single rating curve was applicable to the multiple channels was tested by plotting all the available rating curves for bedrock anastomosing channel types on the same graph axis. They generally overlapped, and displayed similar trends (Figure 28). In this way, although the initial water levels of the different channels in a cross section will vary, their rates of change with discharge will be the same. Clearly, this model will only apply to deep, unconnected channels; yet cross section profiles for the Sabie River show that the multiple channels combine at medium to high flows, eventually forming a single channel across the whole macro channel in extreme events. In reality, distinct adjacent channels must join at the same elevation, but the Non-Horizontal model dictates that one channel will reach the 'threshold' point separating it from an adjacent channel at a lower discharge than the adjacent channel(s), as they initially have different water elevations yet rise at the same gradient. Observations of bedrock distributaries at medium flows have shown that once a channel reaches the elevation 'threshold' dividing it from the next, it overflows into that channel until they are at the same elevation and become one channel.

An idealised account of the Non-Horizontal model for a bedrock anastomosing cross section is given in Figure 27. For an arbitrary discharge, 1, the initial water levels in the five channels vary. The gradient change with increasing discharge, to 2, is the same, but channel B has reached the topographic high overflow threshold to channel A. Therefore, its level remains constant while it contributes its share of the increase in discharge to channel A via overflow until the water levels are equal. An equivalent interpretation applies to channels C, D and E. Channels E and C reach overflow thresholds, thereby remaining at a stationary stage, until the water level in channel D rises to join with them. The resultant rating curves are shown, with the channel containing the lowest initial water elevation controlling the change in stage with discharge.

Direct observation of seasonal channels' recent flow history was possible during the cross section surveys and this information was used to calibrate the Non-Horizontal model at individual cross sections. For example, several macro channel distributaries had no evidence of recent flow through them, therefore they were assumed to have not been inundated for the range of discharges encountered in this study, irrespective of their physical elevation or the result of the Non-Horizontal model analysis.

The procedure for use of the Non-Horizontal model is as follows:

- 1) Survey the water elevation in each active distributary across the cross section for a known low flow discharge.
- 2) Sub-divide the cross section into subsections, separated by highest elevation points or 'thresholds' between the measured active distributaries. In this way, a subsection will comprise one distributary as well as other morphological units such as bedrock core bars or seasonal distributaries.

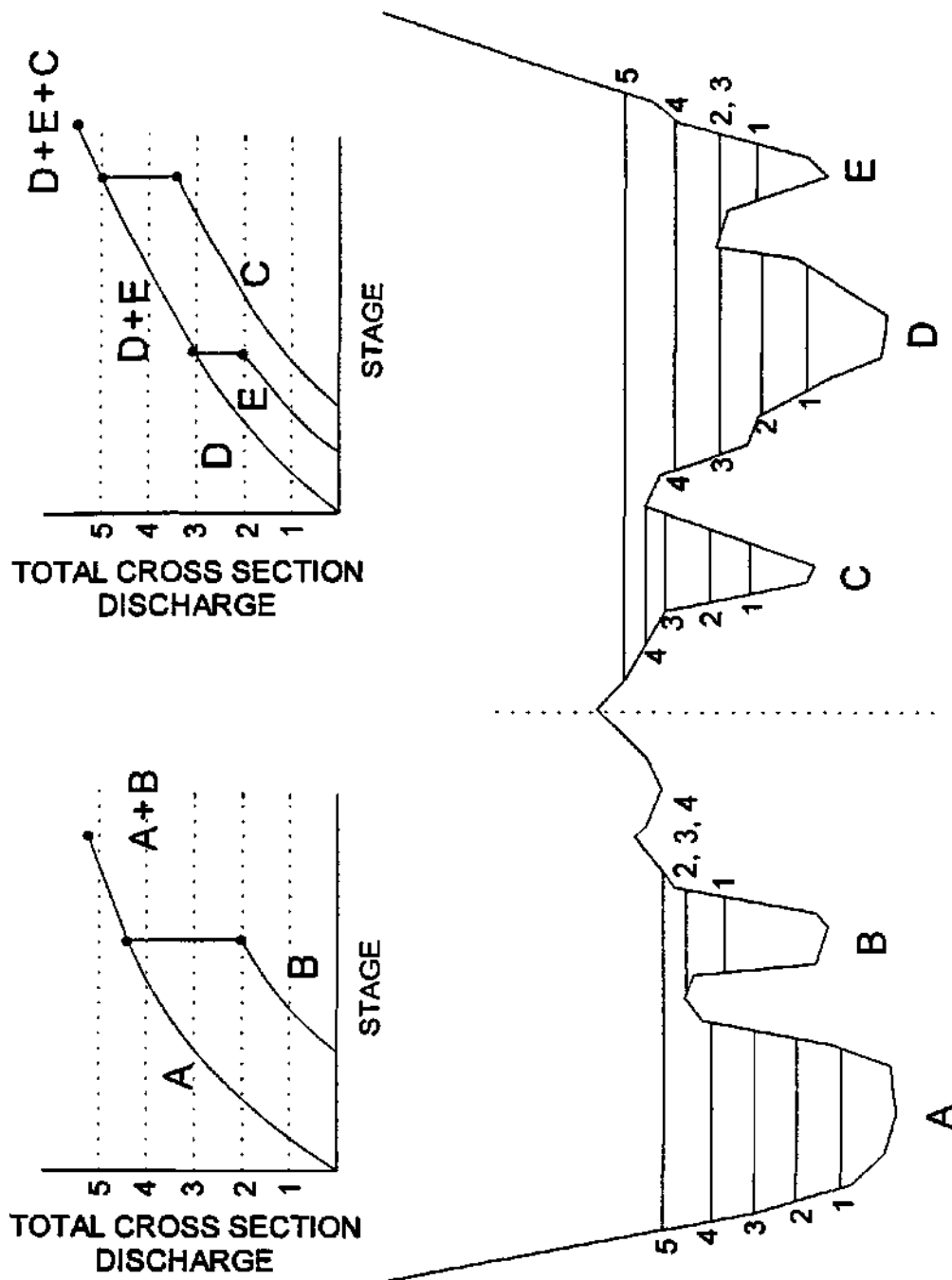


Figure 27: Conceptual diagram of the 'Non-Horizontal' model, for use in bedrock influenced sections, to define flow depth:cross section discharge relationships for individual distributaries.

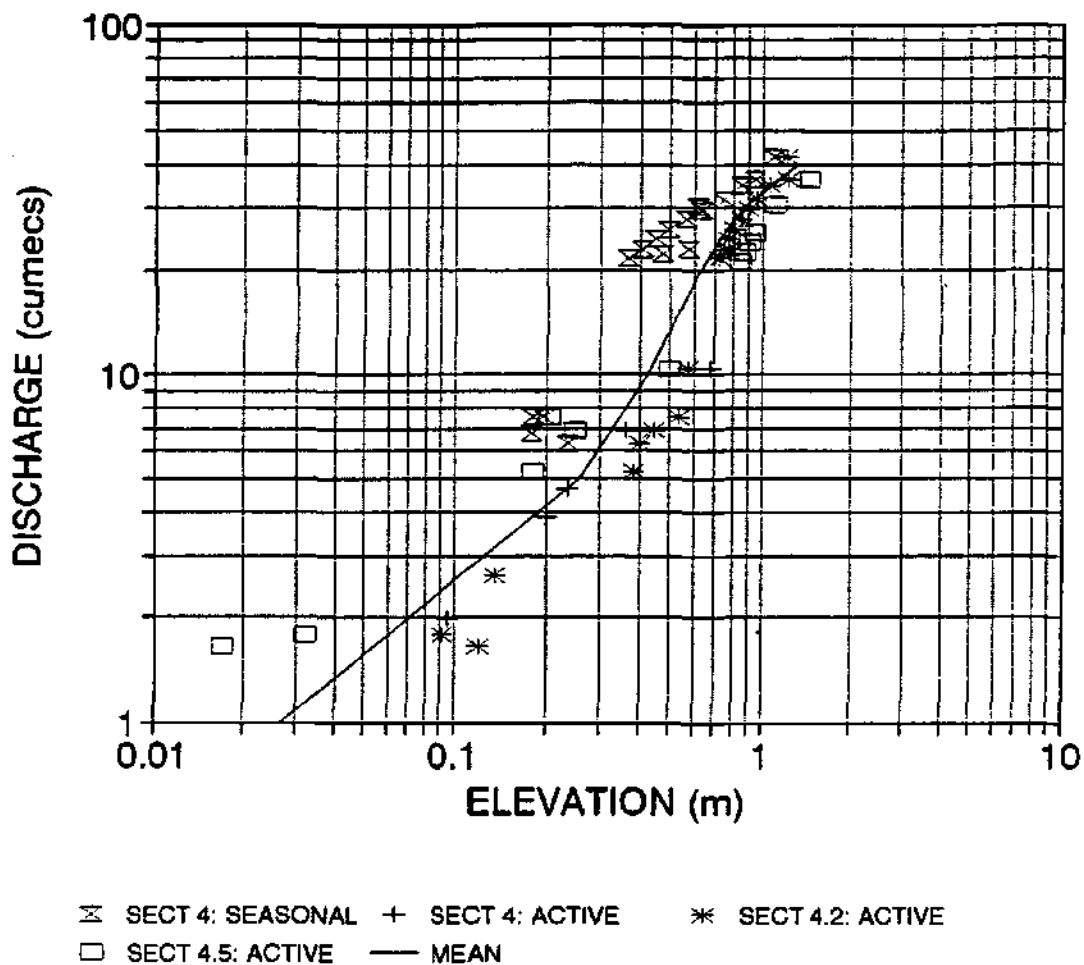


Figure 28: Similarity between bedrock anastomosing rating curves, reduced to a common initial elevation at discharge $1\text{m}^3\text{s}^{-1}$.

- 3) Construct a rating curve by observing water surface elevations over a range of discharges for one distributary channel.
- 4) Assuming each subsection is independent of adjacent ones, generate rating curves for each distributary by applying the gradient of the measured rating curve to the individual initial, low flow elevation in each distributary. The result will be a series of parallel rating curves with different stages against total cross section discharge.
- 5) Starting with the distributary containing the highest water surface elevation, determine the points on the rating curve at which the thresholds to both adjacent subsections are exceeded. The stage at this point must be kept constant until the adjacent channels' elevations have caught up and the three distributaries join. This process must be completed for all the subsections. The rating curves are thus modified to account for distributaries reaching overspill thresholds and eventually joining into a single channel.
- 6) Observational evidence of flow history for seasonal or macro channel distributaries can be used to fine tune the Non-Horizontal model results for specific subsections.
- 7) The resultant rating curves and knowledge of the cross sectional shape can then be used to calculate cross sectional geometry and hydraulic parameters.

A computer program has been developed to calculate the water surface elevation in each distributary for an input discharge using the Non-Horizontal model. Another program quantifies a variety of channel geometry and hydraulic parameters for alluvial sections, where the water surface is horizontal. The output from these programs, as cross section average parameters, was fed into a spreadsheet to calculate flow resistance.

Use of this model will potentially ensure a more representative estimation of total channel area or other channel geometry parameters, that being the sum of the separate distributary channel areas, over a multiple channel cross section and hence average velocity for a given discharge. Comparison of actual cross sectional area and average velocity, representative of the 'Non-Horizontal' model, where individual water surface elevations in each active distributary were measured, and that obtained from the assumption of a horizontal water surface, at a low discharge produced errors in velocity estimation of between 30% and 2500% (Figure 26). These errors relate to a single, low, discharge and at present the actual error, for cross section parameters, between 'Horizontal' and 'Non-Horizontal' model is not available for higher discharges. However, these low flow errors (Figure 26) will be a maximum, as the error will decrease with increasing discharge, until all the discrete distributaries join and the water surface is horizontal. At this high discharge (from observation the distributaries at cross section 4 had not all joined at $650 \text{ m}^3\text{s}^{-1}$), the 'Horizontal' and 'Non-Horizontal' model will predict equal elevations.

Seasonal distributary rating curves were observed at five cross sections within the study reaches, over a range of discharges. These provide a direct test of the 'Non-Horizontal' model performance (Figure 29). According to the 'Non-Horizontal' model, distributary B will have a rating curve of the same gradient as distributary A, but will be at a different starting elevation (predicted curve on Figure 29). The shaded area between the observed and predicted rating curves for distributary B represents the elevation error between the 'Non-Horizontal' model prediction and actual, measured elevation. If a horizontal water surface had been assumed, the error in elevation estimation would have been the 'Non-Horizontal' error plus the area between the measured distributary B rating curve and the measured, distributary A rating curve. The 'Horizontal' and 'Non-Horizontal' errors have been quantified for five seasonal distributaries (Figure 30), where rating curves were observed and compared to elevations predicted from assuming the gradient of the active channel rating curve represented the seasonal channel (using the 'Non-Horizontal' model). Maximum depth between observed and 'Non-Horizontal' model was predicted to between 70% and 165% (Figure 30). This translated to an error of between 55% and 265% in distributary channel area prediction (Figure 31). The 'Horizontal' model predicted negative maximum depth values for one seasonal channel. This was because the water level in the active channel rating curve to be used in the 'Non-Horizontal' model, is lower than the seasonal channel bed elevation.

These 'Non-Horizontal' errors produced are the result of comparison between active channel rating curves, used to drive the 'Non-Horizontal' model and the observed seasonal rating curves. Channel characteristics vary between active and seasonal channels, with the latter tending to have mixed alluvial and bedrock and boulder beds, often with a vegetation cover; this will result in different, actual, rating curves. Therefore, the 'Non-Horizontal' model predictions of channel geometry parameters are likely to be most in error when predicting for seasonal channels and more in agreement when predicting for similar, active channels.

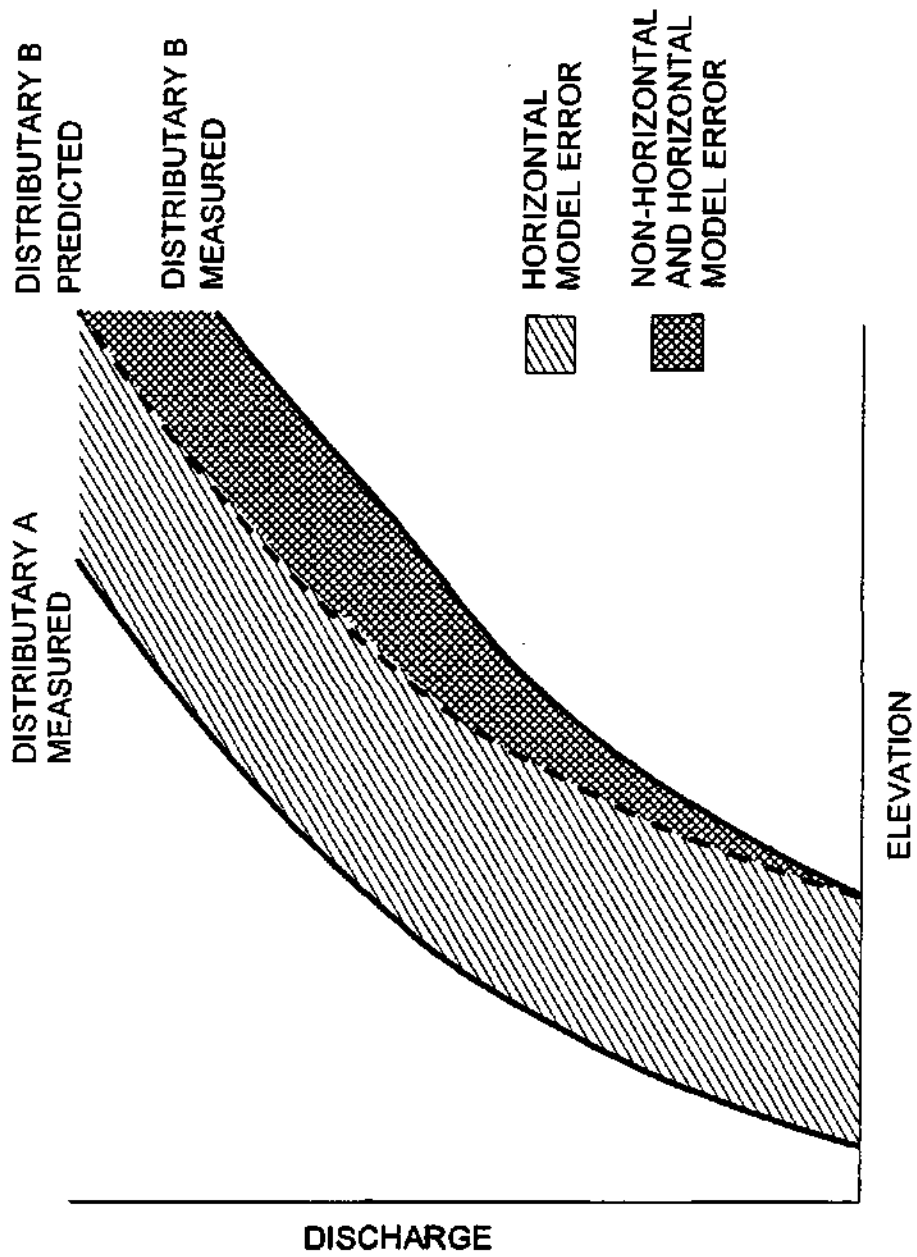


Figure 29: Definition of 'Non-Horizontal' and 'Horizontal' model errors.

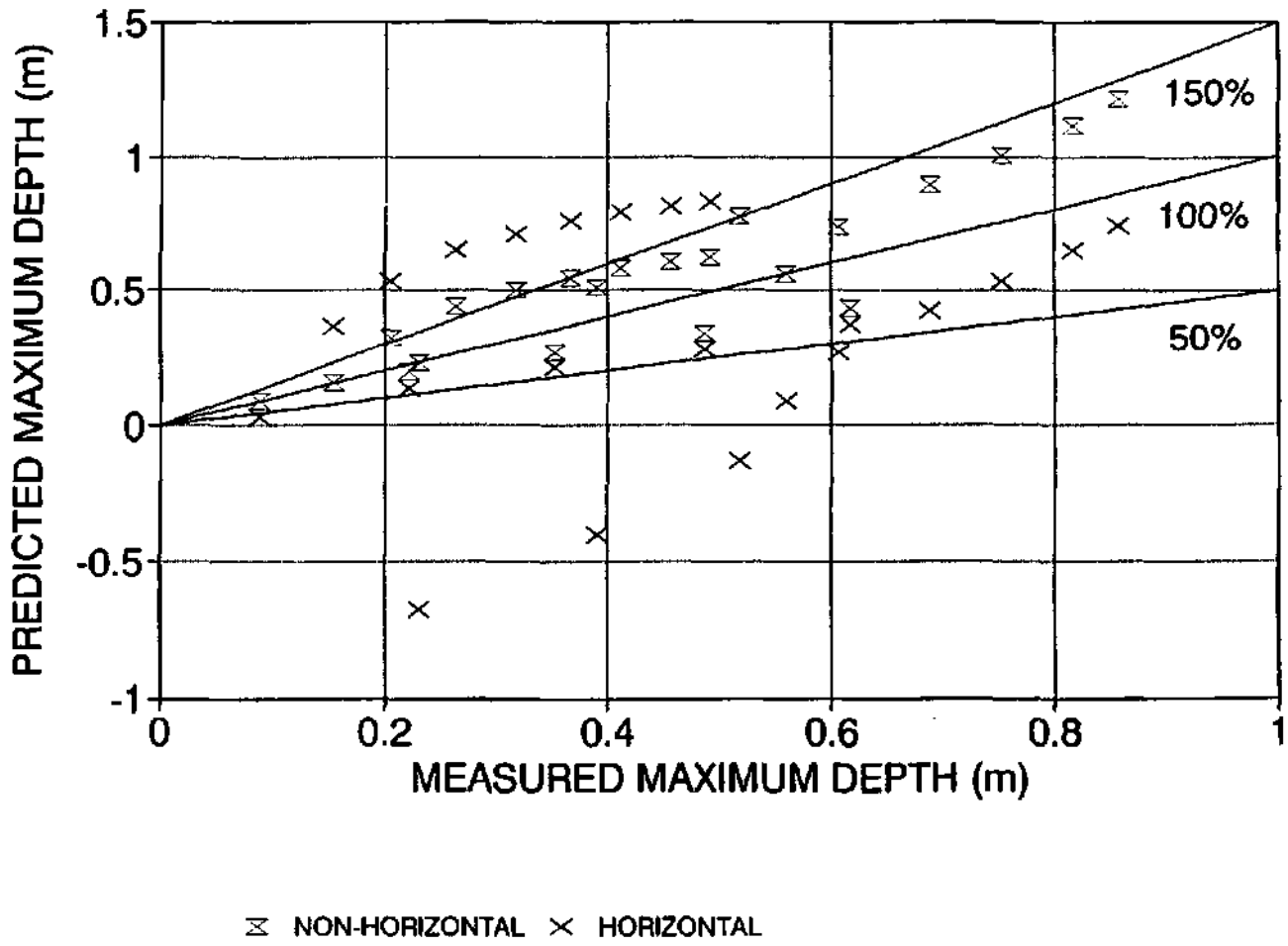


Figure 30: Error between observed and 'Non-Horizontal' and 'Horizontal' model predicted maximum depth, over a range of low and medium discharges for five seasonal distributaries.

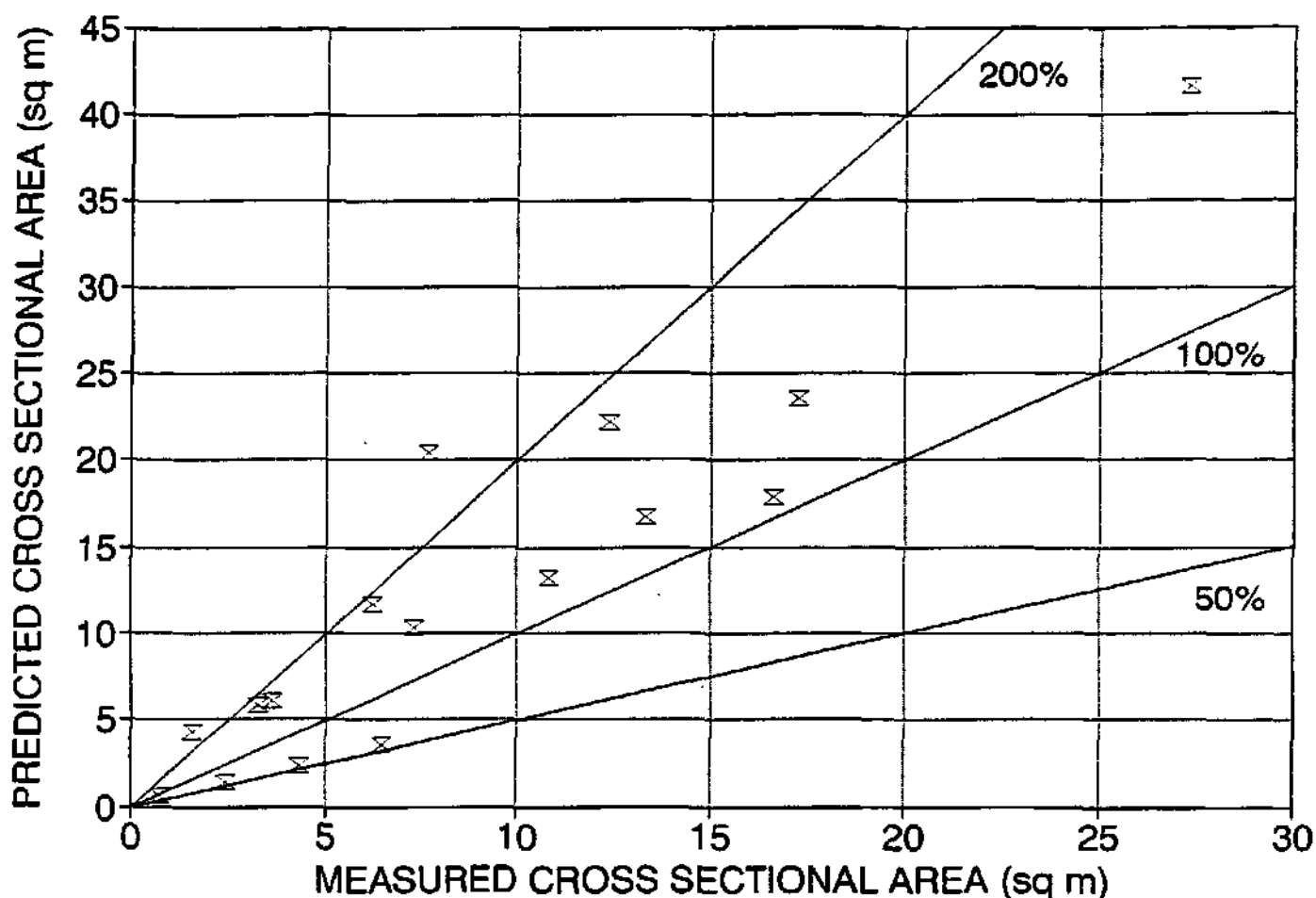


Figure 31: Distributary channel area error between observed and 'Non-Horizontal' model predicted over a range of low and medium discharges for five seasonal distributaries.

Presently, observed rating curves over a range of discharges, are not available for multiple active channels in a cross section, so this hypothesis can not be tested. However, the errors obtained from use of the 'Non-Horizontal' model are well below the corresponding errors produced if the 'Horizontal' model had been used to predict maximum depth in the seasonal channels (Figure 30).

A suggestion for 'refinement' of the 'Non-Horizontal' model is to measure three rating curves for 'characteristic' active, seasonal and macro-channel distributaries per cross section. These three rating curves could then be used to run the 'Non-Horizontal' model, instead of using the single active channel rating curve to predict the flow depth:discharge relationships for the whole cross section.

CHAPTER 7: CHANNEL FLOW RESISTANCE QUANTIFICATION

7.1 Quantification of hydraulic and channel geometry parameters

A variety of channel geometry and hydraulic parameters were derived using the Horizontal model in alluvial or Non-Horizontal model in mixed or bedrock influenced sections. At a cross section these parameters for a given discharge were: average stage h above sea level, width W , hydraulic mean depth \bar{d} , wetted perimeter P , hydraulic radius R , channel area A and average velocity \bar{V} . A width-weighted average elevation was computed to give average stage for multi-channel bedrock sections, as it was thought that wide distributaries would influence the total energy slope for a multiple channel section proportionally more than small, narrow distributaries. The wetted perimeter, channel area and width values were simply the sum of the individual distributary parameters (Figure 32). Therefore, single values of these parameters were determined for the range of measured discharges for each cross section monitored.

$$W_T = W_1 + W_2 + W_3 \quad \bar{V} = \frac{Q}{A_T} \quad \bar{R} = \frac{A_T}{P_T}$$

$$A_T = A_1 + A_2 + A_3$$

$$P_T = P_1 + P_2 + P_3 \quad \bar{d} = \frac{A_T}{W_T}$$

$$\bar{h} = [(h_1 \times W_1) + (h_2 \times W_2) + (h_3 \times W_3)] / W_T$$

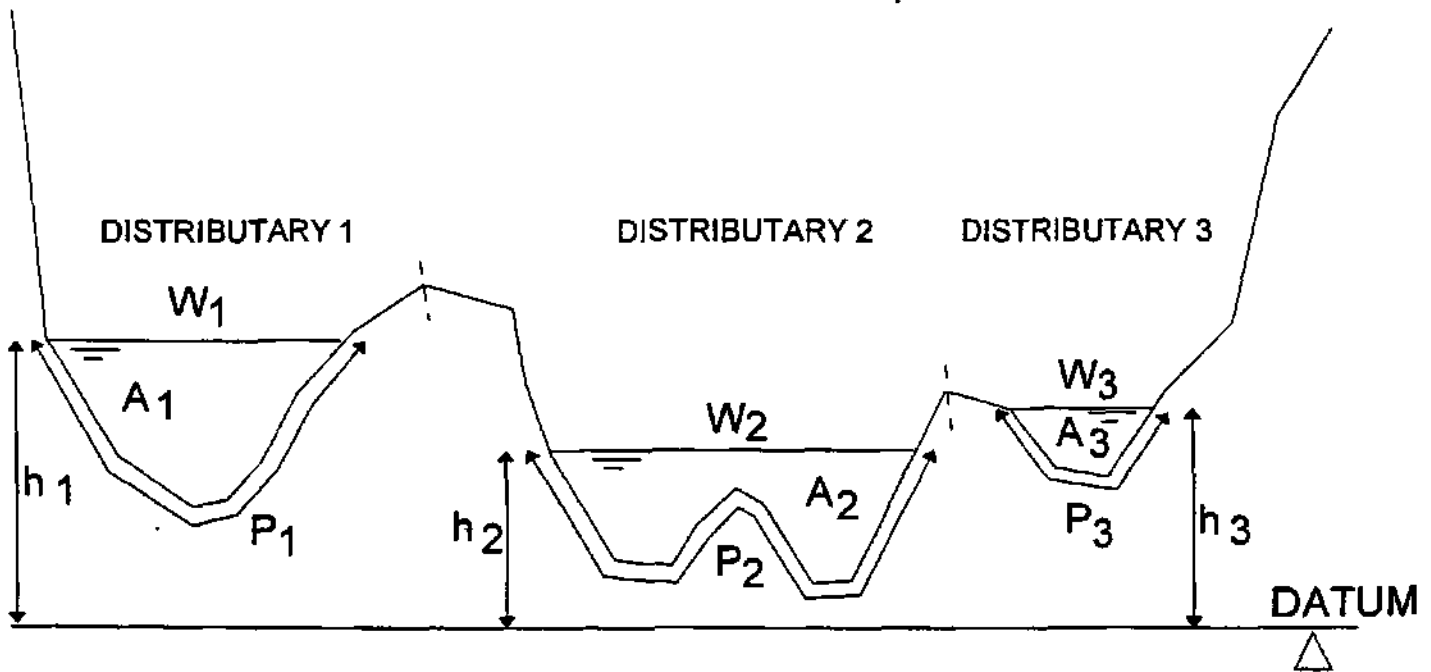


Figure 32: Hydraulic and channel geometry parameter definitions in a bedrock influenced section with a non-horizontal water surface elevation, where W is width, V is velocity, A is area, h is height above datum and P is wetted perimeter.

7.2 Quantification of channel type or 'reach' flow resistance

Following the Barnes (1967) methodology, outlined in Section 4.2, and using the hydraulic and channel geometry parameters derived from either the 'Horizontal' or 'Non-Horizontal' model, reach flow resistance was quantified for the 5 channel types (Figures 33 to 36). Discrete values of discharge and associated cross section parameters were used to generate these discharge:flow resistance relationships, over the range of flows encountered on the Sabie River during the period of study.

As Section 5.3 details, the high magnitude flow levels were only recorded at one or two cross sections per study reach and at three out of the five reaches. Where only one estimate of high discharge stage was recorded within the study reach, equations 1 to 3 were used to calculate flow resistance at a cross section. In these cases, local water surface slope was not available, so the energy slope was assumed to equal the regional bed slope (this assumes that the flow is uniform at high discharges). Therefore, these high discharge flow resistance estimates are less reliable than the multi-cross section derived estimates of the low and medium discharges. Where two high discharge stages were recorded within a study reach, local slope, and hence true energy slope, was available and the Barnes (1967) methodology was used to quantify flow resistance. Table 7 describes the methods used to calculate high discharge flow resistance for all of the channel types.

The bedrock anastomosing channel type has the highest flow resistance values (Figures 34 to 36), but shows the same trend as all of the channel types, with a decrease in flow resistance from low to medium discharges. The alluvial channel types: braided and single thread have the lowest flow resistance coefficients, with mixed anastomosing and pool-rapid reaches giving intermediate values. The mixed anastomosing and braided reach flow resistance increase marginally from medium to high discharges, as opposed to the bedrock anastomosing reach flow resistance which continues to decline throughout the range of discharges monitored.

Table 7: Methodology for high discharge flow resistance quantification

Channel type	Number of cross sections used	Type of slope used
Bedrock anastomosing	1	Regional bed slope
Mixed anastomosing	2	Energy slope
Single thread	0	Not available
Pool-Rapid	0	Not available
Braided	2	Energy slope

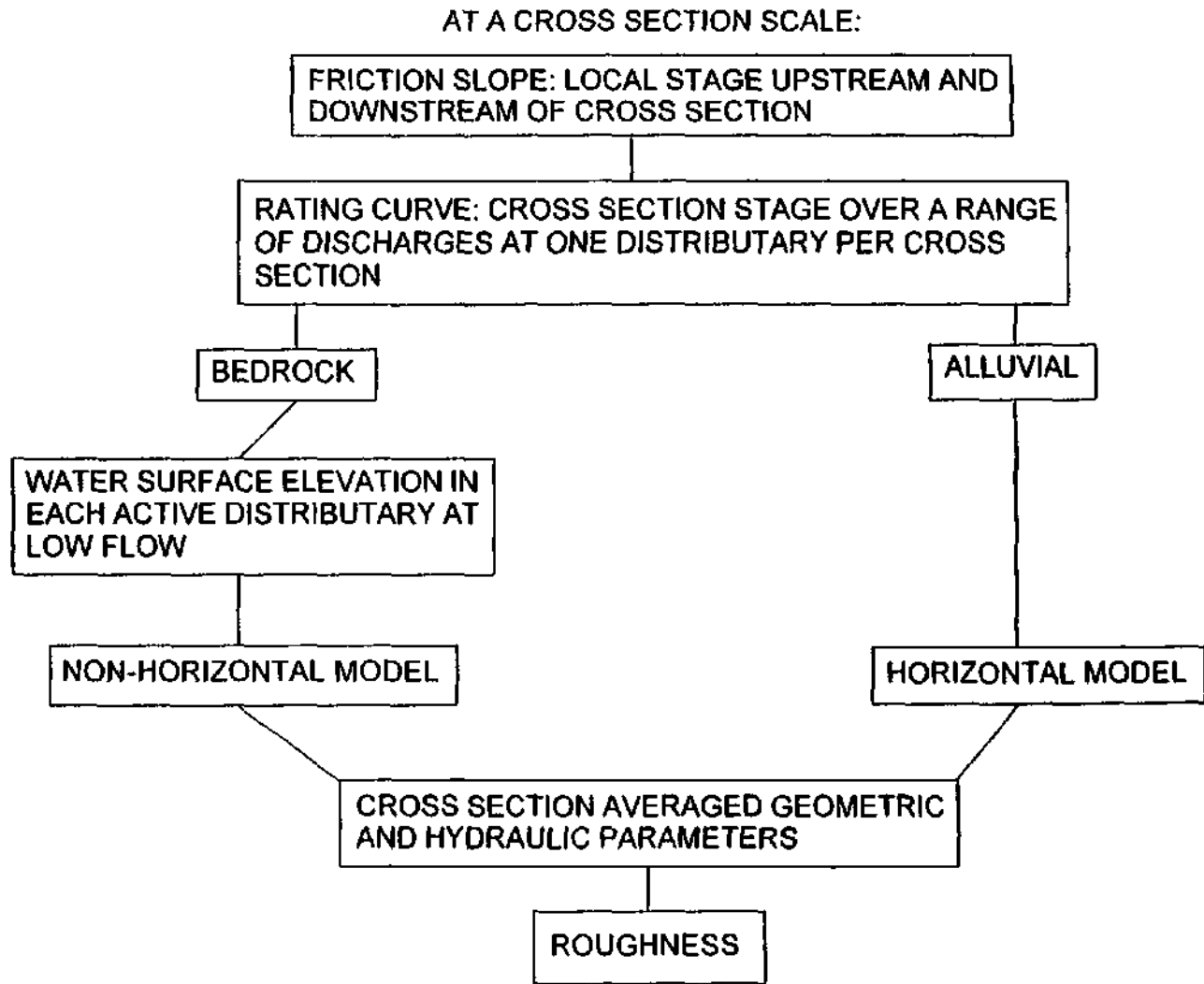
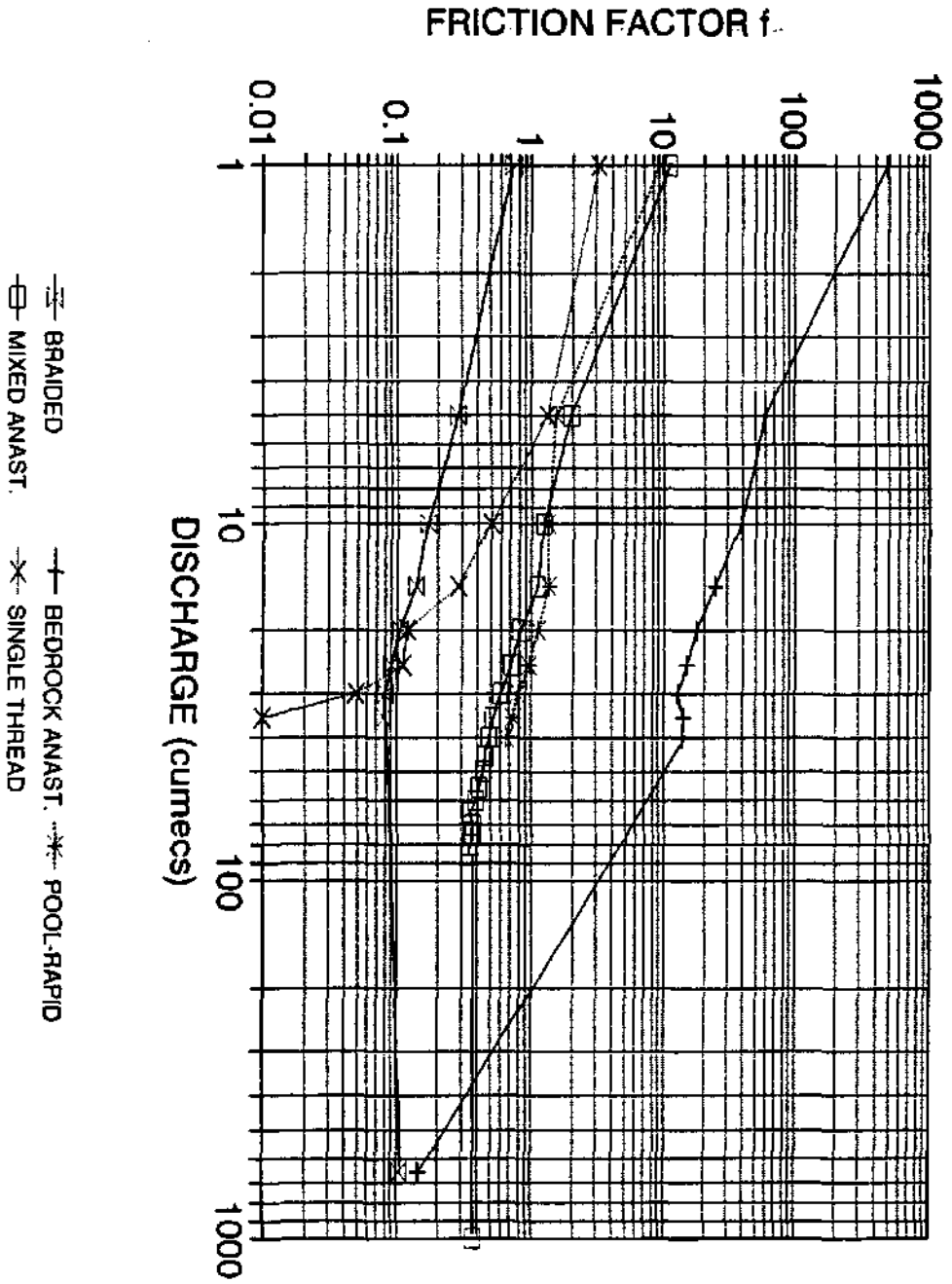
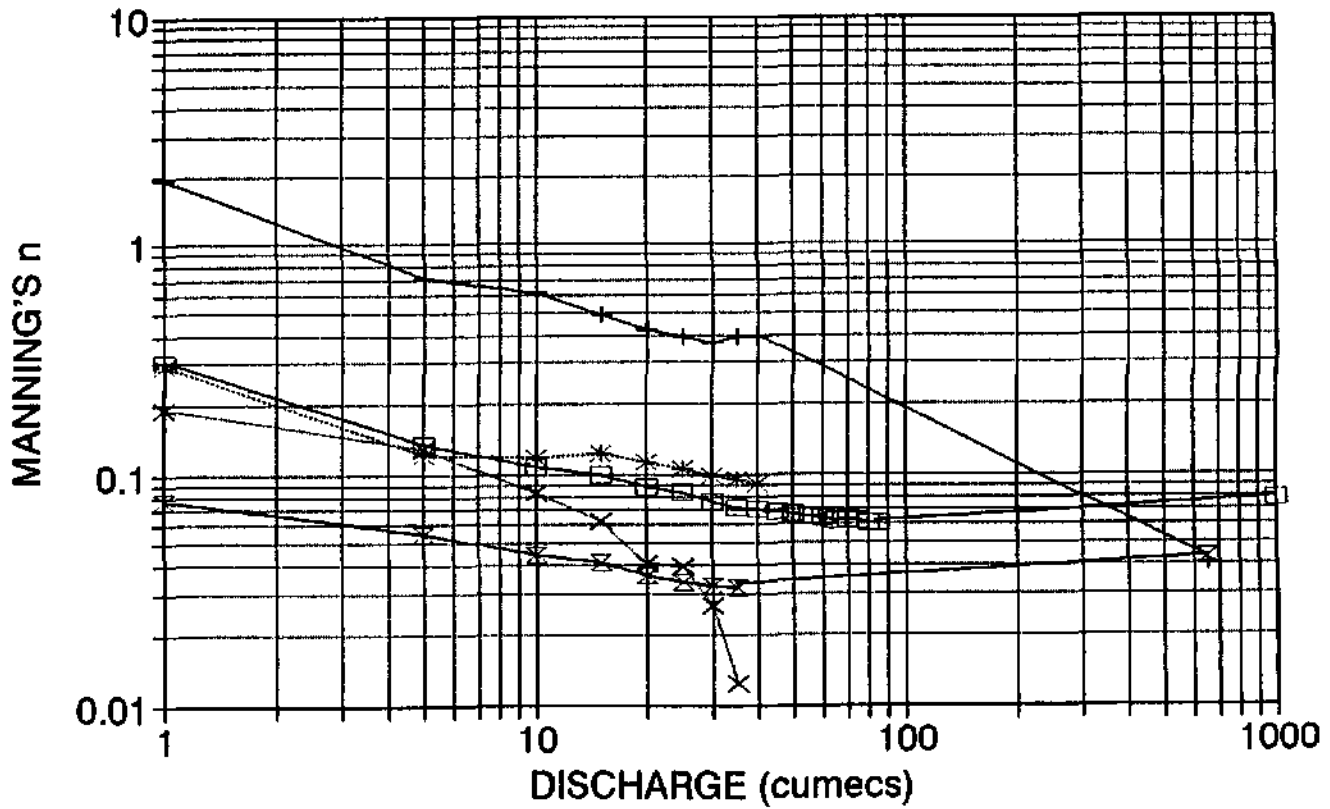


Figure 33: Summary of procedure for calculating flow resistance in alluvial and bedrock sections.

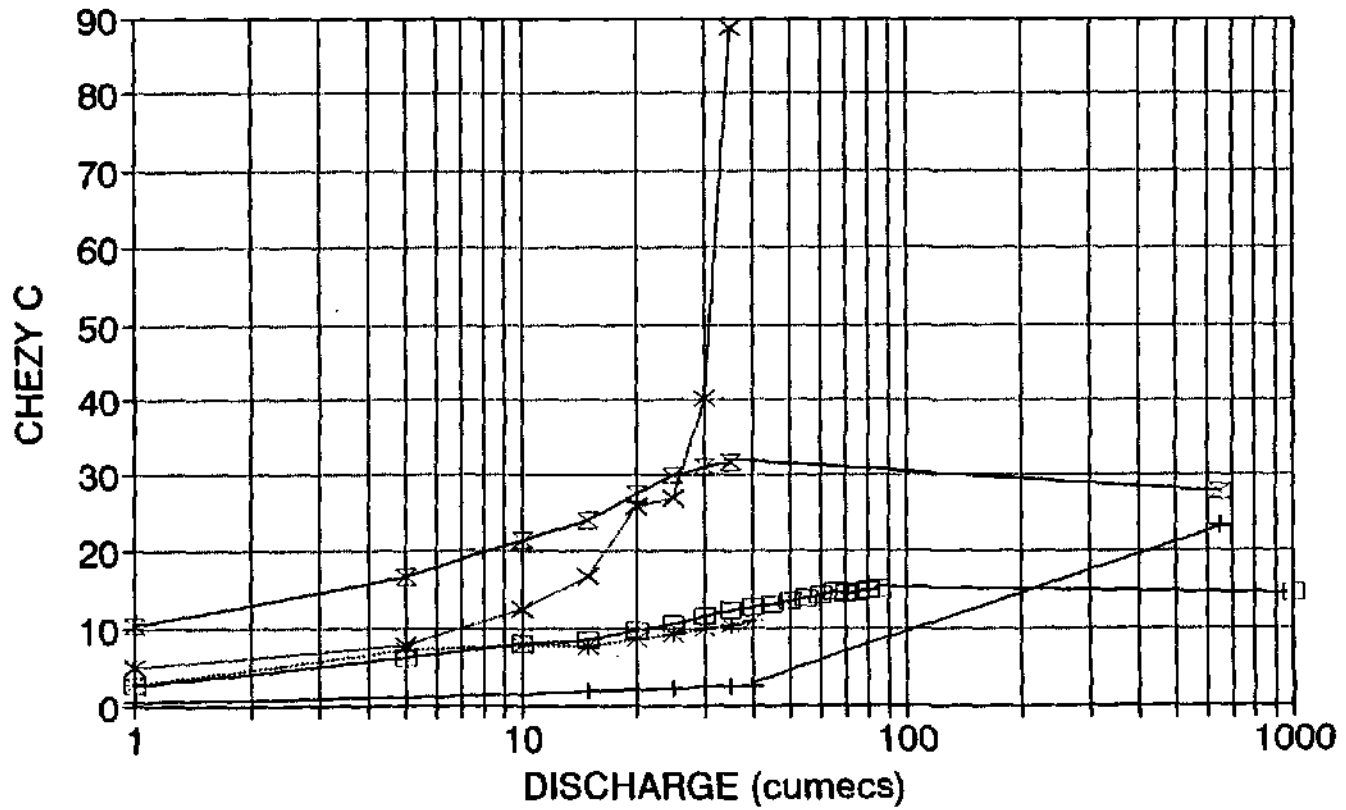
Figure 34: Darcy-Weisbach friction factor, f quantification over the five channel type reaches.





—○— BRAIDED —+— BEDROCK ANAST. —*— POOL-RAPID
 —□— MIXED ANAST. —x— SINGLE THREAD

Figure 35: Manning's n quantification over the five channel type reaches.



—x— BRAIDED —+— BEDROCK ANAST. —*— POOL-RAPID
 —□— MIXED ANAST. —x— SINGLE THREAD

Figure 36: Chezy C quantification over the five channel type reaches.

7.3 Quantification of morphological unit or 'sub-reach' flow resistance

While reach estimations characterise average flow resistance for a whole channel type, there is a need to break down total, reach average flow resistance into smaller spatial components, to quantify more local flow resistance. The data collected on the Sabie River facilitates this local analysis (Section 6.1). Sub-reaches, between two or three cross sections sharing the same morphological unit type, for example a pool section, were fed into the Barnes (1967) model to calculate local flow resistance at the morphological unit scale (Figures 37 to 39). A similar trend of decrease in flow resistance with discharge, as found over the reach scale, occurs for all of the morphological units investigated. The bedrock influenced units, namely rapids and cataracts, display the highest flow resistance values, while the alluvial braid bars and pools have low flow resistance. No high discharge stages were recorded at cross sections used to calculate subreach flow resistance, therefore morphological unit scale flow resistance could not be quantified at high discharge.

Direct measurement of discharge in individual bedrock distributaries (Section 5.4) at the bedrock anastomosing channel type has enabled flow resistance to be quantified for this morphological unit, (Figures 40 to 42) in several active distributaries. Local water surface slope data was used to approximate S_f , the friction slope and cross sectional shape data was measured as part of the gauging exercise. Detailed descriptions of the individual active distributaries morphological form and hydraulic characteristics are given in Table 8.

Table 8: Description of active distributary channels used in morphological unit flow resistance quantification.

Channel	Key	Description
4A	1	Thin dolerite fissure within bedrock pavement; steep slope; smooth but stepped profile; very low discharge
4D	2	Gentle slope over bedrock pavement and boulders; high velocity; upstream of rapids
4F	3	Section of a bedrock cascade: series of pools and rapids
4G	4	Low water surface slope; very low discharge; section of bedrock pavement
4H	5	Dolerite bedrock pavement; large boulders dissecting flow
4.5A	6	Low slope; silty braid bar on smooth bedrock base; low velocity; upstream of rapids
4.5C	7	Low slope; high velocity near critical flow region upstream of rapid in bedrock distributary
4.5D	8	Short rapid section; bedrock and boulders

Note: The channel name corresponds to the active distributaries label in Figure 11. The key refers to the interior label in Figures 40 to 42.

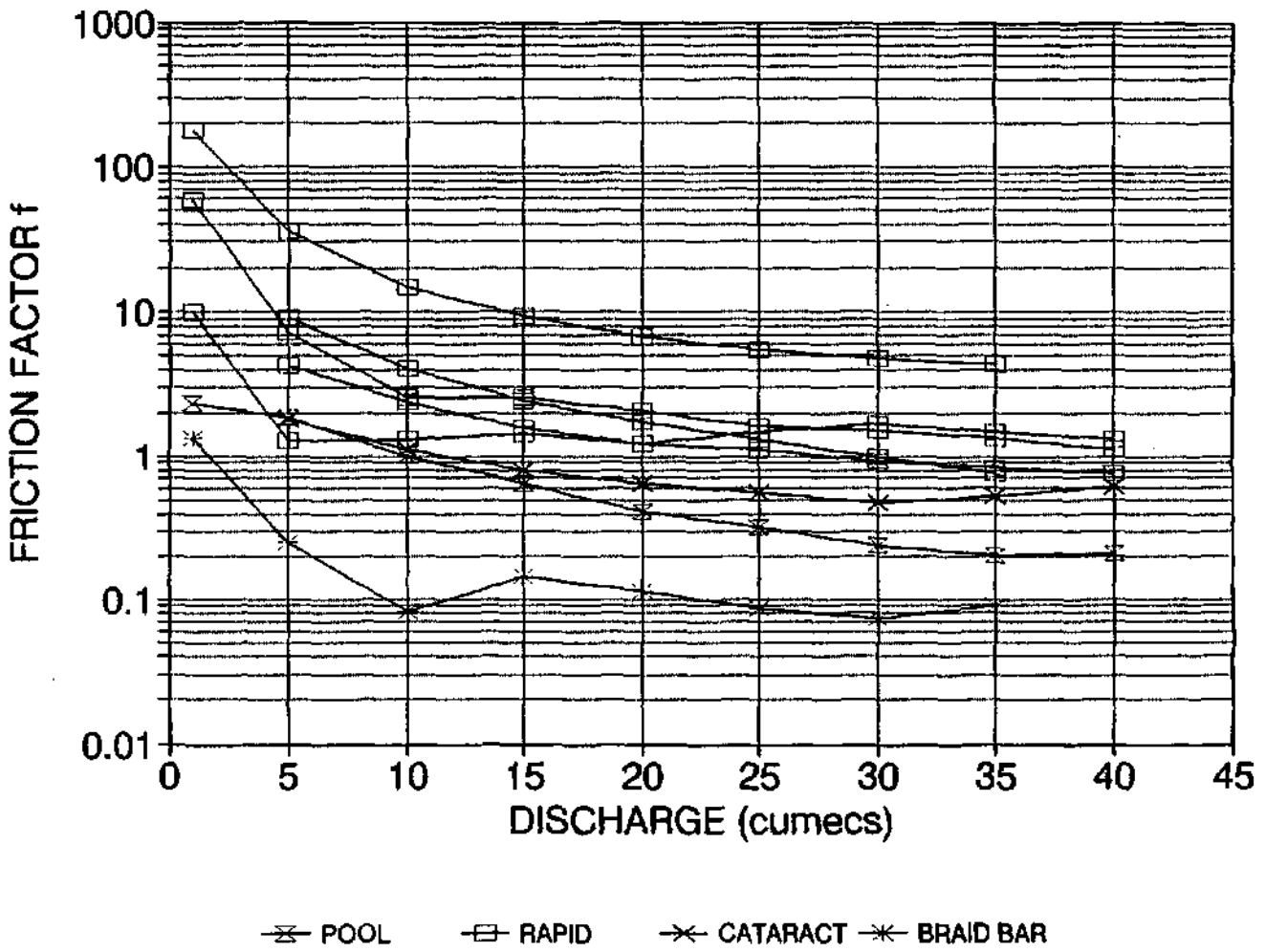


Figure 37: Darcy-Weisbach friction factor, f quantification for a variety of morphological units.

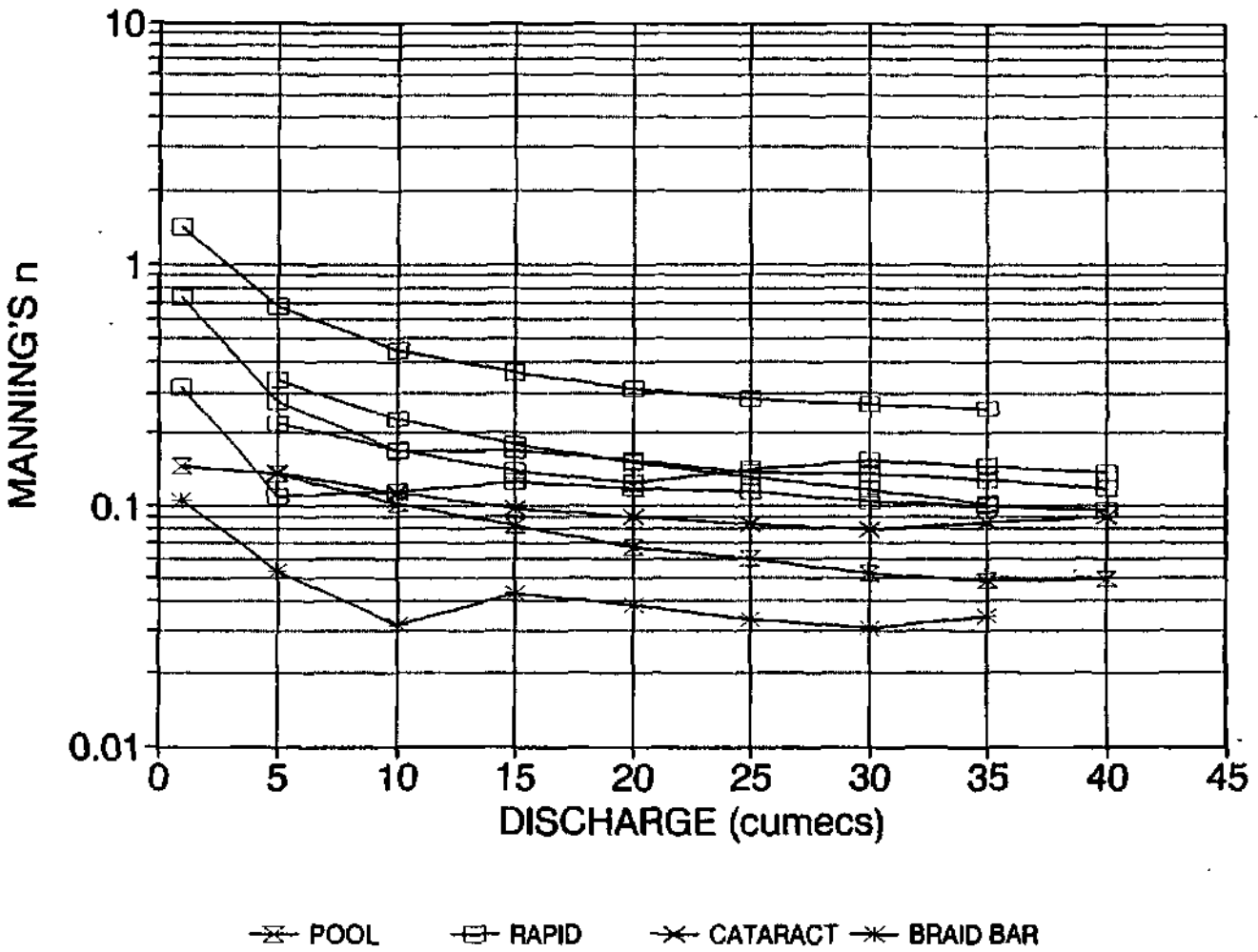


Figure 38: Manning's n quantification for a variety of morphological units.

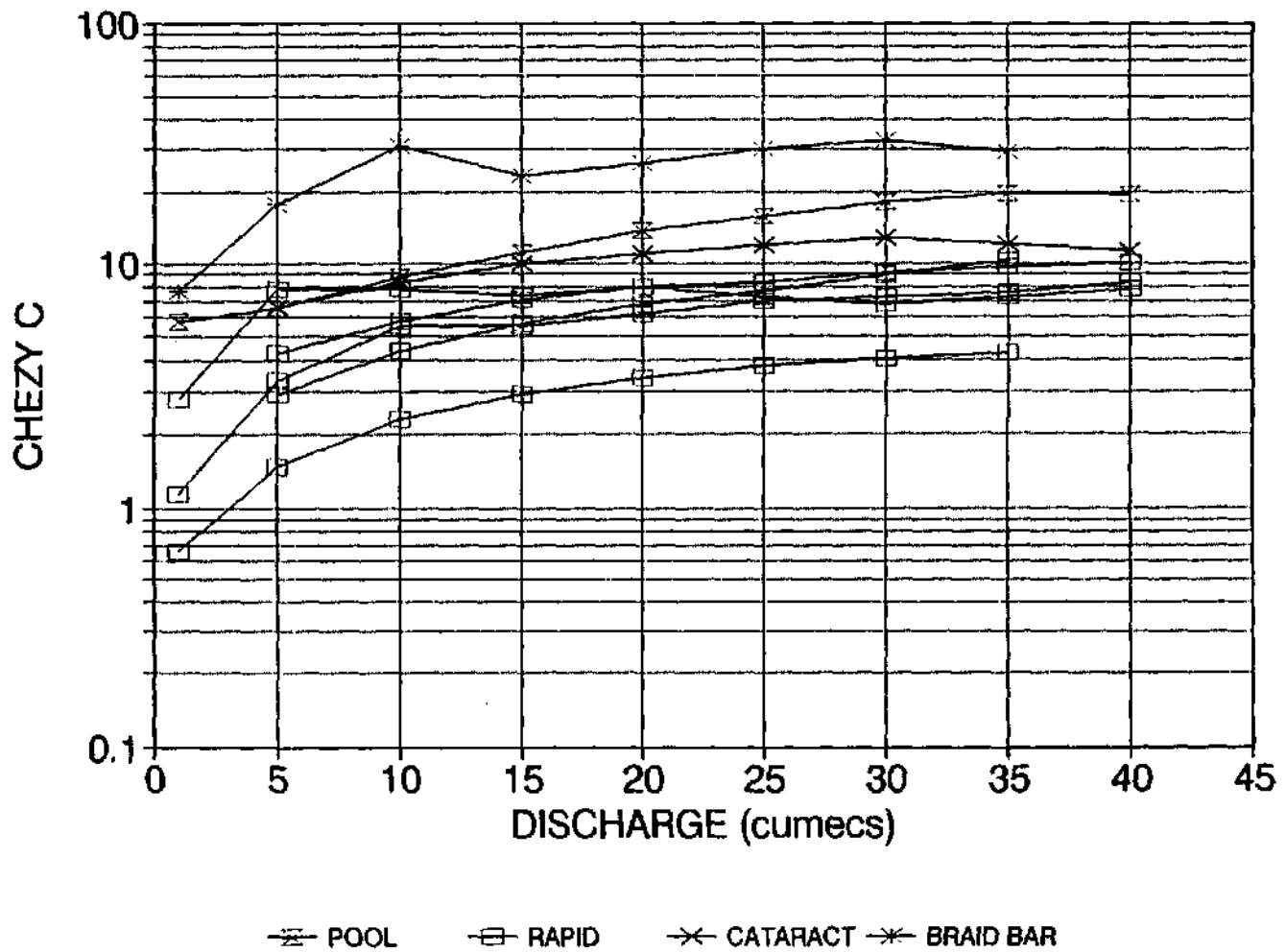


Figure 39: Chezy C quantification for a variety of morphological units.

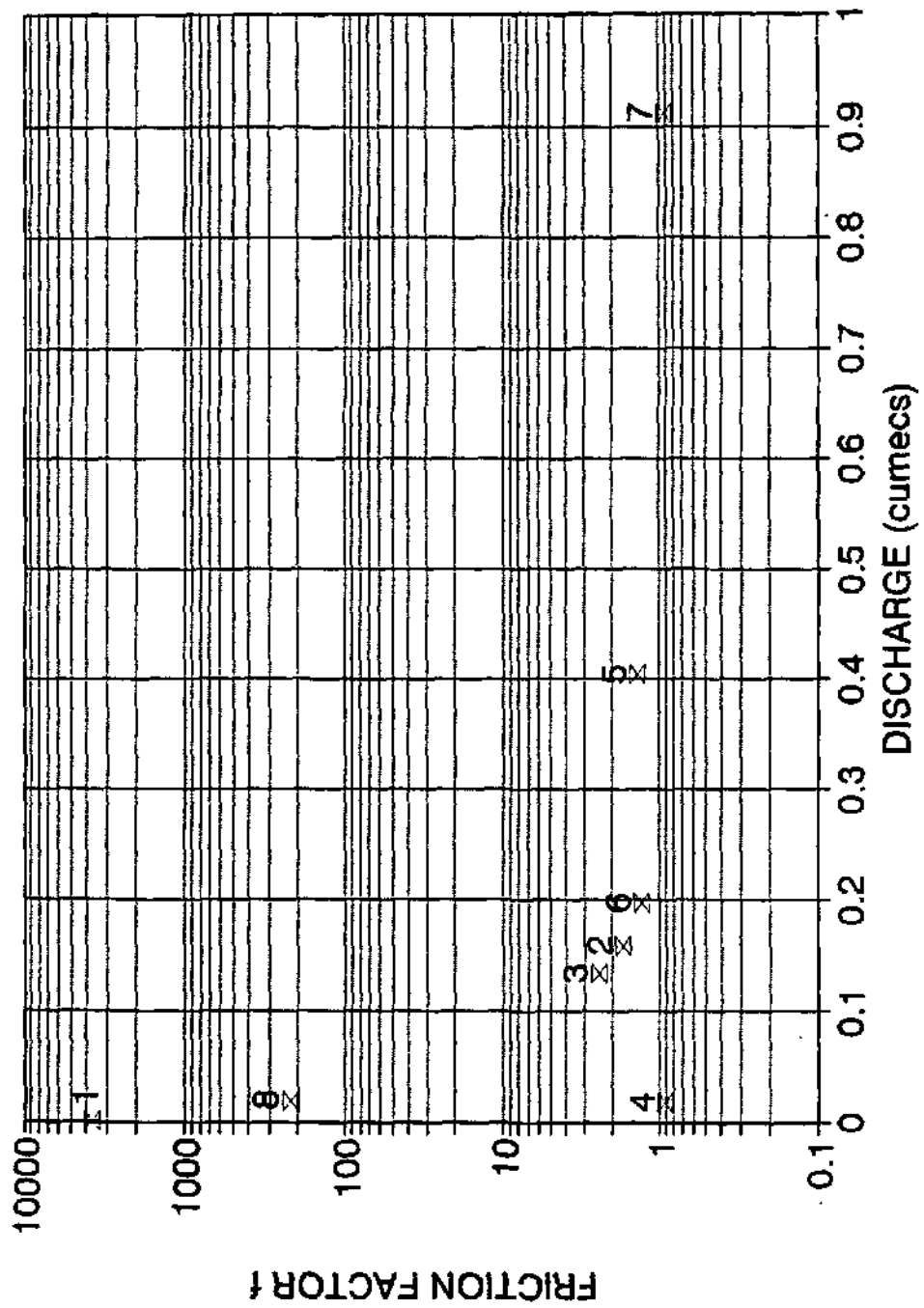


Figure 40: Darcy-Weisbach friction factor, f quantification for bedrock distributaries. Numbers refer to individual distributaries.

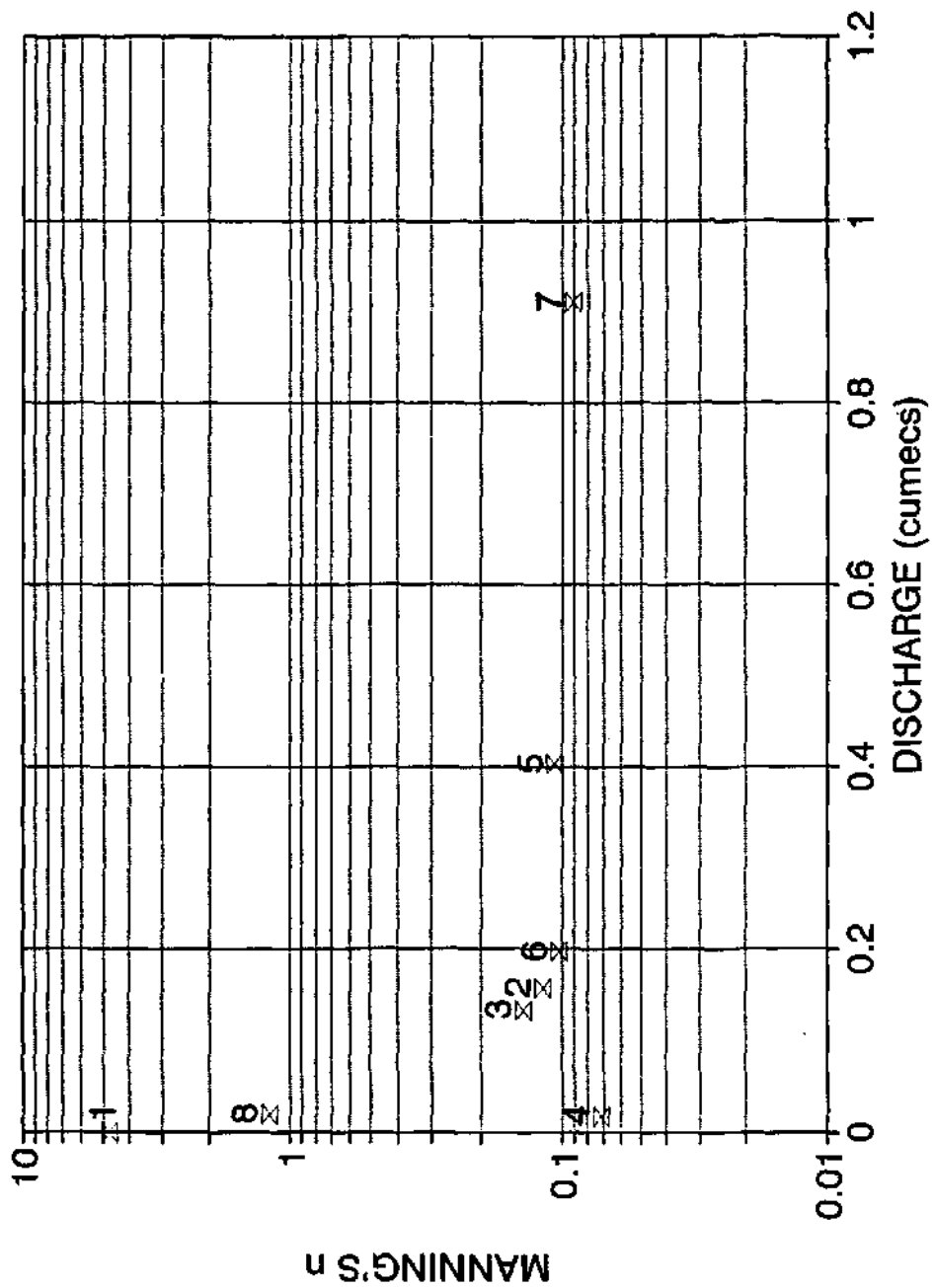


Figure 41: Manning's n quantification for bedrock distributaries. Numbers refer to individual distributaries.

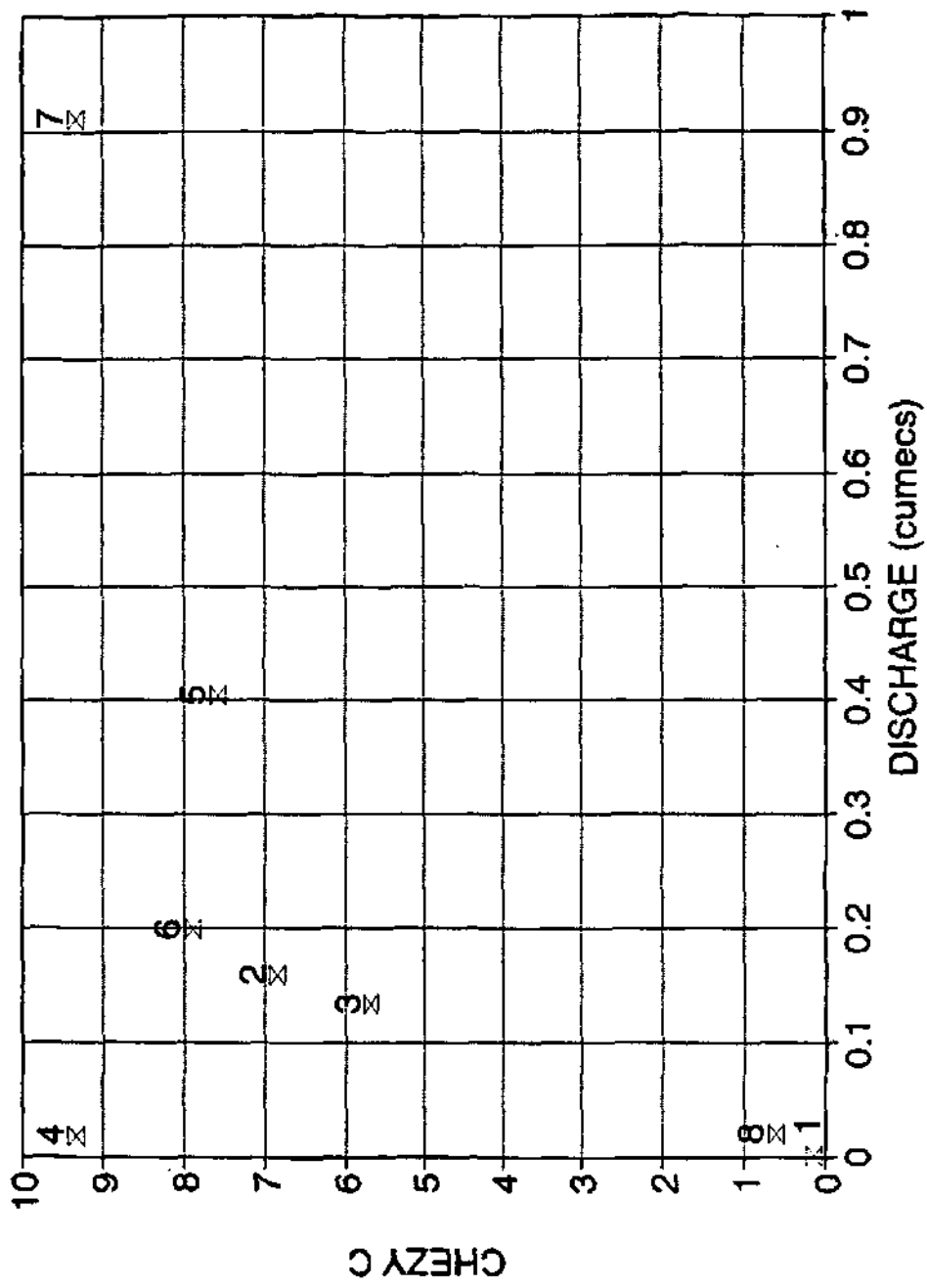


Figure 42: Chezy C quantification for bedrock distributaries. Numbers refer to individual distributaries.

Extreme flow resistance values are associated with very low flows of less than $0.05 \text{ m}^3\text{s}^{-1}$ and steep water surface slopes through fissures in the dolerite bedrock distributaries (Cheshire 1996) (Figures 40 to 42 and Table 8).

7.4 Comparison with flow resistance values reported in similar natural channel environments and quantification of components of flow resistance

Extremely high flow resistance coefficient values have been found on the Sabie River (Figures 34 to 42), particularly at a local scale in small bedrock distributaries, whereas alluvial reaches have generated traditionally recognised flow resistance magnitudes. Table 9 lists the range of Manning's n and Darcy-Weisbach f that have been quoted in channel flow resistance literature for a variety of fluvial environments.

The highest flow resistance coefficients measured at the reach scale were found over the bedrock anastomosing channel type. The extreme reach flow resistance occurs at a low discharge, where the flow is shallow and the cross sectional area is dissected by numerous protruding boulders on a 97% bedrock base, resulting in a tortuous wetted perimeter. Comparable environments, with water surface slopes of greater than 0.0165 and a high incidence of bedrock and boulders in channel have yielded high Manning's n values, for example, 0.27 (Hicks and Mason 1991) and Darcy-Weisbach f values in excess of 40 (Beven *et al.* 1979, Whittaker and Jaeggi 1982). The highest flow resistance value quoted in discussions of extreme flow resistance in natural channels was a friction factor of 1328 (Beven *et al.* 1979), which was recorded in a channel with waterfalls and plunge pools at a very low flow. This value is lower than one local bedrock distributary value on the Sabie River, which generated a friction factor f of 3733 (Figure 40). This value was recorded at a minimal discharge over a dolerite bedrock pavement dissected by fissures, which act as conduits for the flow. This creates a stepped pattern of rapids and pools, forming small scale bedrock cascades within the fissures. The extreme high values of flow resistance obtained by this study confirm that flow through bedrock channels is predominantly influenced by the irregular form of the long profile and that the skin resistance component is negligible, due to the absence of sediment. The flow is severely non-uniform and the resistance coefficients C , n and f are being used to accommodate and subsume the effects of energy dissipation due to hydraulic jumps and internal distortions resulting from bends, boulders, constrictions and other flow disturbances. Under such conditions conventional definitions of hydraulic and channel geometry parameters may not be applicable and equations 1 to 3 inappropriate, as their theoretical and empirical qualifications are not satisfied. Therefore, the absolute magnitudes of flow resistance calculated for low flows in bedrock distributaries must be treated with caution.

The large scale roughness and energy dissipation effect of the irregular bed becomes drowned out as discharge increases, as the flow resistance values decline steadily with increasing discharge for the bedrock anastomosing channel type reach, in addition to the bedrock distributary morphological units. During flood flows, the bedrock anastomosing reach flow resistance values decline markedly, to values indicative of more uniform channels. A vegetation flow resistance component is contributed from inundation of sparsely reeded bedrock core bars, producing flow resistance values within the range of reported vegetation flow resistance (Richards 1982, Bakry *et al.* 1992).

Table 9: Flow resistance coefficients for a variety of channel conditions

Author	Channel description	Manning's n	Friction factor f
Ven te Chow 1959	Vegetation infested	0.1	-
	Dense brush and willows	0.16(max)	-
	Cobble bottom	0.05(max)	-
Barnes 1967	Bedrock base with boulders. High slope, low depth	0.075	-
Bathurst 1978	Mountain stream, low flow	-	3.12(max)
Bathurst <i>et al.</i> 1981	Flume study, large scale roughness	-	4.79(max)
Richards 1982	Clean natural channel	0.03	0.072
	Weedy natural channel	0.07	0.4
	Mountain stream with boulders	0.05	0.196
Thorne and Zevenbergen 1985	Mountain stream, large boulders	0.11(max)	1.55(max)
Bathurst 1985b	Mountain river, high slope	-	0.65 5.46(max)
Hicks and Mason 1991	Boulder bed, low flow	0.27	-
	Large boulder and bedrock, high flow	0.2	-
Whittaker and Jaeggi 1982	Steep-pool mountain streams	-	44.9(max)
Beven <i>et al.</i> 1979	Waterfalls and plunge pools; low flow	-	1328(max)
	Straight, pools and cobbled riffles	-	48
Bridge and Gabel 1992	Low sinuosity, braided	-	0.07 0.13(max)
Bakry <i>et al.</i> 1992	Vegetation infested canals	0.05 0.074(max)	-
Hall and Freeman 1994	Flume study, dense vegetation	0.27 0.7(max)	-

The alluvial reaches, namely braided and single thread, have the lowest flow resistance values and tend, with medium range discharges, to values identical to those reported by authors investigating "clean natural channels" (Richards 1982). In particular, the braided reach compares favourably to other alluvial "low sinuosity braided channels" (Bridge and Gabel 1992). At low discharges of less than $10 \text{ m}^3\text{s}^{-1}$, the flow resistance values resemble the

lower range of values reported for cobble and some boulder bed channel environments (ven te Chow 1959, Barnes 1967, Richards 1982, Thorne and Zevenbergen 1985). The median grain diameter of the active channel sediments in this reach was just over 1mm and therefore not cobble sized. Although this reach is predominantly alluvial, isolated bedrock outcrops and boulders do disrupt the flow at low discharges. The percentage of the wetted perimeter covered by bedrock or boulders is generally less than 5% at this reach, but this is still likely to result in a higher flow resistance, if only at very low discharges and flow depths. High discharge ($650 \text{ m}^3\text{s}^{-1}$) stage data was collected at the braided reach, enabling flow resistance calculation. The flow resistance at this high discharge rises to a friction factor of 0.103, which is higher than the medium discharge range flow resistance values. The corresponding stage inundates 74.1% of the total macro-channel width in a single channel at cross section 12. The features inundated at $650 \text{ m}^3\text{s}^{-1}$ along this reach include heavily reeded macro-channel and seasonal lateral bars. The effect of channel form flow resistance will be minimal, as the braid bars and lateral bars become drowned out under several metres of flow. Therefore, this increase in flow resistance can only be attributed to vegetation flow resistance, although the actual flow resistance magnitude falls slightly below the range reported in flow resistance literature (Bakry *et al.*, 1992).

A braid bar morphological unit was isolated at a subreach within the braided channel type and flow resistance was quantified (Figures 37 to 39). The flow resistance magnitudes are similar to the braided reach values, but are slightly higher. This increase reflects an additional channel form flow resistance derived from the irregular cross sectional shape arising from the presence of the mid-channel braid bar.

Calculation of flow resistance over the whole single thread reach led to a marked increase in flow resistance at $20 \text{ m}^3\text{s}^{-1}$. This can partly be attributed to vegetational resistance of the fringing river cliff reeds and shrubs, but it is largely the result of a noticeable steepening of the water surface slope over the upstream half of the reach at this discharge (Reach 1, Figure 9). Inspection of the cross section profiles through this reach revealed a narrow, constricting section in the upstream portion of the reach. The width of the active channel will not constrict the flow at low discharges, but this effect will become important as the discharge increases. Therefore, the narrow cross section controls the water surface slope in the upstream sections of the single thread reach, leading to the observed increase in total flow resistance. A representative, reach flow resistance for single thread channels was re-calculated using the downstream half of the reach, so as to eliminate the constriction control upstream (Figures 34 to 36). The new, representative, single-thread reach values follow the same decreasing flow resistance trend with increasing discharge as the braided reach curve, to values similar to those in clean natural channels (Richards 1982). High discharge flow resistance could not be calculated at the single thread reach, due to a lack of stage data.

Mixed anastomosing and pool-rapid reach flow resistance coefficients show an almost identical trend of decline in value with discharge until mid range discharge, as the braided reach. However, the actual values are higher, being similar to those measured in mountain streams (Bathurst 1978, Thorne and Zevenbergen 1985, Bathurst 1985b). This corresponds to the greater presence of bedrock and boulders at these sections. At rapid morphological unit sections within the pool-rapid reach and throughout the mixed anastomosing reach, active distributaries are more than 70% bedrock or large boulders, creating large scale roughness and higher magnitude flow resistance. A slight increase in reach flow resistance is found over

the mixed anastomosing channel type at the $1000 \text{ m}^3\text{s}^{-1}$ flood, compared to the medium flow, flow resistance values. The stage at this discharge inundates every active and seasonal morphological unit, with only the macro-channel banks not inundated at site 20 (Table 10). This represents 75% of the total macro-channel width. The successive inundation of morphological units with increasing discharge (Table 10), is represented by the state of consecutive cross section points and corresponding morphologies as either "A", active or "NA", not active.

Table 10: Inundation pattern of morphological units at cross section 20 with increasing discharge

Discharge								
Distance	Elevation	5	20	40	60	80	1000	Morphology
0.01	206.03	NA	NA	NA	NA	NA	NA	Macro-channel bank
63.48	200.43	NA	NA	NA	NA	NA	A	Macro-channel bank
73.59	199.14	NA	NA	NA	NA	NA	A	Macro-ch mix dist
78.86	200.71	NA	NA	NA	NA	NA	A	Macro-ch lat bar
131.46	198.91	NA	NA	NA	NA	NA	A	Seasonal lat bar
163.66	199.27	NA	NA	NA	NA	NA	A	Seasonal levee
164.22	198.75	NA	NA	NA	A	A	A	Seasonal levee
169.02	198.34	NA	NA	A	A	A	A	Seasonal levee
178.53	197.02	A	A	A	A	A	A	Act alluvial dist
189.19	197.5	NA	A	A	A	A	A	Active braid bar
207.33	197.12	A	A	A	A	A	A	Active braid bar
224.74	196.96	A	A	A	A	A	A	Active mixed dist
232.69	197.96	NA	A	A	A	A	A	Seasonal lat bar
239.84	198.26	NA	NA	A	A	A	A	Seasonal lat bar
246.25	198.8	NA	NA	NA	A	A	A	Seasonal lat bar
282.59	198.9	NA	NA	NA	NA	A	A	Seasonal lat bar
308.31	199.45	NA	NA	NA	NA	NA	A	Seasonal levee
316.35	198.57	NA	NA	NA	NA	NA	A	Seasonal mix dist
365.13	201.38	NA	NA	NA	NA	NA	A	Macro-channel bank
465.77	206.08	NA	NA	NA	NA	NA	NA	Macro-channel bank

NA = Not active; A = Active

Inspection of inundation patterns for every cross section within reach 21 has shown that flow remains generally confined to unvegetated active distributaries at most sections at discharge $85 \text{ m}^3\text{s}^{-1}$. Therefore, at discharges lower than $85 \text{ m}^3\text{s}^{-1}$ the flow resistance is attributable to either large scale, channel form, or skin resistance. The seasonal alluvial anastomosing bars and lateral bars at the mixed anastomosing study sites are generally sparsely vegetated, although sections 20.1, 20.3, 21.2 and 22 have small, locally dense areas of *Phragmites mauritianus*. These morphological units are inundated at the high discharge of $1000 \text{ m}^3\text{s}^{-1}$, hence vegetation flow resistance will be introduced. At this high discharge, the flow depth is such that the effect of skin and large scale roughness will be minimal, so the increase in flow resistance can be attributed to the vegetation. This is confirmed by the fact that the flow resistance magnitude at discharge $1000 \text{ m}^3\text{s}^{-1}$ falls within the range, Manning's n 0.05-0.1, of vegetation flow resistance quoted by other authors (ven te Chow 1959, Richards 1982, Bakry *et al.* 1992).

An indication of the variation in flow resistance found at pool and rapid morphological units within the pool-rapid reach is given in Figures 37 to 39. The difference in flow resistance between the pool and rapid morphological units represents the non-uniformity of the long profile and is a manifestation of channel form flow resistance.

A summary of the reach and morphological unit scale flow resistance, over a range of discharges, is given in Table 11.

7.5 Transfer of the flow resistance values to independent sections

Reach flow resistance has been calculated at each of the five major channel types found on the Sabie River over a range of discharges (Section 7.2). To assess the applicability and generality of these flow resistance values to the morphological conditions investigated, stage-discharge relationships were synthesised at independent sites on the Sabie River, which had similar morphological characteristics to the study reaches. Two methods for synthesising stage-discharge relationships were used to compare with the actual, measured, rating curves at six independent cross sections. These methods are outlined below.

For cross sections where the rating relationship and cross section shape are known, cross sectional area, A and hydraulic radius R , can be calculated for a given stage. The friction slope S_f , was assumed to be the water surface slope between the independent cross section and the nearest upstream cross section, as no local slope information exists for the independent sites. A flow resistance that is representative of either the cross section shape parameters, for a given stage, or the discharge must be determined, to enable a new, synthesised discharge, Q^1 , to be calculated from equation 52.

$$Q^1 = \frac{A}{n} R^{\frac{2}{3}} S^{\frac{1}{2}} \quad (52)$$

The value for Manning's n in equation 52 was calculated by two methods.

Table 11: Summary of flow resistance coefficients calculated at a reach and at a morphological unit scale.

Scale and morphology	Discharge m ³ s ⁻¹	n	C	f
Bedrock distributary	0.001364	4.703551	0.145728	3733.177
	0.15839	0.117281	6.846849	1.69115
	0.133898	0.138383	5.677126	2.459839
	0.018461	0.071632	9.342399	0.908337
	0.404276	0.10573	7.587317	1.377169
	0.198381	0.101805	7.893636	1.272358
	0.911669	0.091066	9.341191	0.908571
	0.02052	1.199775	0.597837	221.8187
	Pool	1	0.146	5.766
5		0.136	6.486	1.866
10		0.102	8.846	1.003
20		0.0672	13.749	0.415
30		0.0523	18.195	0.237
40		0.0498	19.428	0.208
Rapid		1	1.414	0.659
	5	0.679	1.481	35.784
	10	0.449	2.298	14.866
	20	0.311	3.406	6.765
	30	0.266	4.061	4.758
	35	0.256	4.26	4.325
Cataract	5	0.137	6.604	1.8
	10	0.114	8.359	1.123
	20	0.0896	10.99	0.65
	30	0.0787	12.808	0.478
	40	0.0903	11.351	0.609
Braid bar	1	0.1056	7.631	1.3477
	5	0.0535	17.619	0.2528
	10	0.0319	30.911	0.0821
	20	0.0384	26.157	0.1147
	30	0.0309	32.72	0.0733
	35	0.0347	29.399	0.0908
Rapid	5	0.337	2.917	9.221
	10	0.229	4.377	4.097

	20	0.151	6.761	1.717
	30	0.116	8.897	0.992
	35	0.101	10.206	0.753
Reach braided	1	0.0772	10.407	0.725
	5	0.0549	16.649	0.283
	10	0.0448	21.49	0.17
	20	0.0363	27.394	0.105
	30	0.0325	31.031	0.0815
	35	0.0319	31.548	0.0789
Reach bedrock anastomosing	1	1.9388	481.417	0.4038
	5	0.7095	59.615	1.1474
	10	0.6074	38.45	1.4287
	20	0.4248	17.835	2.0977
	30	0.369	12.679	2.488
	40	0.39052	13.724	2.391
Reach pool-rapid	1	0.2951	2.946	9.044
	5	0.121	7.216	1.509
	10	0.117	7.784	1.295
	20	0.113	8.523	1.08
	30	0.0982	9.95	0.793
	40	0.0912	10.895	0.661
Reach mixed anastomosing	1	0.3062	2.674	10.976
	5	0.136	6.3	1.977
	10	0.107	8.017	1.221
	20	0.089	9.754	0.825
	30	0.0758	11.487	0.595
	40	0.0699	12.697	0.487
	60	0.0642	14.26	0.386
	80	0.0617	14.972	0.35
	1000	0.0779	14.609	0.368
Reach single thread	1	0.191	4.998	3.142
	5	0.129	7.779	1.297
	10	0.0826	12.492	0.503
	20	0.0406	25.902	0.117
	30	0.0265	40.287	0.0484
	35	0.0122	88.7	0.01

1) The discharge:flow resistance relationship was calculated directly, for all the channel types found on the Sabie River (Figures 34 to 36). These relationships were used to predict flow resistance at similar channel types for a given point on the rating curve.

2) Hydraulic radius, R:flow resistance relationships were established for the different channel type reaches studied (Figure 43). These relationships displayed distinct trends between the channel types and with change in hydraulic radius. Regression analysis was used to quantify the relationships. Therefore, for a given stage at an independent site, hydraulic radius could be calculated and fed into the hydraulic radius:flow resistance regression equation, to determine the representative flow resistance for the new cross section.

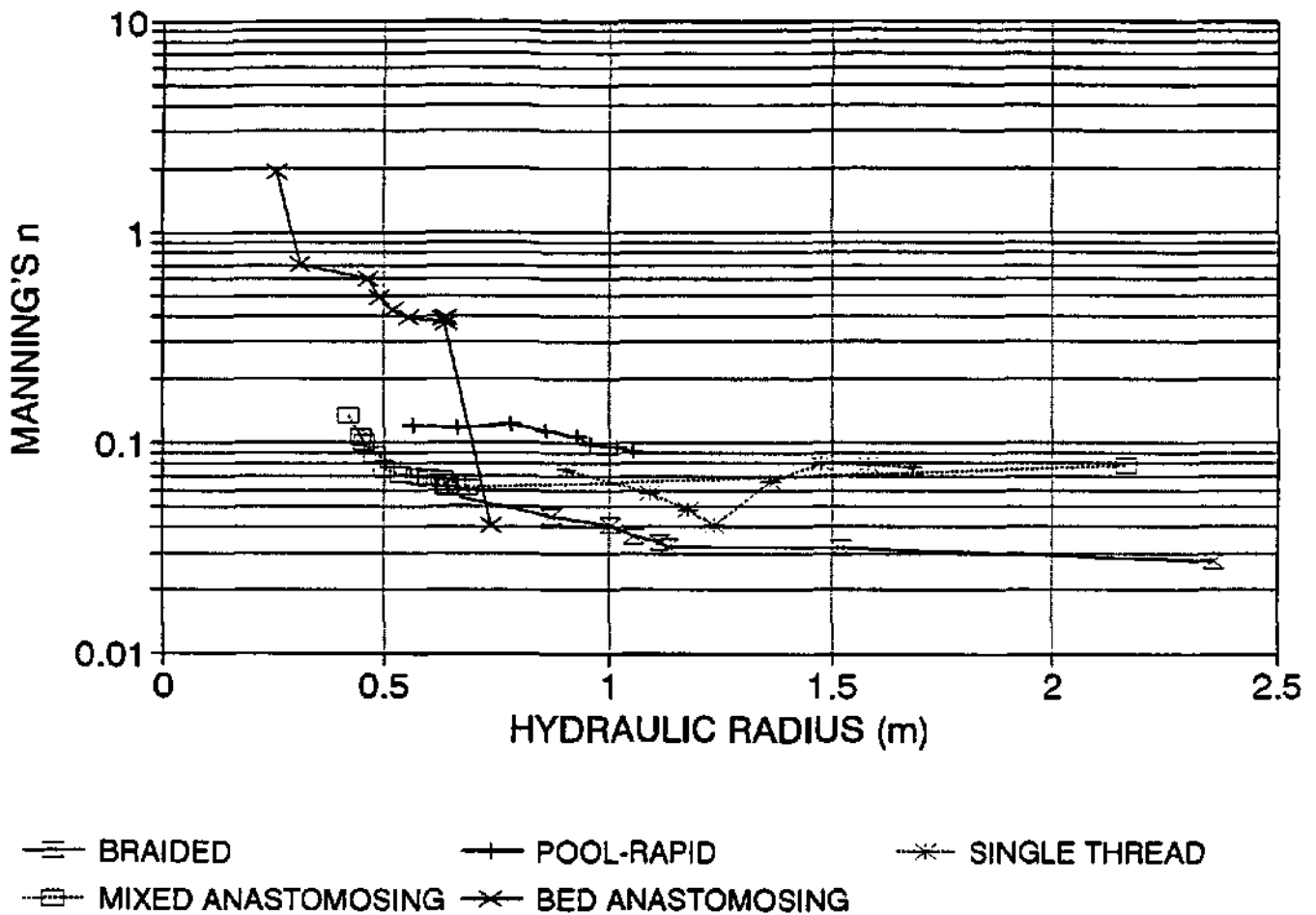


Figure 43: Manning's n:hydraulic radius relationship, for use in synthesising independent rating curves.

For a given stage at an independent cross section, therefore, estimates of Manning's n from two different methods, cross sectional area, hydraulic radius and slope can be used to synthesise a new discharge, Q' (equation 52) and thus a rating curve. A comparison of the actual, measured, rating curve and the two synthesised relationships for several channel types is given (Figures 44 to 49).

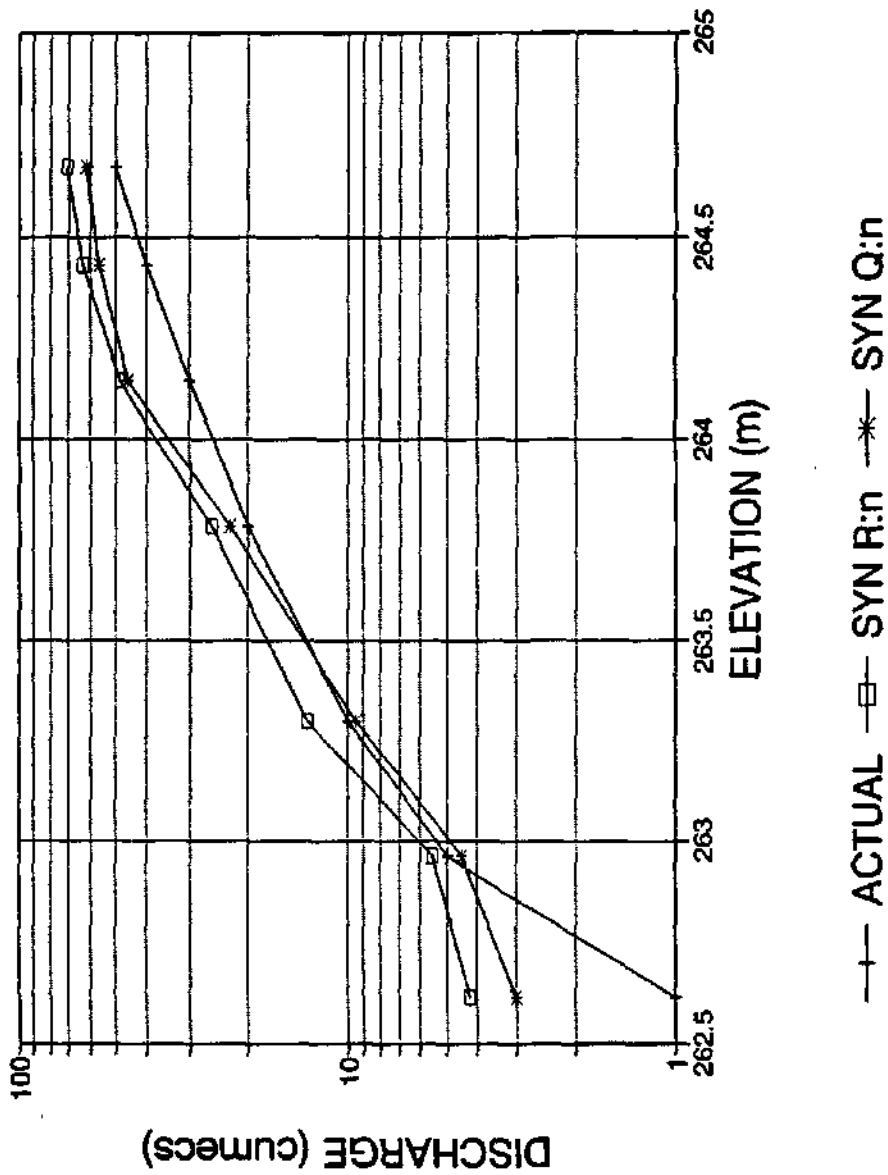


Figure 44: Synthesised rating curves (SYN) for the Narina study site, a braided cross section. The SYN R:n curve was synthesised using a hydraulic radius to flow resistance relationship; the SYN Q:n curve was synthesised using a discharge to flow resistance relationship.

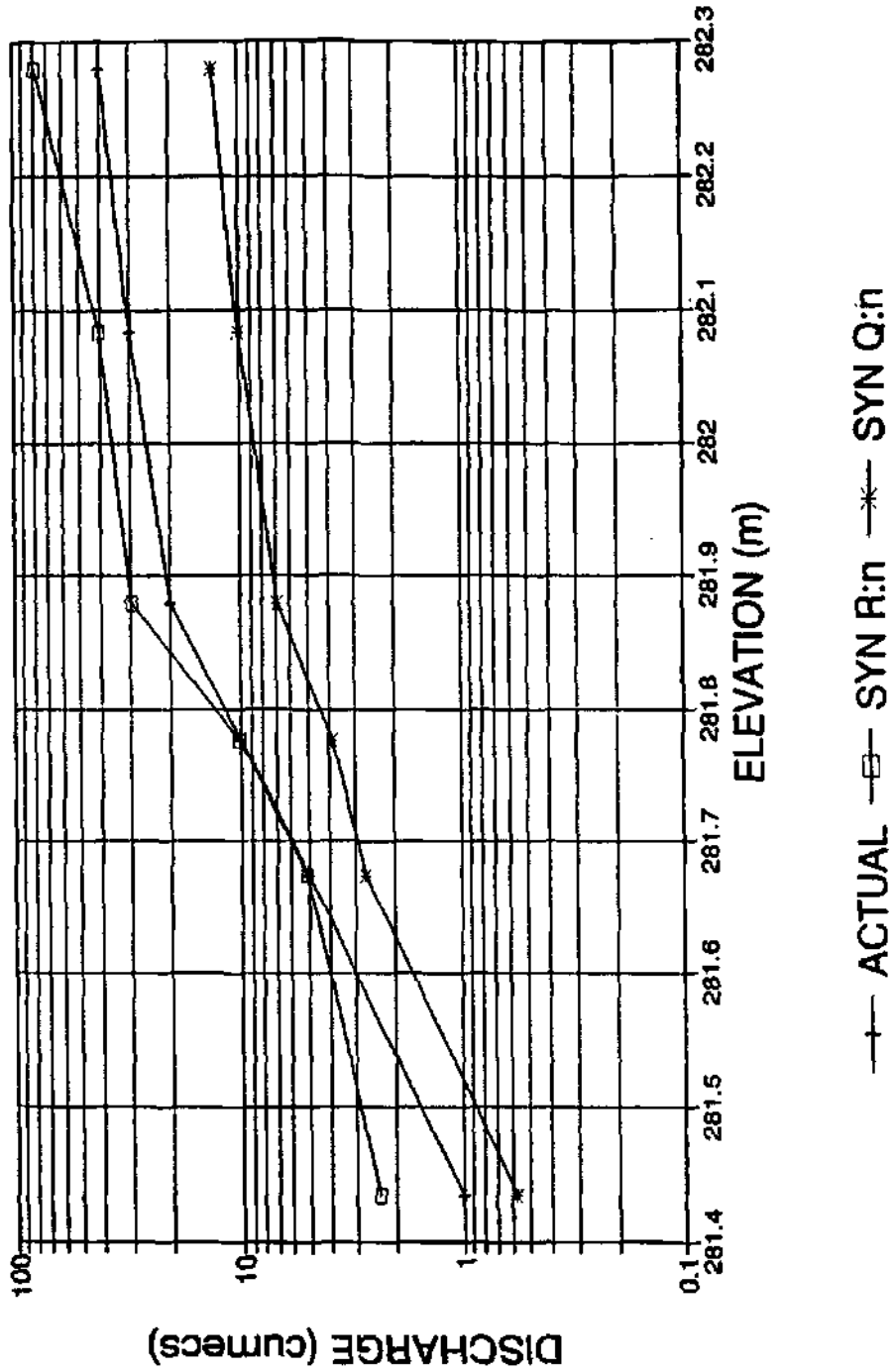


Figure 45: Synthesised rating curves (SYN) for Section 11, a bedrock anastomosing cross section. The SYN R:n curve was synthesised using a hydraulic radius to flow resistance relationship; the SYN Q:n curve was synthesised using a discharge to flow resistance relationship.

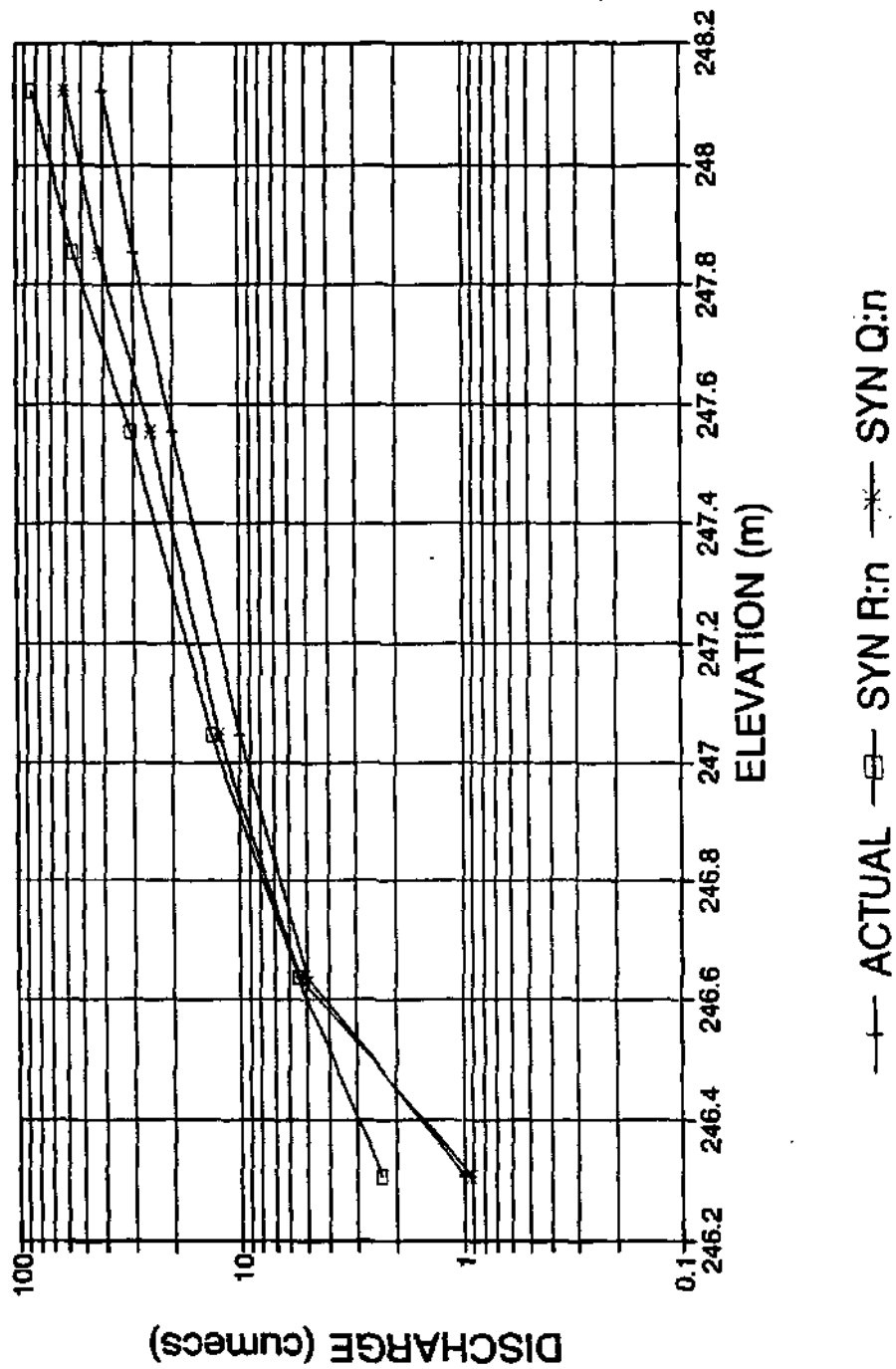


Figure 46: Synthesised rating curves (SYN) for Section 16, a pool-rapid cross section. The SYN R:n curve was synthesised using a hydraulic radius to flow resistance relationship; the SYN Q:n curve was synthesised using a discharge to flow resistance relationship.

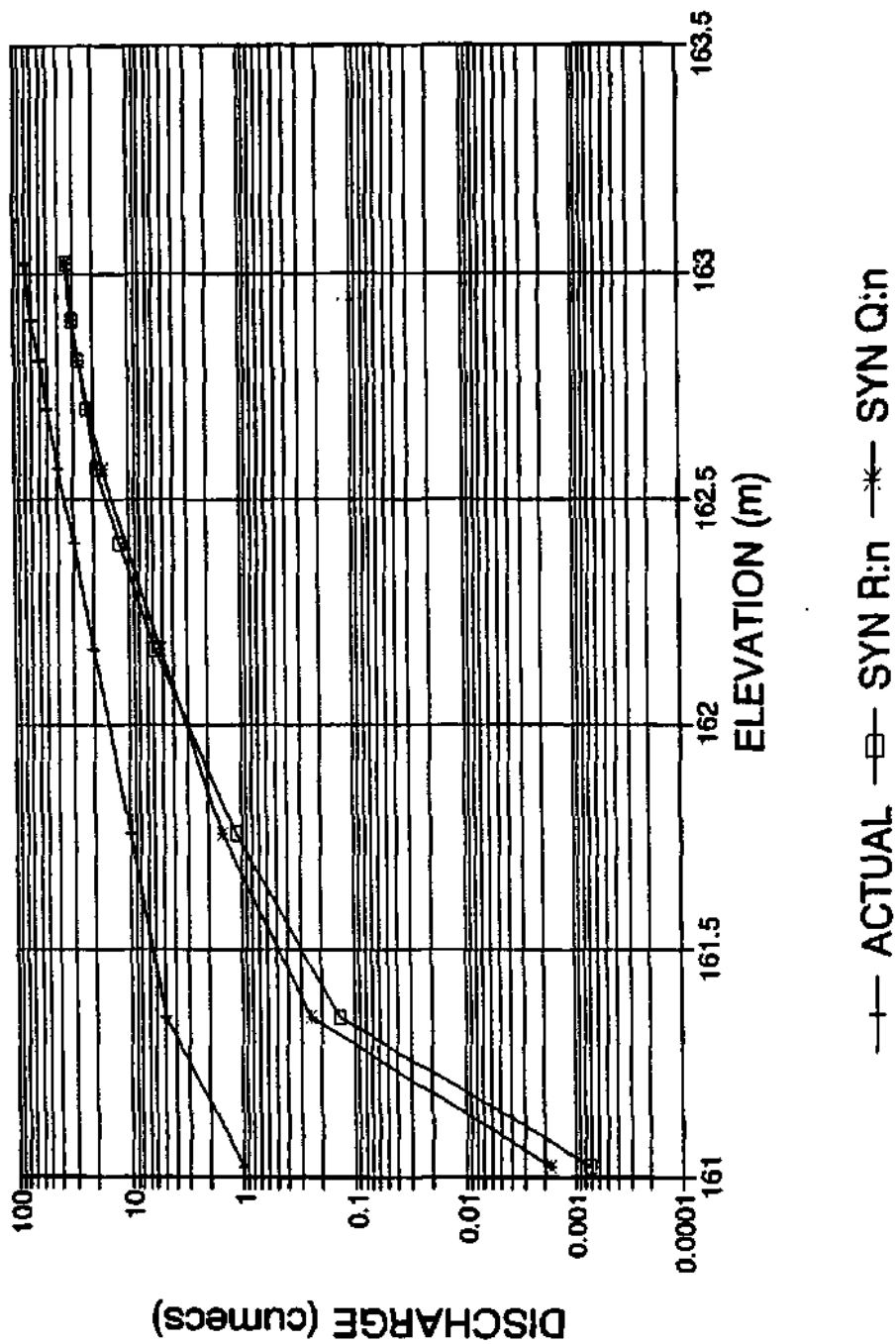


Figure 47: Synthesised rating curves (SYN) for Section 27, a mixed anastomosing cross section. The SYN R:n curve was synthesised using a hydraulic radius to flow resistance relationship; the SYN Q:n curve was synthesised using a discharge to flow resistance relationship.

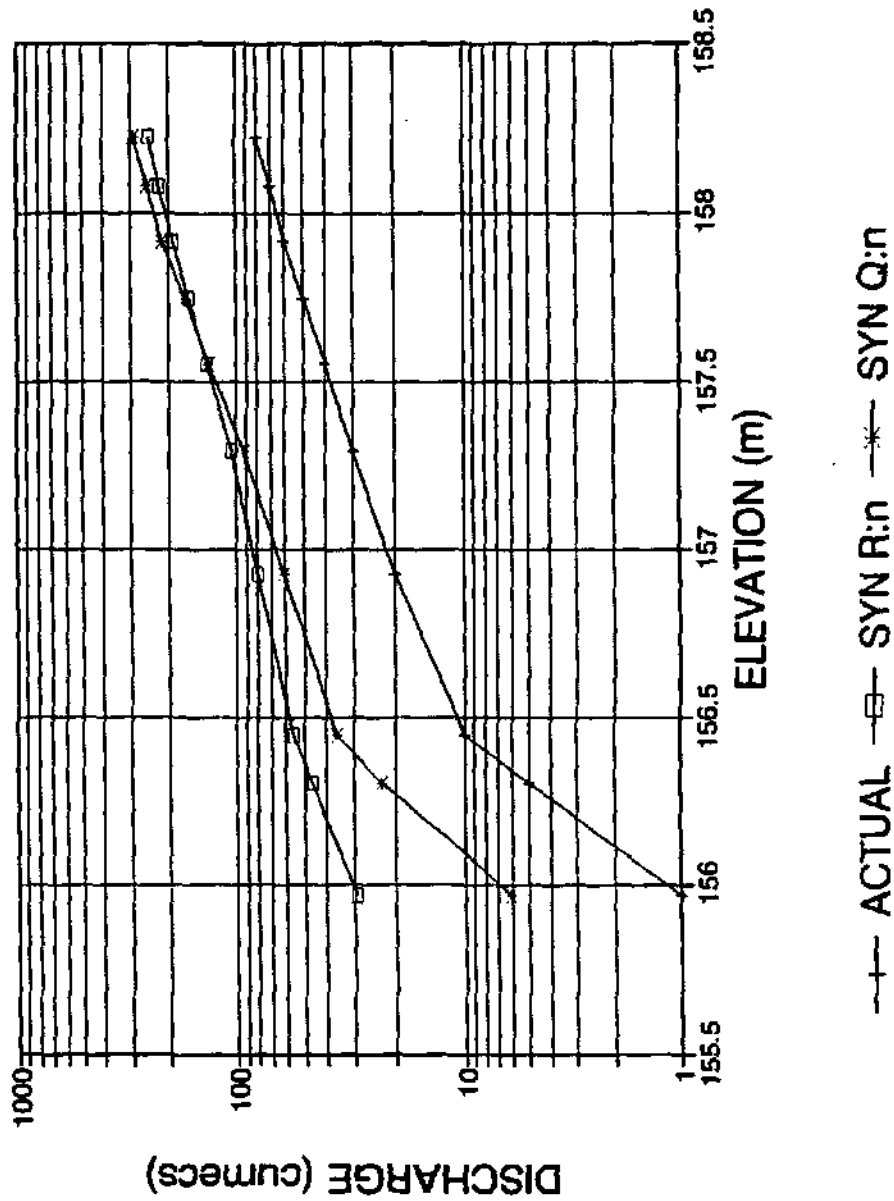


Figure 48: Synthesised rating curves (SYN) for Section 29, a mixed anastomosing cross section. The SYN R:n curve was synthesised using a hydraulic radius to flow resistance relationship; the SYN Q:n curve was synthesised using a discharge to flow resistance relationship.

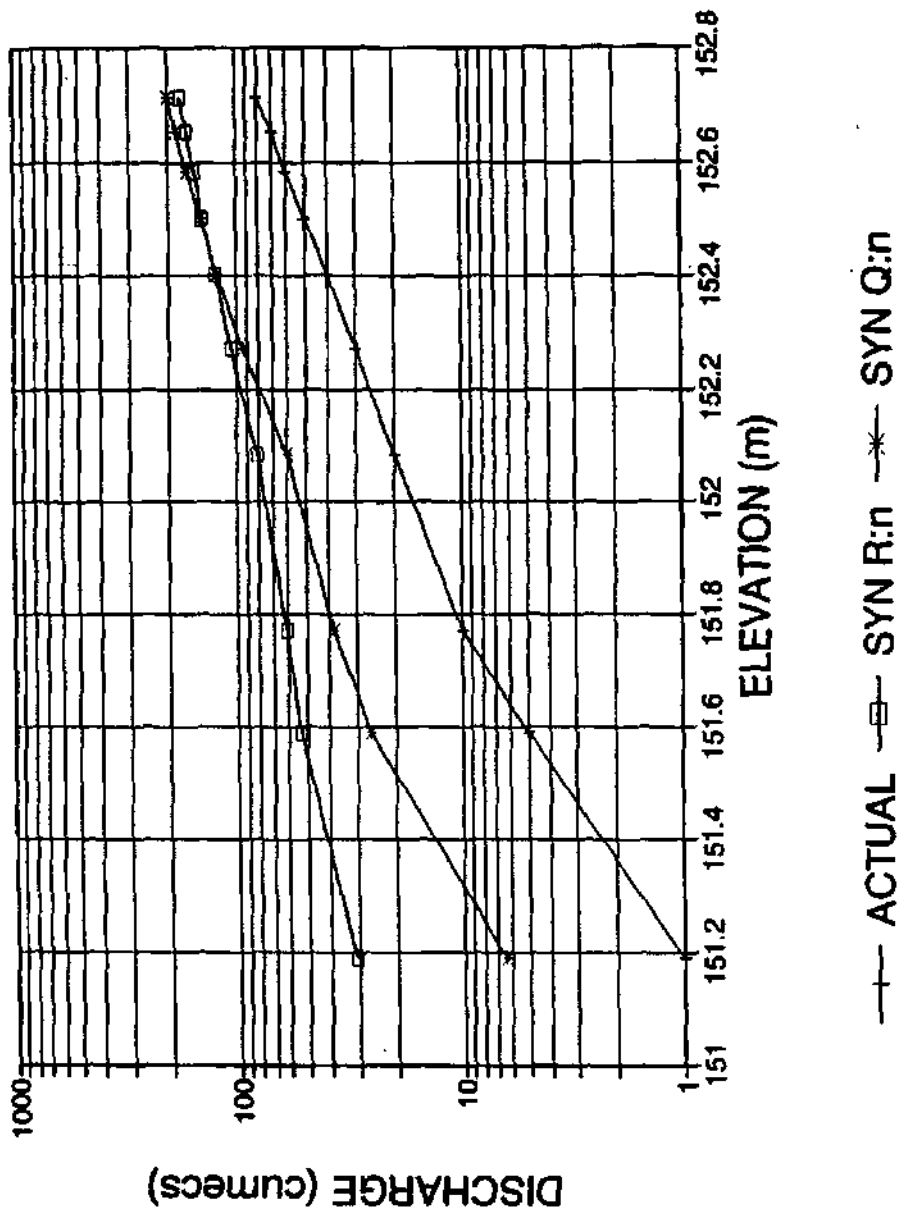


Figure 49: Synthesised rating curves (SYN) for Section 30, a mixed anastomosing cross section. The SYN R:n curve was synthesised using a hydraulic radius to flow resistance relationship; the SYN Q:n curve was synthesised using a discharge to flow resistance relationship.

The alluvial, braided synthesised rating curve (Figure 44) shows the closest fit to the actual data, with the predominantly alluvial, pool-rapid independent site showing a good fit also. The mixed anastomosing synthesised rating curves are generally a poor comparison to the actual curves, particularly at low discharges (Figures 47 to 49). This discrepancy is probably due to the use of the 'Horizontal' model to calculate hydraulic radius and cross sectional area at inappropriate cross sections, where numerous distributaries in a wide macro-channel create a markedly non horizontal water surface across a cross section. Individual water surface elevations are not known for the active distributaries at the independent sites, making application of the 'Non-Horizontal' model impossible. Misuse of the 'Horizontal' model at the mixed anastomosing sections will particularly affect low flow channel geometry parameters, where the difference in water elevations between active distributaries is at its greatest. It is the low flow synthesised rating curve points that deviate most from the actual curve, suggesting the misuse of the 'Horizontal' model is the cause of the deviation.

The use of water surface slope between the independent site and the nearest upstream rated cross section, to represent friction slope, is another inaccurate assumption, but the lack of detailed local stage data upstream and downstream from the independent site makes it a necessary one.

Generally, the Q:n synthesised rating curves fit to the actual data better than the R:n synthesised curves. The latter method is more dependent on site specific channel geometry conditions than the Q:n method, so transfer to independent sites will be more erroneous.

CHAPTER 8: CONCLUSIONS AND RECOMMENDATIONS

The 'Translating discharge into local hydraulic conditions on the Sabie River: an assessment of channel flow resistance' project provides a link between the data requirements of geomorphologists and biologists, and the constraints of water resource managers. This is achieved through the prediction of local hydraulic conditions from a known flow regime.

This report identifies and quantifies flow resistance over the range of fluvial environments encountered on the Sabie River, many of which experience hydraulic conditions which have previously been unstudied.

The principal conclusions that have been reached in this study are:

- 1) The Sabie River has a diverse set of morphological units which form associations, termed channel types. Each morphological unit has a variety of complexly interacting flow resistance components.
- 2) The interaction of multiple resistance components precludes quantitative isolation of the individual components, therefore total flow resistance was calculated.
- 3) Four physical scales for resistance analysis have been proposed, following the geomorphological hierarchy (van Niekerk *et al.*) and the physical, spatial scale of resistance components, namely, at reach, subreach, cross section and distributary scales.
- 4) Conventional methods for assessing hydraulic and channel geometry parameters in alluvial cross sections were found to be accurate.
- 5) Non horizontal water surface elevations in distributaries across bedrock influenced cross sections, led to errors of up to 2500% in the prediction of average velocity, if the conventional horizontal water surface was used to calculate hydraulic and channel geometry parameters. Therefore, these parameters, for use in flow resistance quantification, were predicted using a 'Non-Horizontal' model in bedrock reaches.
- 6) Testing of the 'Non-Horizontal' model has shown a large reduction in maximum depth prediction error, when using the 'Non-Horizontal' model, when compared to the 'Horizontal' model.
- 7) Flow resistance quantification at the bedrock anastomosing channel type and at bedrock morphological units has produced extreme, unique magnitudes of flow resistance, at low discharges. These high resistance values suggest that the widely used flow resistance equations, Darcy-Weisbach, Chezy and Manning's, are inappropriate for use in bedrock fluvial environments at low flows. Under these conditions the flow resistance coefficients are reflecting energy dissipations due to hydraulic jumps and internal distortions.

- 8) High discharge flow resistance at all the channel types investigated reflect the influence of vegetation on the inundated seasonal and macro-channel features.
- 9) Independent testing of the flow resistance reach values, in similar geomorphic environments produced a good correlation in synthesised rating curves at alluvial cross sections. However, there was a poor correlation in bedrock influenced sections, which was probably due to lack of data precluding the use of the 'Non-Horizontal' model to predict hydraulic and channel geometry variables at these sections.

8.1 Uses of the products of this research

The products of this research form three major output areas:

- 1) Appropriate methodologies for establishing a monitoring network, enabling hydraulic and channel geometry data to be collected at a number a physical scales.
- 2) Conceptual models to predict hydraulic and channel geometry data in both alluvial and bedrock influenced, multiple channel sections. This can be used to model channel behaviour over all channel environments, from fully bedrock through mixed channels, to fully alluvial.
- 3) This investigation has generated a large data base of flow resistance coefficients over a range a physical scales and fluvial environments, in addition to hydraulic and channel geometry data. Quantification of the flow resistance coefficients has aided an assessment of channel dynamics (Heritage *et al.* 1996) hence, biotic change (Figure 1) and flow resistance values have been successfully transferred to other reaches (Birkhead *et al.* 1996). These uses of the outputs from this research form integral components of the Kruger National Park Rivers Research Programme (Figures 1 to 3) and are of use to a variety of river scientists.

8.2 Recommendations for further research

Limited calibration and testing of the 'Non-Horizontal' model has been possible for this project and has highlighted errors involved in the prediction of channel geometry variables. Further testing, leading to better calibration and refinement of the model is a priority for further research. Measurement of rating curves, over a range of discharges, at each distributary in a cross section is necessary, to test the model rigorously.

8.3 Guidelines

Knowledge arising from the 'Translating discharge into local hydraulic conditions on the Sabie River: an assessment of channel flow resistance' project, has led to the following guidelines, which are suggested as an appropriate methodology for quantifying flow resistance in environments similar to those found on the Sabie River.

- 1) Use the 'Horizontal' model to predict hydraulic and channel geometry parameters in alluvial sections.

- 2) Use the 'Non-Horizontal' model to predict hydraulic and channel geometry parameters in bedrock influenced sections.
- 3) Apply Barnes (1967) methodology to quantify multi-section reach flow resistance over a variety of scales.
- 4) The reach or channel type flow resistance values reported in this project can be reliably transferred to similar channel environments. However, the bedrock morphological unit resistance values need to be treated with caution, as the flow resistance values obtained represent major energy dissipation due to hydraulic jumps and other flow disturbances. Under such conditions conventional definitions of hydraulic and channel geometry parameters may not be applicable and equations to quantify flow resistance may be invalid.

REFERENCES

- Abdelsalam M.W., Khattab A.F., Khalifa A.A. and Bakry M.F. (1992) Flow capacity through wide and submerged vegetal channels, *J. Irrig. and Drainage Eng.*, ASCE, 1992, Vol. 118, No. 5, 724-732.
- Alam, A.M.Z., Cheyer, T.F. and Kennedy, J.F. (1966) Friction factors for flow in sand bed channels. *Hydrodynamics Lab. Rep. No. 78*, Massachusetts Instit. Tech., Cambridge, Mass..
- Allen, J. (1939). The resistance to flow of water along a tortuous stretch of river and in a scale model of the same. *J.Inst. Civ. Eng. (London)*, 11 (5161), 115-132.
- Bagnold, R.A. (1960). Some aspects of the shape of river meanders. *U.S. Geol. Surv. Prof. Paper 282-E*, U.S. Geol. Surv., Washington, D.C., 135-143.
- Bakry, M.F., Gates, T.K. and Khattab, A.F., (1992) Field measured hydraulic resistance characteristics in vegetation infested canals. *J. Irrig. and Drainage Eng.*, ASCE, 118 (2), 256-274.
- Barnes, H.H. (1967) Roughness characteristics of natural channels. *U.S. Geo. Surv. Water Supply Paper 1849*, U.S. Geol. Surv., Washington, D.C., 1-9.
- Bathurst, J.C. (1978) Flow resistance of large scale roughness. *J. Hydr. Engrg.*, ASCE, 104 (HY12), 1587-1603.
- Bathurst, J.C. (1981). Discussion of Bar resistance of gravel bed streams. *J. Hydr. Engrg.*, ASCE, 107 (10), 1276-1278.
- Bathurst, J.C. (1982). Theoretical aspects of flow resistance. In "Gravel Bed Rivers." Eds Hey, R.D, Bathurst, J.C. and Thorne, C.R., Wiley and Sons Ltd., Chichester, England, 83-105.
- Bathurst, J.C. (1985a) *Literature review of some aspects of gravel bed rivers*. Instit. Hydrology, Wallingford, Uk.
- Bathurst, J.C. (1985b) Flow resistance estimation in mountain rivers. *J. Hydr. Engrg.*, ASCE, 111 (4), 625-643.
- Bathurst, J.C., Thorne, C.R. and Hey, R.D. (1979) Secondary flow and shear stress at river bends. *J. Hydr. Div.*, ASCE, 105 (HY10), 1277-1293.
- Bathurst, J.C. Li, R.M. and Simons, D.B. (1981) Resistance equation for large scale roughness. *J. Hydr. Engrg.*, ASCE, 107 (HY12), 1593-1613.
- Beven, K., Gilman, K. and Newson, M. (1979) Flow and flow routing in upland channel networks. *Intl. Ass. Hydrol. Sci., Hydrol. Sci. Bull.*, 24 (3), 303-325.

Birkhead, A.L, Olbrich, B.W., James, C.S. and Rogers K.H. (1996). Developing an integrated approach to predicting water use of riparian vegetation. WRC Report No. K5/474/0/1.

Bray, D.I. (1979) Estimating average velocity in gravel bed rivers. **J. Hydr. Div., ASCE**, 105 (HY9), 1103-1122.

Bridge, J.S. and Gabel, S.L. (1992) Flow and sediment dynamics in a low sinuosity, braided river: Calamus River, Nebraska Sandhills. **Sedimentology**, 39, 125-142.

Brownlie, W.R. (1983) Flow depth in sand-bed channels. **J. Hydr. Div., ASCE**, 109 (7), 959-990.

Burkham, D.E. and Dawdy, D.R. (1976) Resistance equation for alluvial channel flow. **J. Hydr. Div., ASCE**, 102 (10), 1479-1489.

Cheshire, P. (1996) Geology and geomorphology of the Sabie River, Kruger National Park and its catchment area, Water Research Commission Report No. k5/376/0/3.

Church, M., Wolcott, J. and Maizels, J. (1990). PalaeoveLOCITY: a parsimonious proposal. **Earth Surface Processes and Landforms**, 15, 475-480.

Cook H.L. and Campbell F.B. (1939) Characteristics of some meadow strip vegetations, **Agricultural Engineering**, Vol. 20, 345-348.

Cowan W.L. (1956) Estimating hydraulic roughness coefficient, **Ag. Eng.**, Vol 37, 473-475.

Eastgate W. (1969) Vegetated stabilisation of grassed waterways and dam bywashes, **Water Research Foundation of Australia, Bull.** 16.

Einstein, H.A. and Barbarossa, N. (1952) River channel roughness. **Trans ASCE**. 117, 1121-1146.

El-Hakim, D. and Salama, M.M. (1992) Velocity distribution inside and above branched flexible roughness. **J. Irrig. and Drainage Eng.**, ASCE, 118, 6, 914-927.

"Friction factors in open channels." (1963) Progress report of the Task Force on Friction Factors in Open Channels of the Committee of Hydromechanics, Hyd. Div., **J. Hydr. Div., ASCE**, 89 (HY2), Proc. Paper 3464, 97-143.

Hall, B.R. and Freeman, G.E. (1994) Study of hydraulic roughness in wetland vegetation takes new look at Manning's n. **Bull. Wetlands Res. Prog.**, 4, 1, 1-4.

Hammer D.E. and Kadlec R.H. (1986) A model for wetland surface water dynamics, **Water Resources Research**, Vol. 22, No. 13, 1951-1958.

Heritage, G.L. and van Niekerk, A.W. (1994) Morphological response of the Sabie River to changing flow and sediment regimes. **Proc. 50 years of Water Engineering in South Africa SAICE**, Johannesburg, 389-402.

Heritage, G.L., van Niekerk, A.W. & Moon, B.P. (1995) Classifying bedrock influenced semi-arid river systems: extending the continuum concept. In: **Proc. Int. Ass. of Geomorphologists South East Asia Conf. on Geomorphology: Abstracts**, June 1995, Singapore.

Heritage, G.L., van Niekerk, A.W., Moon, B.P., Broadhurst, L.J., Rogers, K.H. and James, C.S. (1996) Geomorphological response to the changing flow regimes of the Sabie and Letaba River systems. WRC Report No. K5/376/0/1.

Hey, R.D. (1979) Flow resistance in gravel bed rivers. **J. Hydr. Div., ASCE**, 104 (6), 869-885.

Hey, R.D. (1988) Bar form resistance in gravel bed rivers. **J. Hydr. Div., ASCE**, 114 (12), 1498-1508.

Hicks, D.M. and Mason, P.D. (1991) In: **Roughness characteristics of New Zealand rivers**. Water Res. Survey, DSIR, 1-13.

Hydraulics Research (1985) Hydraulic roughness of vegetated channels. Report No. SR36. Hydraulics Research, Wallingford, England.

Hydraulics Research (1992) Hydraulic roughness of vegetated channels. Report No. SR305. Hydraulics Research, Wallingford, England.

Jadhav, R.S. and Buchberger S.G. (1994) Modelling flow through dense vegetation in free surface constructed wetlands. In: **Proc. 14th Annual Am. Geophys. Union, "Hydrology Days"**, April 1994, Colorado State University, Fort Collins, Colorado. Hydrology Days Publications, Atherton, California. Ed: H.J. Morel-Seytoux, 165-176.

Jarrett, R.D. (1984) Hydraulics of high gradient streams. **J. Hydr. Engrg., ASCE**, 110 (11), 1519-1539.

Kadlec, R.H. (1990) Overland flow in wetlands- vegetation resistance, **J. Hyd. Eng., ASCE**, Vol. 116, No. 5, 691-706.

Keulegan G.H. (1938) *Laws of turbulent flow in open channel*, **J. of Research, Pap. RP1151**, US Nat. Bureau Standards, Vol. 21, 707-741.

Klaassen G.J. and van der Zwaard J.J. (1974) Roughness coefficients of vegetated flood plains, **J. Hyd. Res.**, Vol. 12, No. 1, 43-63.

Kouwen, N. (1988) Field estimation of the biomechanical properties of grass, **J. Hyd. Res.**, Vol. 26, No. 5, 559-568.

- Kouwen, N. (1992) Modern approach to design of grassed channels, **J. Irrig. and Drainage Eng.**, ASCE, Vol. 118, No. 5, 733-743.
- Kouwen N. and Li R-M. (1980) Biomechanics of vegetative channel linings, **J. Hyd. Div.**, ASCE, Vol. 106, No. HY6, 1085-1103.
- Kouwen, N. and Unny, T.E. (1973) Flexible roughness in open channels. **J. Hyd. Div.**, ASCE, 99, HY5, 713-728.
- Kouwen N., Unny T.E. and Hill H.M. (1969) Flow retardance in vegetated channels, **J. Irrig. and Drainage Div.**, ASCE, Vol 95, No. IR2., 329-342.
- Kouwen N., Li R-M and Simons D.B. (1981) Flow resistance on vegetated waterways, **Trans ASAE**, Vol. 21, 684-690.
- Larsen T., Frier J-O. and Vestergaard K. (1990) Discharge/stage relations in vegetated Danish streams, In: **Proc. of International Conference on river flood hydraulics**, 187-195.
- Leopold, L.B., Bagnold, R.A, Wolman, M.G. and Brush, L.M. (1960). Flow resistance in sinuous or irregular channels. **Prof. Paper 282D**, US. Geol. Surv., Washington DC, 111-134.
- Li R-M and Shen H.W. (1973) Effect of tall vegetation on flow and sediment, **J. Hyd. Div.**, ASCE, Vol. 99, No. HY5, 793-814.
- Limerinos, J.T. (1970) Determination of the Manning coefficient for measured bed roughness in natural channels. **Water Supply Paper 1898-B**, U.S. Geol. Surv., Washington, D.C..
- Maheshwari, B.L.(1992) Suitability of different flow equations and hydraulic resistance parameters for flows in surface irrigation, **Wat. Res. Res.**, Vol 28, No 8, 2059-2066.
- Miller, B.A. and Wenzel, H.G. (1985). Analysis and simulation of low flow hydraulics. **J. Hydr. Div.**, ASCE, 111 (12), 1429-1446
- Moon, B.P., van Niekerk, A.W., Heritage, G.L. (in press). A geomorphological approach to the management of the rivers in the Kruger National Park: the case of the Sabie River. **Trans. Instit. British Geographers**.
- Nikuradse, J. (1933). **Stromungsgesetze in Rauhen Rohren**. (Laws of flow in rough pipes.), **Forschungsheft Verein duetscher Ingenieure**, 361.
- Parker, G. and Peterson, A.W. (1980). Bar resistance of gravel-bed rivers. **J. Hydr. Div.**, ASCE, 106 (10), 1559-1575.
- Petryk S. and Bosmajjian G. (1975) Analysis of flow through vegetation, **J Hyd. Div.**, ASCE, Vol. 101, No. HY7, 871-884.

- Prandtl, L. (1952). **Essentials of Fluid Dynamics**. Blackie, London, 452pp.
- Ree W.O., Wimberley F.L. and Crow F.R. (1977) Manning n and the overland flow equation, **Trans. ASAE**, 1977, Vol. 20, 89-95.
- Richards, K. (1982) **Rivers: Form and Process in Alluvial Channels**. Methuen, London.
- Rogers, K.H., Pullen, R.A., O'Keeffe, J.H. and Moon, B.P. (1992) An integrated programme for research on the Kruger National Park rivers. Unpublished report.
- Smith, R.J., Hancock, N.H. and Ruffini, J.L. (1990). Flood flow through tall vegetation, **Ag. Wat. Mngmt.**, Vol. 18, 317-332.
- Streeter, V.L. (1942) The kinetic energy and momentum correction factors for pipes and for open channels of great width. **Civ. Eng.**, 12 (4), 212-213.
- Strelkoff T. and Fangmeier D.D. (1974). Discussion of Flow resistance from cylindrical roughness, by Nanji S. and Wu I., **J. Irrig. Drain. Div.**, ASCE, 1974, Vol. 100, 390-393.
- Thompson G.T. and Roberson J.A., (1976). A theory of flow resistance for vegetated channels. **Trans. Am. Soc. Agr. Engrs.**, Vol. 19, No. 2, 288-293.
- Thompson, S.M. and Campbell, P.L. (1979). Hydraulics of a large channel paved with boulders. **J. Hydr. Res.**, 17 (4), 341-354.
- Thorne, C.R. and Zevenbergen, L.W. (1985) Estimating mean velocity in mountain rivers. **J. Hydr. Eng.**, ASCE, 111 (4), 612-624.
- Turner, A.K. and Chanmeesri, N. (1984) Shallow flow of water through non-submerged vegetation. **Ag. Wat. Mngmt.**, 8, 375-385.
- Turner, A.K., Langford, K.J., Myo win and Clift, T.R. (1978) Discharge depth equation for shallow flow. **J. Hyd. Div.**, ASCE, 104, 95-110.
- USDA (1954), **Handbook of channel design for soil and water conservation**. US Soil Conservation Service, Washington DC, No. SCS-TP61, 1-34.
- van Collier, A.L., Heritage, G.L. and Rogers, K.H. (1995) Linking riparian vegetation distribution and flow regime of the Sabie River through fluvial geomorphology. In: **Proc. of Seventh S. African Nat. Hyd. Symposium.**, Ghramestown, South Africa.
- van Collier, A.L., Rogers, K.H. and Heritage, G.L. (Submitted) Linking riparian vegetation types and fluvial geomorphology along the Sabie River within the Kruger National Park. **African J. Ecology**.

van Niekerk, A.W. and Heritage, G.L. (1993) **Geomorphology of the Sabie River: overview and classification.** Centre for Water in the Environment Report No. 2/93. University of the Witwatersrand, Johannesburg.

van Niekerk, A.W., Heritage, G.L. and Moon, B.P. (1995) **River classification for management: the geomorphology of the Sabie River in the E. Transvaal.** S. A. Geog. J.

Ven te Chow (1959) **Open Channel Hydraulics.** McGraw Hill, Tokyo, 680pp.

Von Karman, T. (1930) **Mechanical similarity and turbulence.** Proc. Third Int. Congress of Applied Mechanics, Stockholm, Sweden, Vol. 1, 85-92.

Wadson, R. and Rowntree, K. (1995) **A hierarchical geomorphological model for classification of South African river systems.** In: **Classification of Rivers and Environmental Health Indicators.** Ed: Uys, M.C., Water Research Commission, S. Africa, Report No. TT63/94, Proc. of joint S. African-Australian workshop, February 1995, Cape Town, 49-67.

Whittaker, J.G. and Jaeggi, M.N.R. (1982) **Origin of step-pool systems in mountain streams.** J. Hyd. Div., ASCE, 108 (HY6), 758-773.

Wolman, G.M. (1954). **A method of sampling coarse river bed material.** Trans. Am. Geophys. Union, 35 (6), 951-956.

NOTATION

a	Hydraulic cross section shape parameter (Hey 1979)
A	Channel cross sectional area
A_{BED}	Area of bed
A_F	Total wetted frontal area of boulders protruding through the free surface
A_i	Exposed vegetation area
A_N	Projected area normal to the flow
B	Boundary characteristics (Prandtl-von Karman 1952)
C	Chezy's roughness coefficient
C_D	Vegetation drag coefficient
C_{D0}	Cylinder drag coefficient
C_E	Local expansion and contraction coefficient (Miller and Wenzel 1985)
C_o	Keulegan roughness coefficient
d	Mean depth
d'	Average depth defined by actual cross sectional area of flow, excluding roughness element frontal area and dividing by water surface width
d_m	Maximum depth
Δ	Average depth of free water
D	Roughness height
D_b	Bar form roughness height
D_g	Grain roughness height
D_n	n% of sediment sample less than or equivalent to D_n
D_s	Stem diameter
D_t	Total roughness height
EI	Flexural rigidity of the vegetation stem
f	Darcy-Weisbach roughness coefficient
F	Drag force around cylinders
F_R	Froude number
g	Gravitational acceleration
G	Coefficient of flow resistance, independent of slope
h	Water surface elevation
h_f	Head loss due to boundary friction
h_v	Velocity head
i	Coefficient dependent on the extent the vegetation is bent
I	Mean depth (Bathurst 1981)
I_0	Residual depth
j	Coefficient dependent on the extent the vegetation is bent
k	Energy loss due to acceleration or deceleration coefficient
k_e	Coefficient describing the geometry of the surface
k_s	Equivalent roughness height
L	Reach length
m	Number of cross sections in reach
M	Stem density
n	Manning's roughness coefficient
n_b	Manning's n in absence of vegetation
p	Length of vegetation

P	Wetted perimeter
q	Subarea discharge
Q	Discharge
Q_G	Hypothetical discharge due to grain resistance
r	Subscript to denote riffle data
R	Hydraulic radius
R'	Subreach average velocity
R_D	Stem Reynold's number
R_E	Reynold's number
S_f	Friction slope
S_{FM}	Energy losses due to from resistance (Miller and Wenzel 1985)
S_L	Local energy losses due to flow contraction and expansion
S_x	Chainage of study site x
S_{50}	Median vertical axis of boulders
t	Exponent to reflect degree of mixing in the flow
T_x	Time flood peak passes weir x
v	Subarea velocity
V	Mean velocity
V'	Subreach average velocity
V_o	Average superficial velocity
V_{max}	Maximum velocity
V^*	Shear velocity
V^*_{crit}	Critical shear velocity
w	Width of subarea
W	Width of channel
W_x	Chainage of weir x
X	A factor equal to $AR^{1/2}$
y	Distance from bed boundary
y'	Perpendicular distance from channel perimeter to point of maximum velocity
Y	A factor equal to A^2R
Y_{50}	Median cross stream axis of boulders
Z	A factor equal to $AR^{2/3}$
α	Velocity head coefficient
γ	Unit weight of water
σ	Standard deviation of bed material size distribution
ν	Kinematic viscosity
ν	Local velocity
κ	von Karman's universal constant
ρ	Density
λ	Imperial or S.I. units correction factor
λ_E	Roughness concentration of exposed roughness elements
θ	Fitted parameters in the discharge-depth equation (Smith <i>et al.</i>)
ϵ	Fitted parameters in the discharge-depth equation (Smith <i>et al.</i>)
ω	Fitted parameters in the discharge-depth equation (Smith <i>et al.</i>)
ϕ	Exponent to reflect vertical stem density gradient
τ_0	Total boundary shear
Ψ	Bottom elevation distribution (Kadlec 1980)

APPENDIX 1: LOCATION OF BENCHMARKS AND FLOW MONITORING STATIONS FOR THE CHANNEL FLOW RESISTANCE INVESTIGATION

REACH 1

This single thread active channel flows over alluvial deposits for the central sections 0.1A to 1.0. Bedrock outcrops as rapids and cascades upstream of 0.1A and downstream of 1.0. The macro-channel consists of a series of alluvial terraces, which may represent a former meander pattern. Site accessed from 536 Hazyview Road. Turn left immediately before the Sabie River bridge. Follow track along river to first farm gate on left (section 0.0). Due to narrowing of cross section at section 0.2, representative single thread reach taken to be sections 0.4 to 1.0.

REACH 4

The reach, from sections 4.2 to 4.7, is a bedrock anastomosing one, with a wide macro channel controlled by the lithology. Topographic highs, between active bedrock distributary channels, are bedrock core bars. The bedrock core bars are densely vegetated with *Breonadia salicina* often forming a dense canopy layer. Where the canopy is less thick, dense woody shrubs proliferate. There is generally a sparse ground cover. Upstream of the anastomosing section, due to backwater effects, there is much deposition in the form of lateral bars and braid bars, as seen at site 4.1. The downstream end of the study reach is a prominent bedrock rapid. Site accessed from the 536 Hazyview Road. Left at 20km post; keep left past through farm gate and past farm building. Turn left at river road junction and section 4.0 is 500m downstream. Representative bedrock anastomosing reach taken to be between sections 4.2 and 4.5.

SITE 14

The reach is a single thread/braided active channel, meandering within the macro channel between lateral bars. The seasonal lateral bars are heavily reeded, whereas the macro channel banks are wooded, often with 3 stories of vegetation. Large well established fig trees and areas of impenetrable woody shrubs are common at the bottom of the macro channel bank. Site accessed from H11, past NO ENTRY track to Kruger Weir for 7.2km, to site 14 or from Skukuza, follow signs to Golf Club. Turn right at stop street, past Lake Panic. Right at NO ENTRY after 1.7km. Straight along track past Narina study site. Site 14 marked by cairn. Representative braided reach taken to be between sections 12.2 and 12.10.

REACH 15

The active channel of this reach flows through a series of pool-rapids, controlled by resistant bedrock outcrops. Throughout the reach there has been deposition, with braid bars and lateral bars common, particularly upstream of rapid areas. Reeds are often found fringing the active channel on seasonal lateral bars and braid bars, giving way to dense woody shrubs on the macro channel lateral bars. Bedrock core bars and seasonal rapid areas tend to be sparsely vegetated. Much of the right bank vegetation downstream of section 15.7 has been cleared. Site accessed from Skukuza. Follow signs for the Golf Club. Turn right at the junction with the club house. Right onto NO ENTRY where road bends sharply. Take track past pump

station on left, to site 15 which runs parallel to the power lines. Representative pool-rapid reach taken to be between sections 15.1 and 15.10.

REACH 21

This mixed anastomosing active channel flows as a series of distributary channels through a wide sand filled macro channel, over bedrock. Several ephemeral or seasonal distributaries dissect the macro channel deposits, which are locally heavily reeded. Section 20 is on the H4-1 road to Lower Sabie, at the 23.5km post, just before a NO ENTRY on the right. Representative mixed anastomosing reach taken to be between sections 20 and 22.

REACH 1

BMK	BMK POSITION	CHAINAGE	FMS	SITE DESCRIPTION
0.0	BMK "SCT4A", next to white rock outside fence	-702.9	1	Upstream of bedrock control
0.1		-630.2	-	
0.1A	Downstream from pylon on right bank	-536.1	2	
0.2		-363.3	2	Start of upper terrace on right bank. No terrace on left bank
0.3	1m upstream from large tree, next to gate post	-244.2	-	Cross section through low mid channel braid bar
0.4		-179.0	2	Left bank upper terrace start
0.5		-83.4	-	
1.0	2km from Hazyview road	0	2	
1.1		177.5	1	Bedrock cascade
1.2	Next to fence in agricultural field	236.9	1	Bedrock cascade

REACH 4

BMK	BMK POSITION	CHAINAGE	FMS	DESCRIPTION
4.1	Left at river road junction. Fence sprayed.	19760	1	Upstream of anastomosing section. Single thread.
4.2	Left at river road junction. Fence sprayed.	20092.6	1	Upstream end of anastomosing section.
4.3	225m upstream of BMK4. Sprayed fence and cairn.	20237.3		Active channel anastomoses around bedrock core bars.
4.4	100m upstream of BMK4. Road turns away from river.	20348.3		Dense canopy vegetation (Breonadia common) on bedrock core bars.
4.0	Left at river road junction for 500m. BMK is over grid by sprayed post.	20417.6	1	Centre of anastomosing section. Wide macro channel controlled by lithology.
4.5	130m along road from BMK4.	20667.6		4 major active channels. Some alluvial deposits.
4.6	230m from BMK4. Sprayed fence and cairn.	20843.9	2	Downstream end of anastomosing section. 2 major active channels.
4.8	390m from BMK4. BMK is 3m into KNP and 10m downstream of sprayed post.	21012.2	1	Single thread channel. Upstream of bedrock control.
4.9	11 posts upstream of sprayed post. 2m into KNP.	21137.4	2	Braided active channel. Downstream of bedrock control.

REACH 14

BMK	BMK POSITION	CHAINAGE	FMS	DESCRIPTION
12	Next to cairn	41275	2	Large lateral bar on right bank.
12.1	BMK next to road.	42534.3	1	Upstream of a control.
12.2	BMK next to road.	42736.4	2	Downstream of control. Lateral bar on right bank and mid channel island.
12.3	BMK near road, before it bends away from river.	42913.9		Upstream end of lateral bar on left bank. No mid channel bar.
12.4	BMK on break of slope, 30m from road. Cairn on road.	43041.7	1	Monitors large lateral bar on left bank, which is densely reeded.
12.5	BMK next to macro channel cliff, 30m from road. 3 cairns.	43225.5		Upstream end of braid bar. Active channel fringe reeded; lateral bars have woody shrubs.
12.6	BMK next to road. Cairn marks.	43308.0		Downstream end of mid channel bar and start of lateral bar on left bank.
12.7	BMK next to road.	43400.7		Active channel meander apex;lateral bar on left bank.
12.8	Before road bends away from channel sharply.	43548.2	2	Extensive lateral bar on right bank covered with dense, tall reeds.
12.9	BMK 35m from road: along path to river.	43701.6		Mid channel island and downstream end of right bank lateral bar.
12.10	New BMK 50m from road.	43862.5	2	Left bank point bar upstream of active channel control.
12.11	BMK 100m from road on edge macro channel. Follow cairns.	43975.0	1	Downstream of control. Large areas of bedrock outcrops on banks.
14	Section marked by cairn.	44525.0	3	Point bar deposit on right bank.

REACH 15

BMK	BMK POSITION	CHAINAGE	FMS	DESCRIPTION
15.1	250m upstream from 15. BMK in clearing on macro channel top.	49082.2	2	Upstream of a bedrock control. Lateral bars on both banks.
15.2	120m upstream from 15. Next to large animal burrow.	49196.4		In a pool section downstream of the control.
15.0	Follow road past the pump house. BMK is under powerline.	49300		Bedrock core bars and lee deposits occur.
15.3	140m downstream from 15. BMK on macro chl top, upslope from disused braai area.	49462.2		Large areas of bedrock outcrops, with some deposition (bedrock core bars).
15.4	300m from 15. BMK on upstream edge of wooden 'treehouse'.	49660.0	1	Reeds well established on active channel braid bars.
15.5	425m from 15. BMK is 15m upstream from fence.	49745.9	1	On a control. Bedrock core bars sparsely vegetated.
15.6	BMK is 20m downstream from fence and 3m downslope of gravel pile.	49867.0		Lateral bars and active channel bedrock core bars heavily reeded.
15.7	600m from 15. BMK 10m upstream from trib.	49937.3	2	Upstream edge of bedrock control.
15.8	700m from 15. BMK 5m downslope from fence, in line with water intake.	50006.4	1*	Bedrock control. Evidence of increased deposition in sand splays.
15.9	BMK on bedrock.	50096.0		
15.10	840m from 15. BMK 10m downslope from fence, in line with gate.	50161.9	1	Downstream of control. Relic macro channel island prominent.

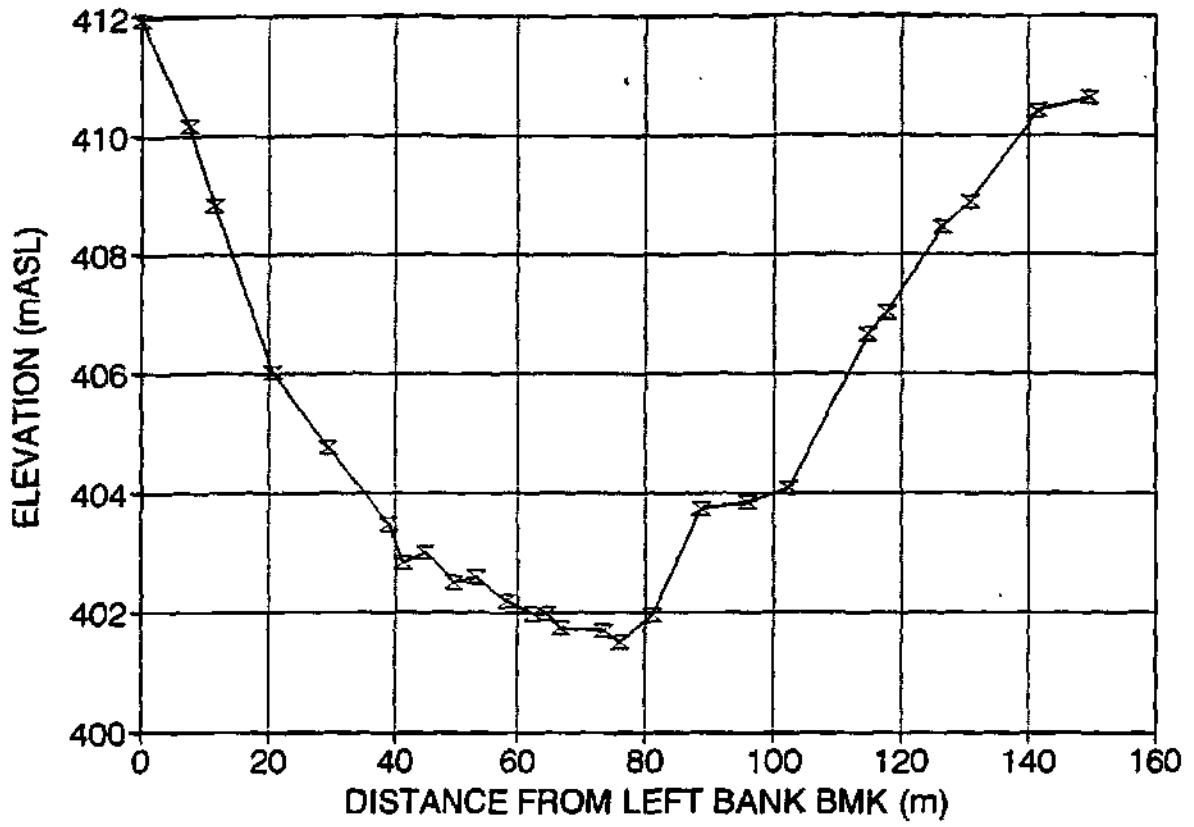
* FMS is a water intake structure

REACH 21

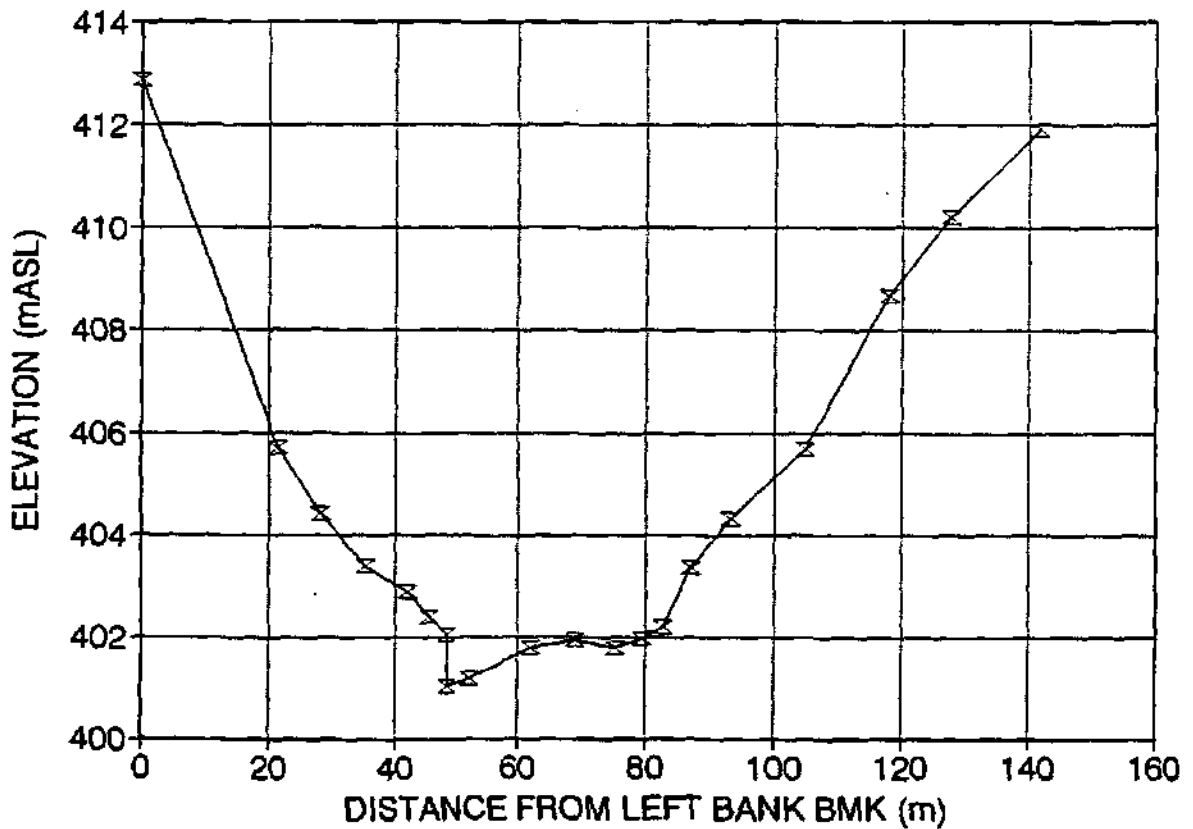
BMK	BMK POSITION	CHAINAGE	FMS	DESCRIPTION
20	23.5km along road to Lower Sabie. Before no entry on right.	73635	2	Braided channel with bed rock core bars.
20.1	23.8km. 0.3km before Nwatimwambu bridge.	73985	2	Bedrock core bars dissected by seasonal distributaries.
20.2	24.4km. On sharp bend in road. Cross section start 200m downslope from road.	74786.4		Section upstream of tributary on the left bank. A very wide macro channel.
20.3	24.9km. Cross section start on old Lower Sabie road, 100m in from road.	75091.7	2	Sand deposits heavily reeded, with occasional trees.
20.6	26.4km.	76601.9	2	Confluence of 2 active distributaries.
20.7	26.7km. 20m upstream of small loop.	76967.1		Heavily vegetated with reeds, dense shrub and willow.
21	27.4km.	77477.1	2	
21.1	0.35km along S79 turnoff from Lower Sabie road.	78164.5		Bedrock largely covered by sand deposition.
21.2	0.7km along S79. 0.1km upstream of Nwatimhiri bridge.	78769.2	2	Active channel is a deep, wide pool.
21.3	0.8km along S79. BMK is upstream left corner of bridge support.	79026.7	1	Dead trees common on seasonal bedrock core bars.
22	2.4km along S79. BMK is 30m from road.	80326.7	2	3 active channels with bedrock core bars.

APPENDIX 2: CROSS SECTION SURVEY DATA

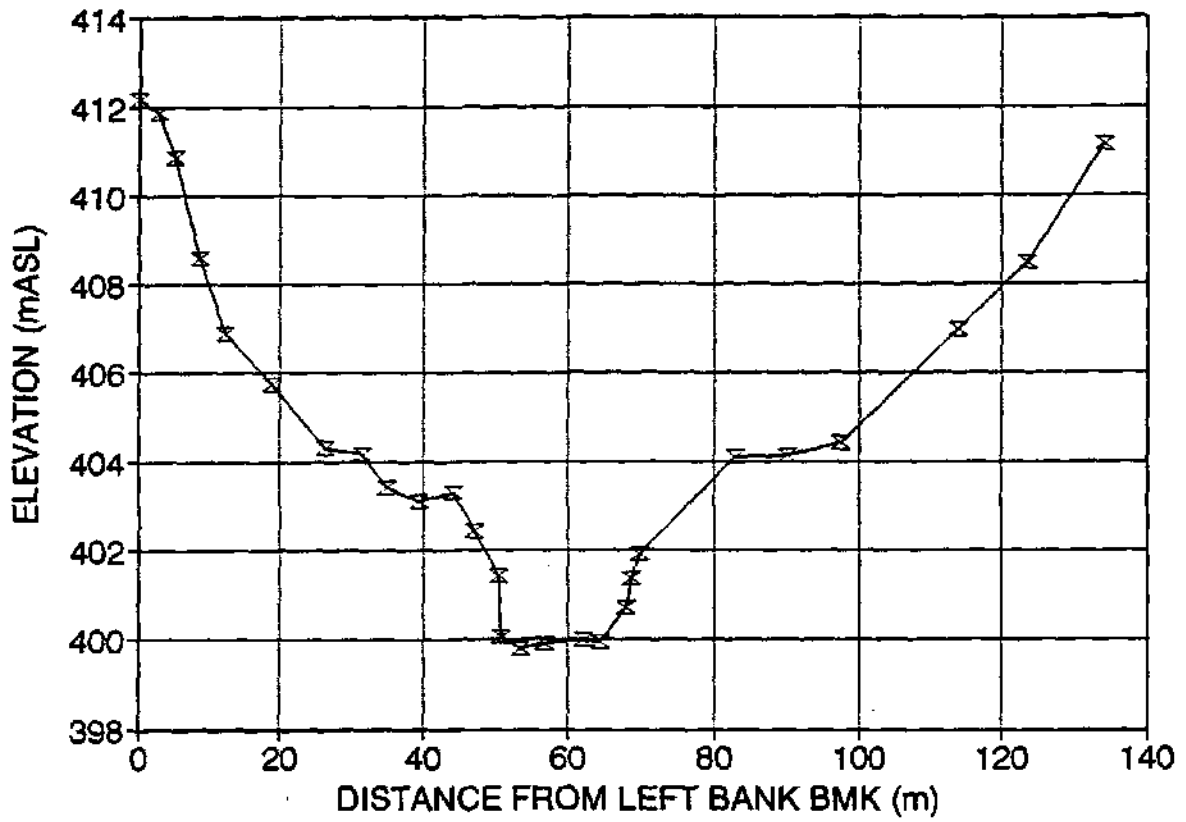
CROSS SECTION 0.0



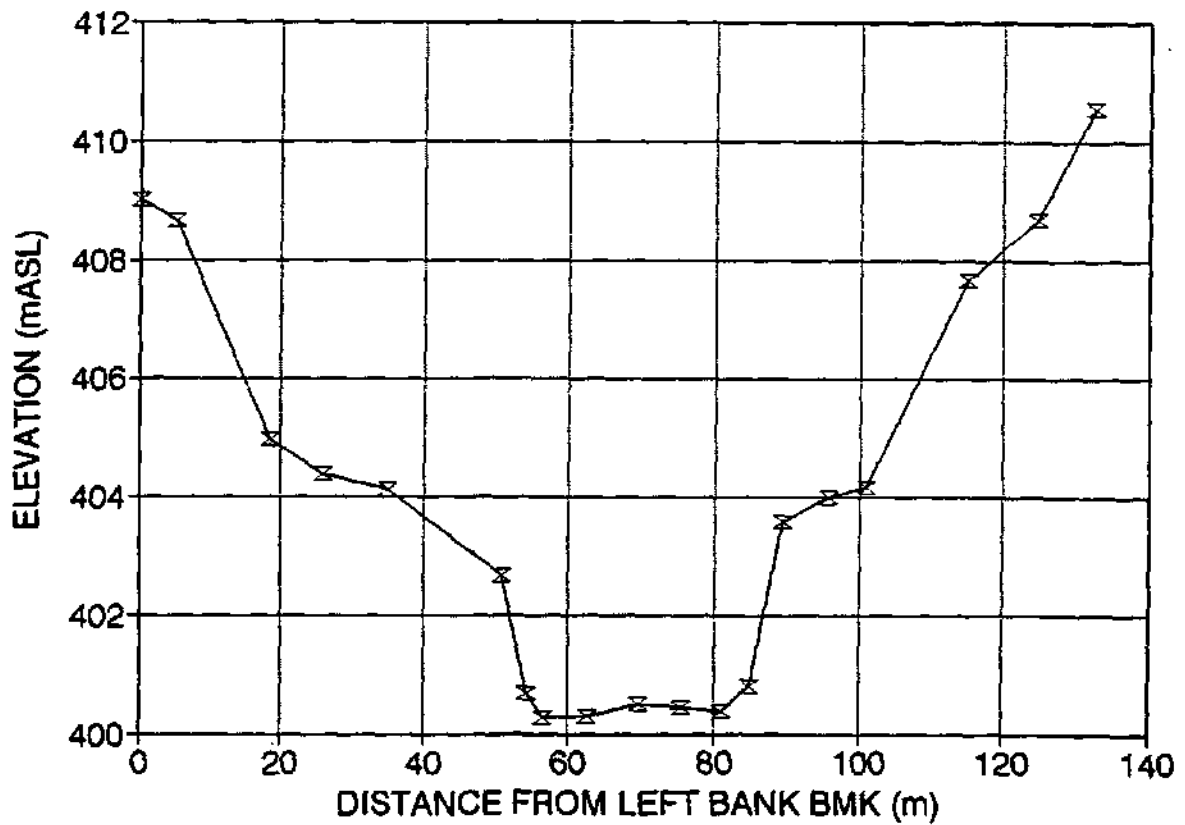
CROSS SECTION 0.1



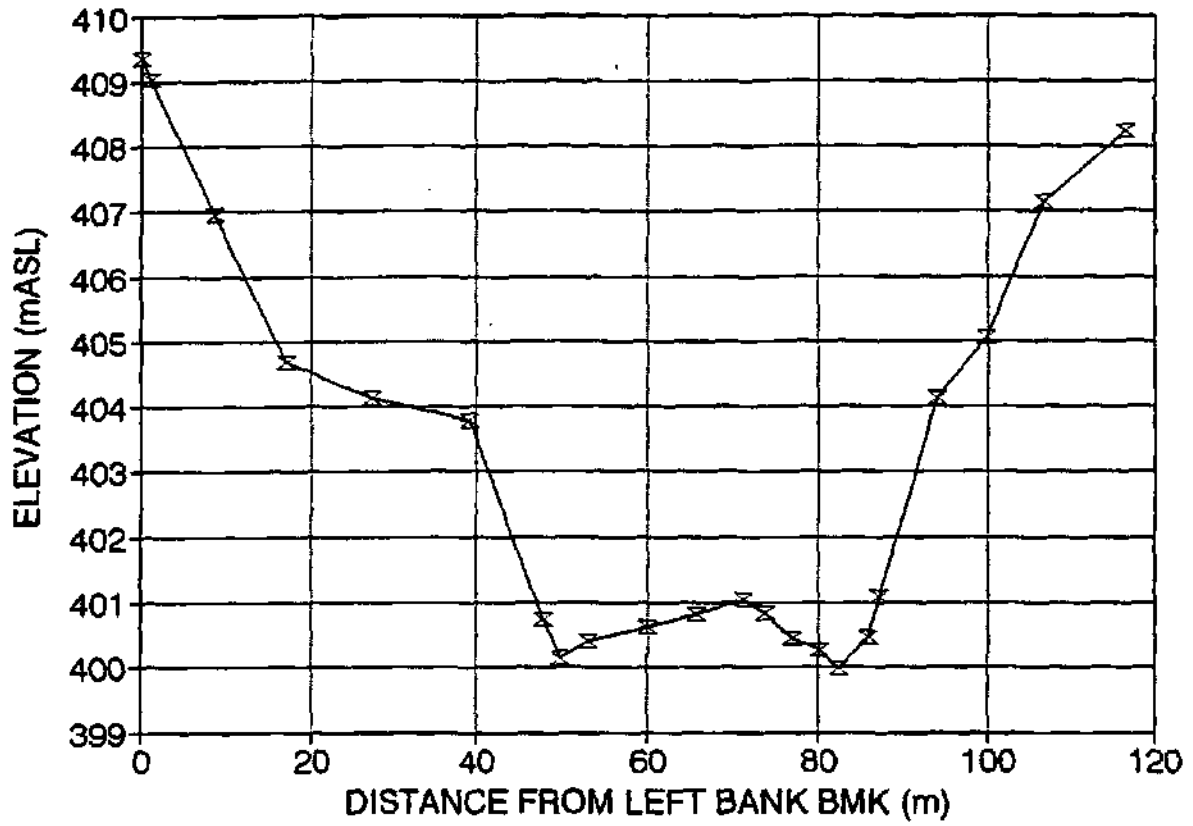
CROSS SECTION 0.1A



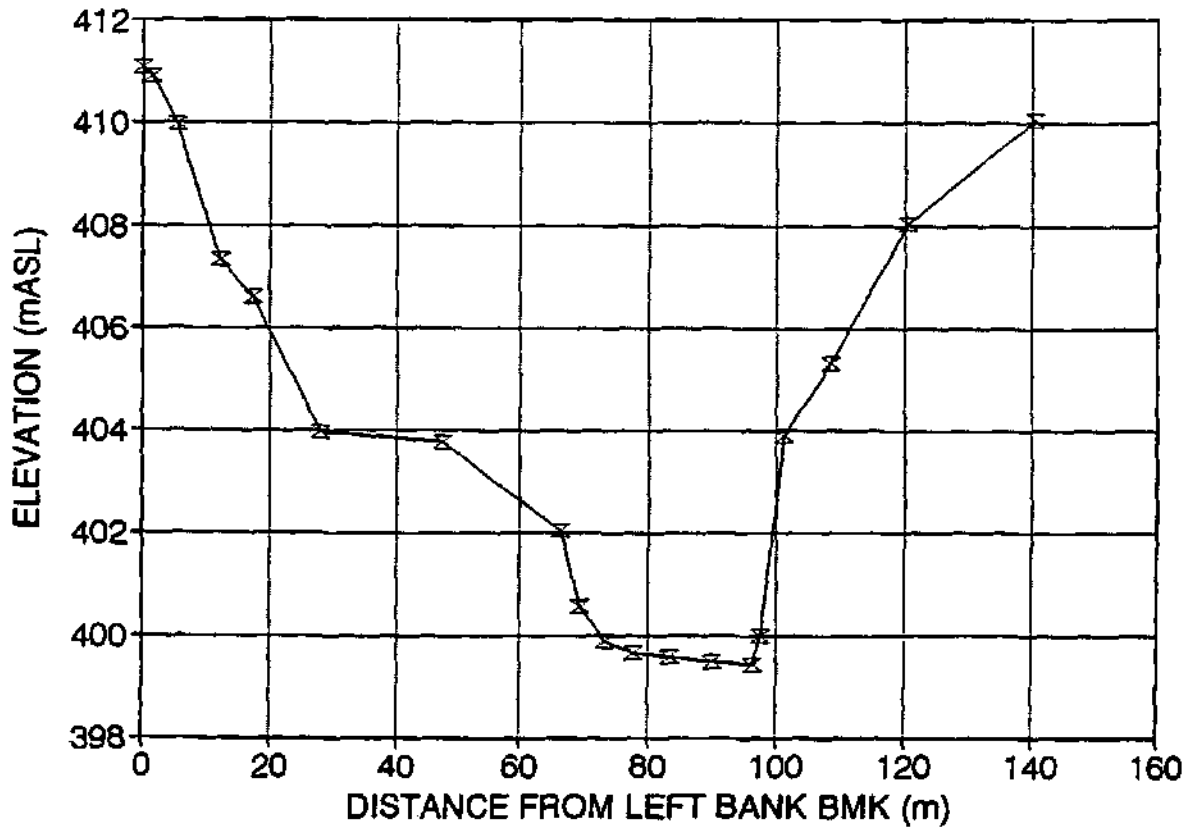
CROSS SECTION 0.2



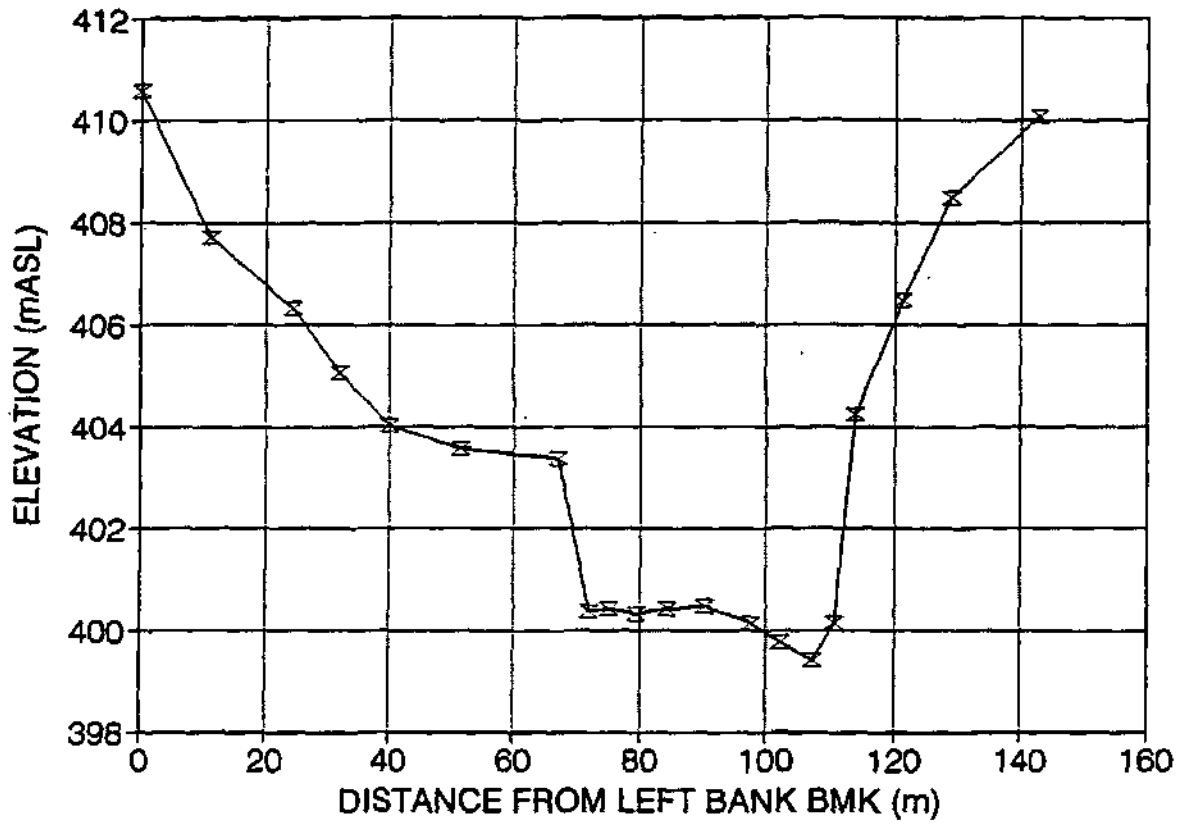
CROSS SECTION 0.3



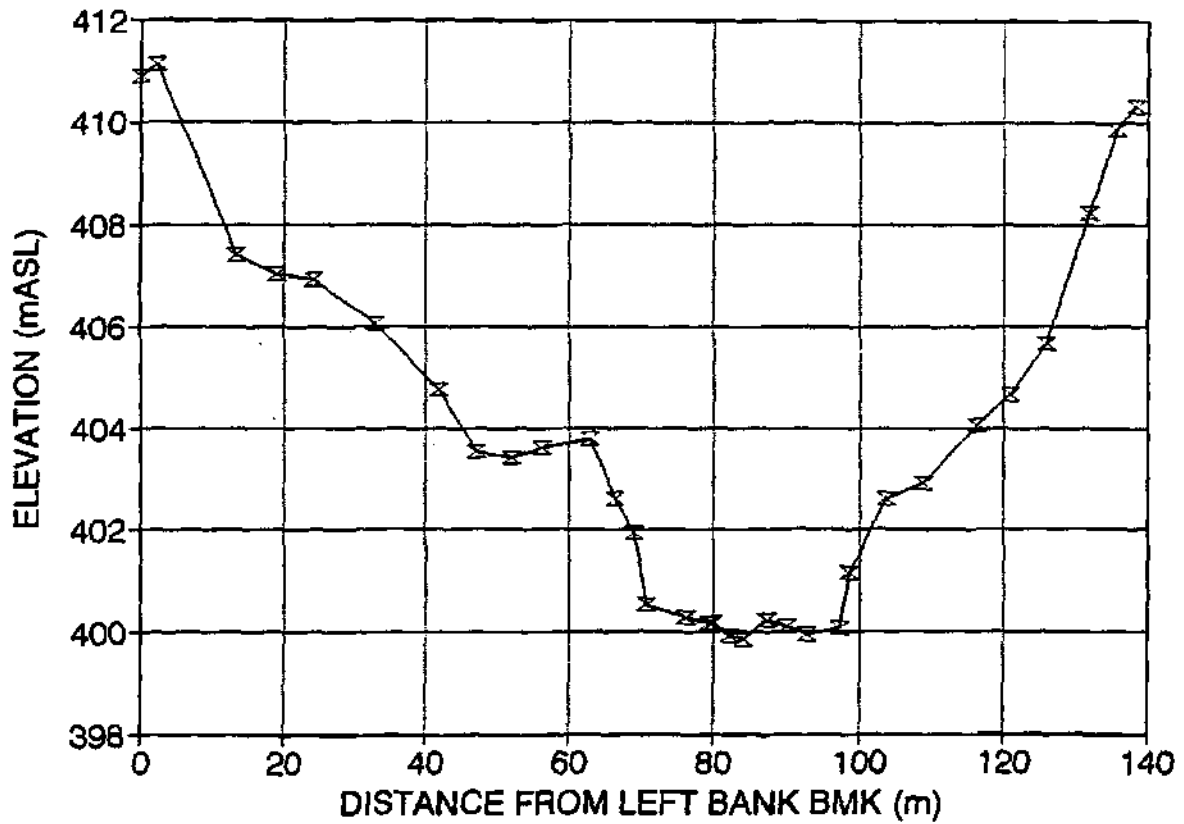
CROSS SECTION 0.4



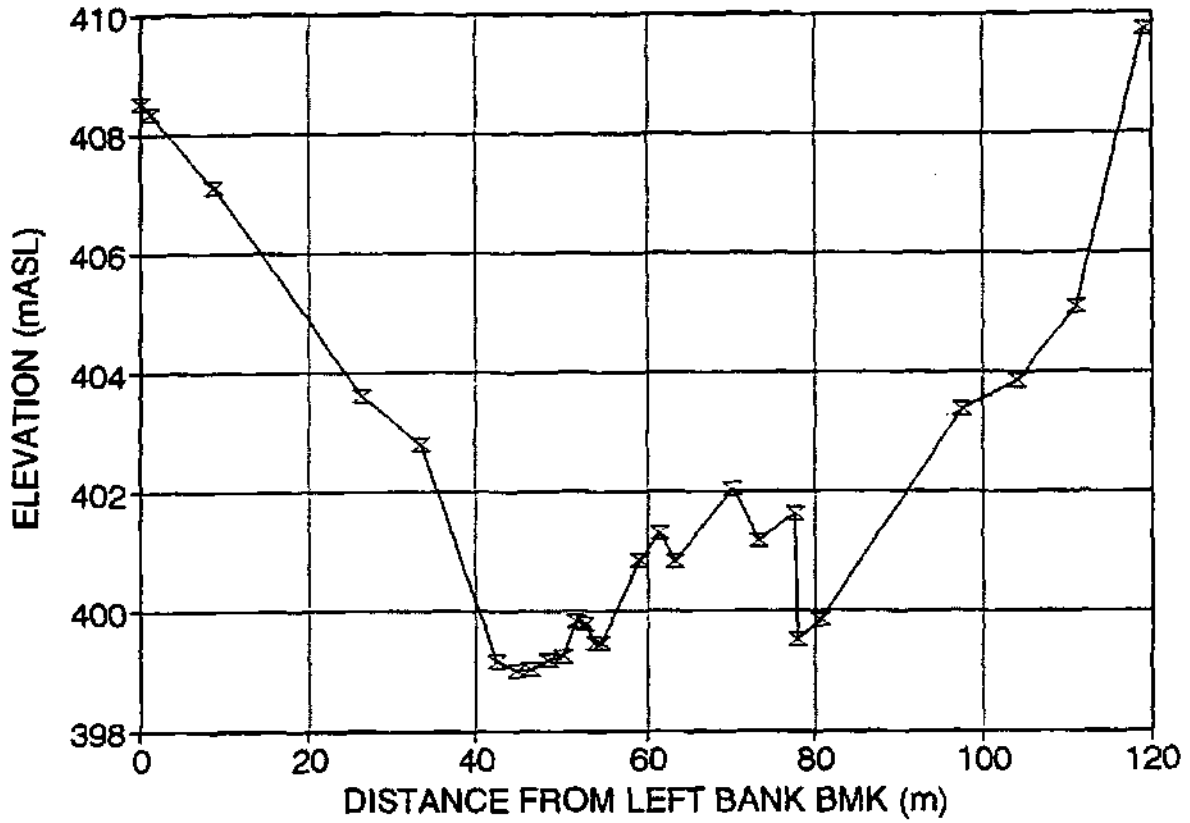
CROSS SECTION 0.5



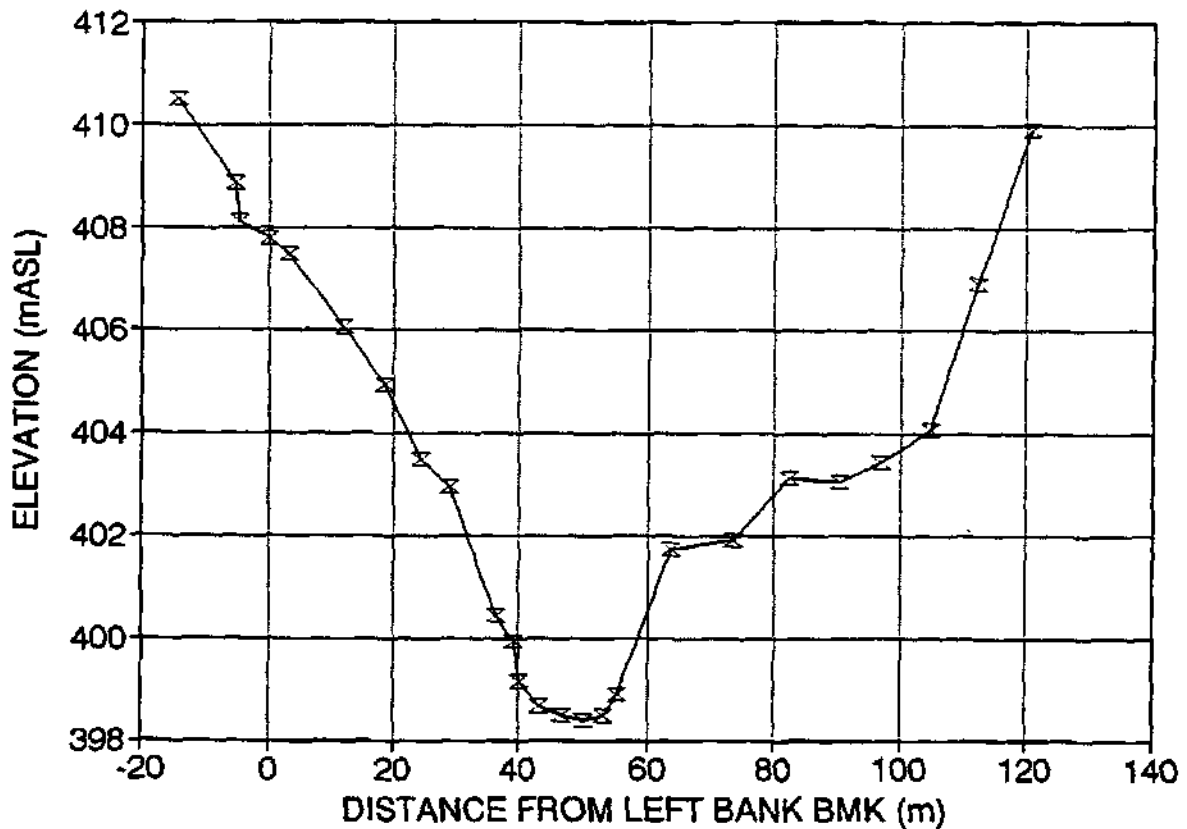
CROSS SECTION 1



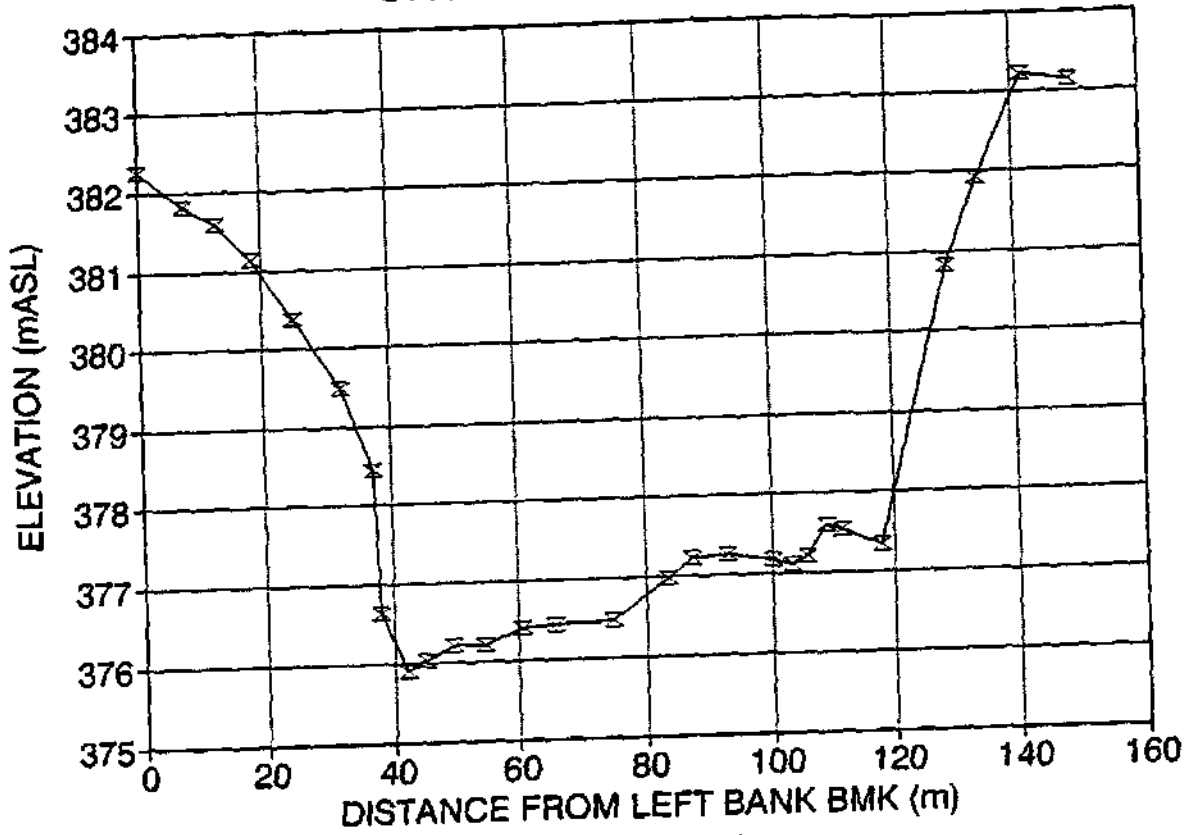
CROSS SECTION 1.1



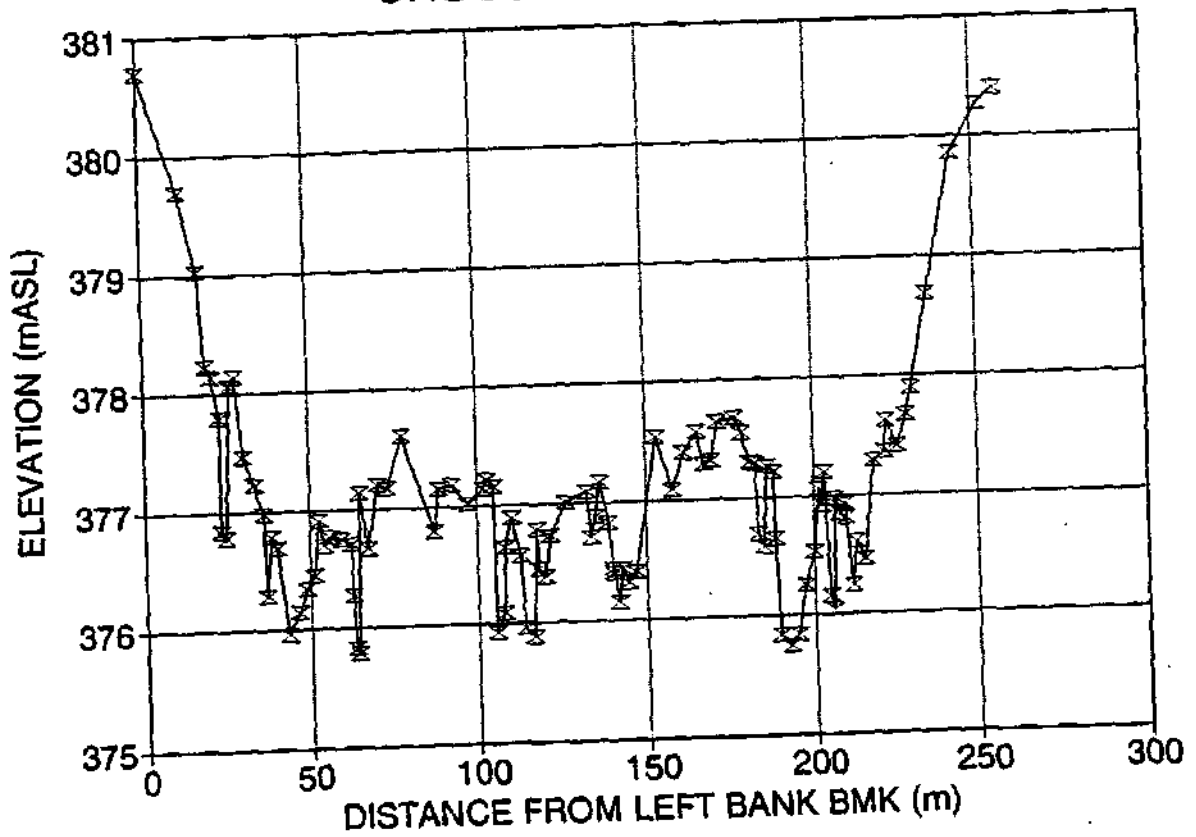
CROSS SECTION 1.2



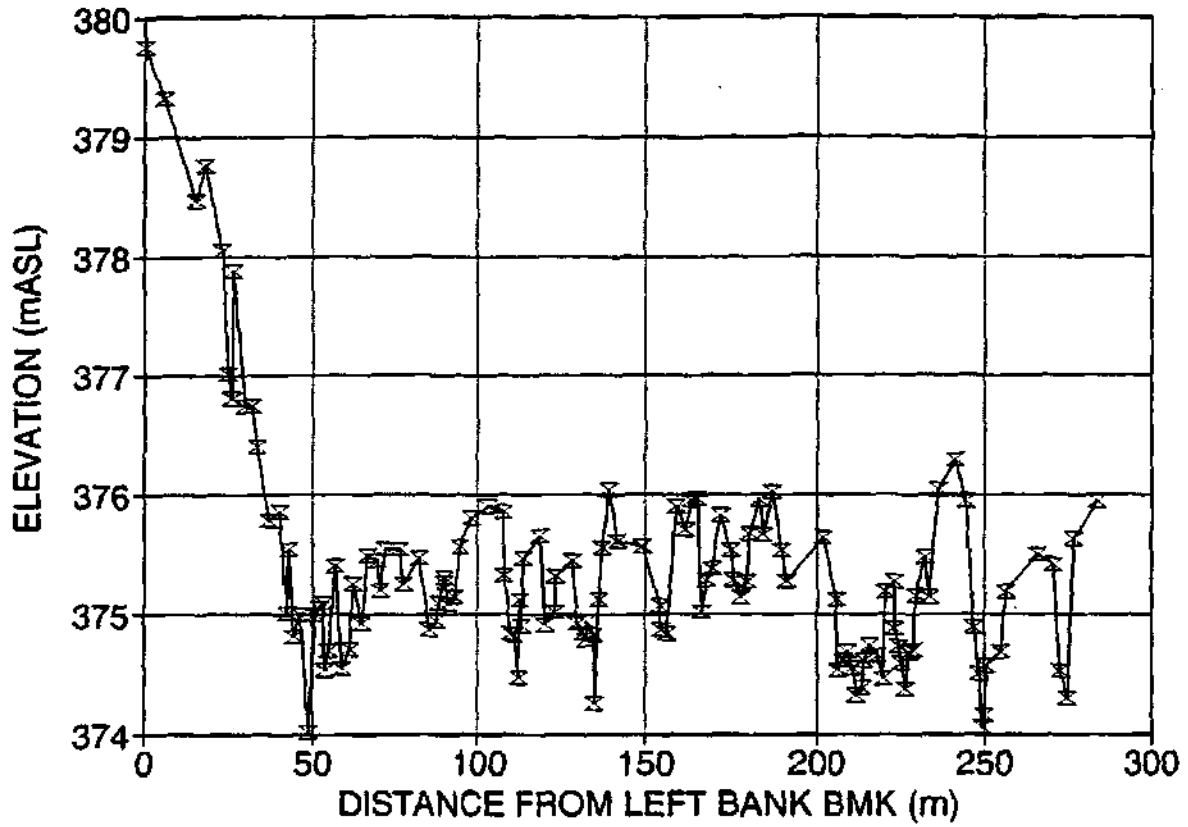
CROSS SECTION 4.1



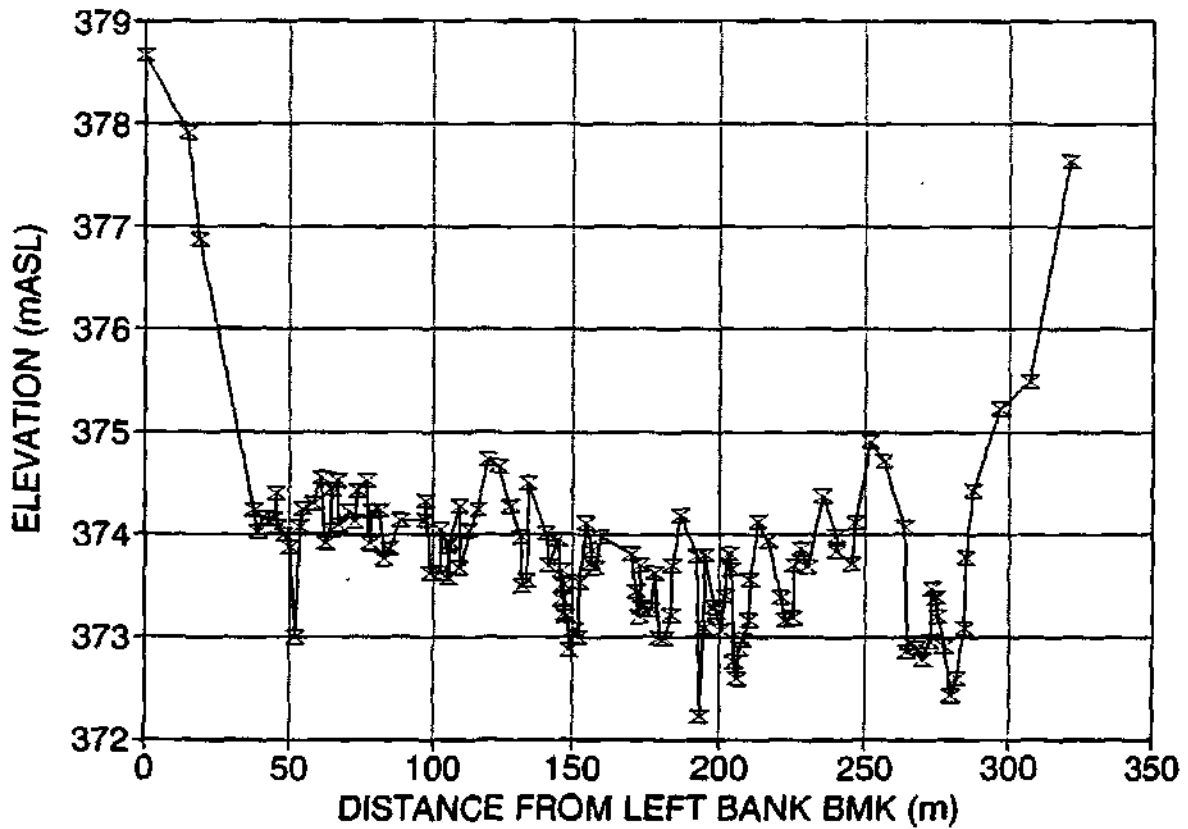
CROSS SECTION 4.2



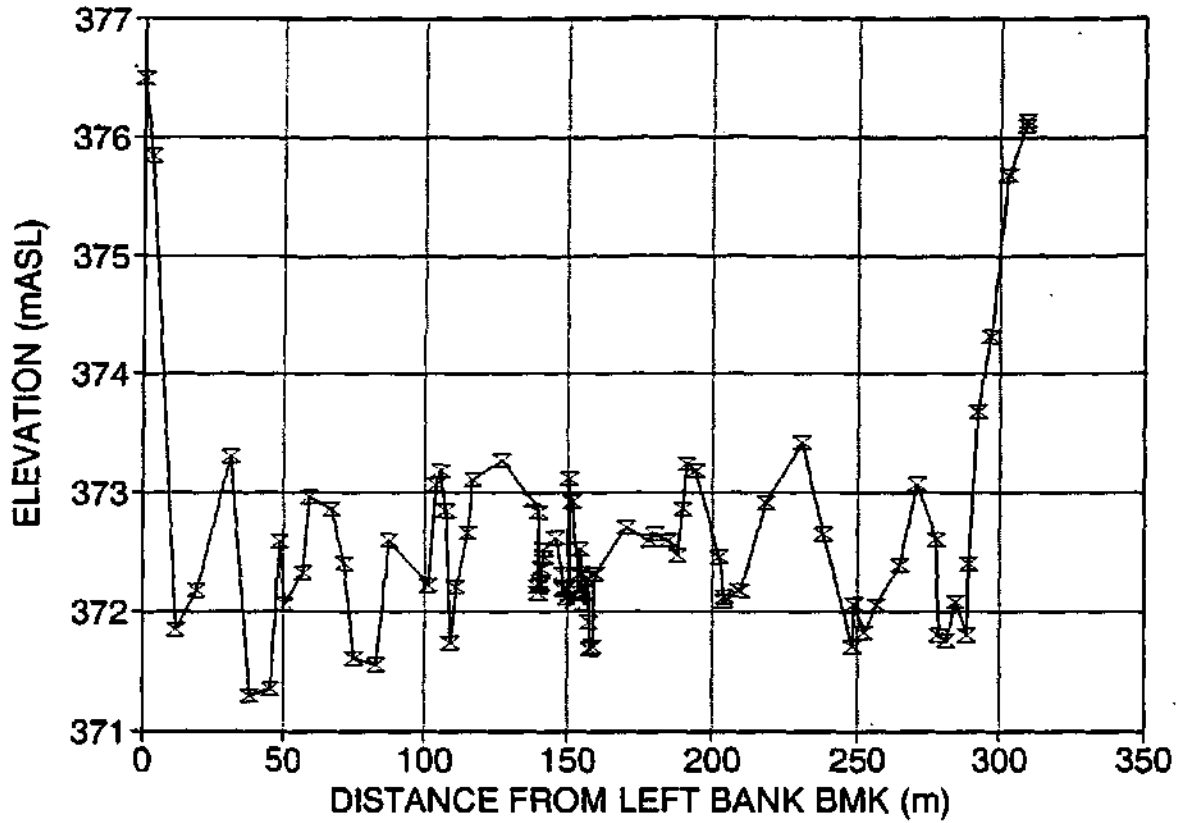
CROSS SECTION 4.3



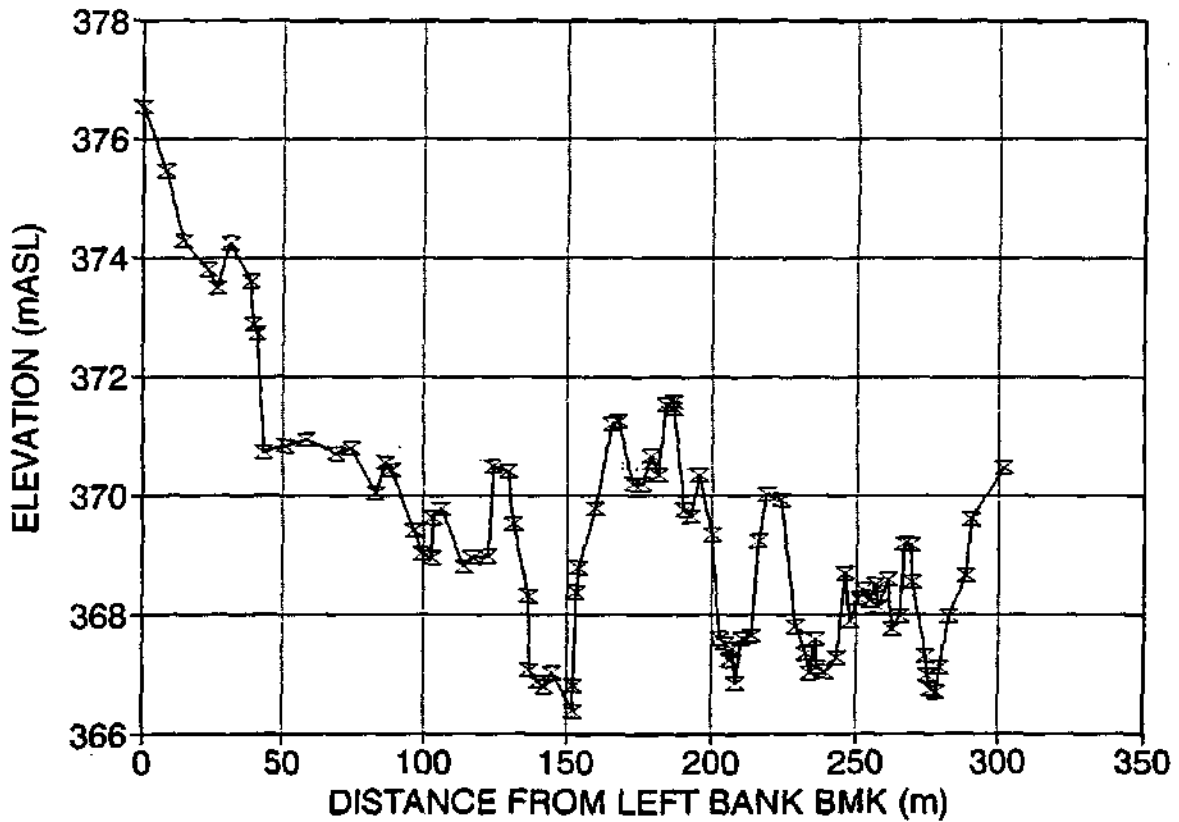
CROSS SECTION 4.4



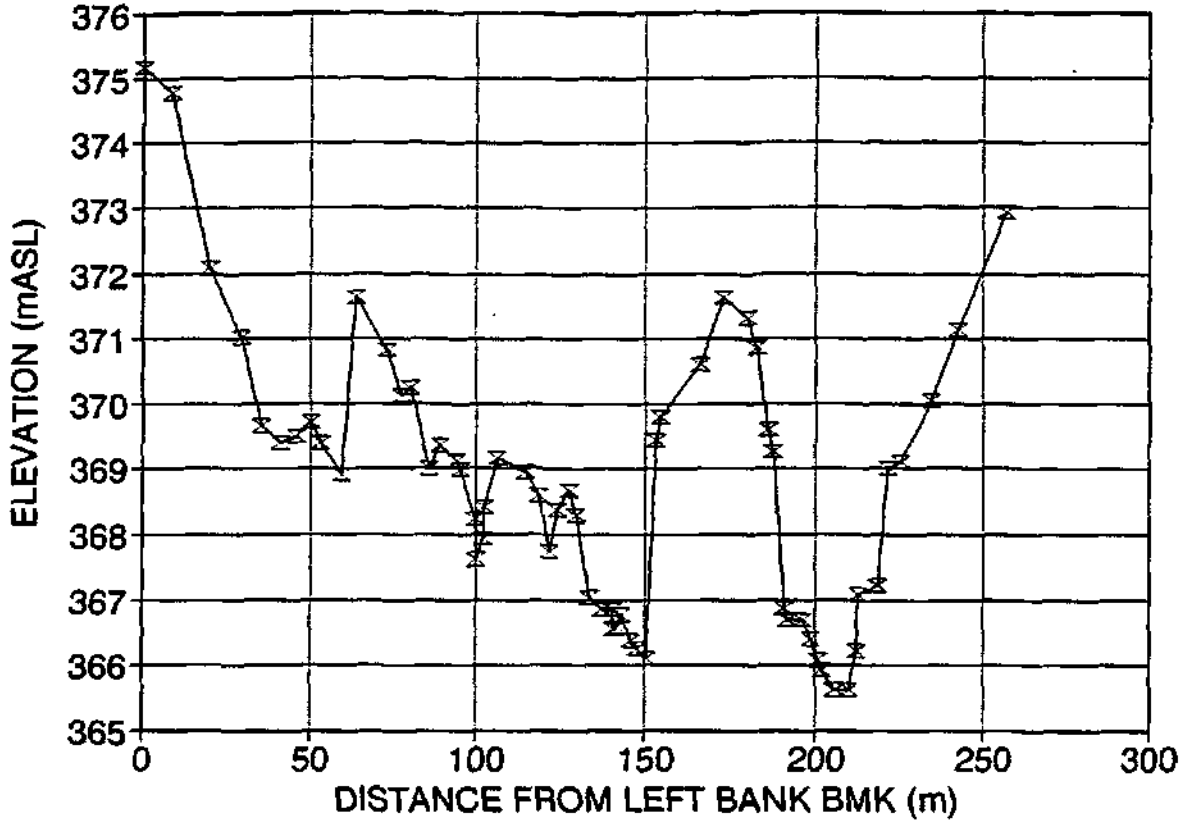
CROSS SECTION 4



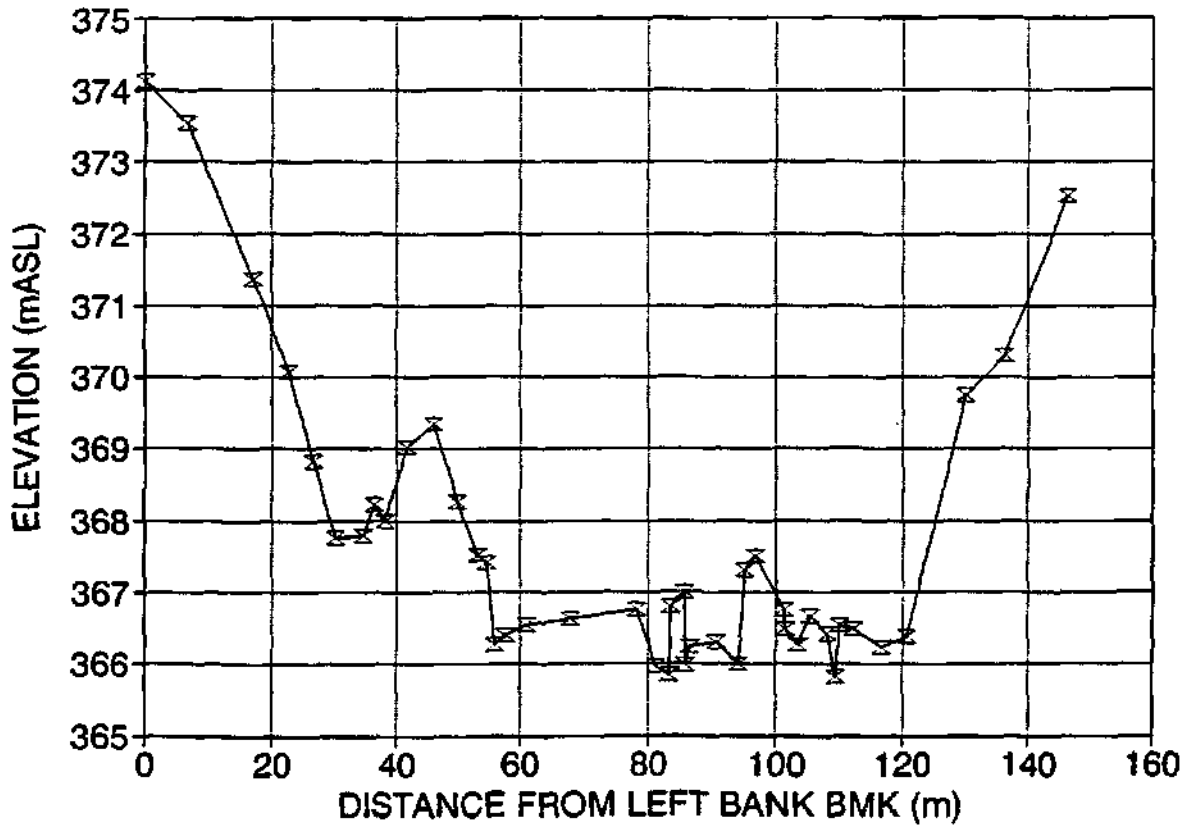
CROSS SECTION 4.5



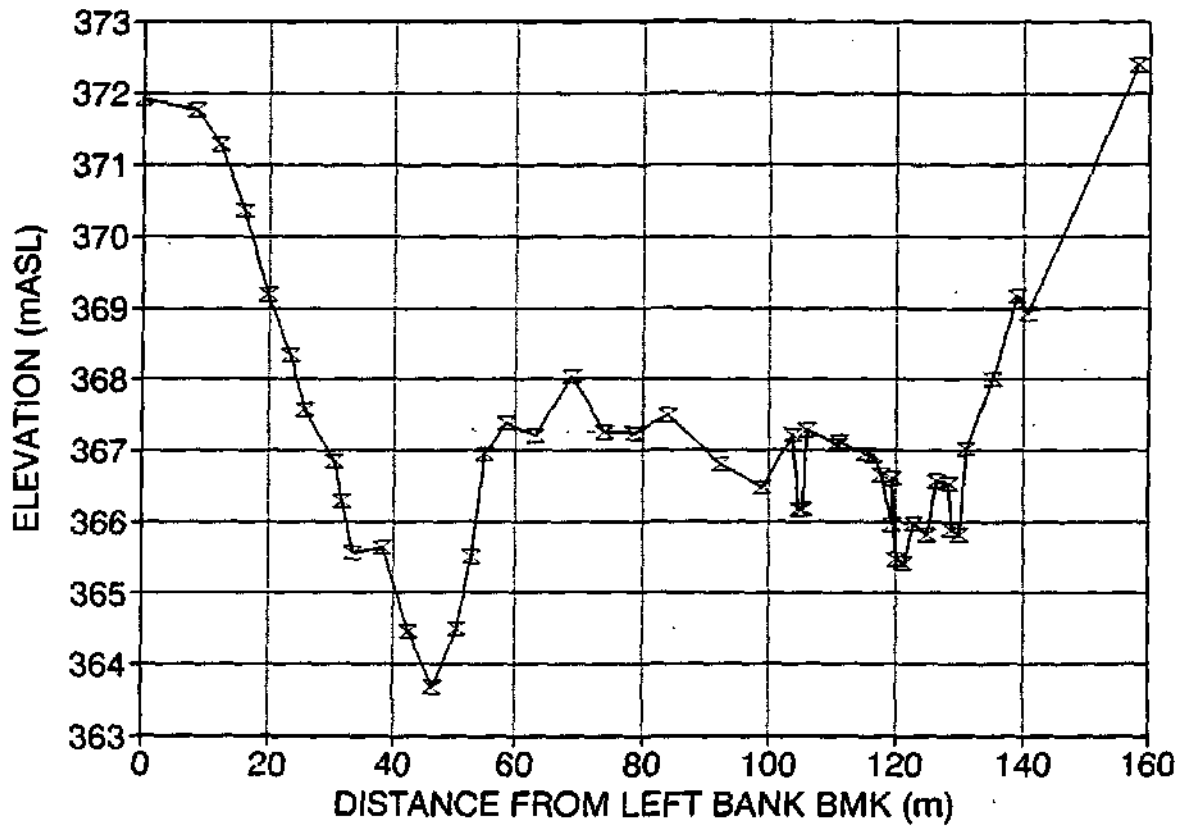
CROSS SECTION 4.6



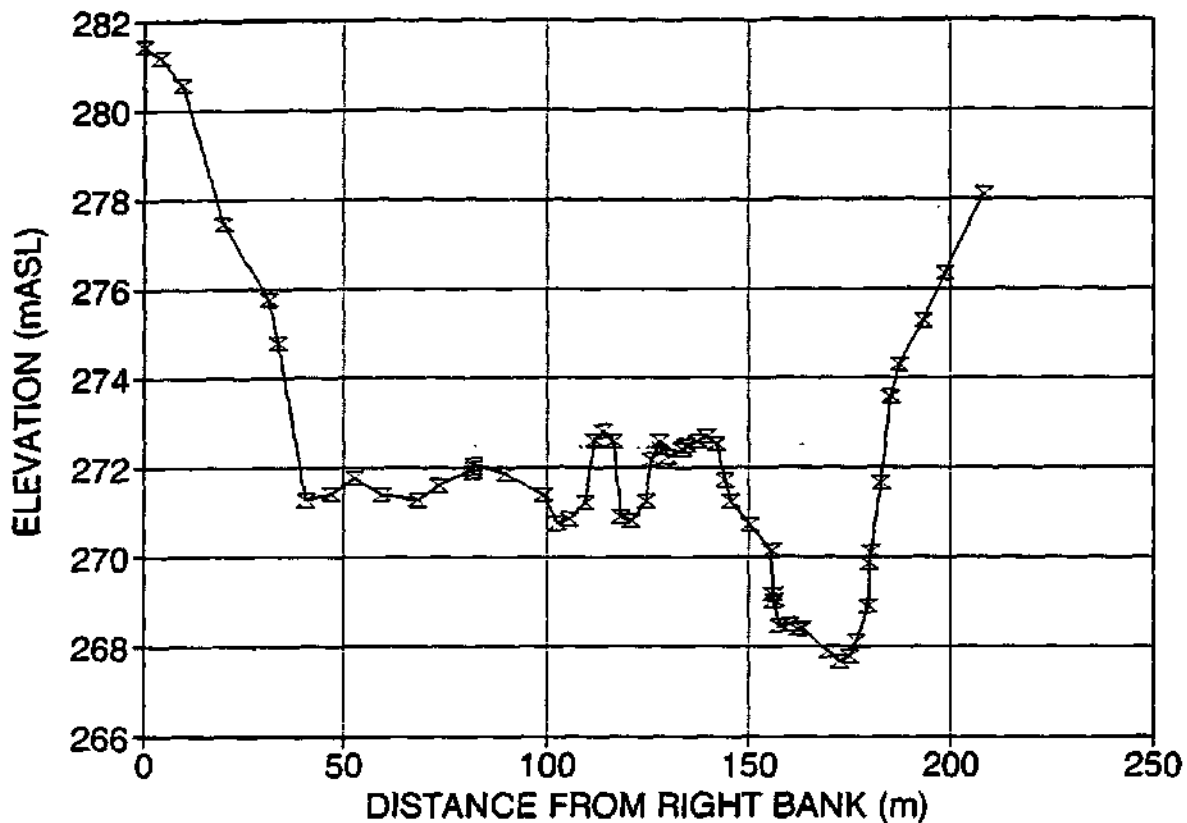
CROSS SECTION 4.8



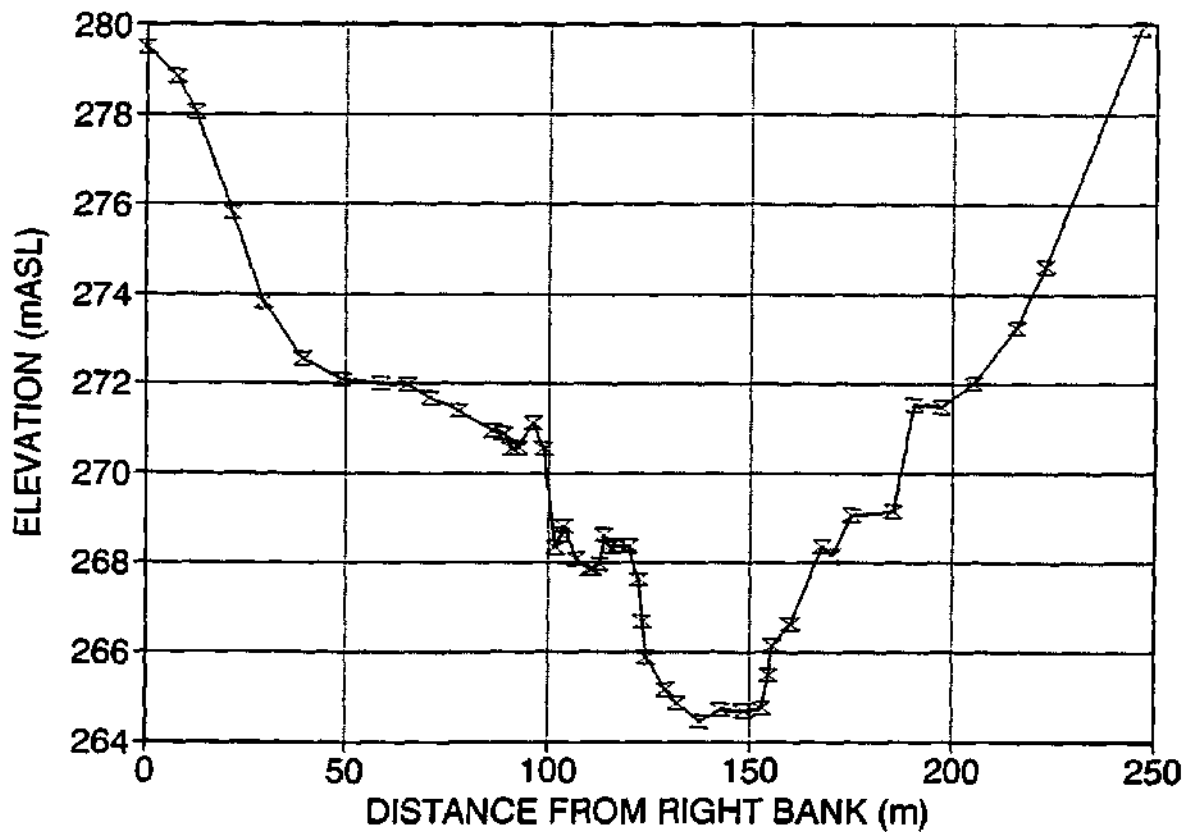
CROSS SECTION 4.9



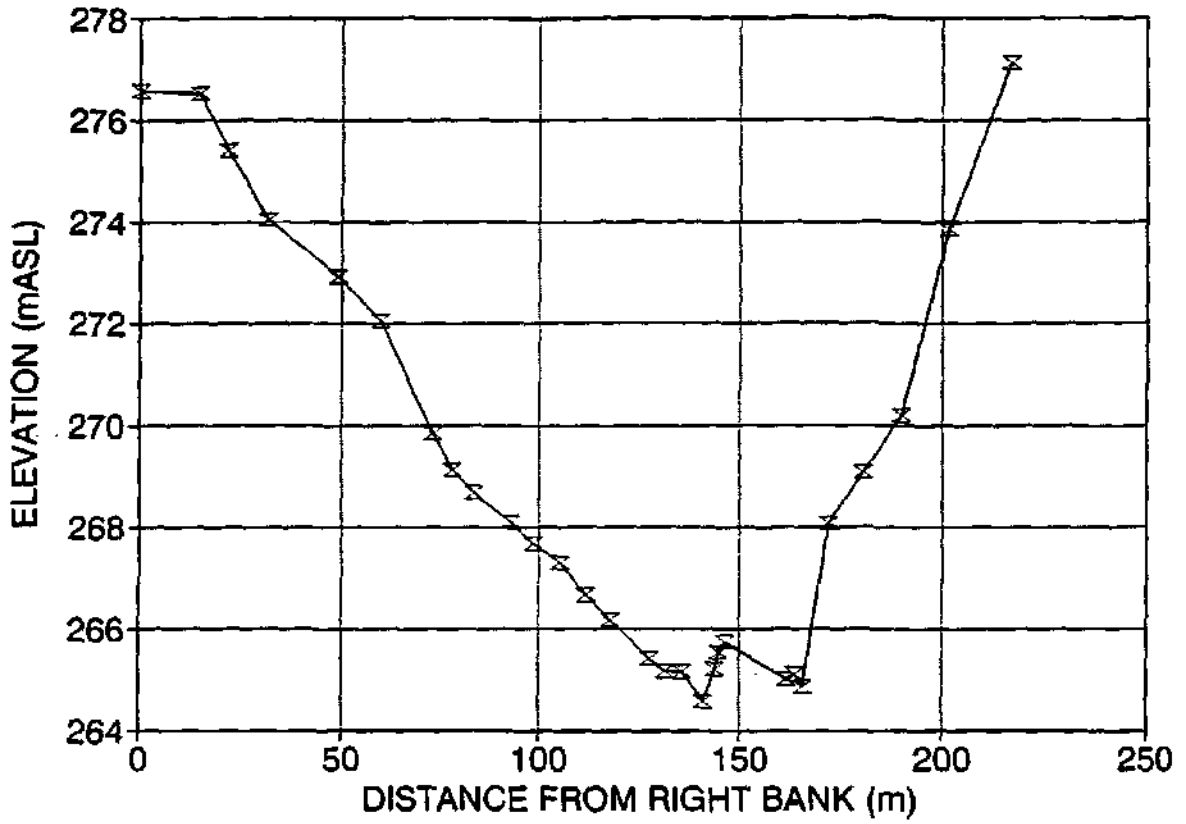
CROSS SECTION 12



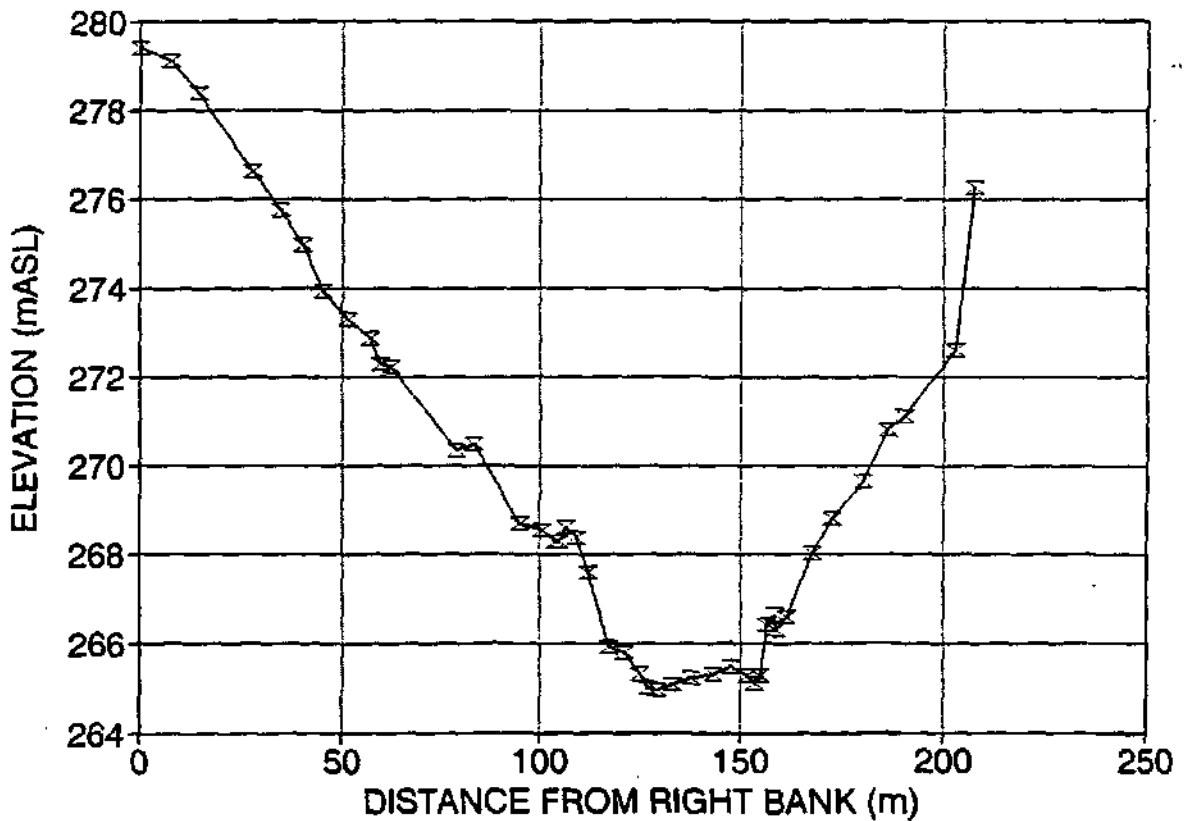
CROSS SECTION 12.1



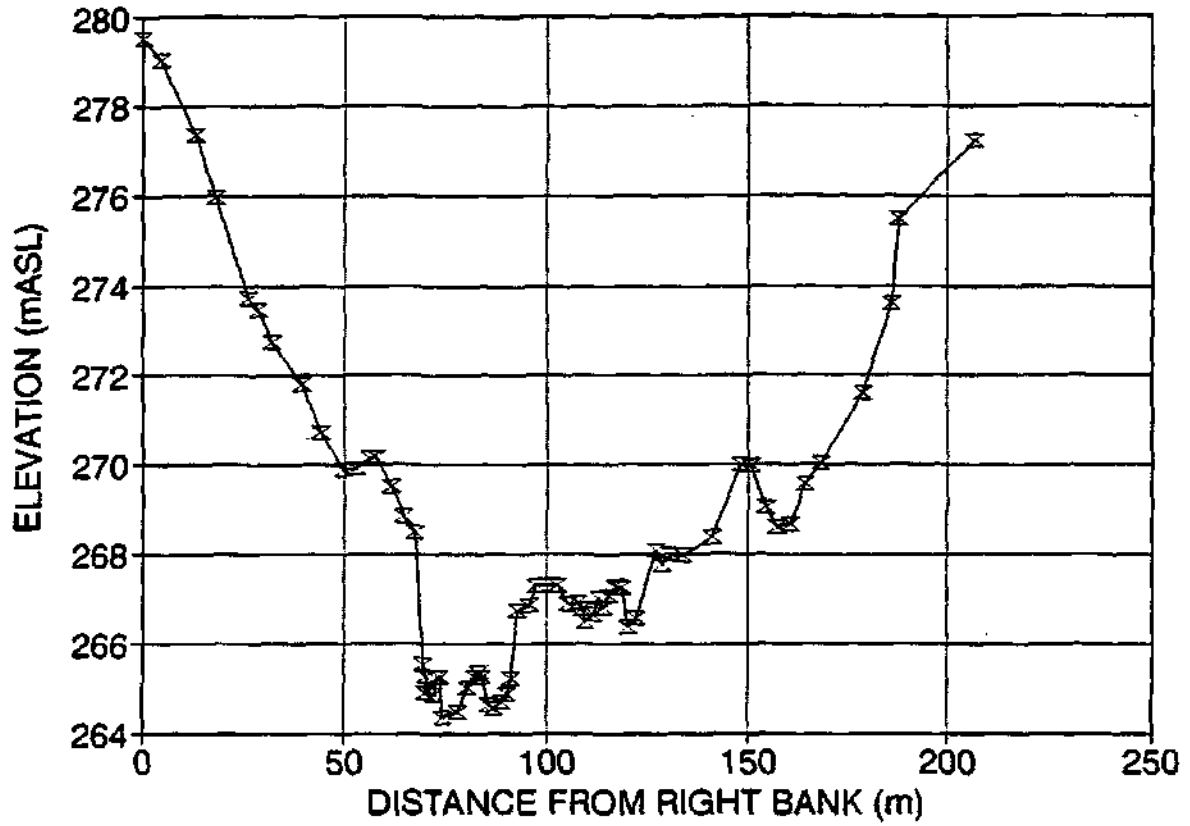
CROSS SECTION 12.2



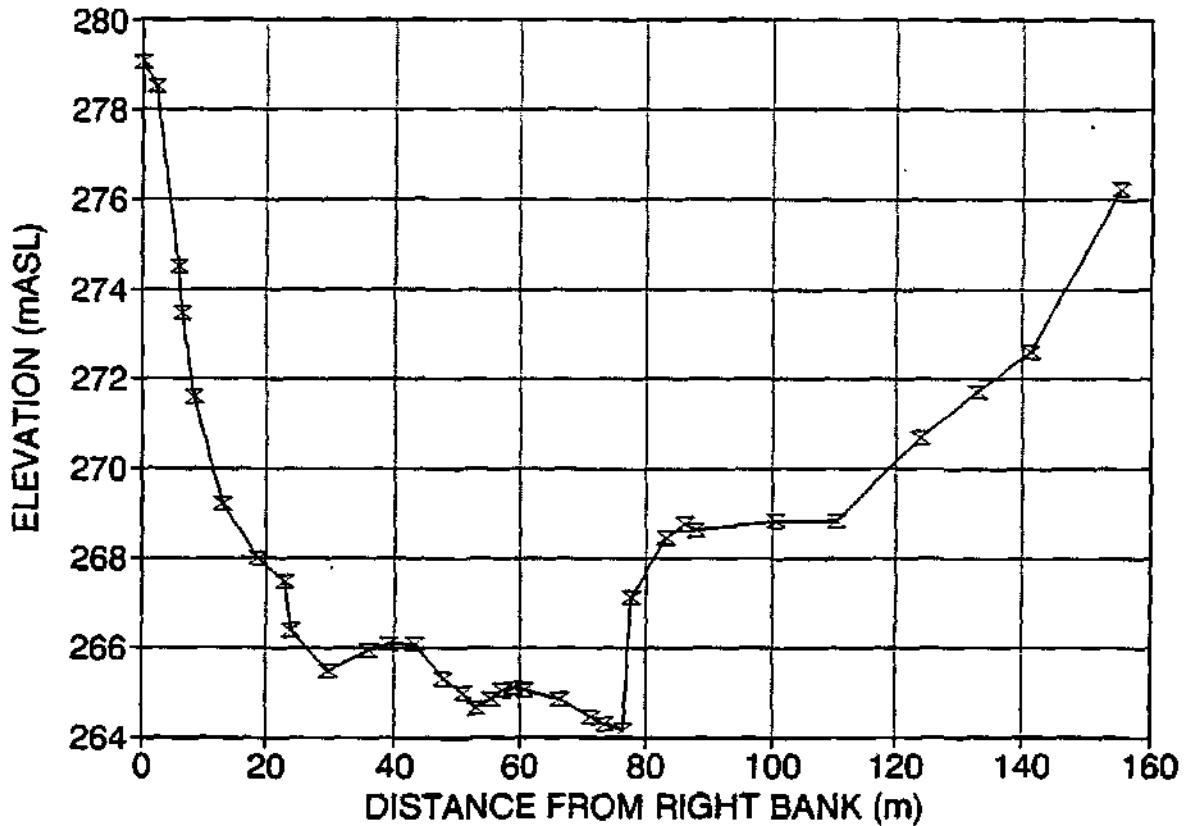
CROSS SECTION 12.3



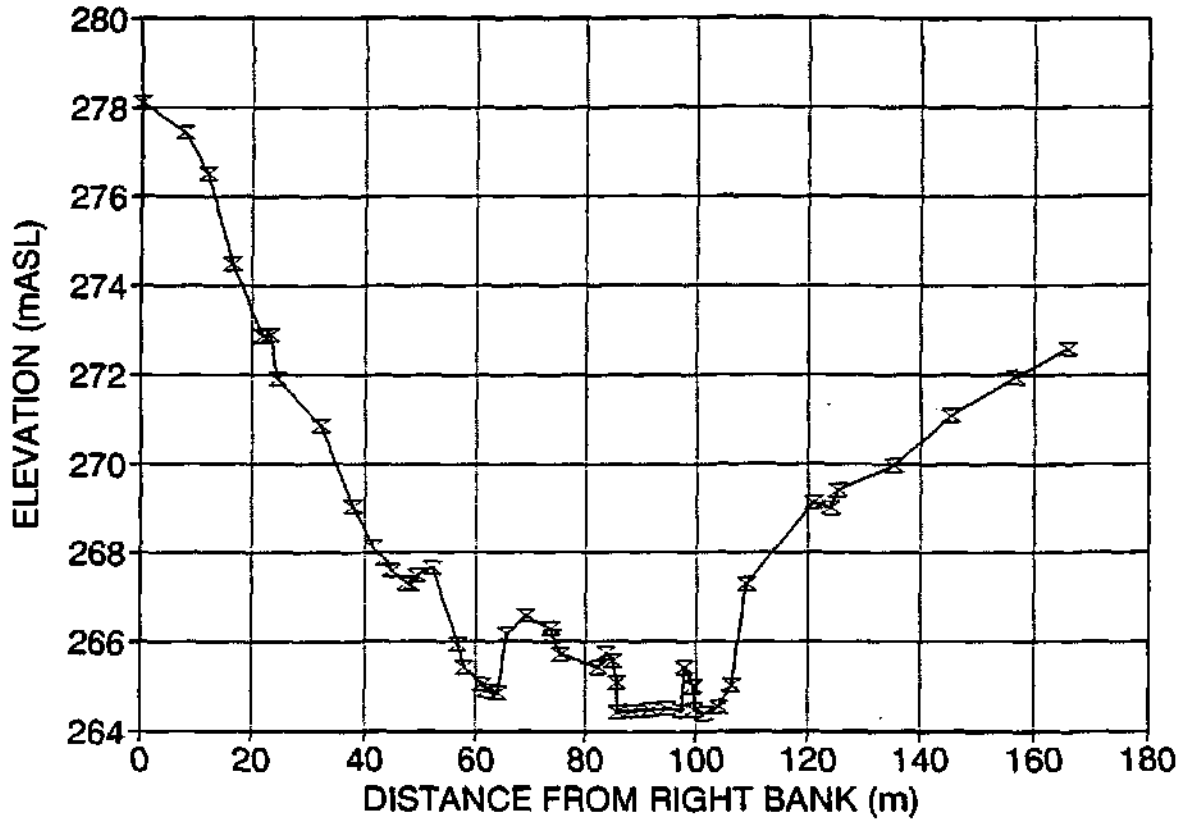
CROSS SECTION 12.4



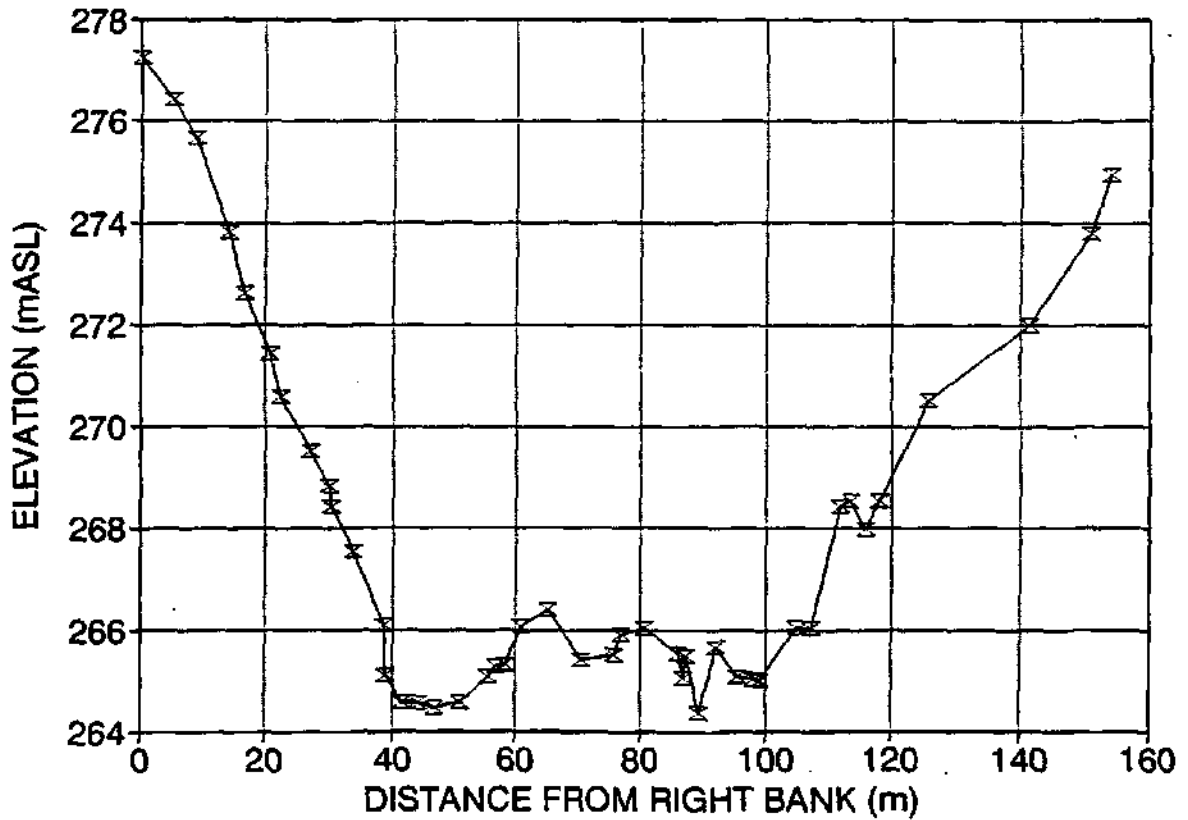
CROSS SECTION 12.5



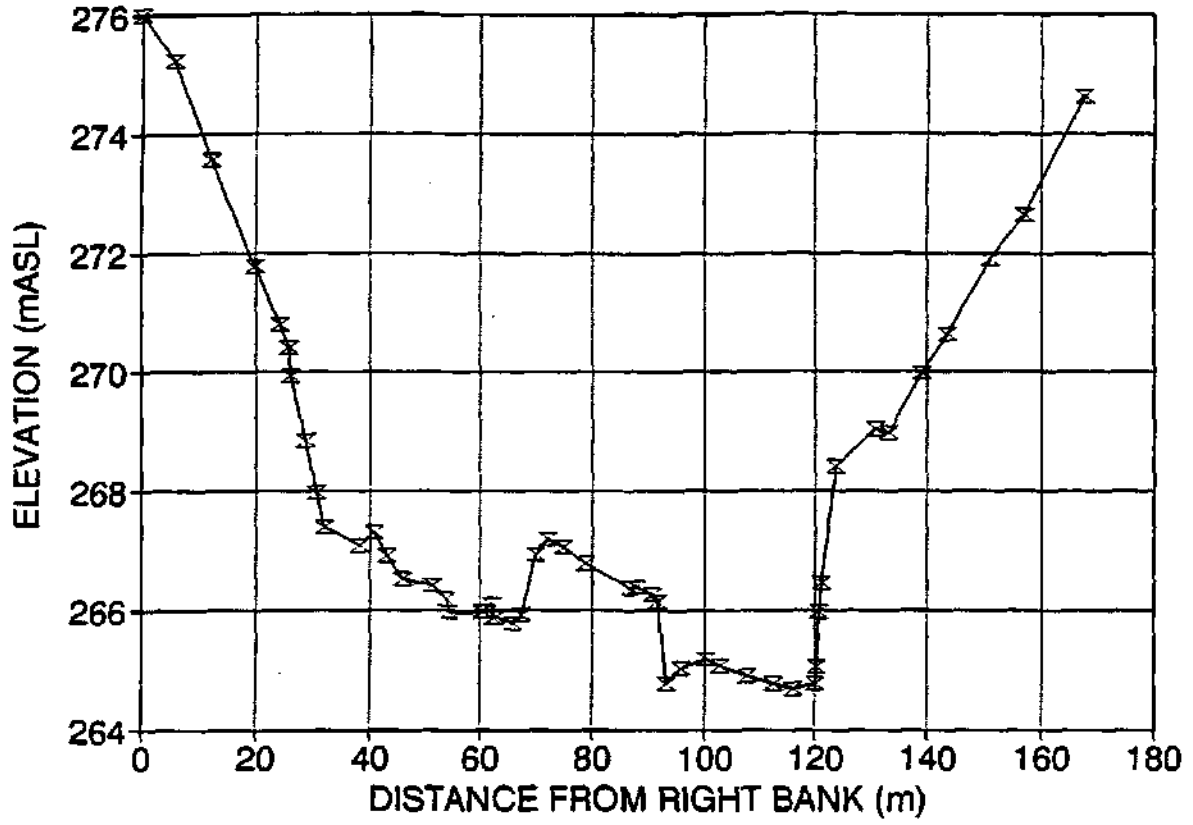
CROSS SECTION 12.6



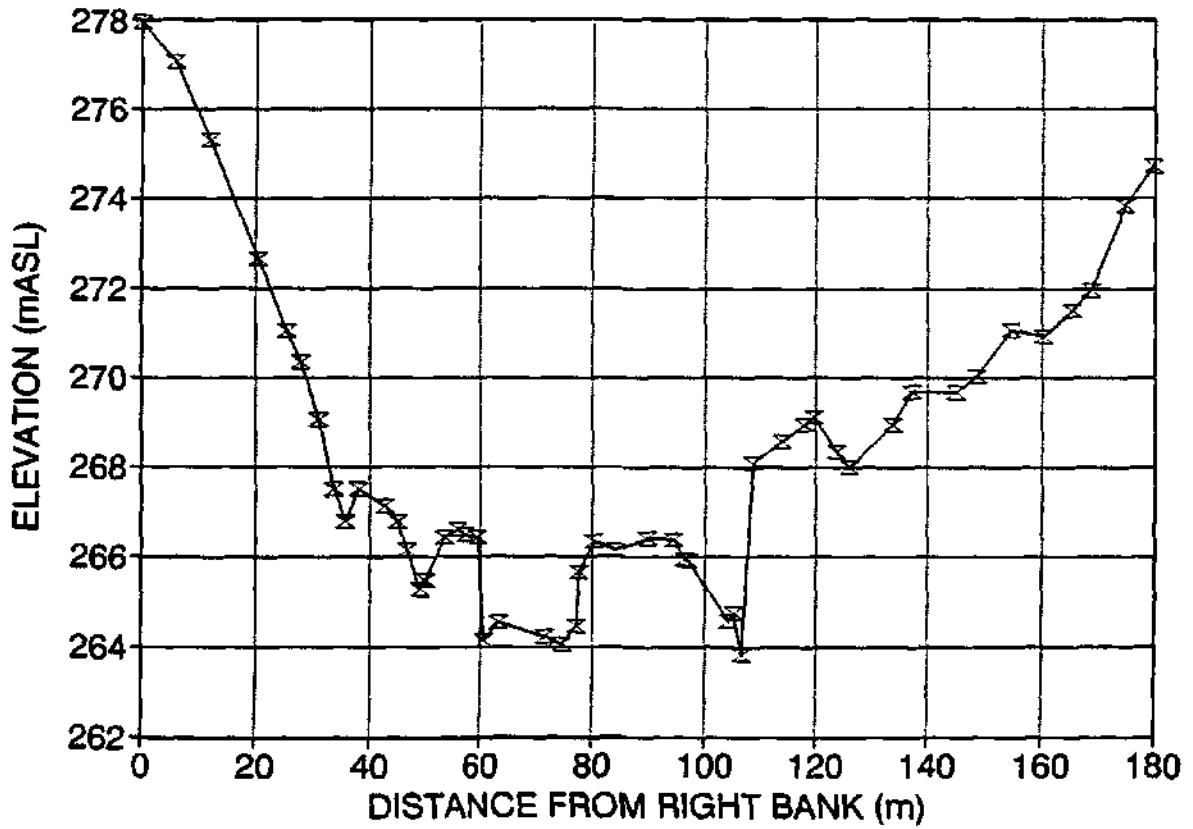
CROSS SECTION 12.7



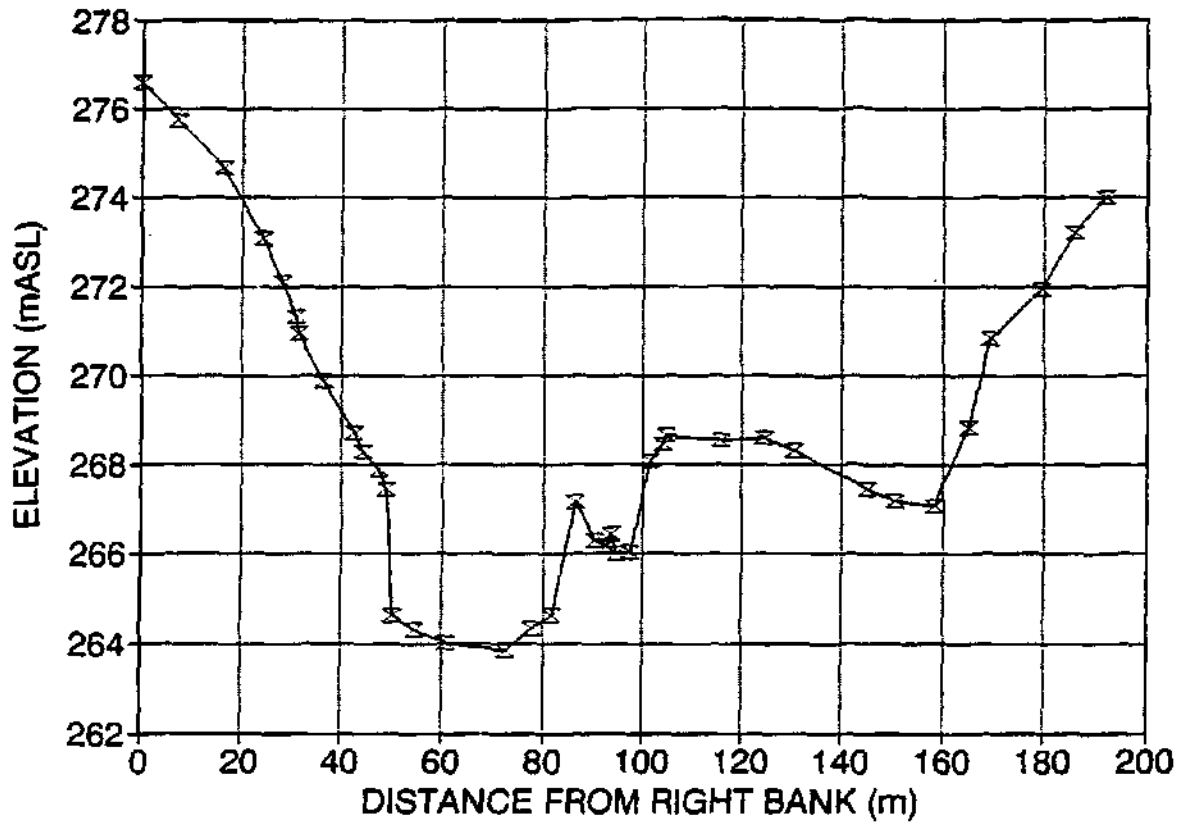
CROSS SECTION 12.8



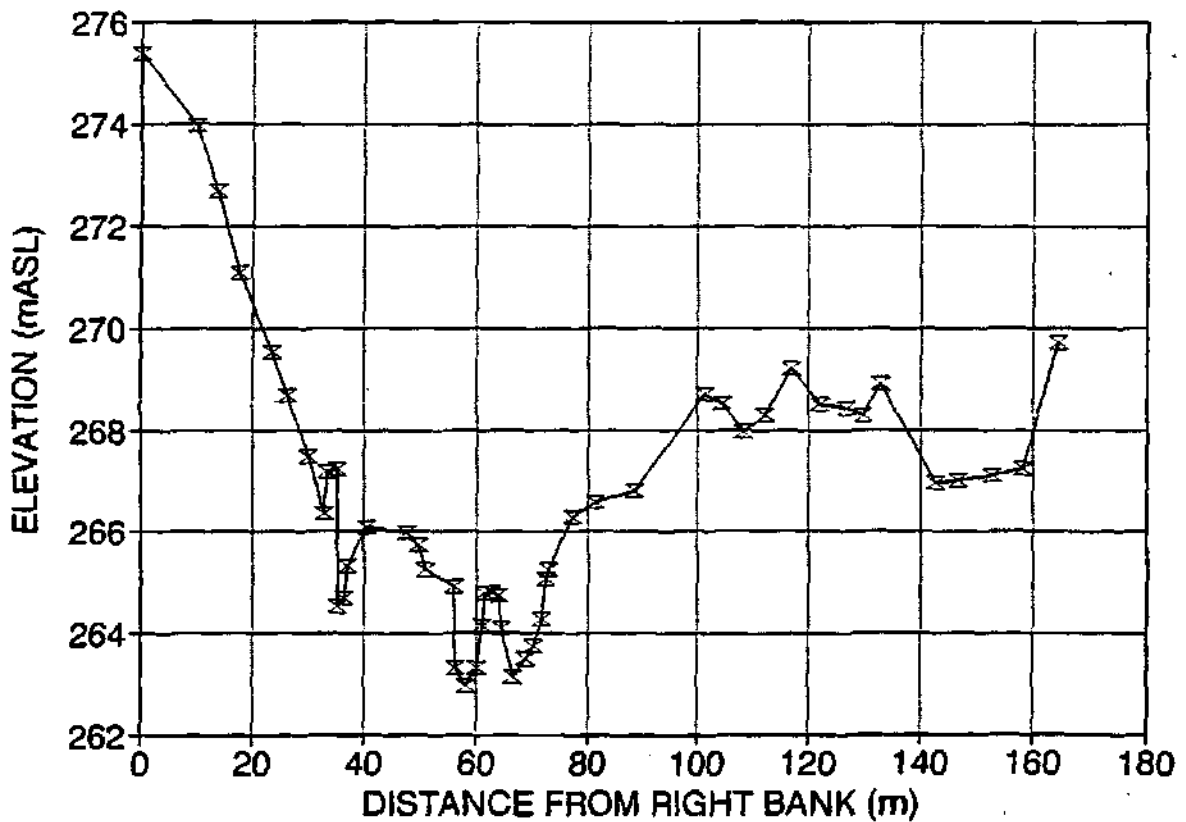
CROSS SECTION 12.9



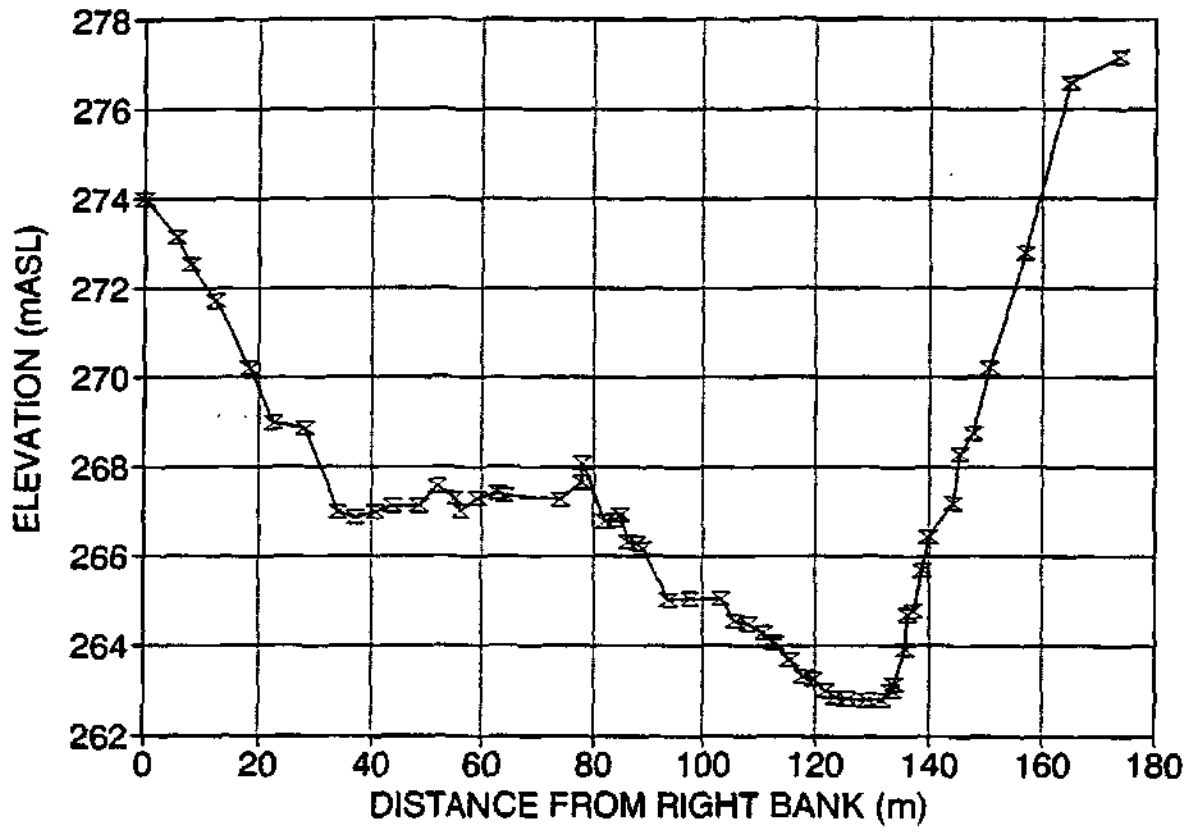
CROSS SECTION 12.10



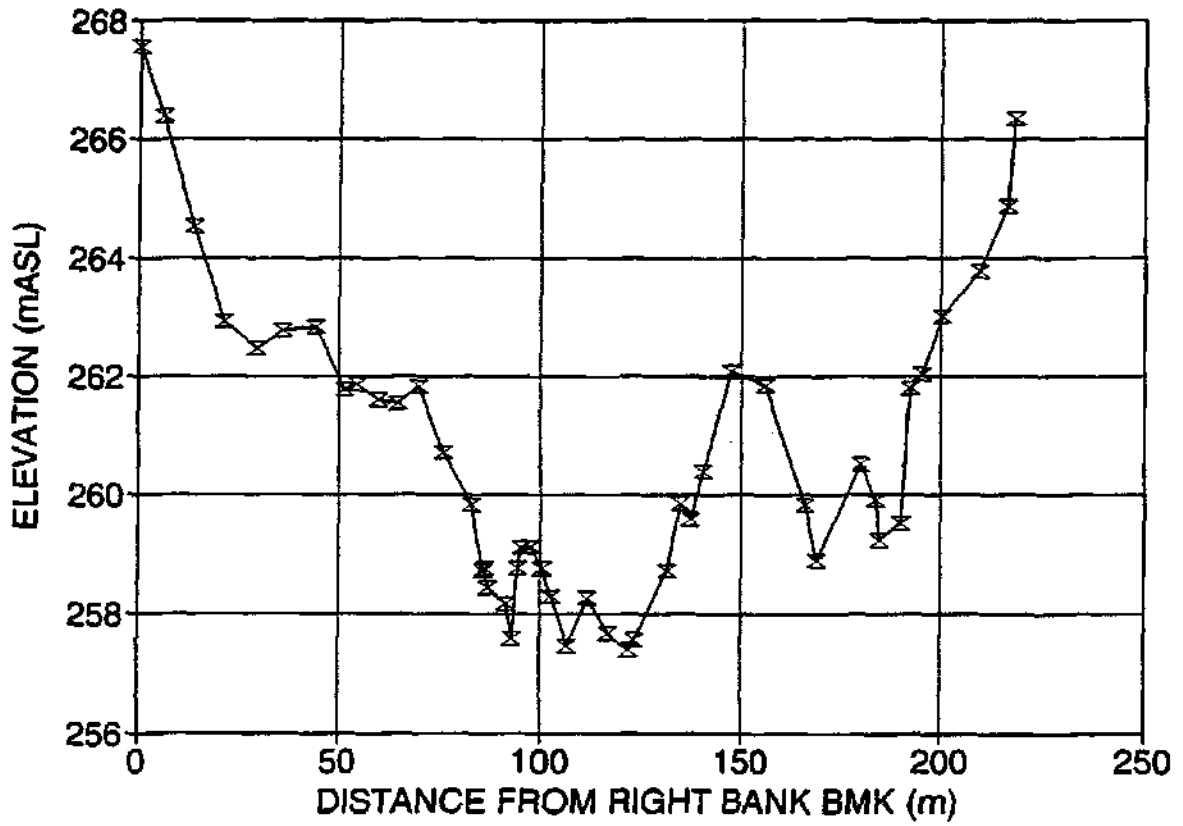
CROSS SECTION 12.11



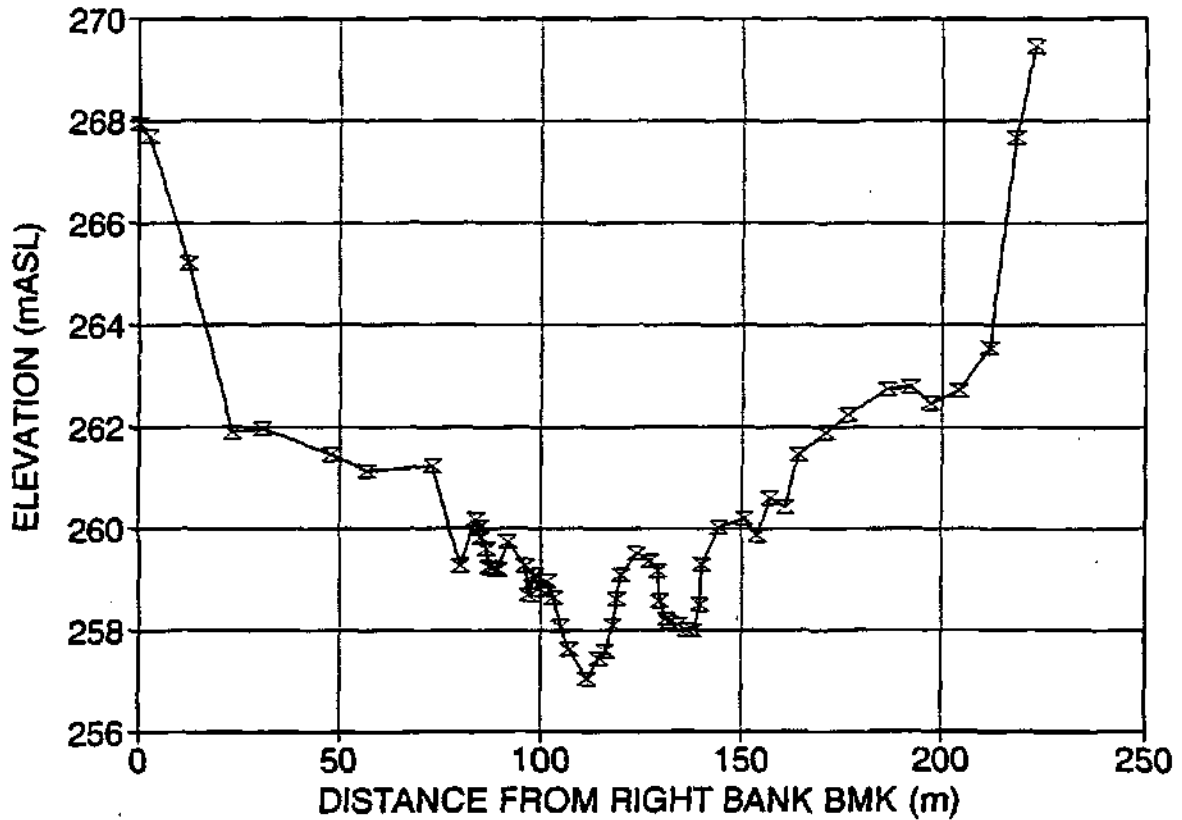
CROSS SECTION 14



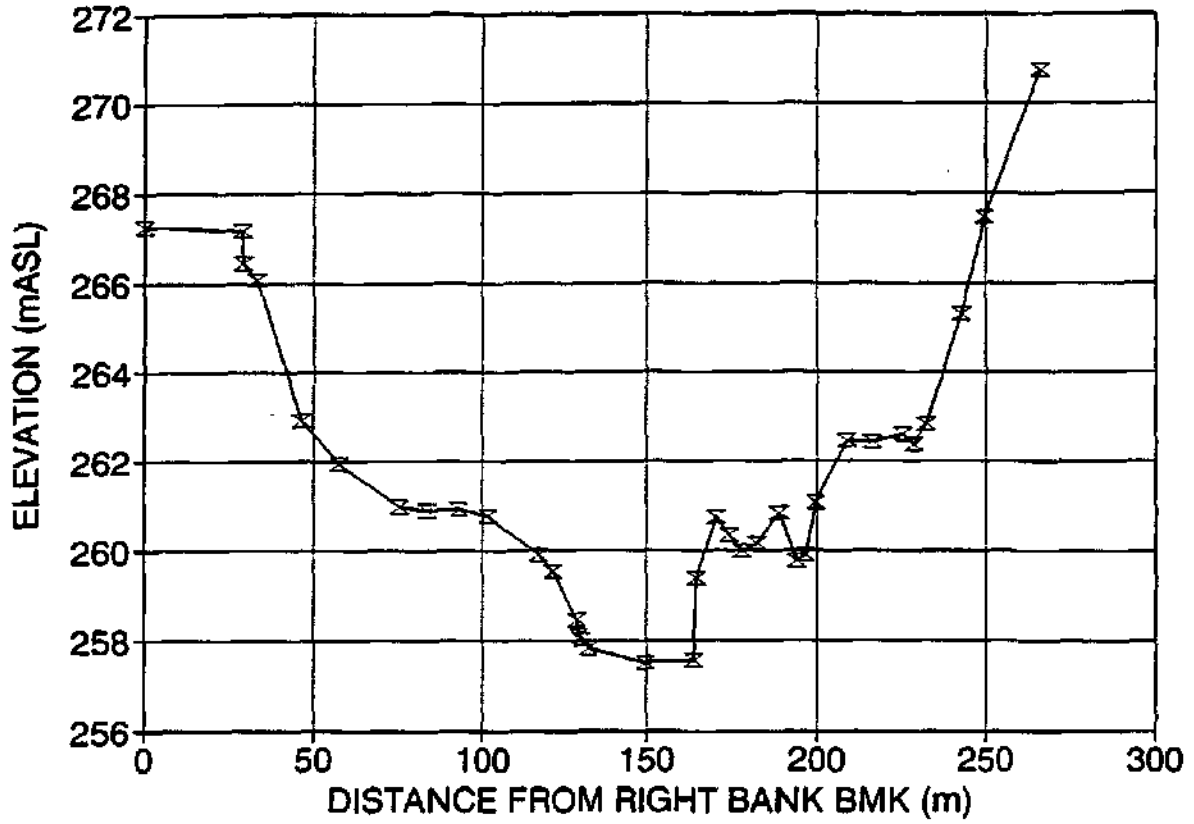
CROSS SECTION 15.1



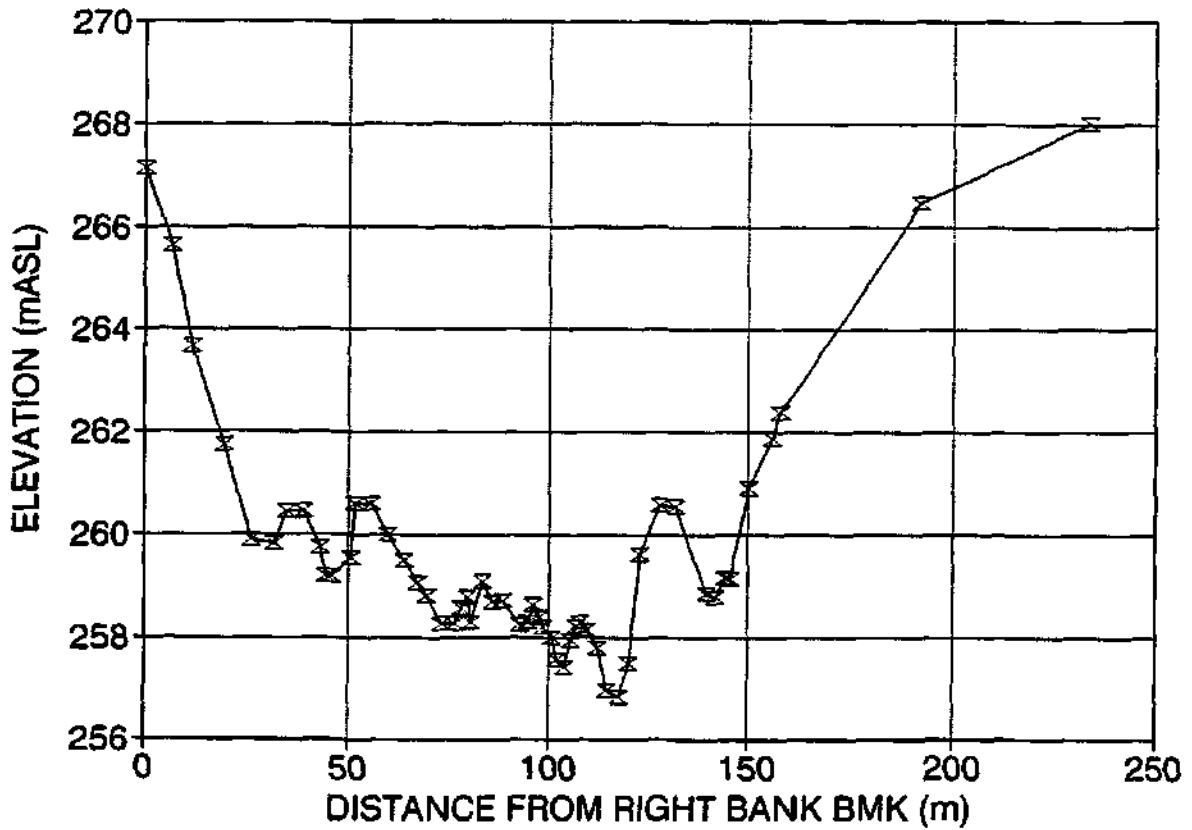
CROSS SECTION 15.2



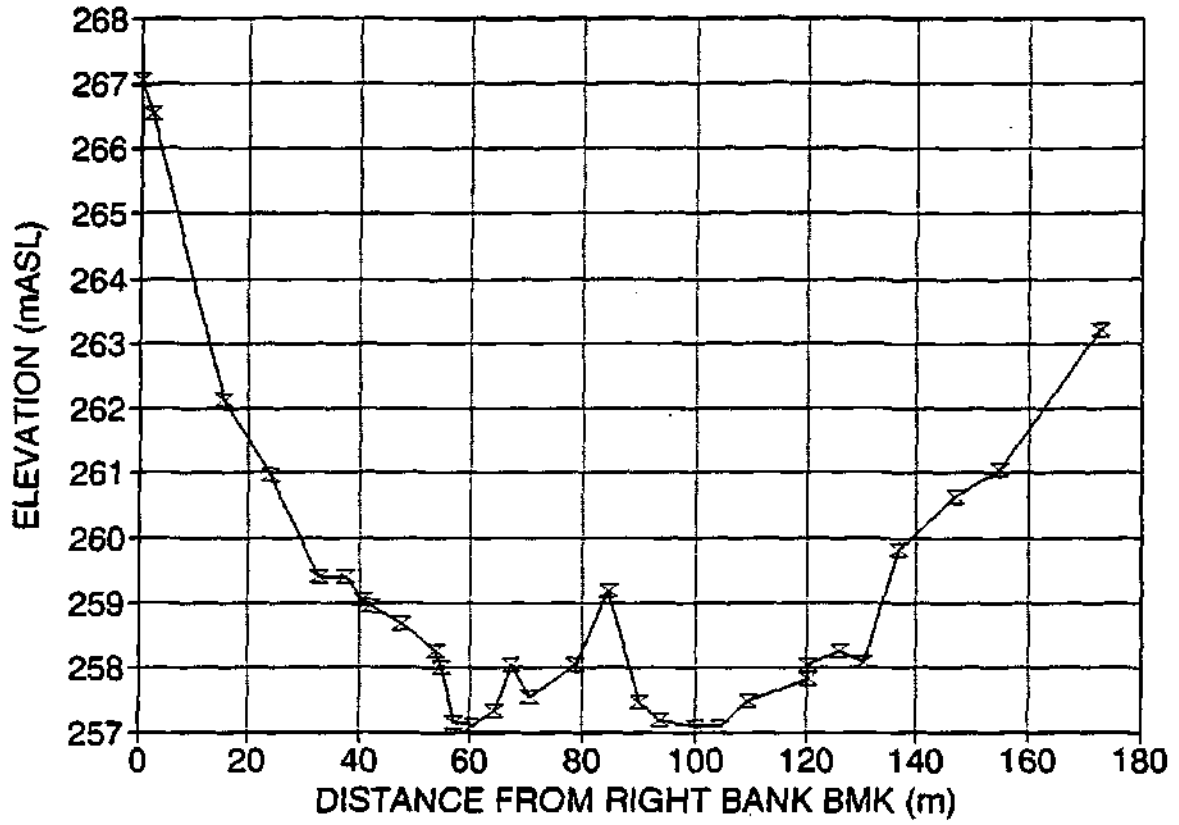
CROSS SECTION 15.0



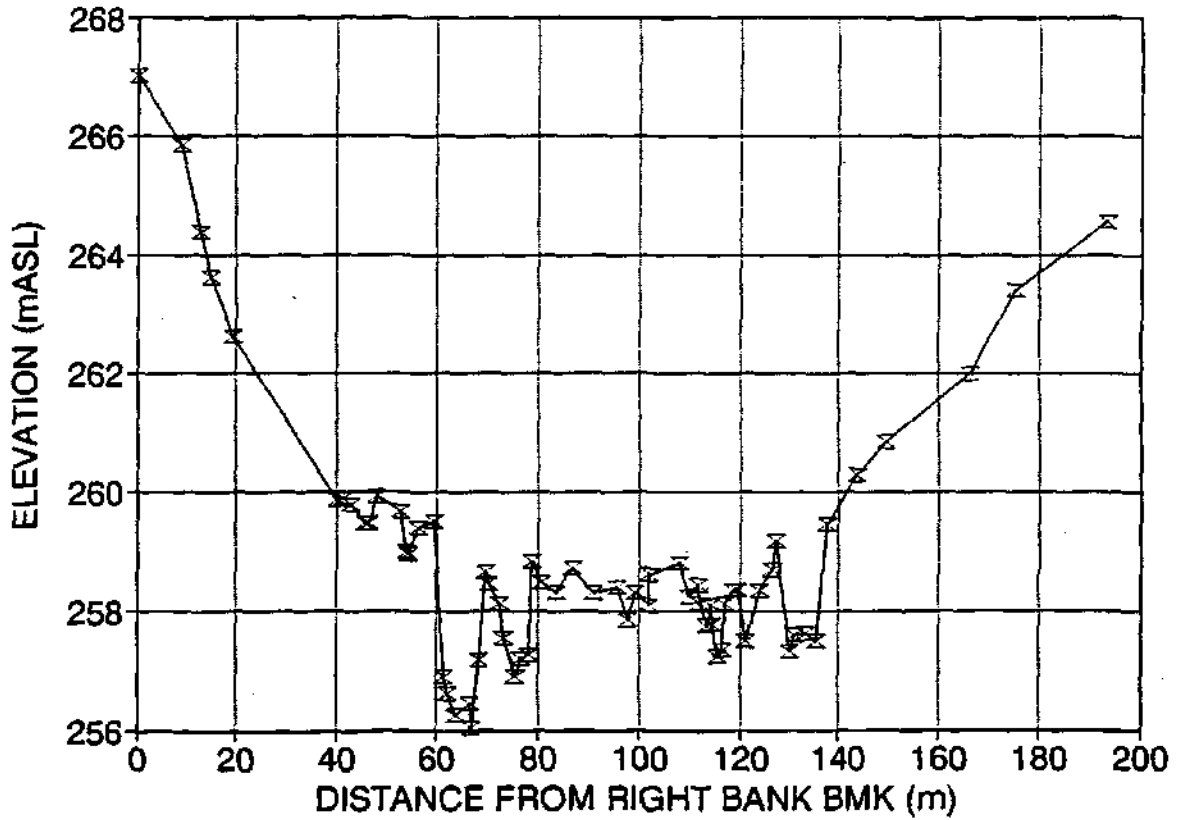
CROSS SECTION 15.3



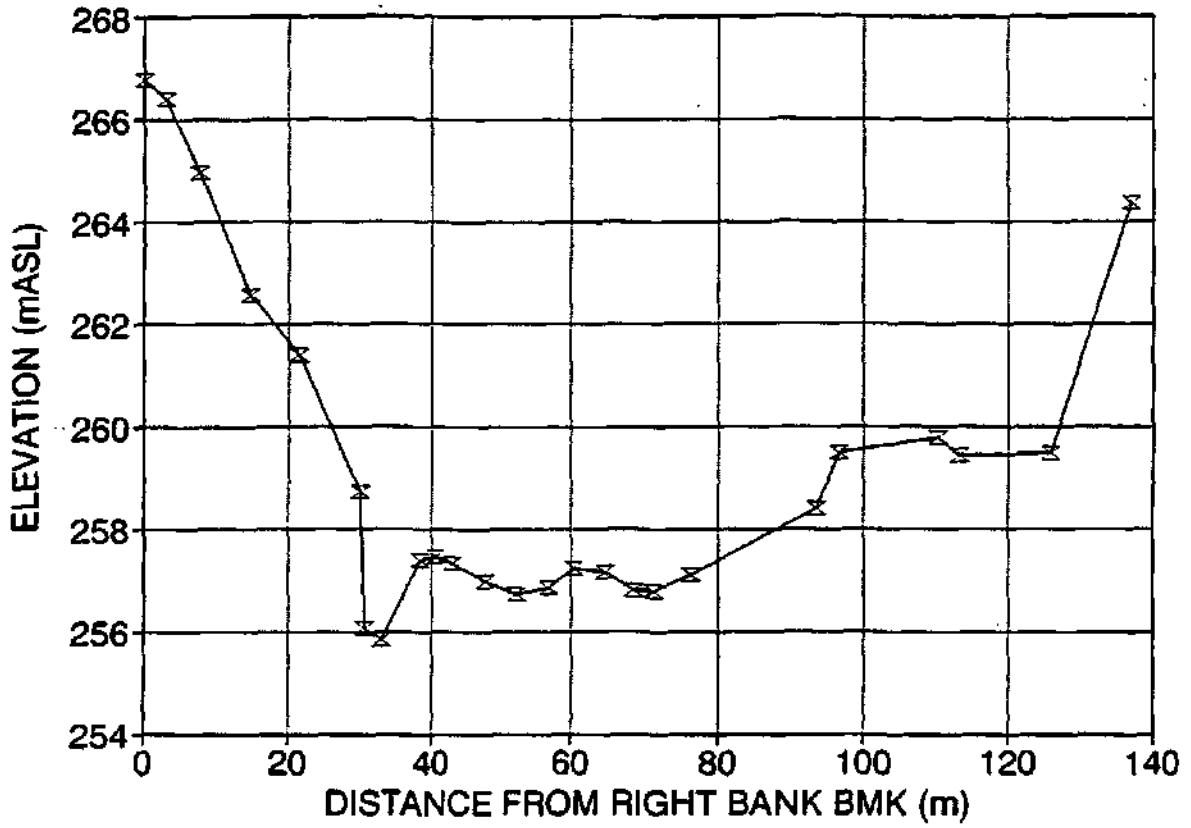
CROSS SECTION 15.4



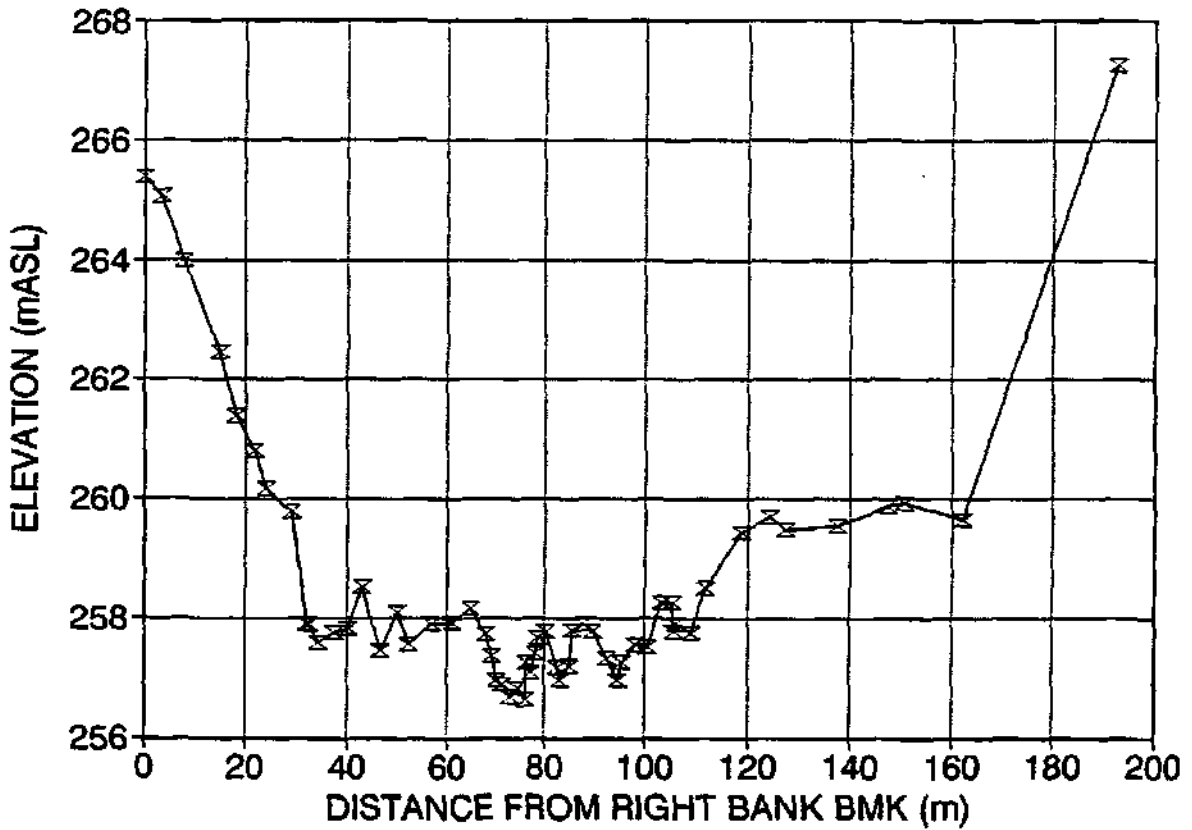
CROSS SECTION 15.5



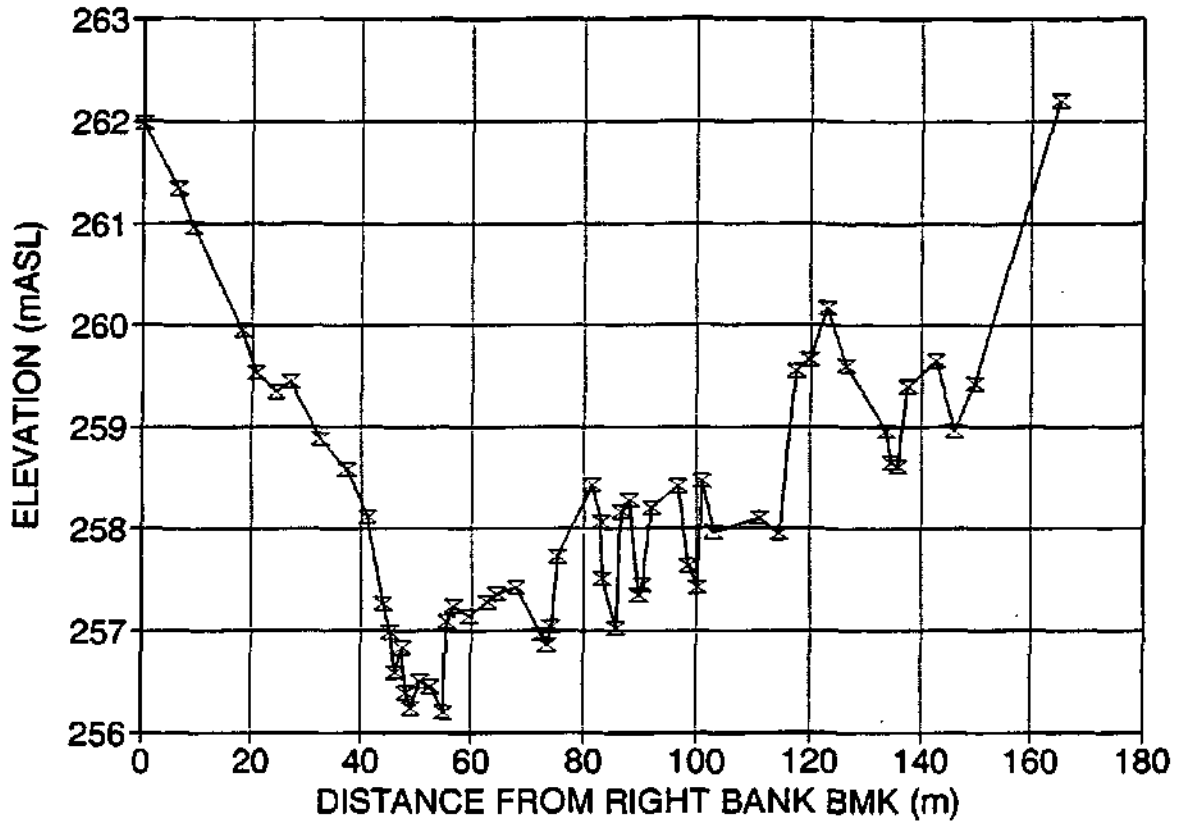
CROSS SECTION 15.6



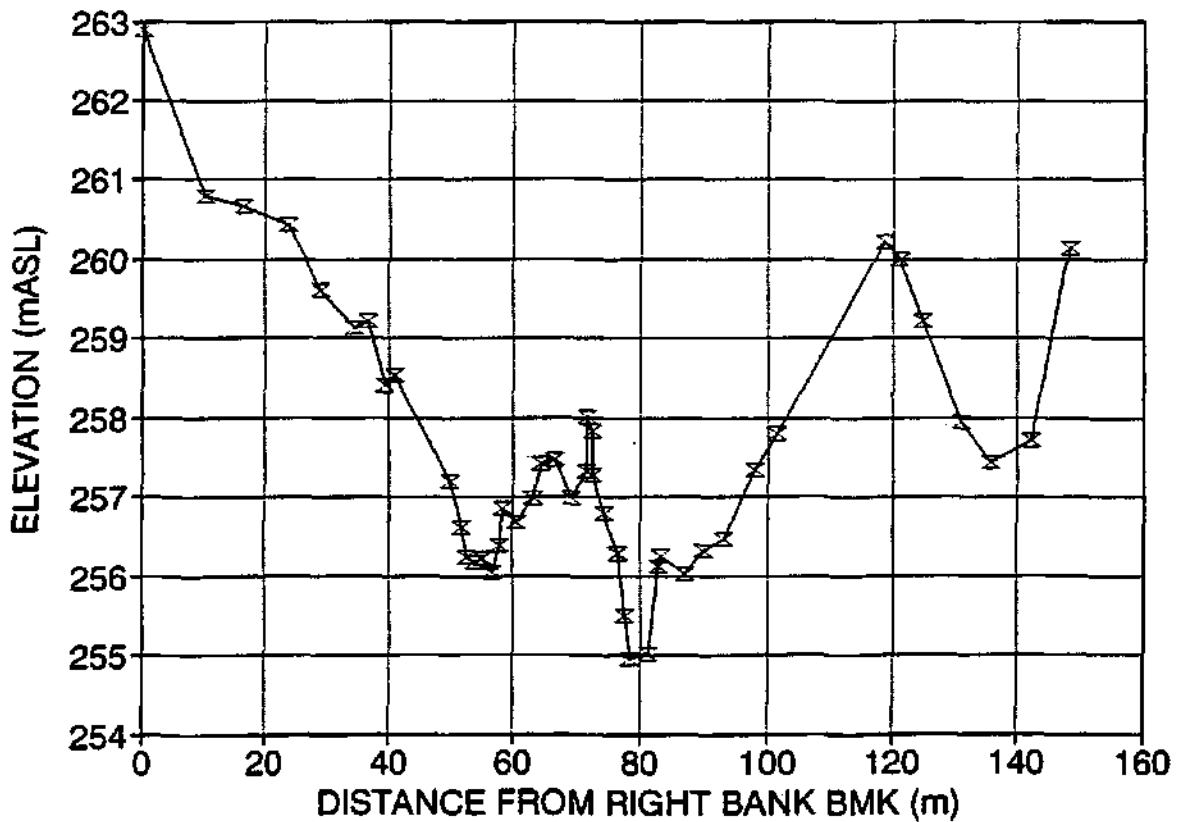
CROSS SECTION 15.7



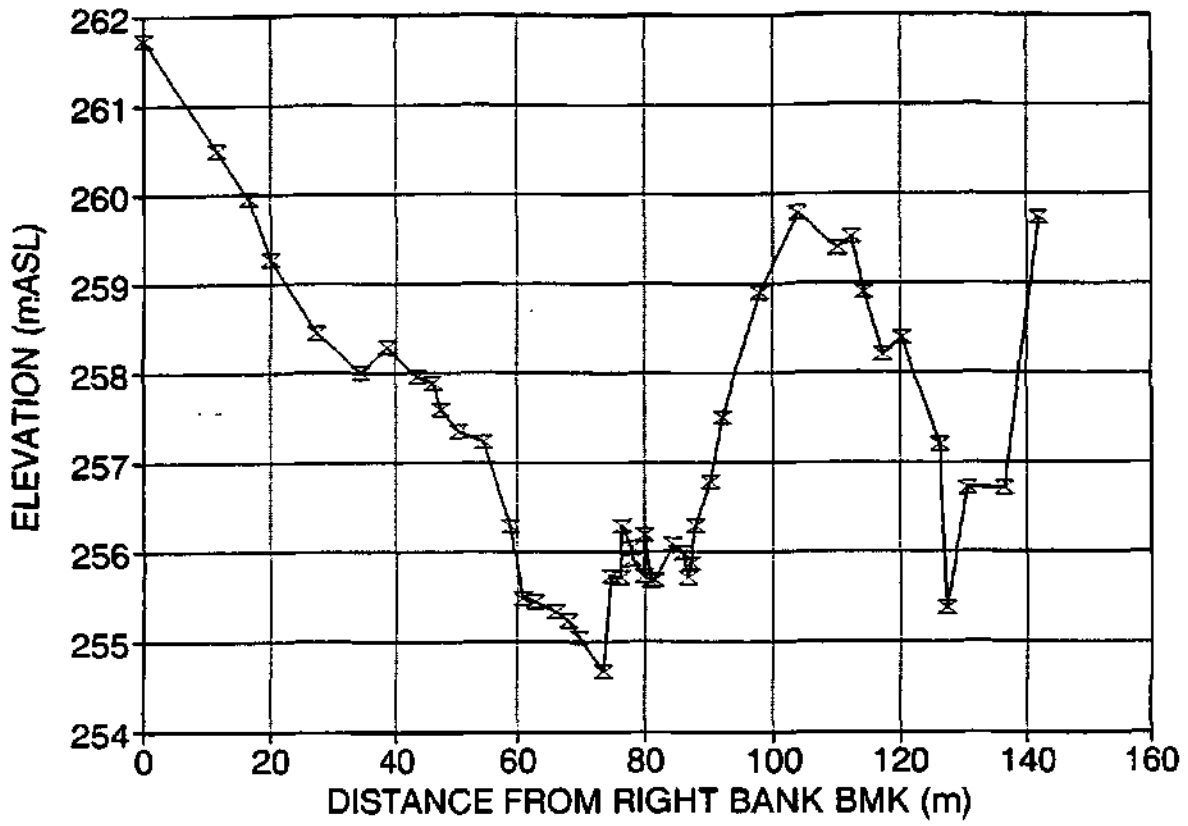
CROSS SECTION 15.8



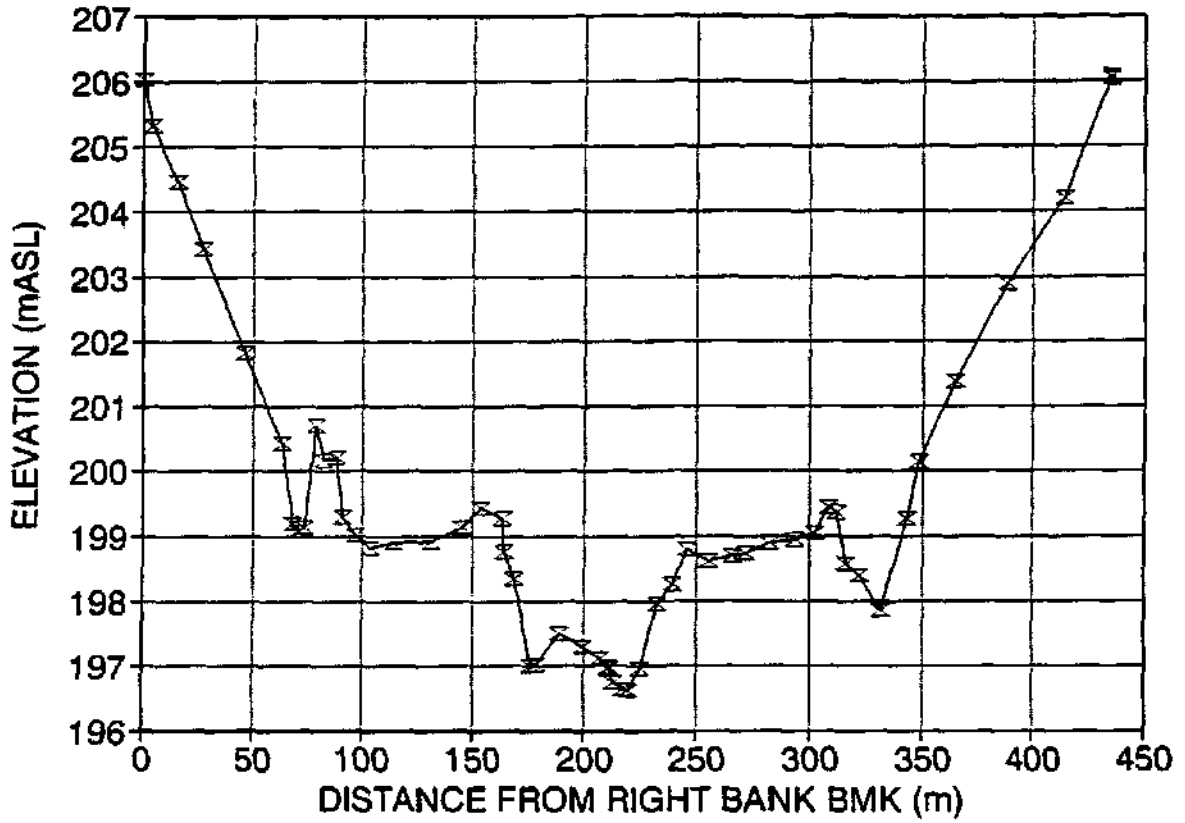
CROSS SECTION 15.9



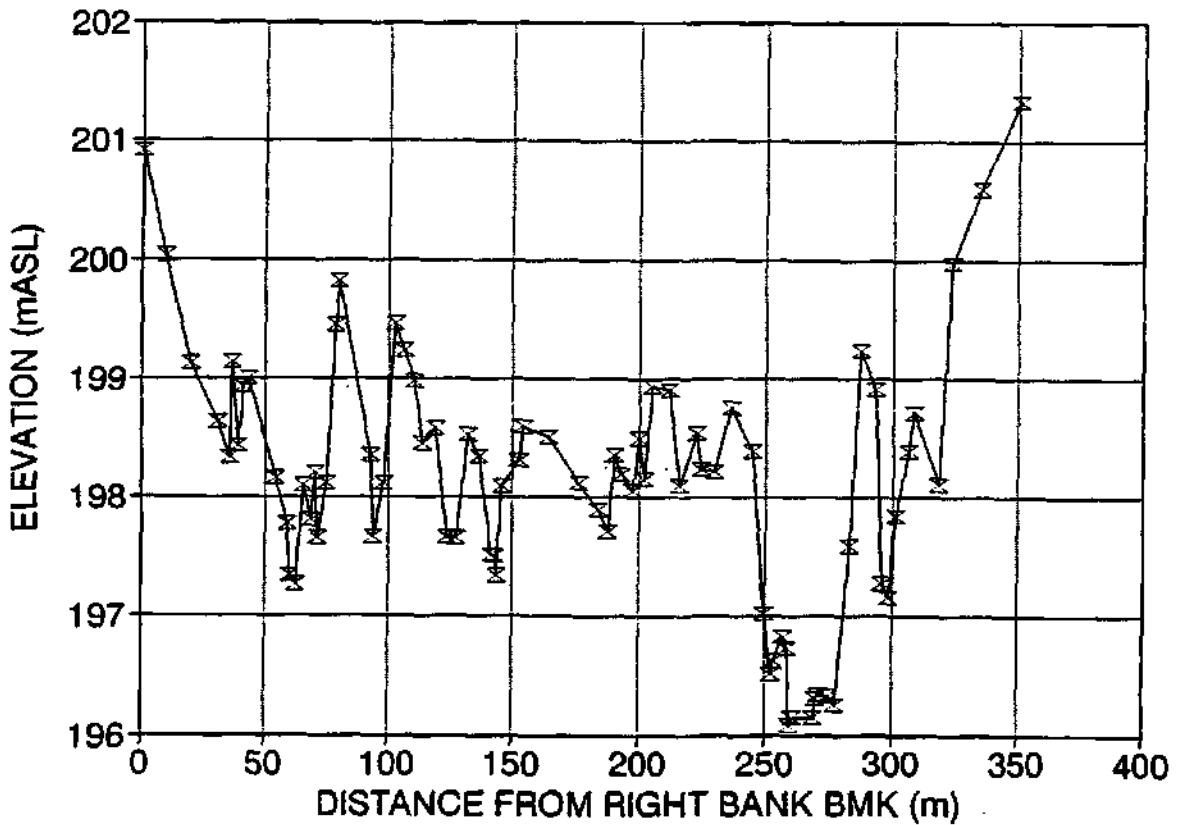
CROSS SECTION 15.10



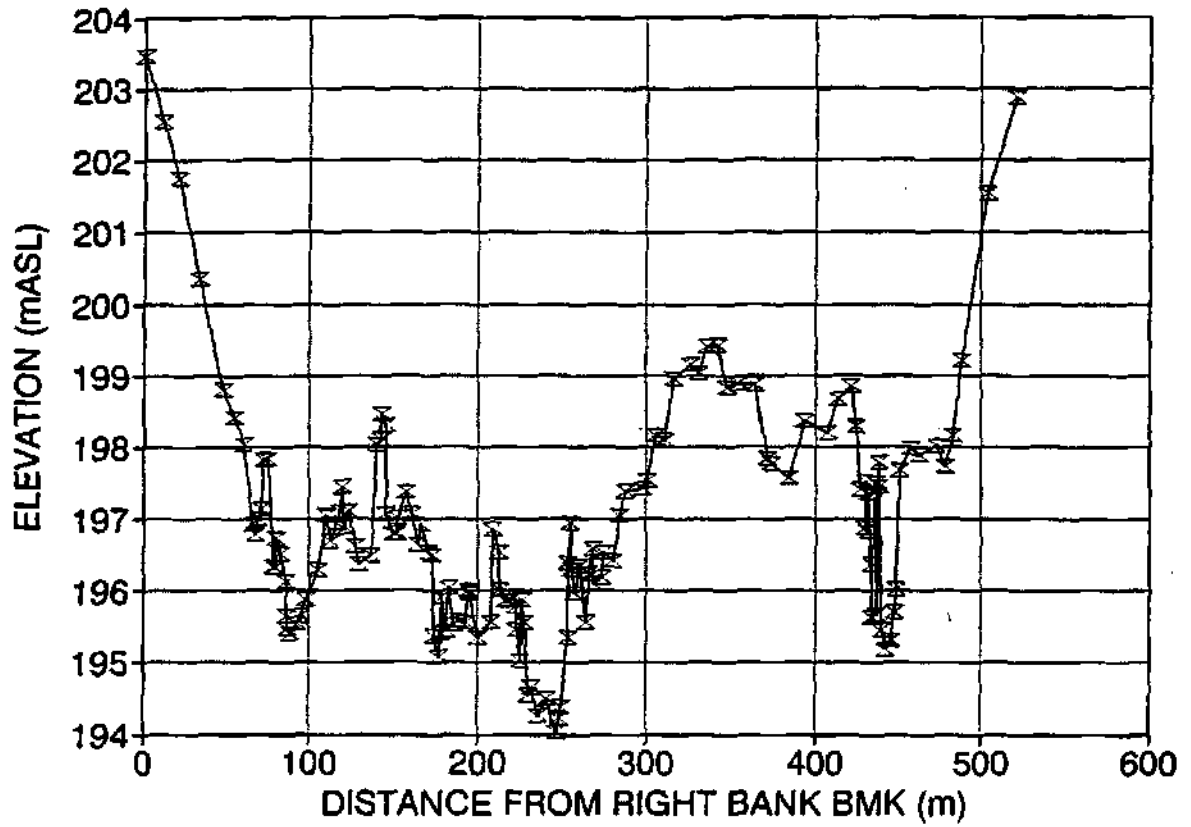
CROSS SECTION 20



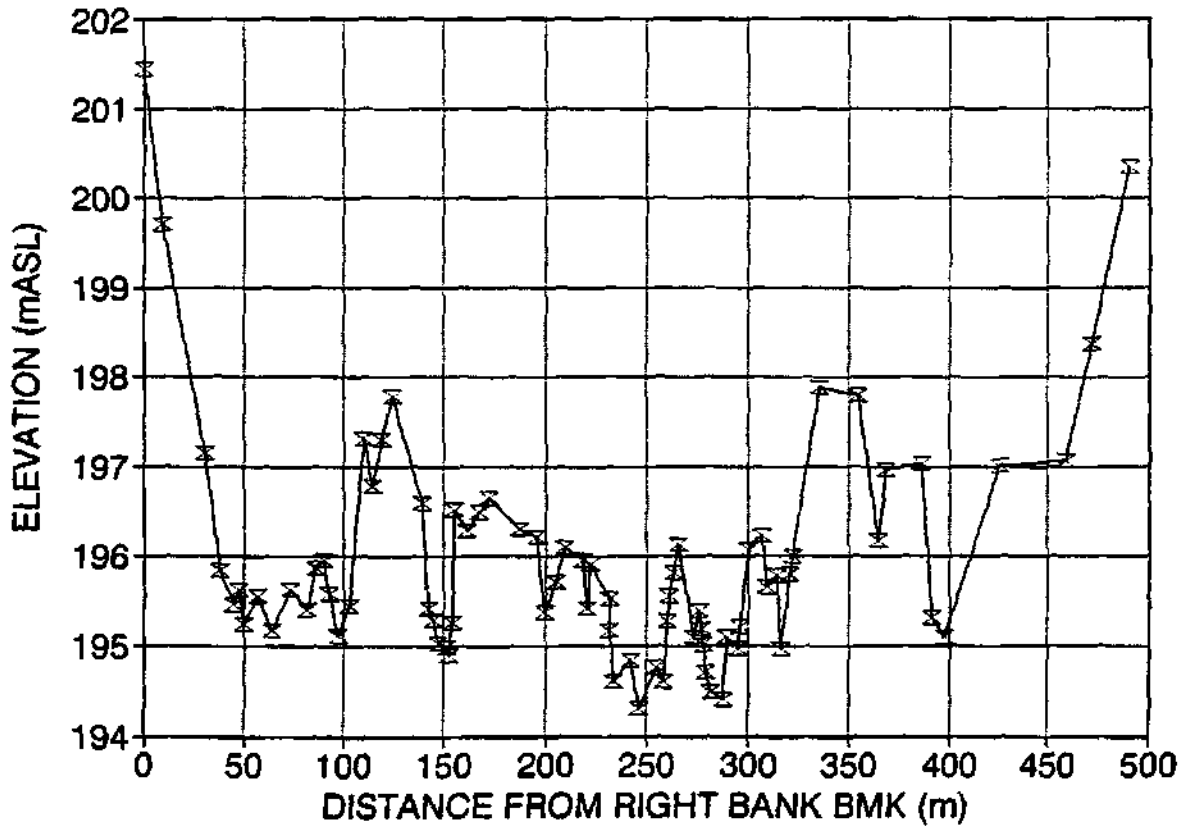
CROSS SECTION 20.1



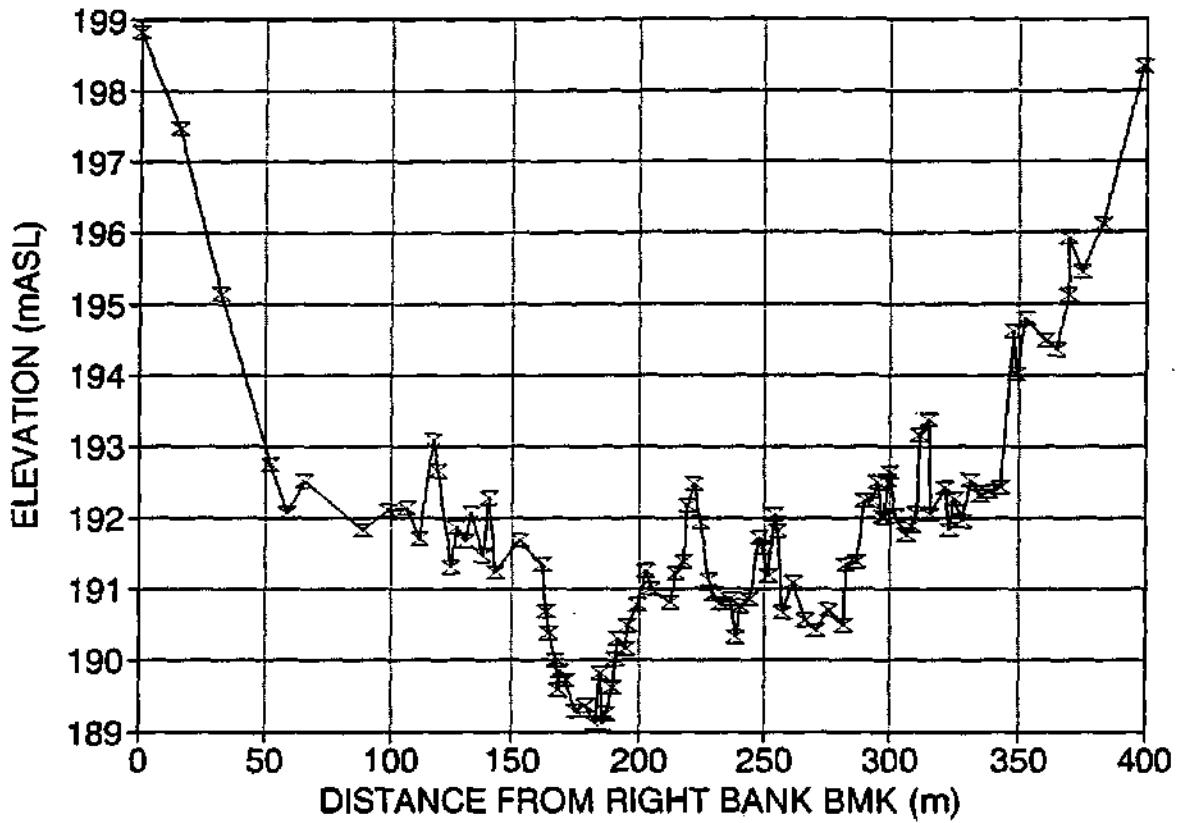
CROSS SECTION 20.2



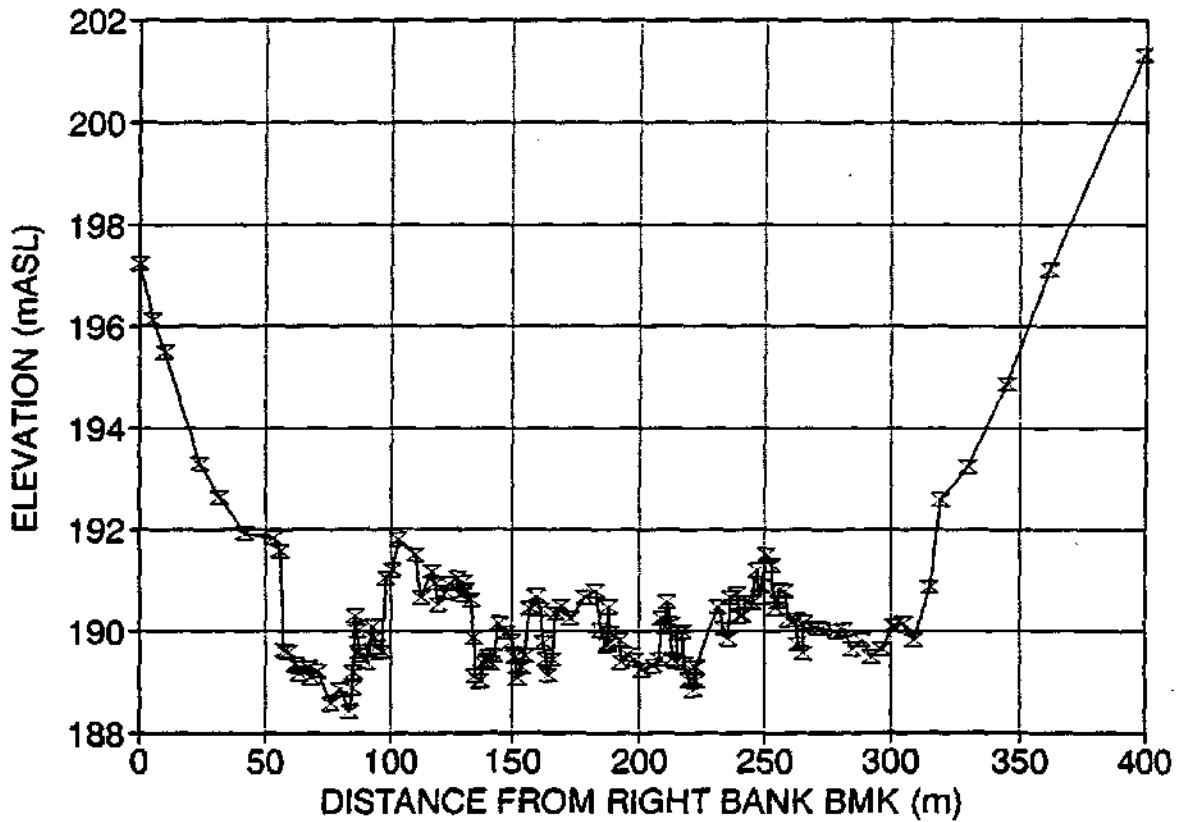
CROSS SECTION 20.3



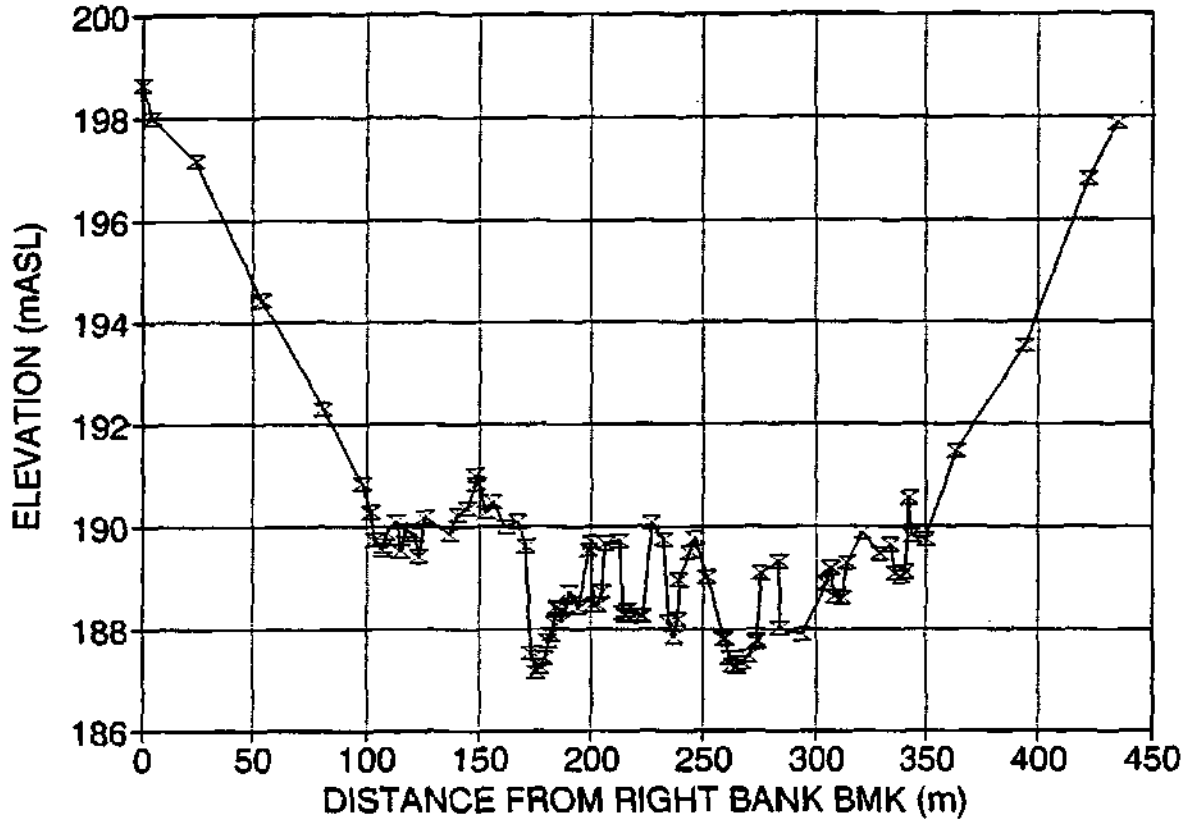
CROSS SECTION 20.6



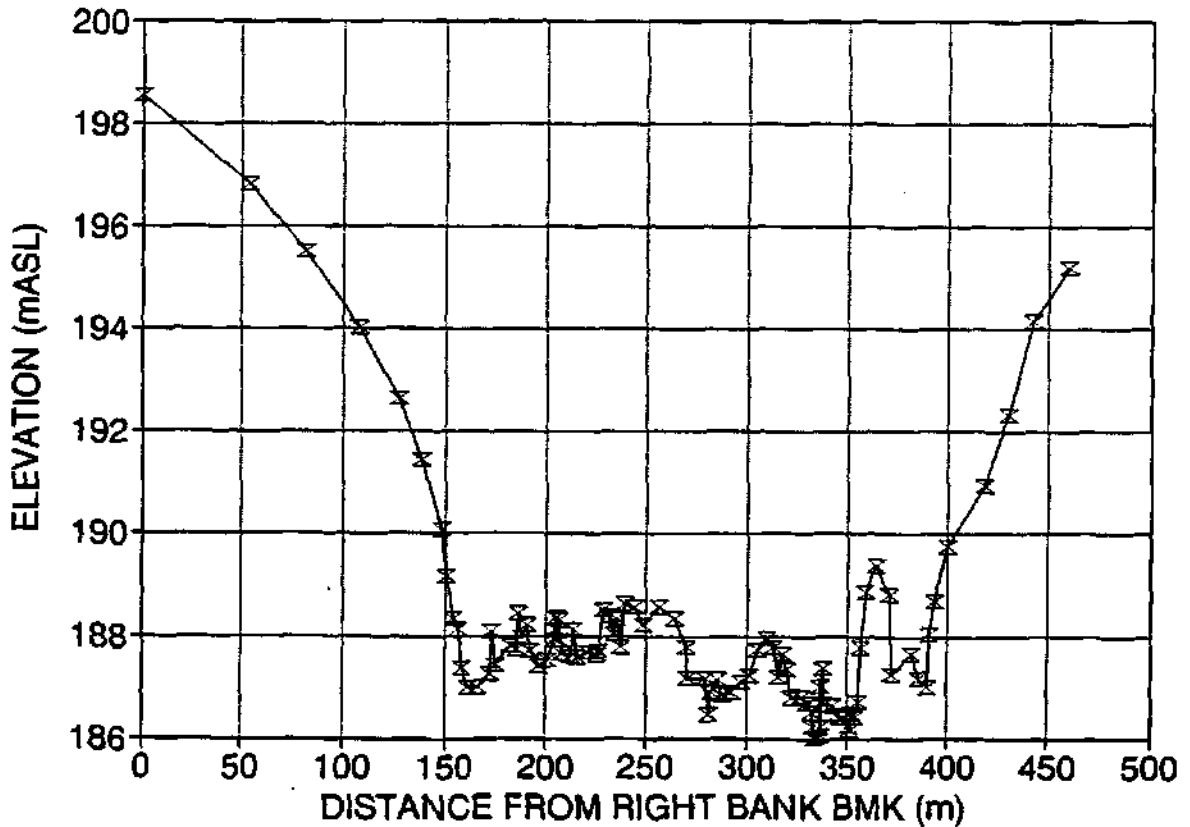
CROSS SECTION 20.7



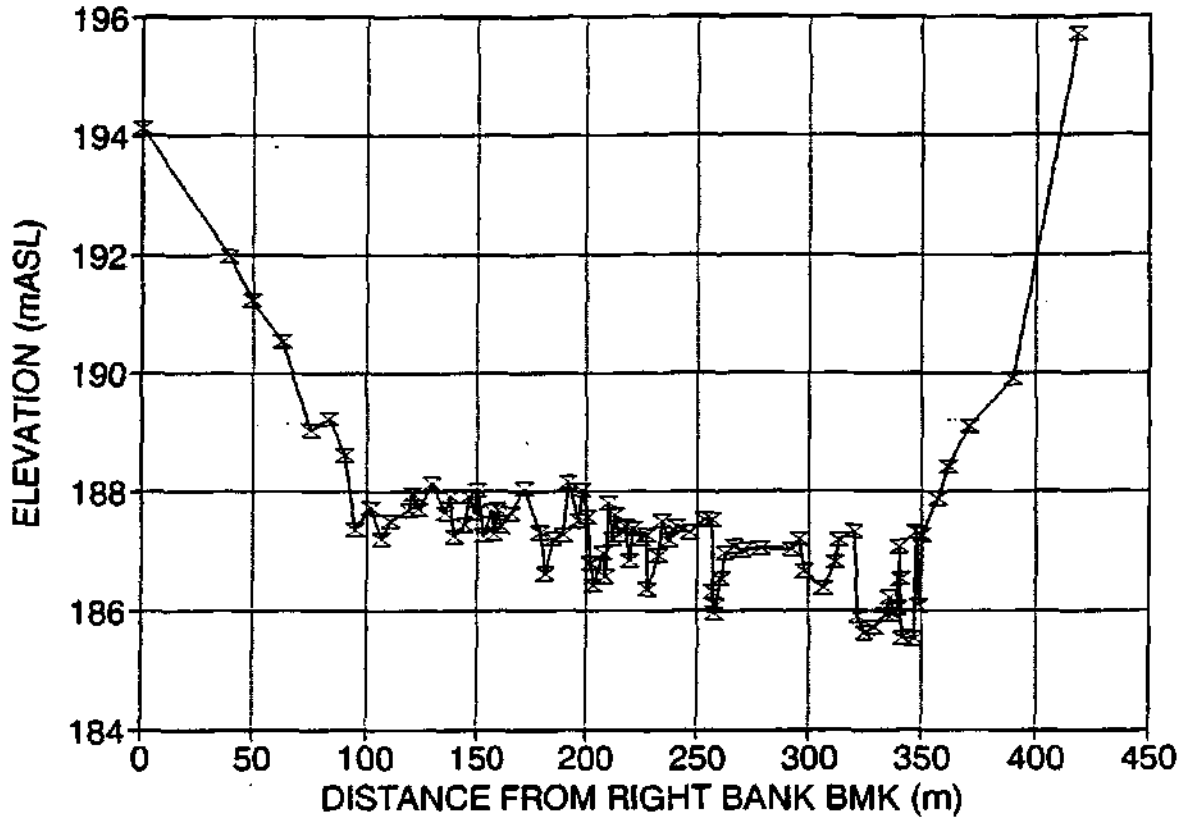
CROSS SECTION 21



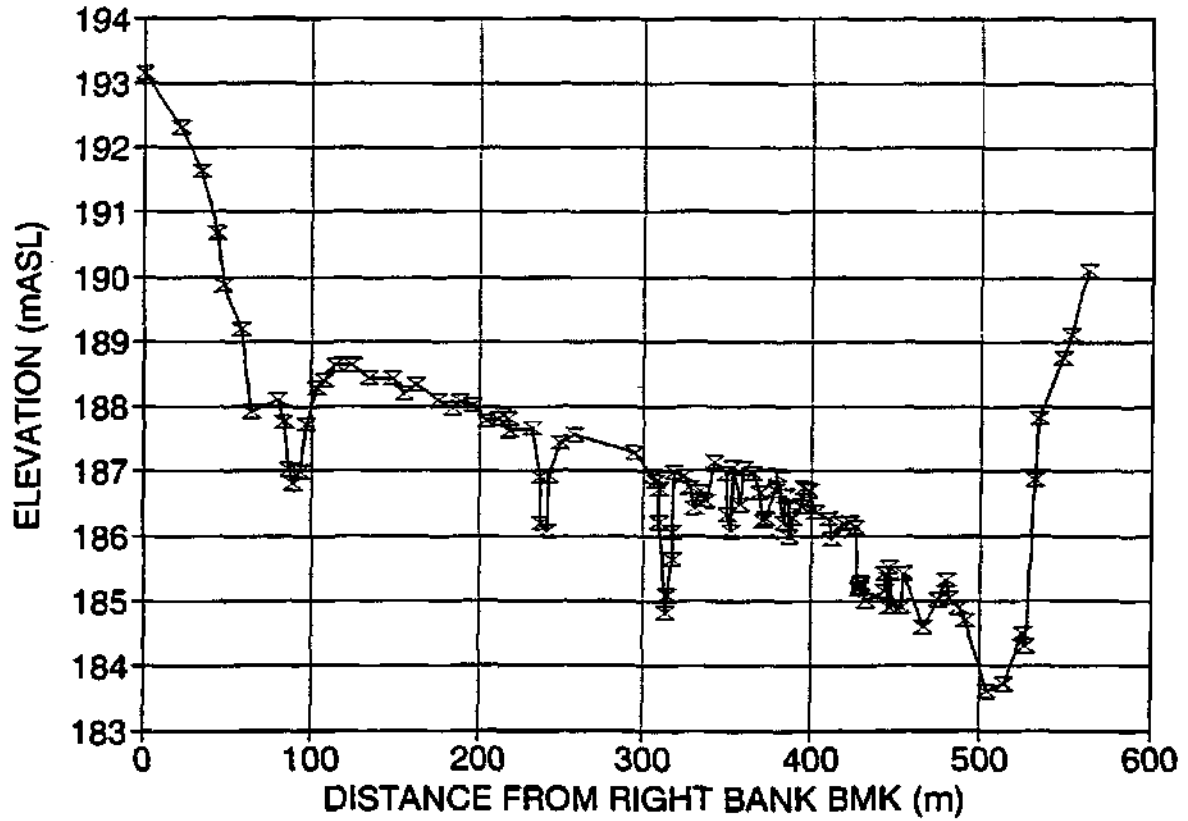
CROSS SECTION 21.1



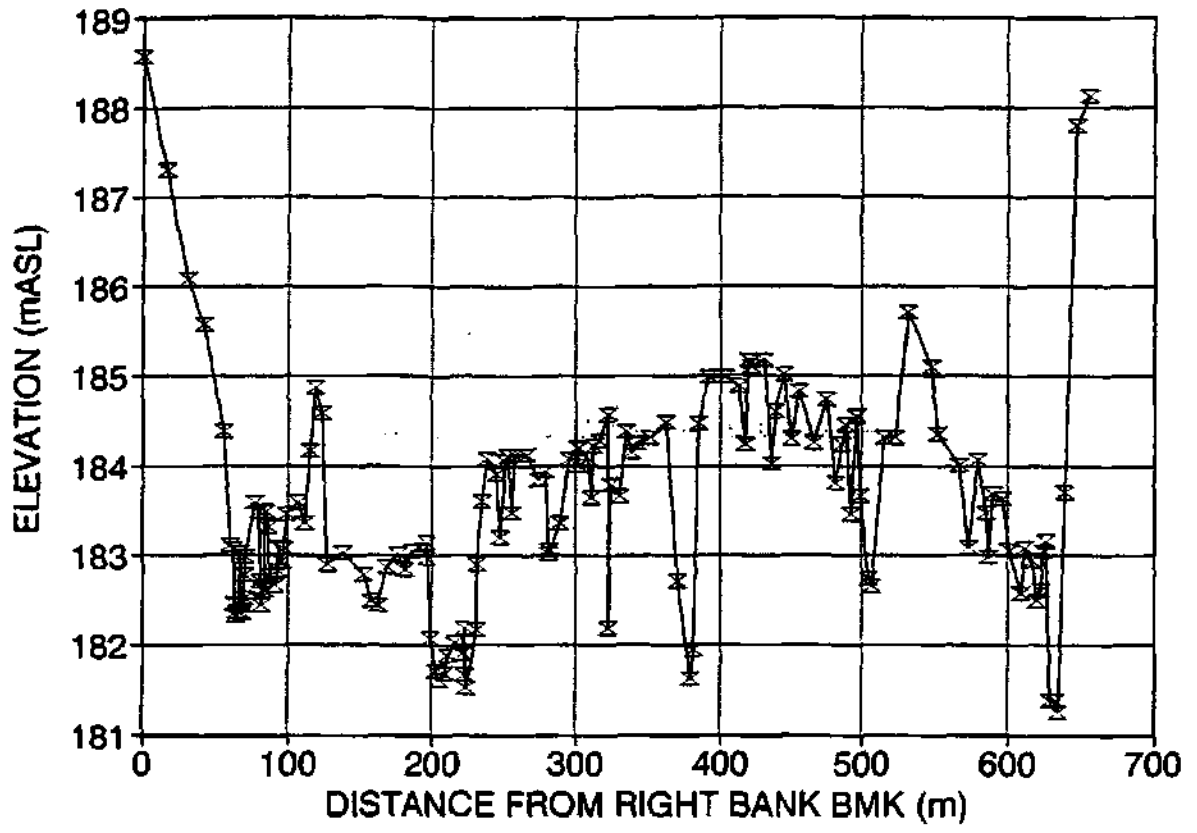
CROSS SECTION 21.2



CROSS SECTION 21.3



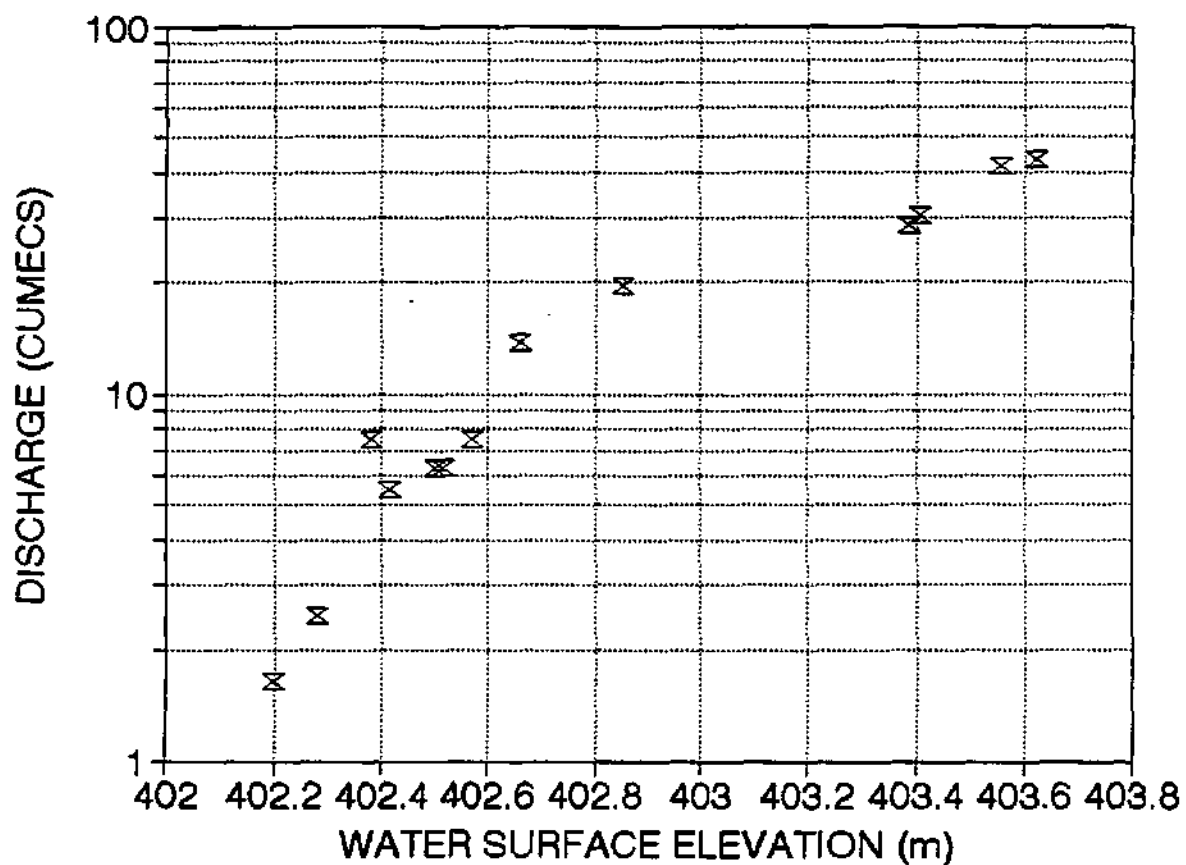
CROSS SECTION 22



APPENDIX 3: STAGE-DISCHARGE RATING CURVES

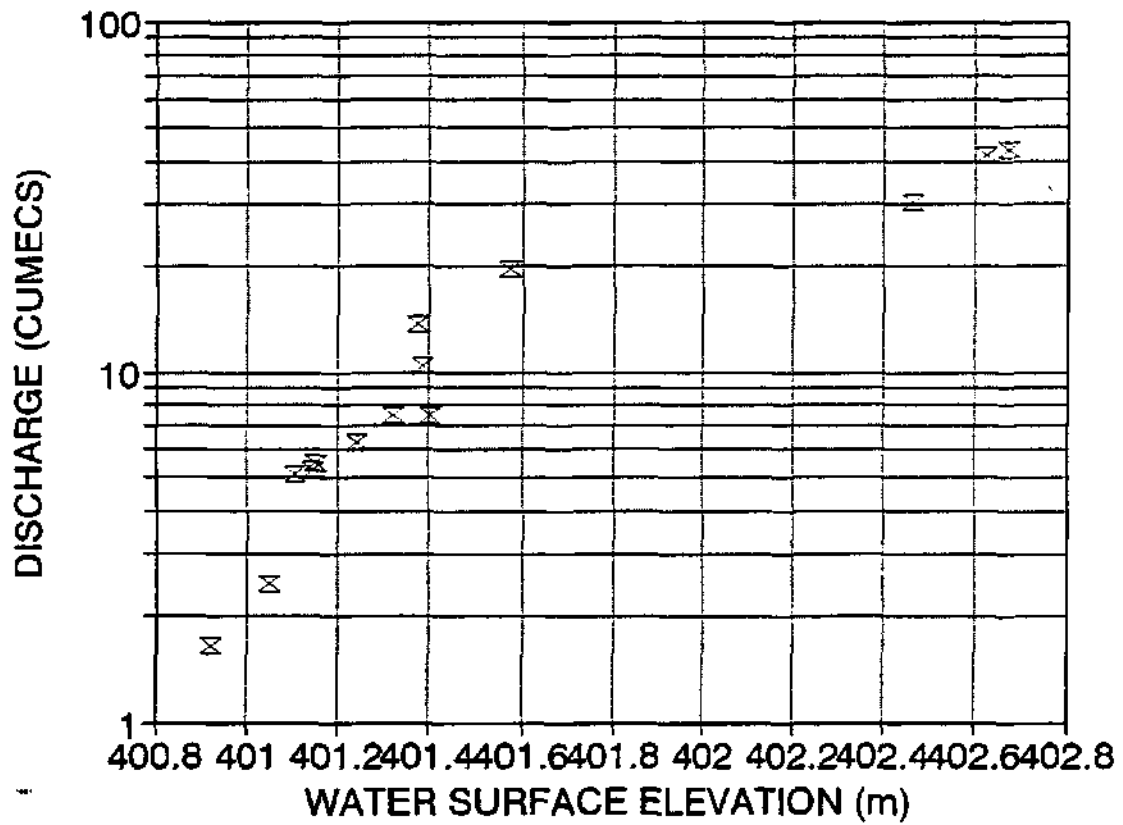
DISCHARGE RATING CURVE

SITE 0.0



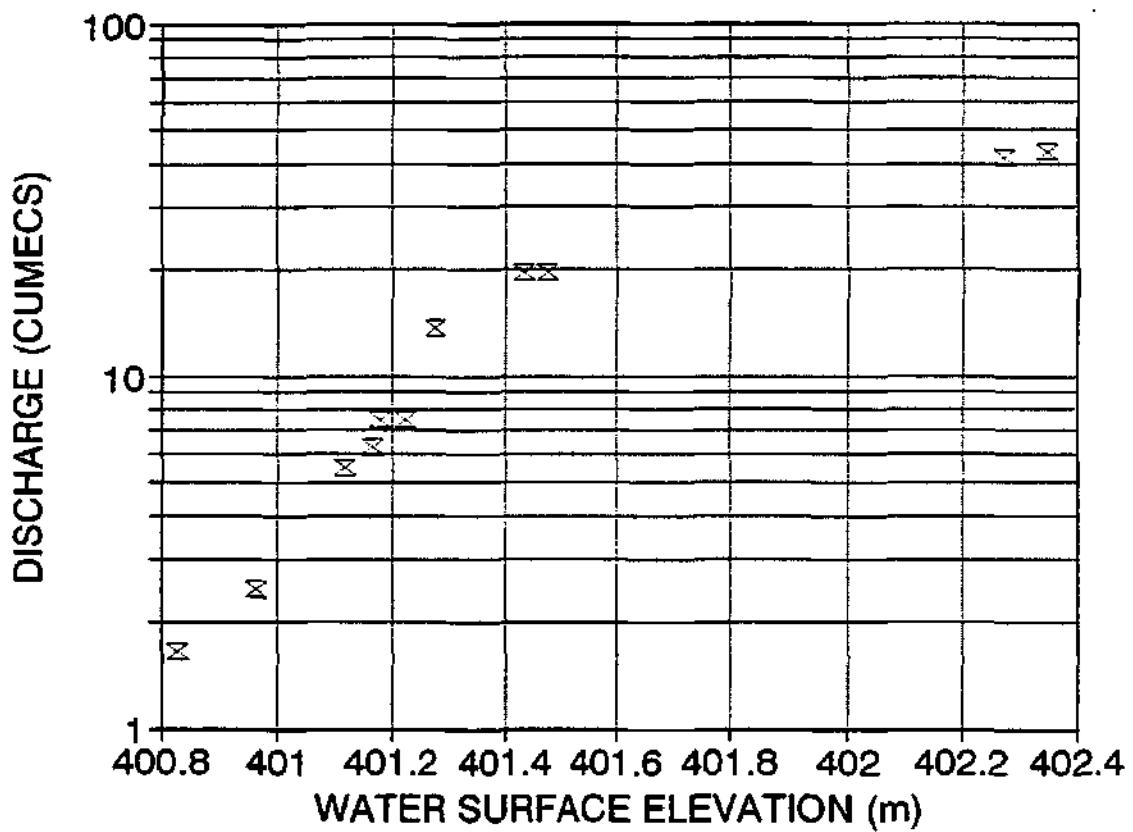
DISCHARGE RATING CURVE

SITE 0.1A



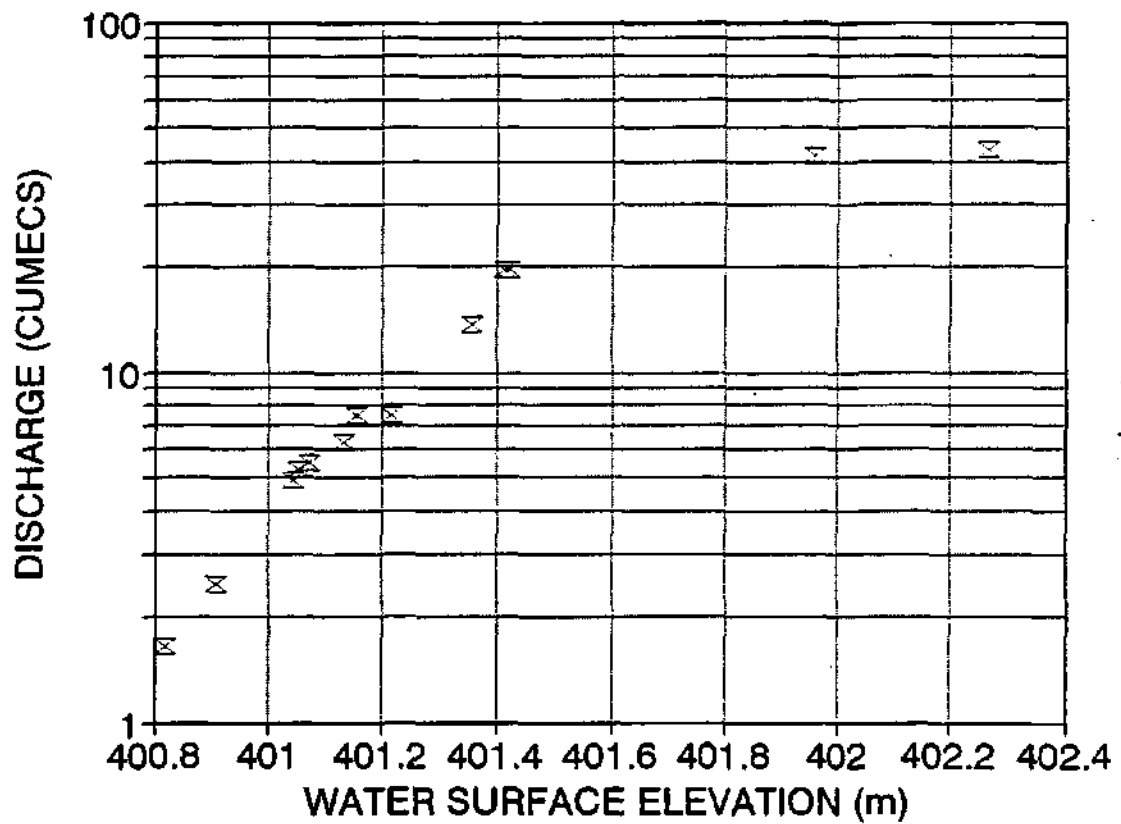
DISCHARGE RATING CURVE

SITE 0.2



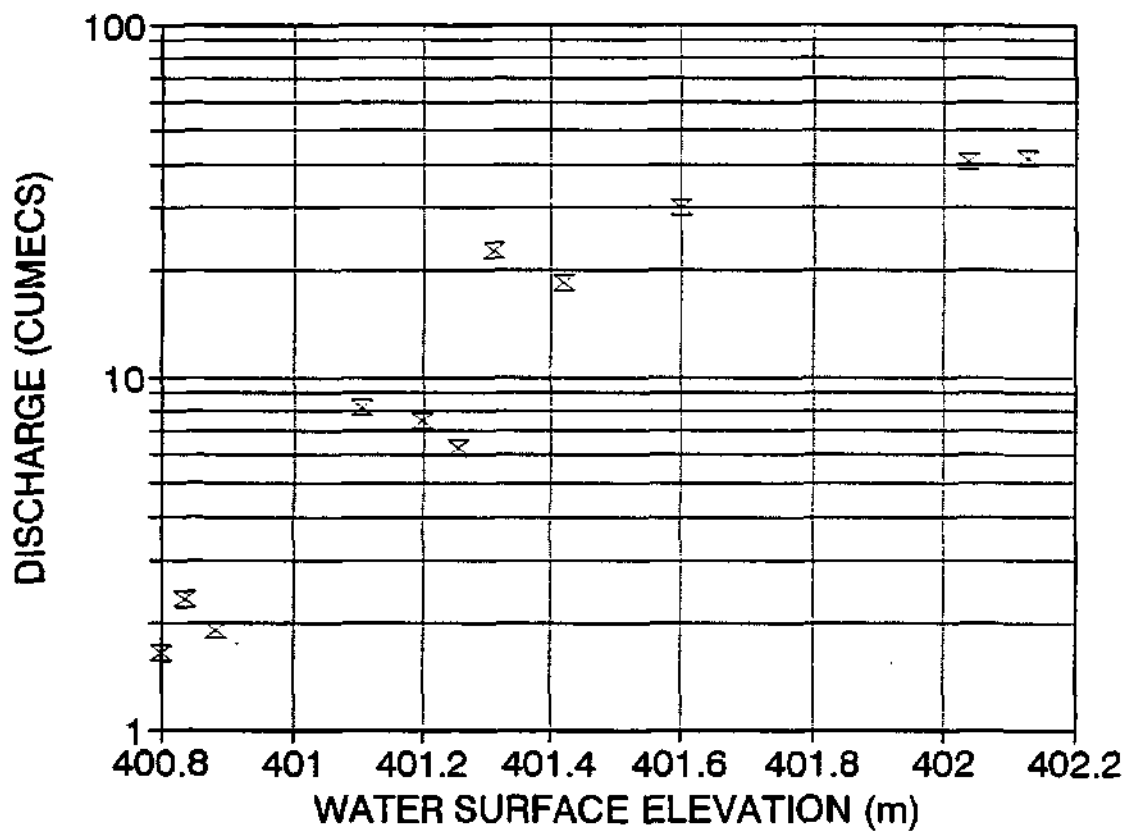
DISCHARGE RATING CURVE

SITE 0.4



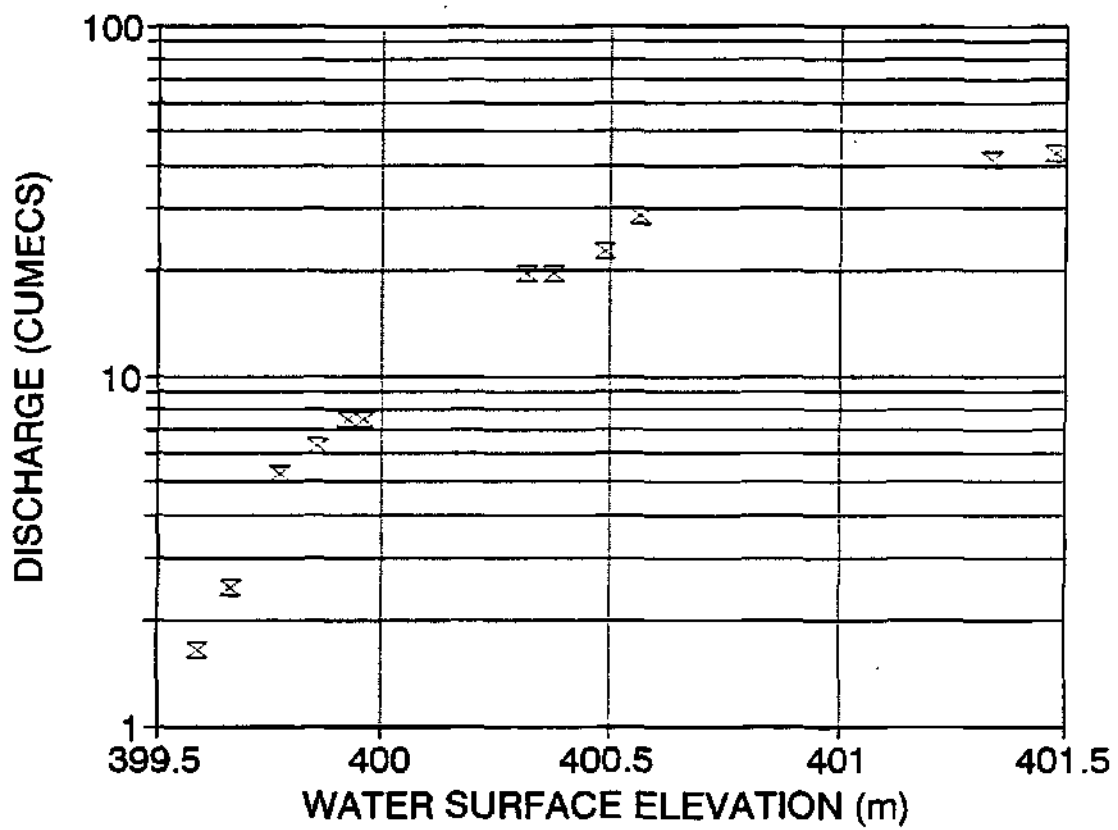
DISCHARGE RATING CURVE

SITE 1



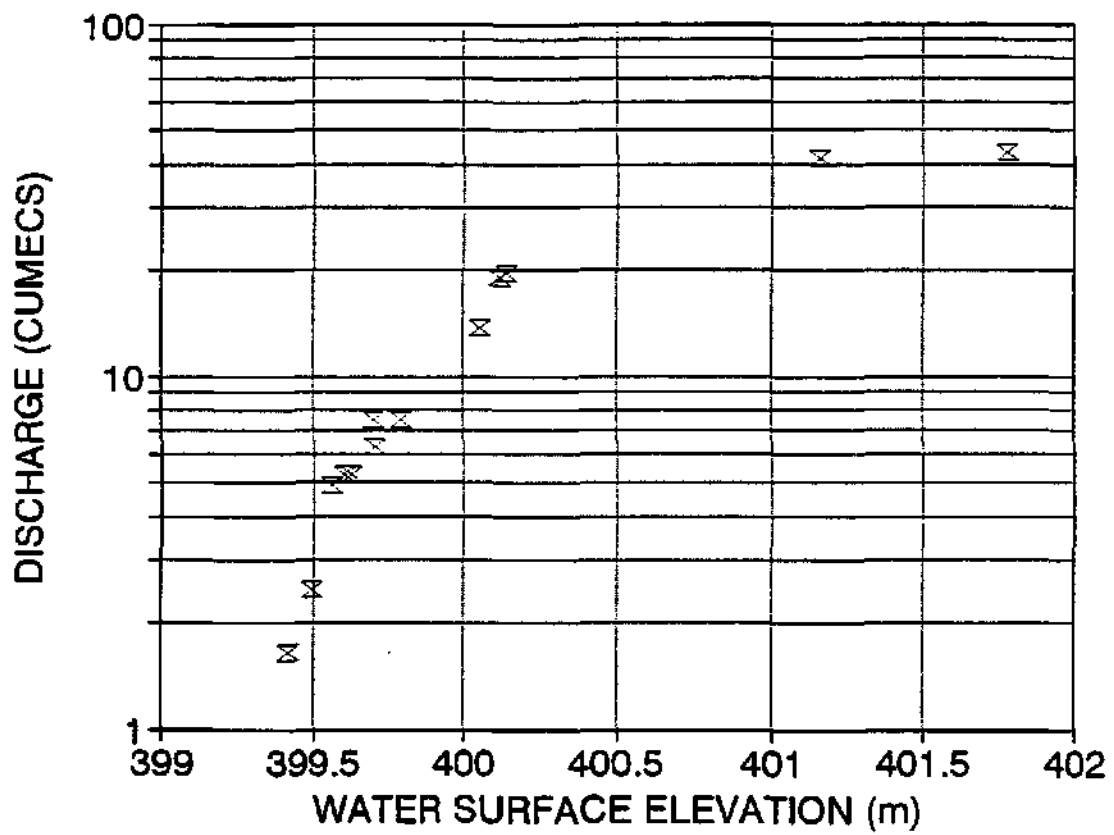
DISCHARGE RATING CURVE

SITE 1.1



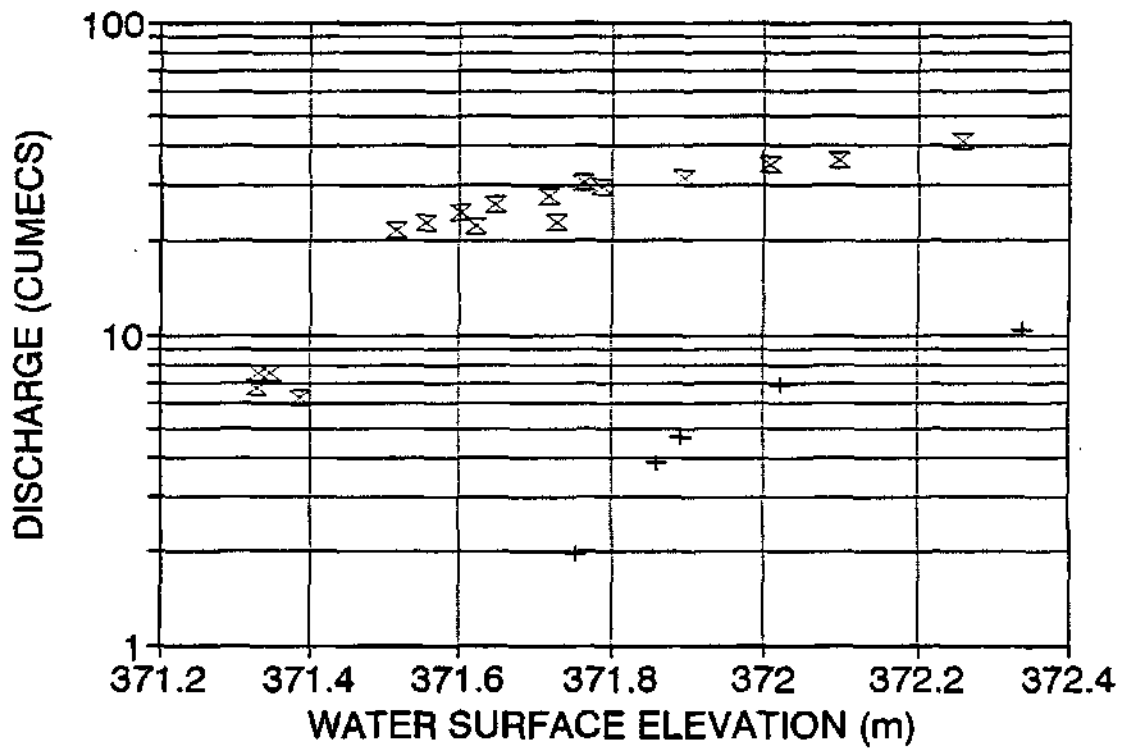
DISCHARGE RATING CURVE

SITE 1.2



DISCHARGE RATING CURVE

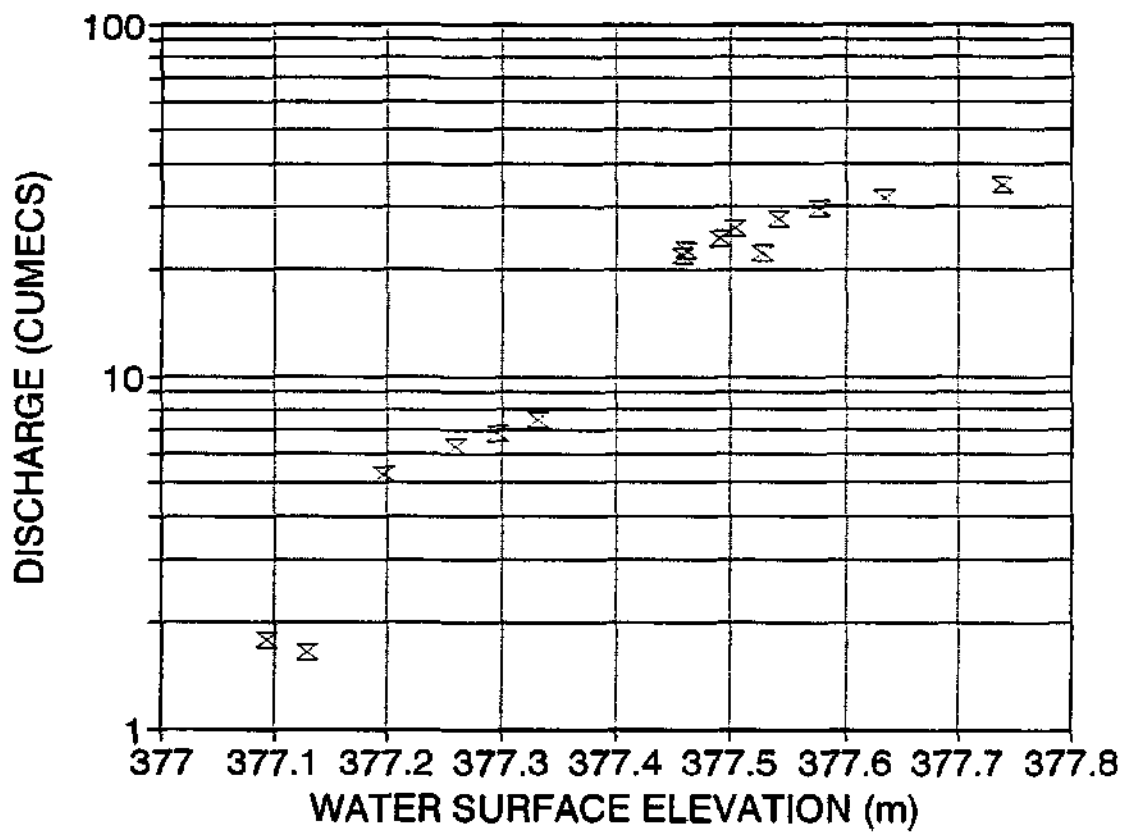
SITE 4.0



⊗ SEASONAL + ACTIVE

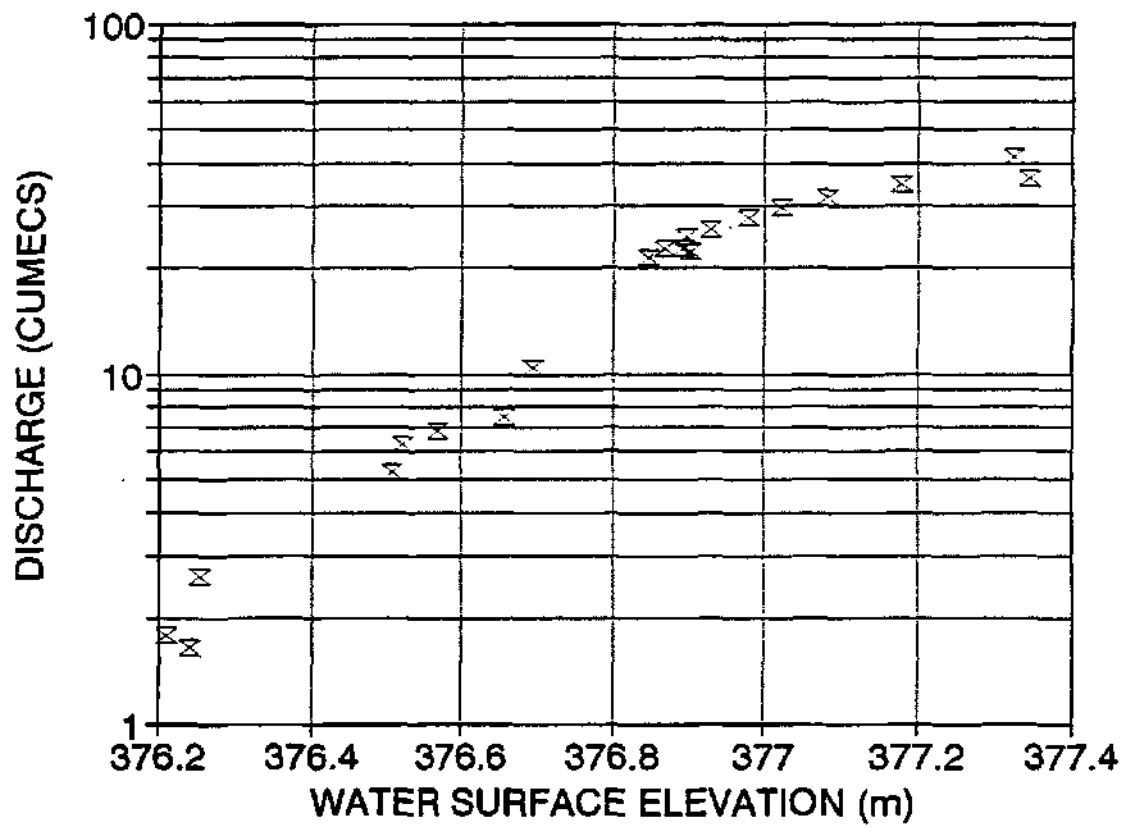
DISCHARGE RATING CURVE

SITE 4.1



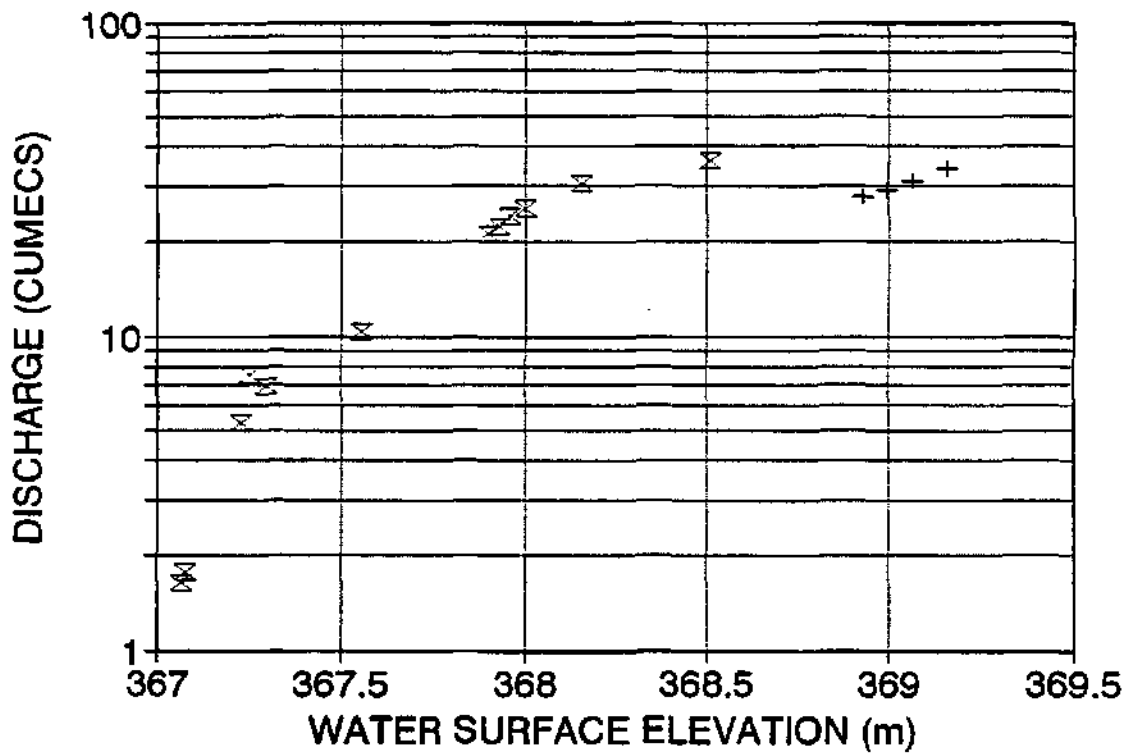
DISCHARGE RATING CURVE

SITE 4.2



DISCHARGE RATING CURVE

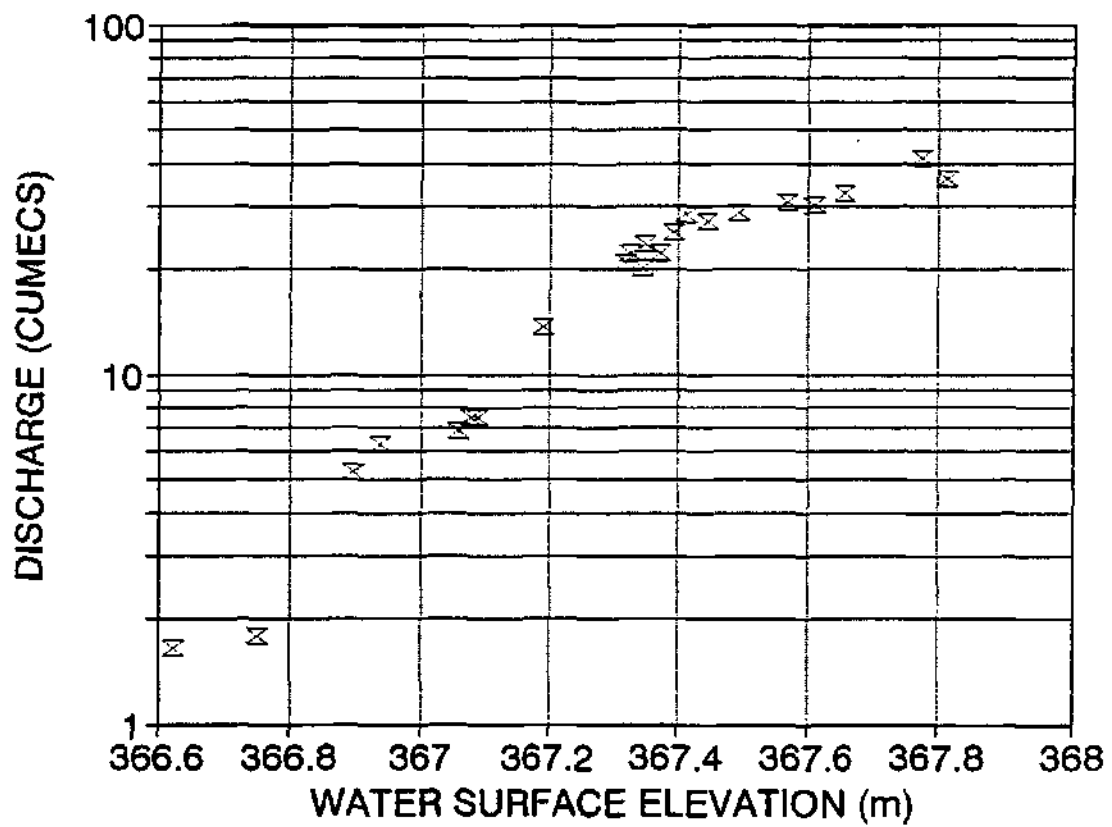
SITE 4.5



x ACTIVE + SEASONAL

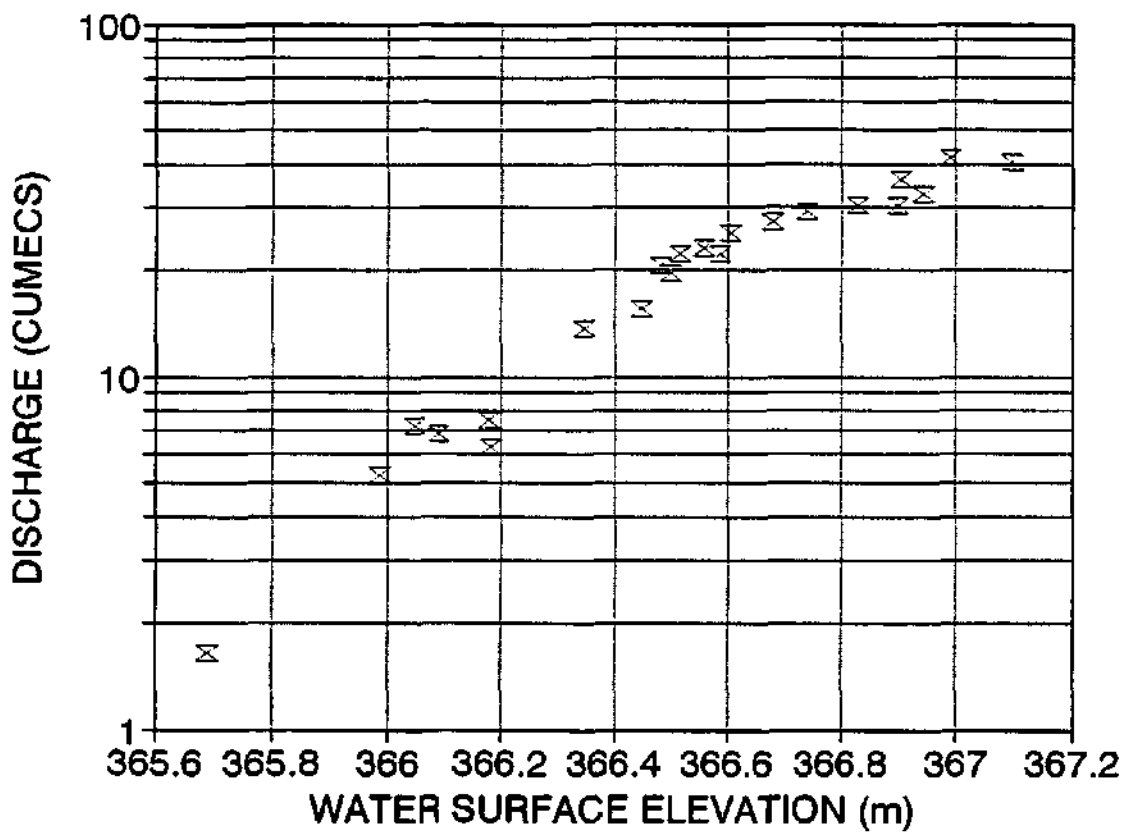
DISCHARGE RATING CURVE

SITE 4.8



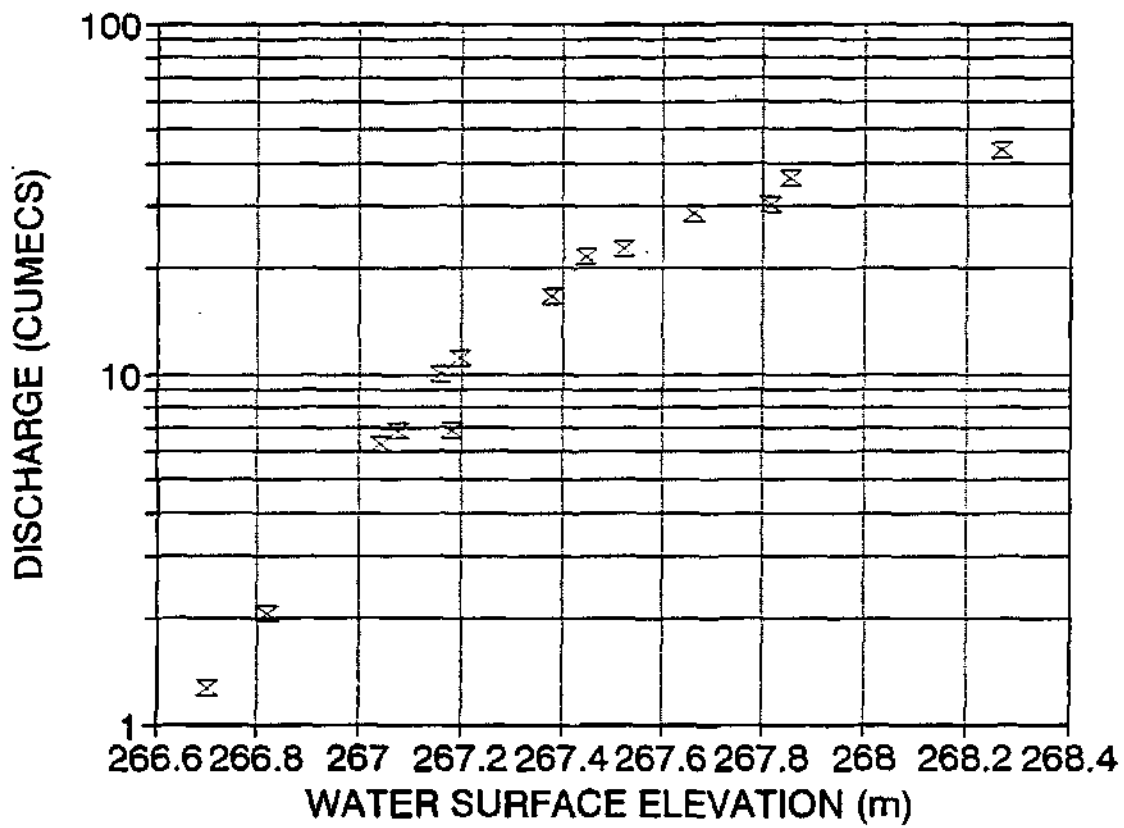
DISCHARGE RATING CURVE

SITE 4.9



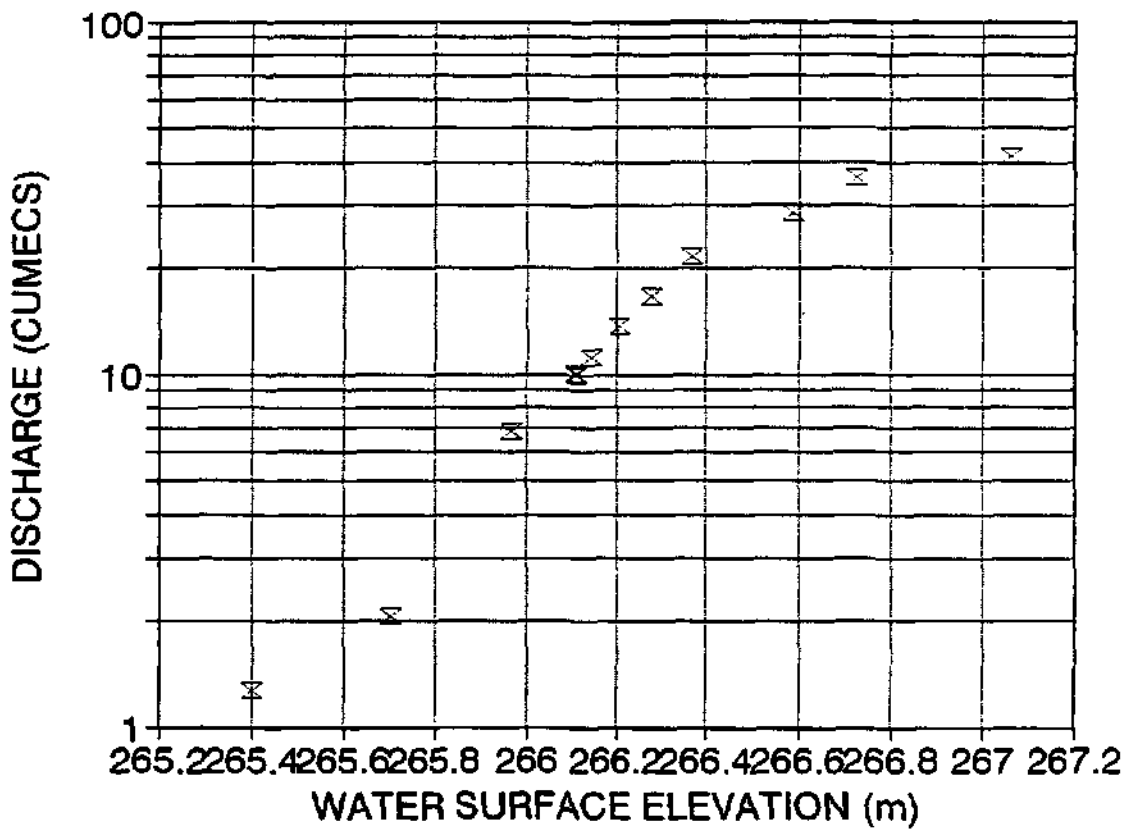
DISCHARGE RATING CURVE

SITE 12.1



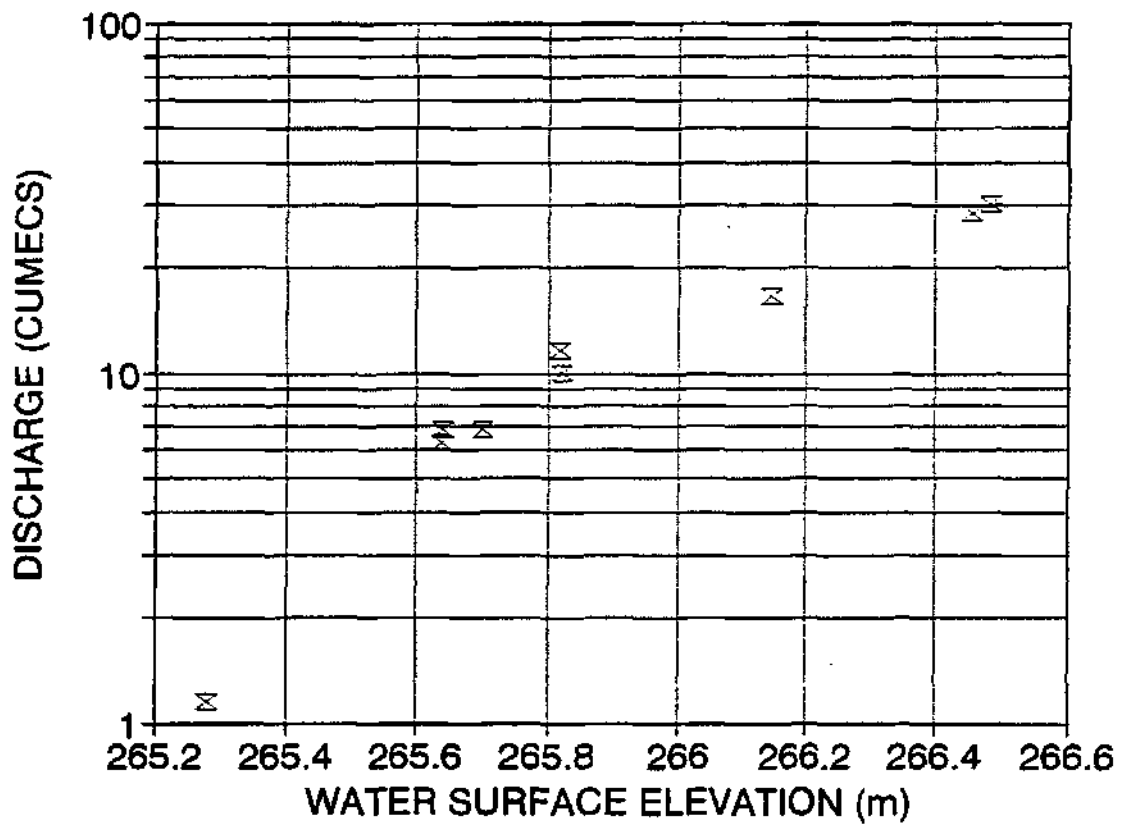
DISCHARGE RATING CURVE

SITE 12.2



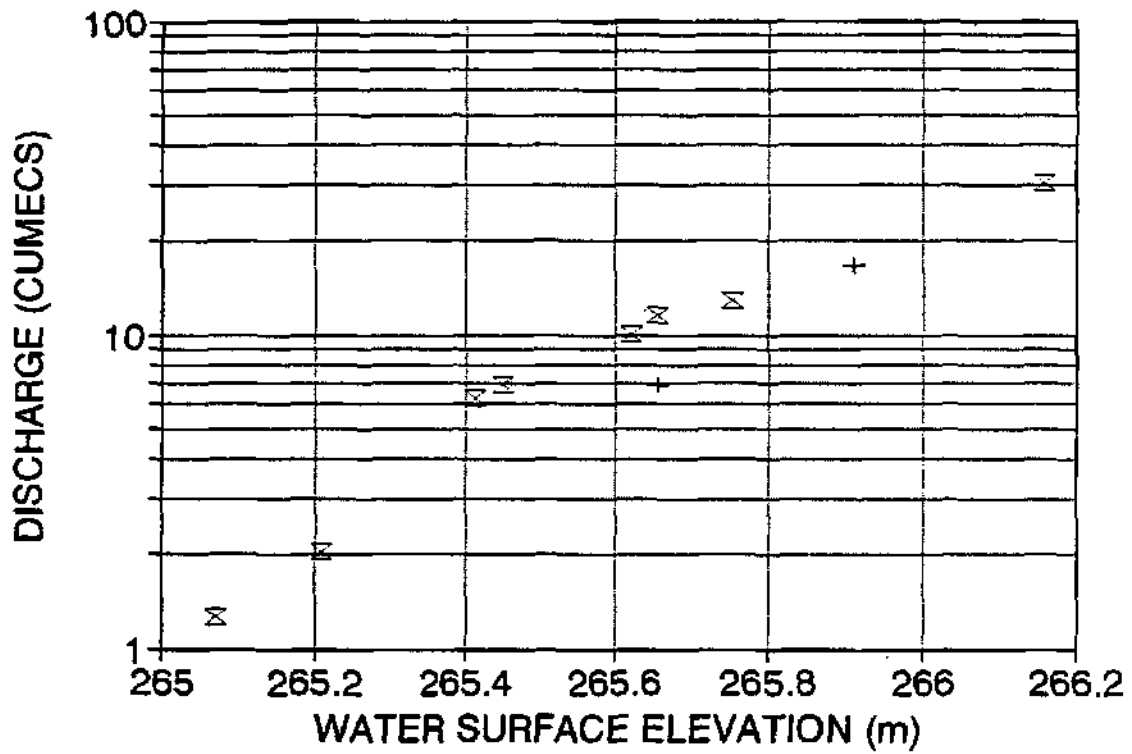
DISCHARGE RATING CURVE

SITE 12.4



DISCHARGE RATING CURVE

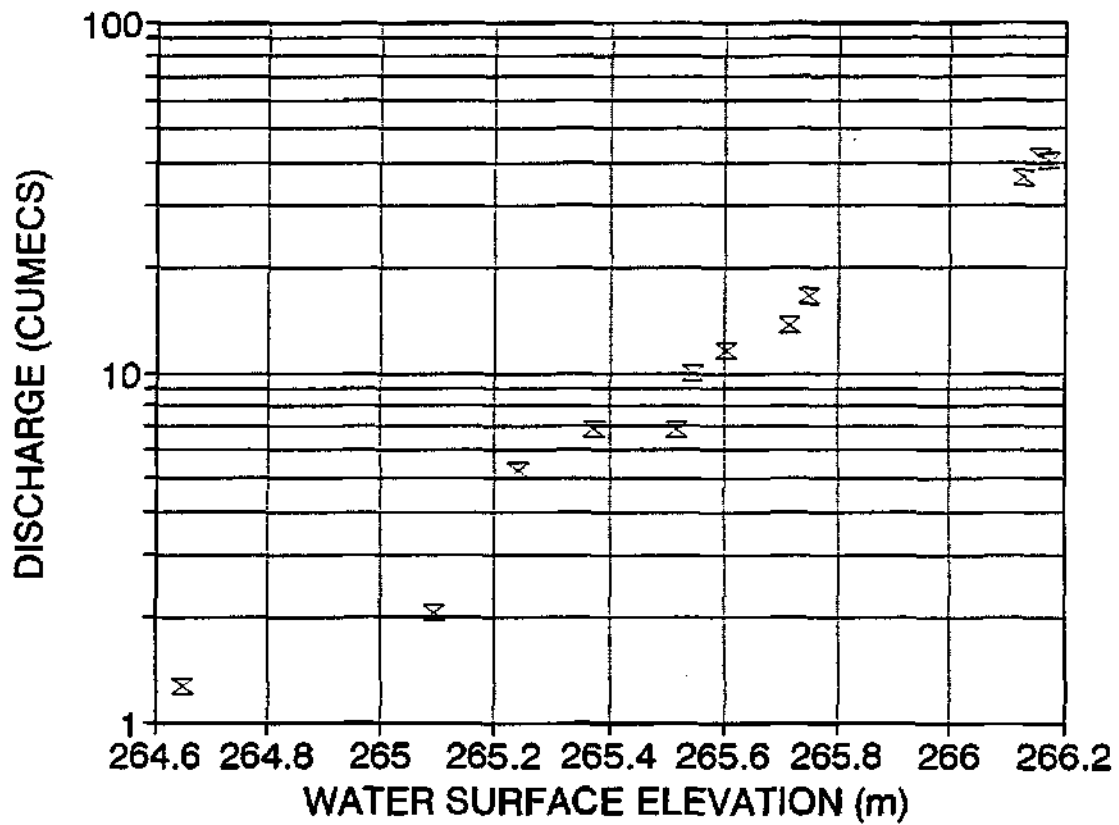
SITE 12.8



x ACTIVE + SEASONAL

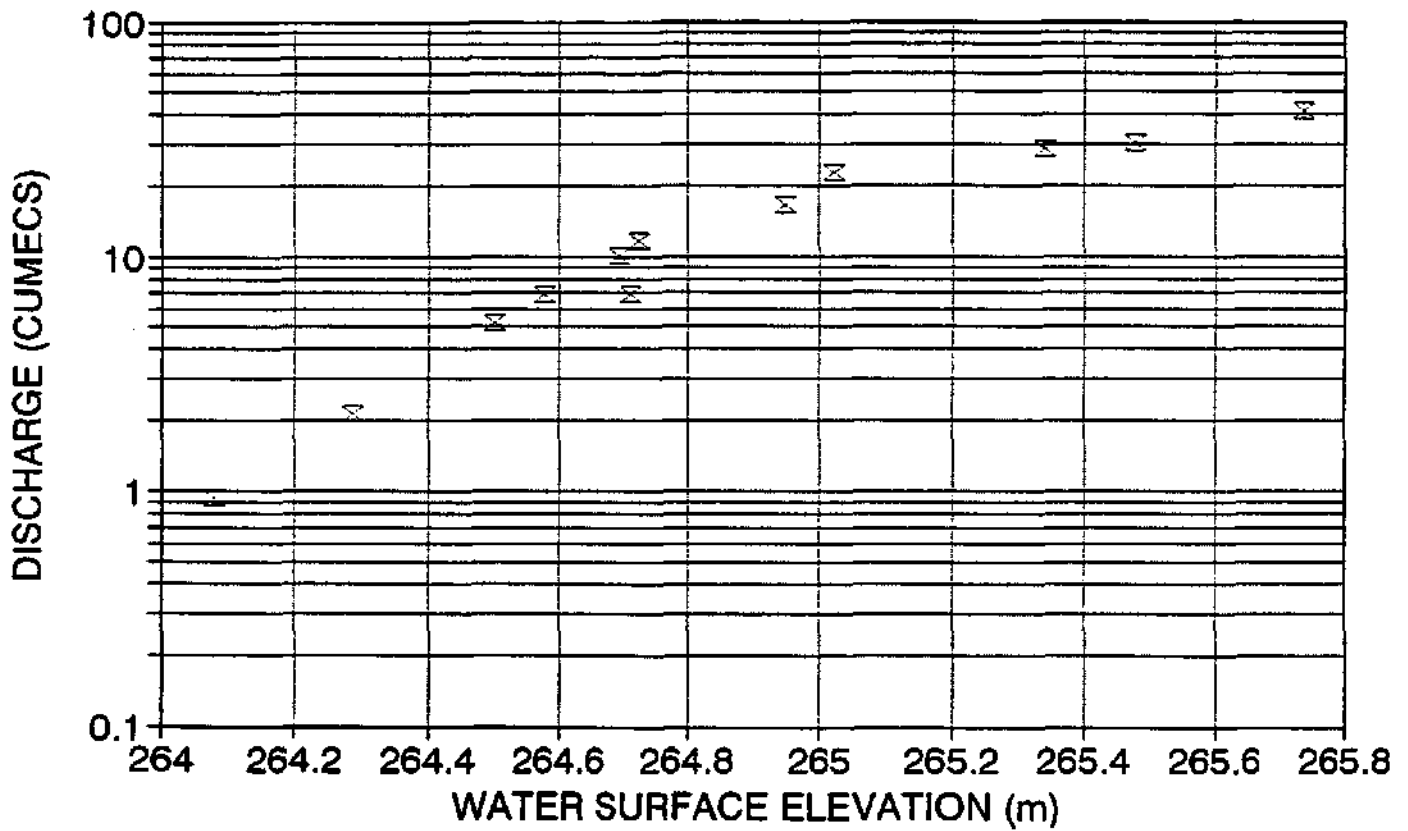
DISCHARGE RATING CURVE

SITE 12.10



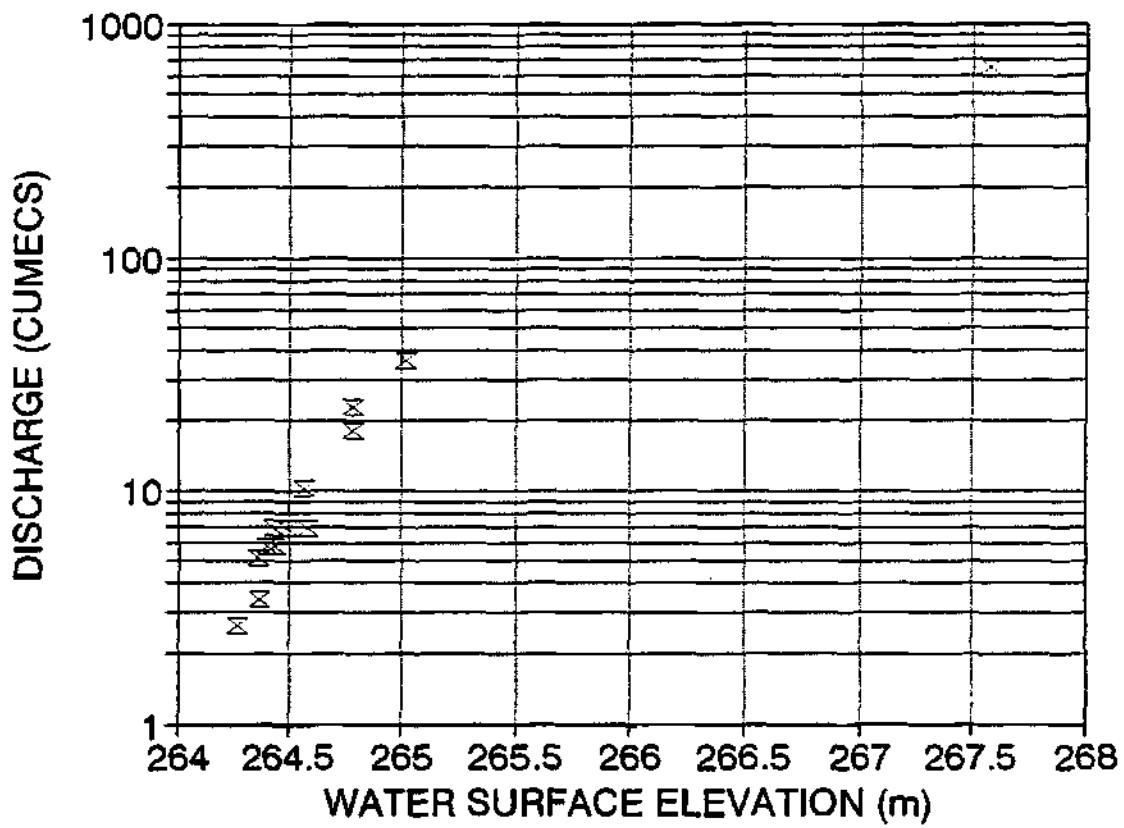
DISCHARGE RATING CURVE

SITE 12.11



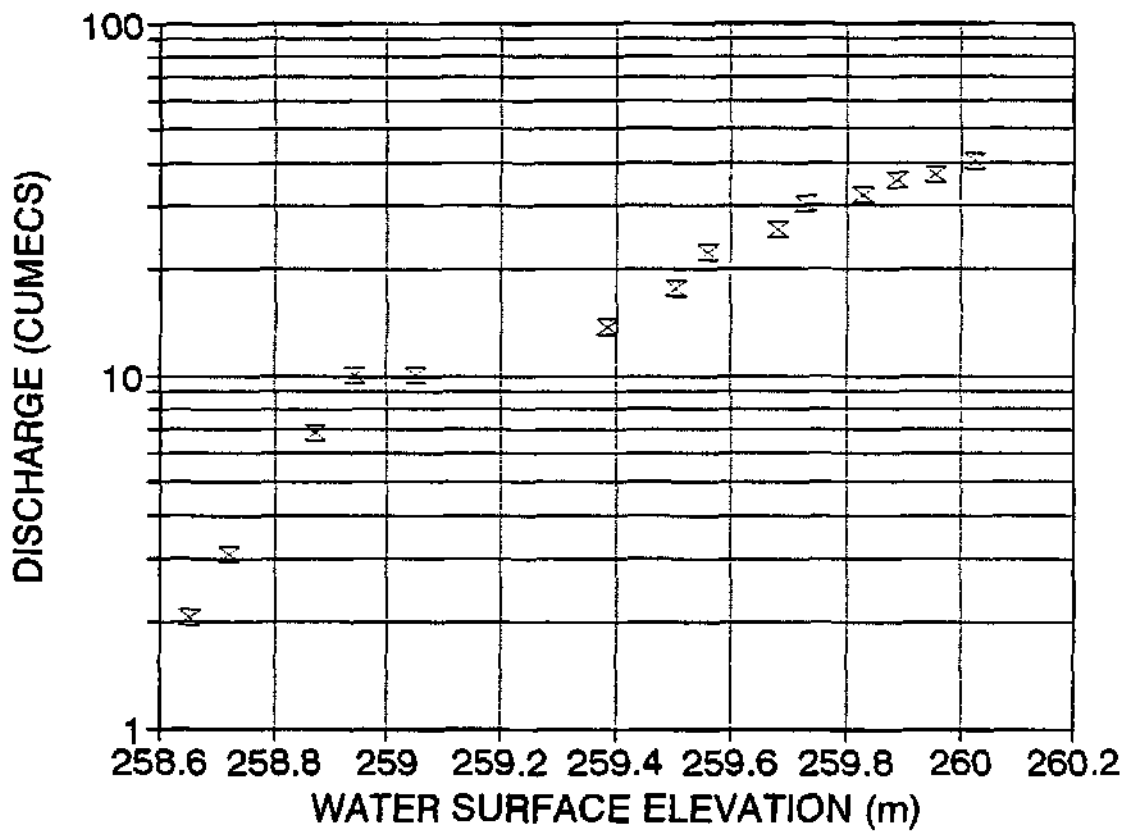
DISCHARGE RATING CURVE

SITE 14



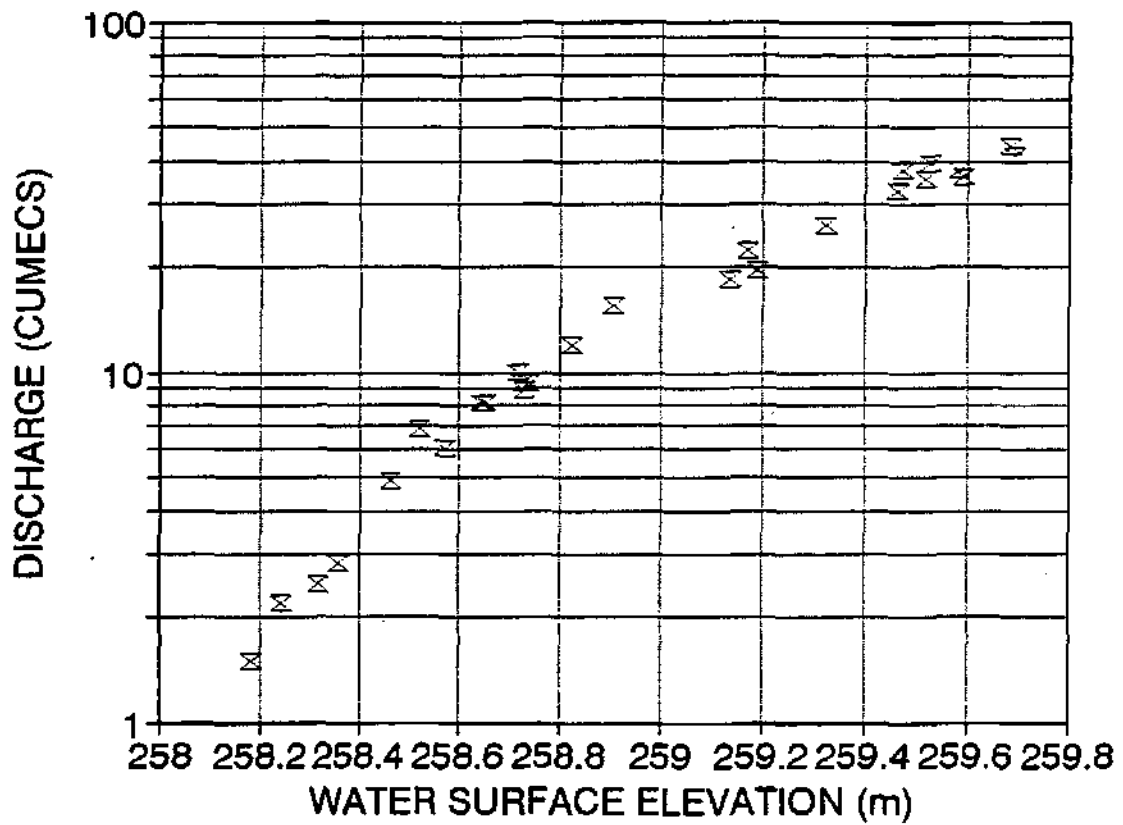
DISCHARGE RATING CURVE

SITE 15.1



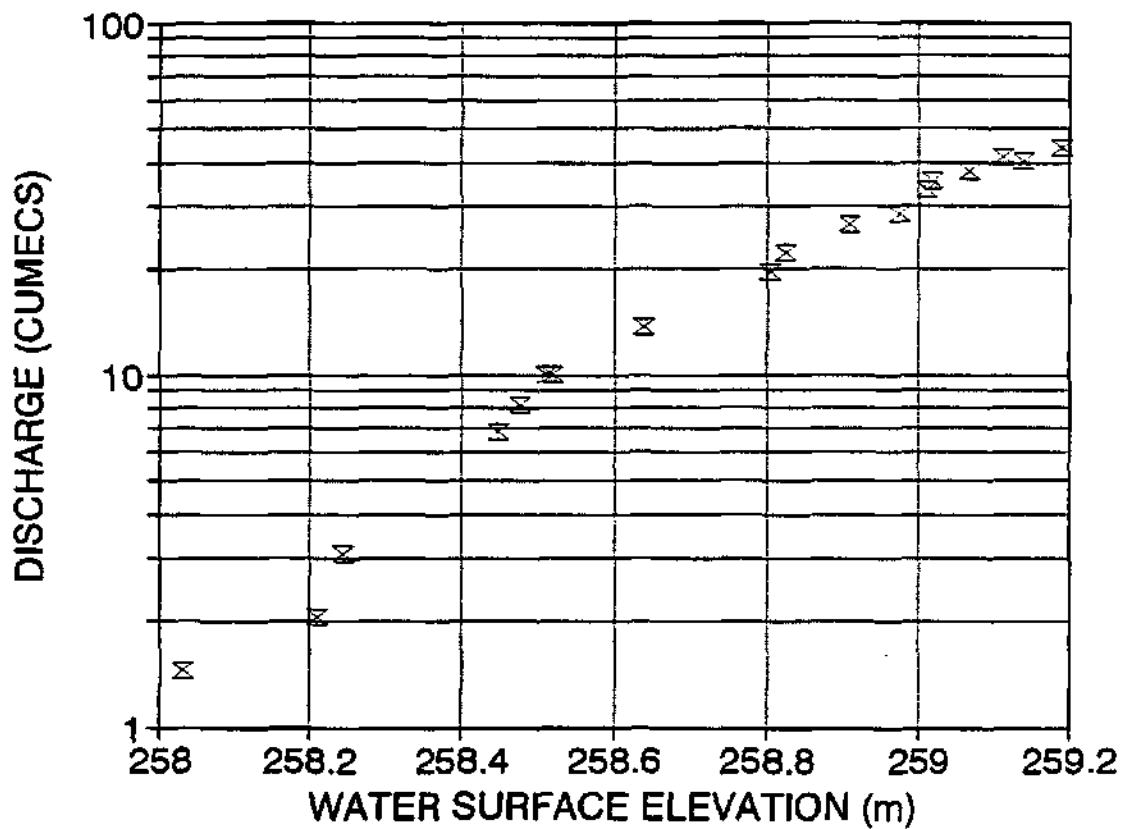
DISCHARGE RATING CURVE

SITE 15



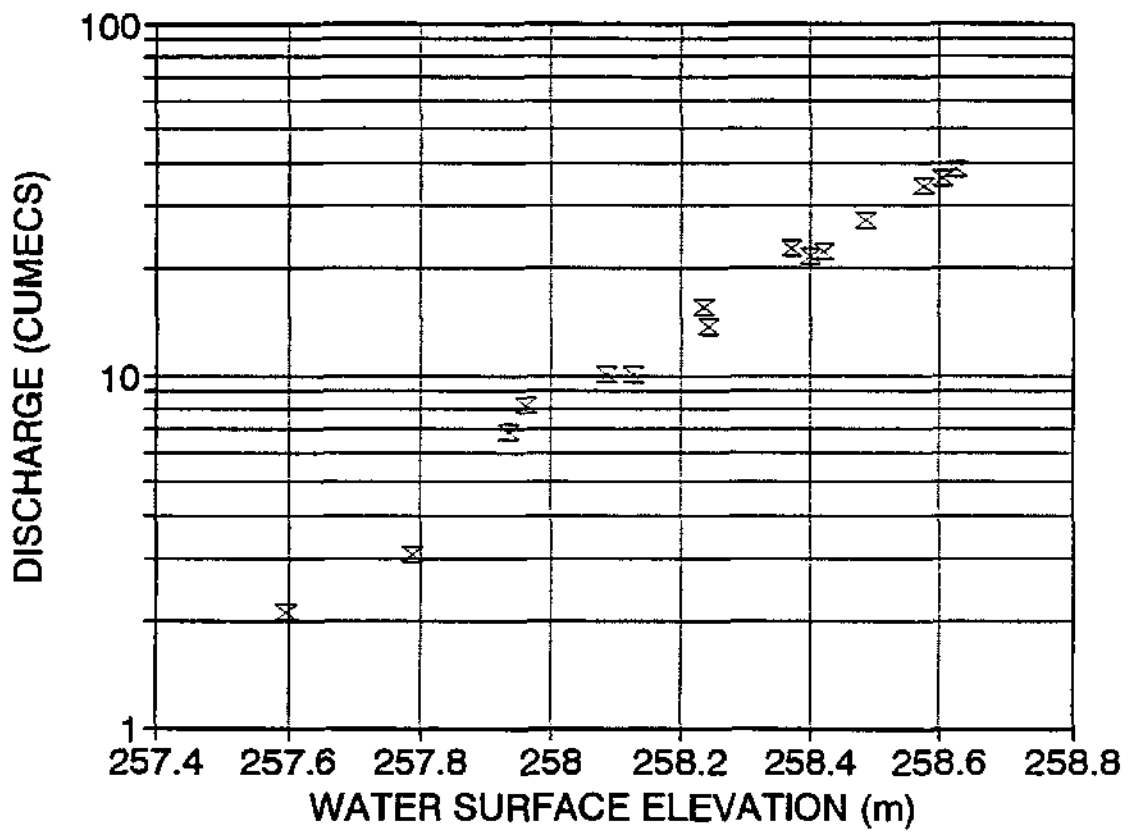
DISCHARGE RATING CURVE

SITE 15.4



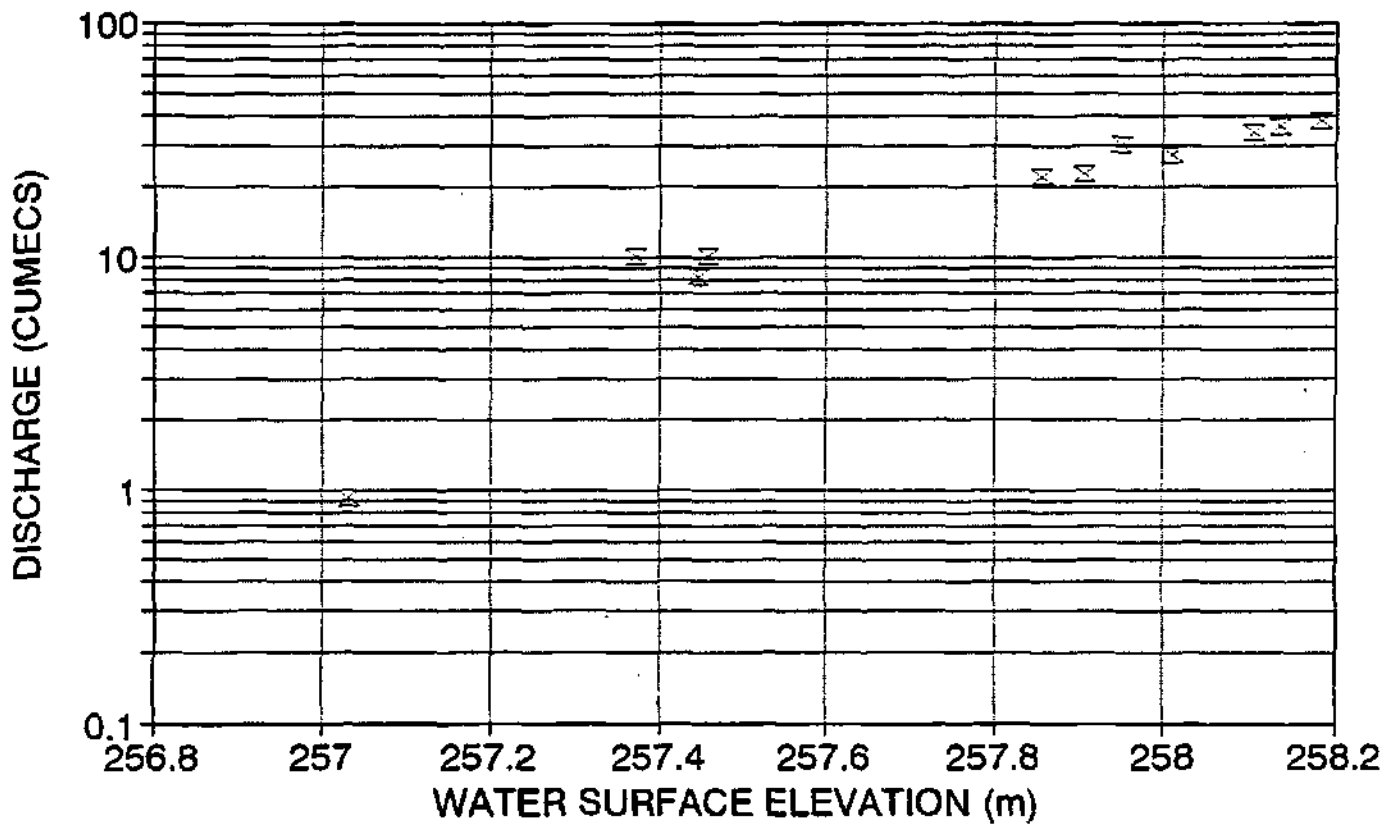
DISCHARGE RATING CURVE

SITE 15.7



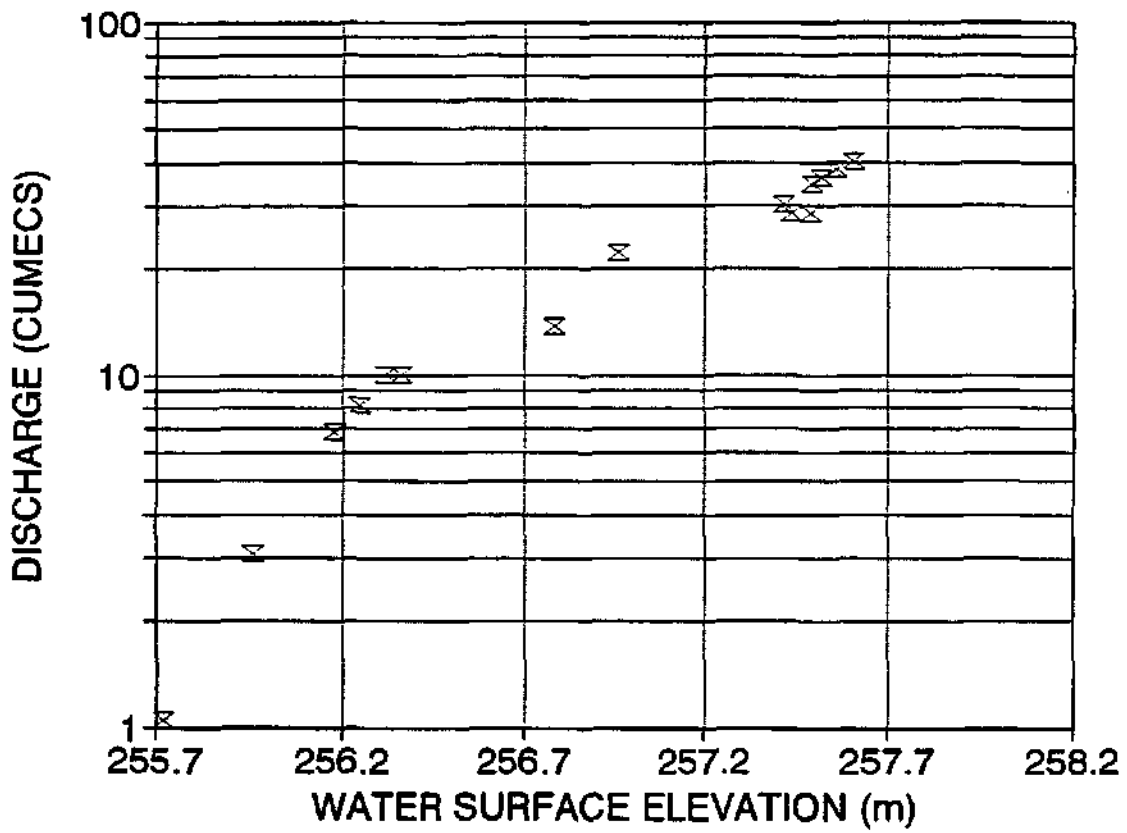
DISCHARGE RATING CURVE

SITE 15.8



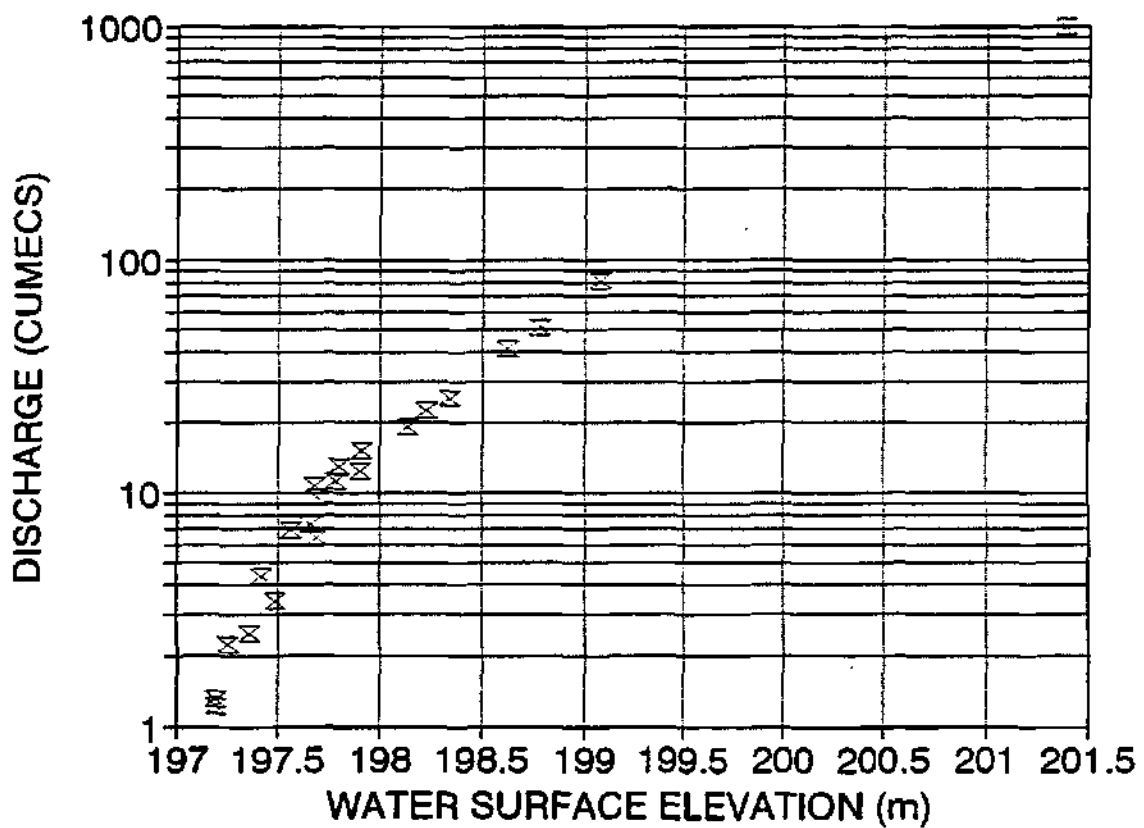
DISCHARGE RATING CURVE

SITE 15.10



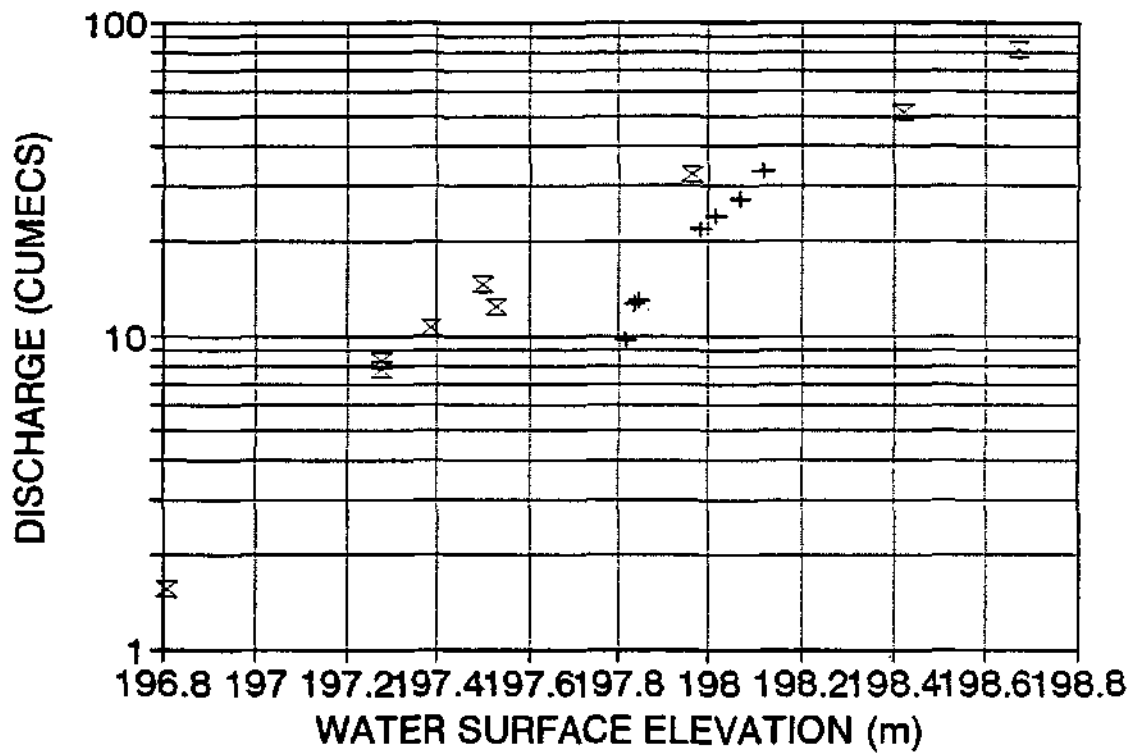
DISCHARGE RATING CURVE

SITE 20



DISCHARGE RATING CURVE

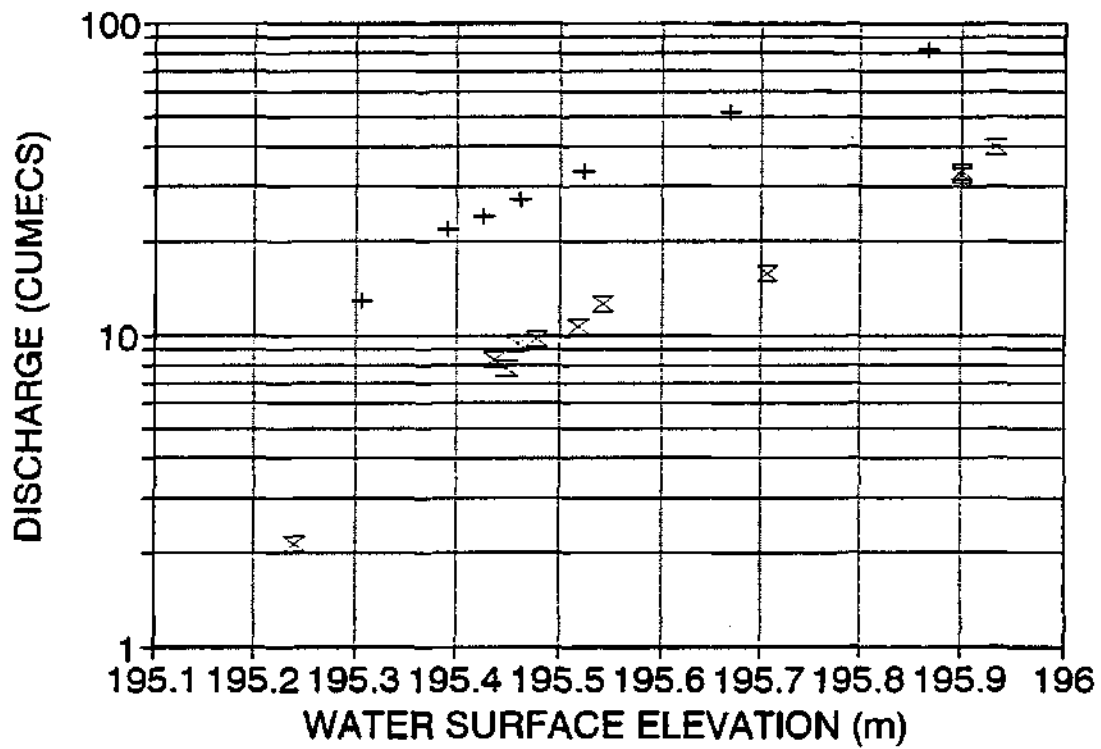
SITE 20.1



⊗ ACTIVE + SEASONAL

DISCHARGE RATING CURVE

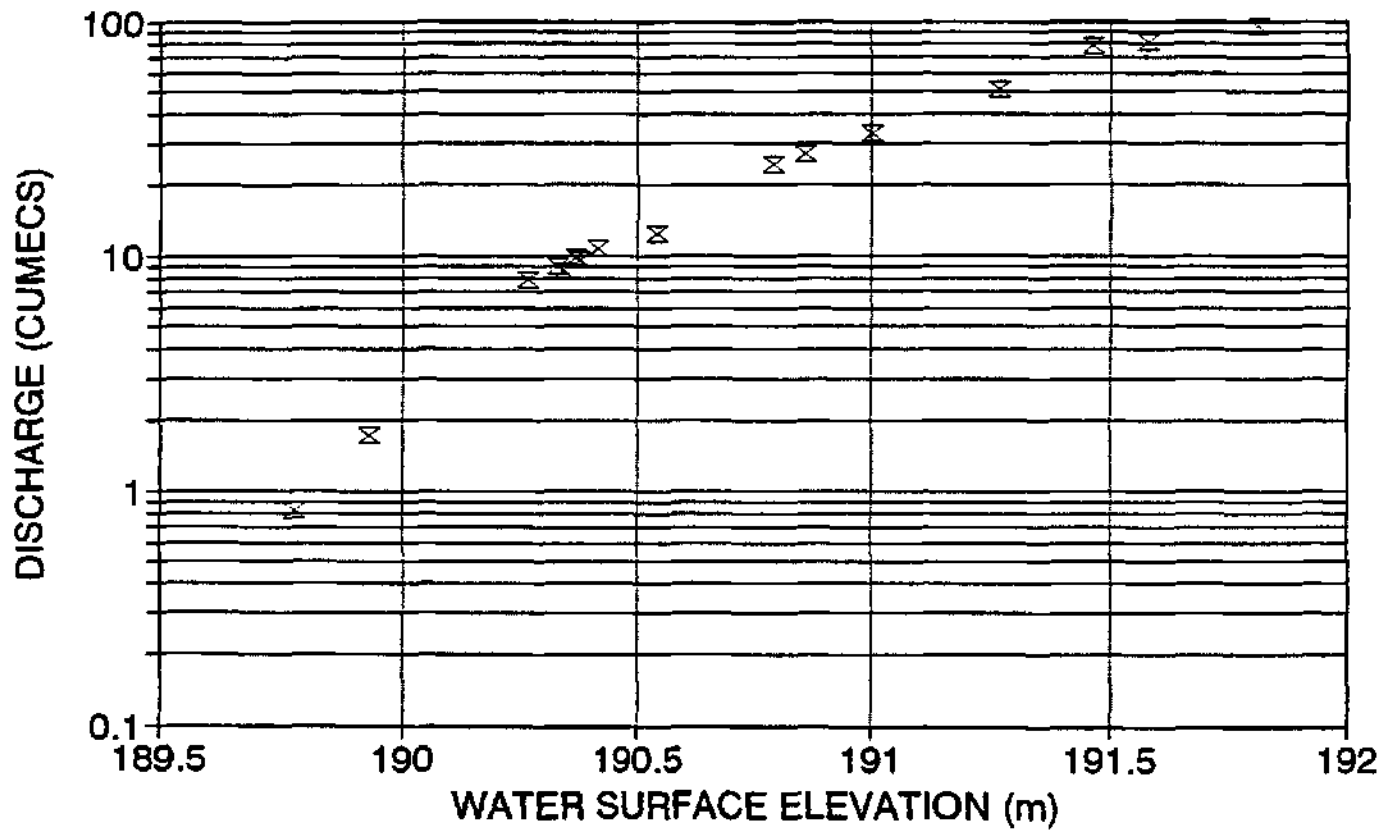
SITE 20.3



X ACTIVE + SEASONAL

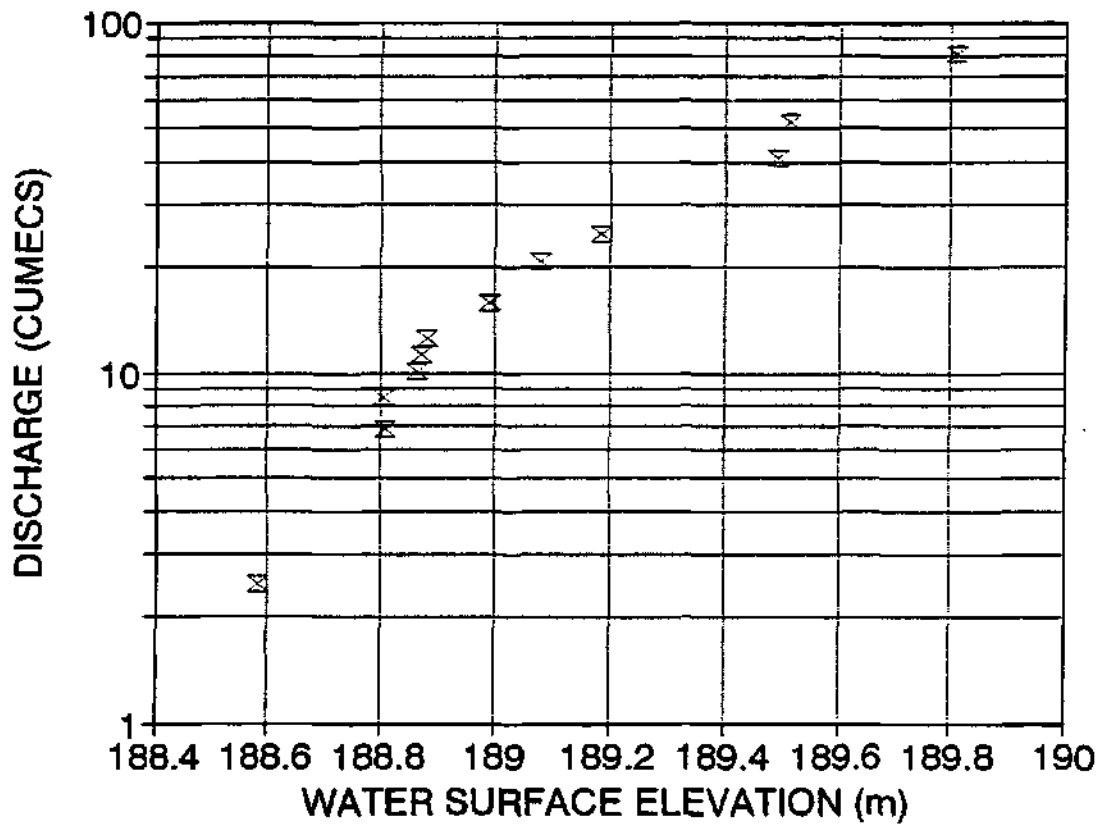
DISCHARGE RATING CURVE

SITE 20.6



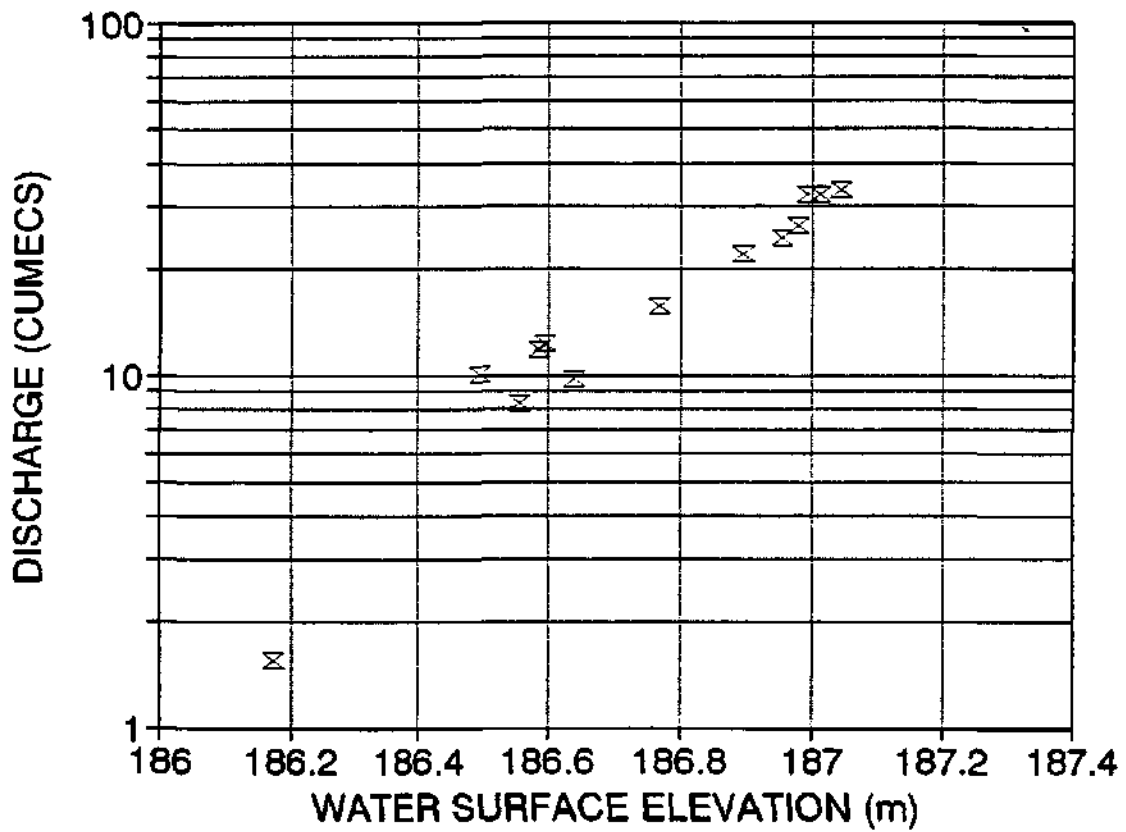
DISCHARGE RATING CURVE

SITE 21



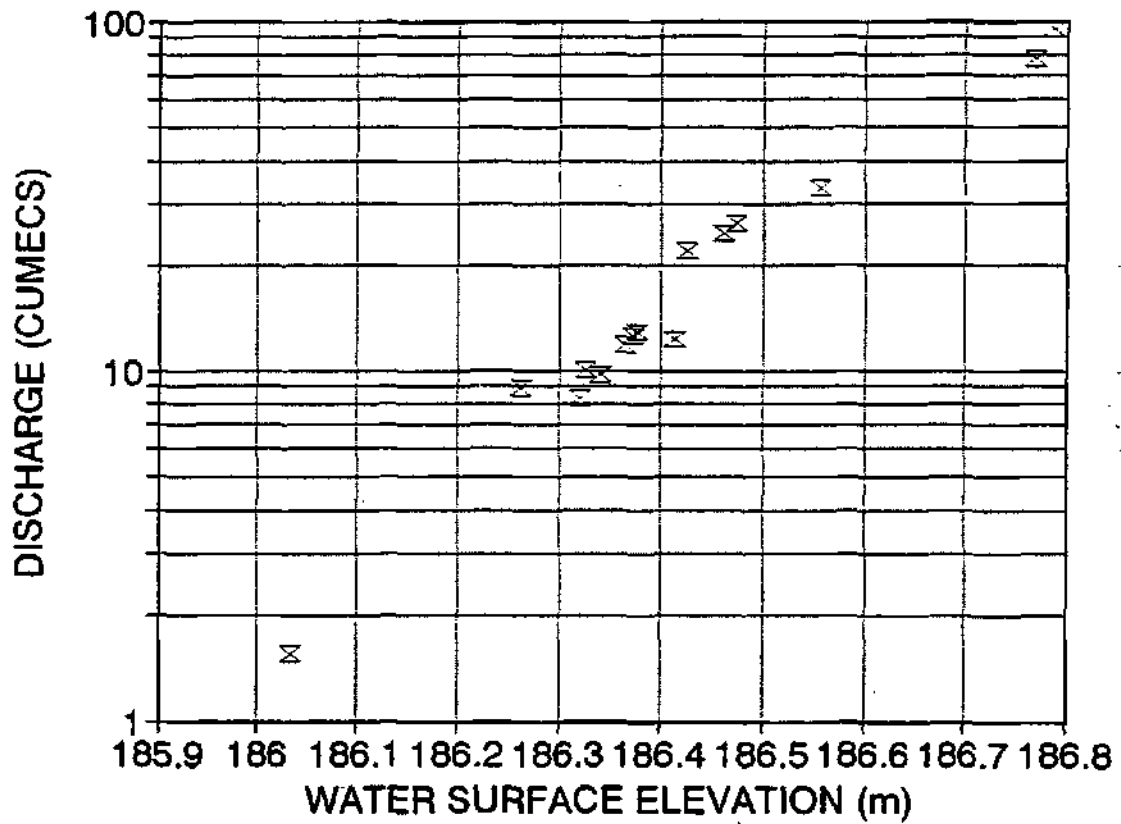
DISCHARGE RATING CURVE

SITE 21.2



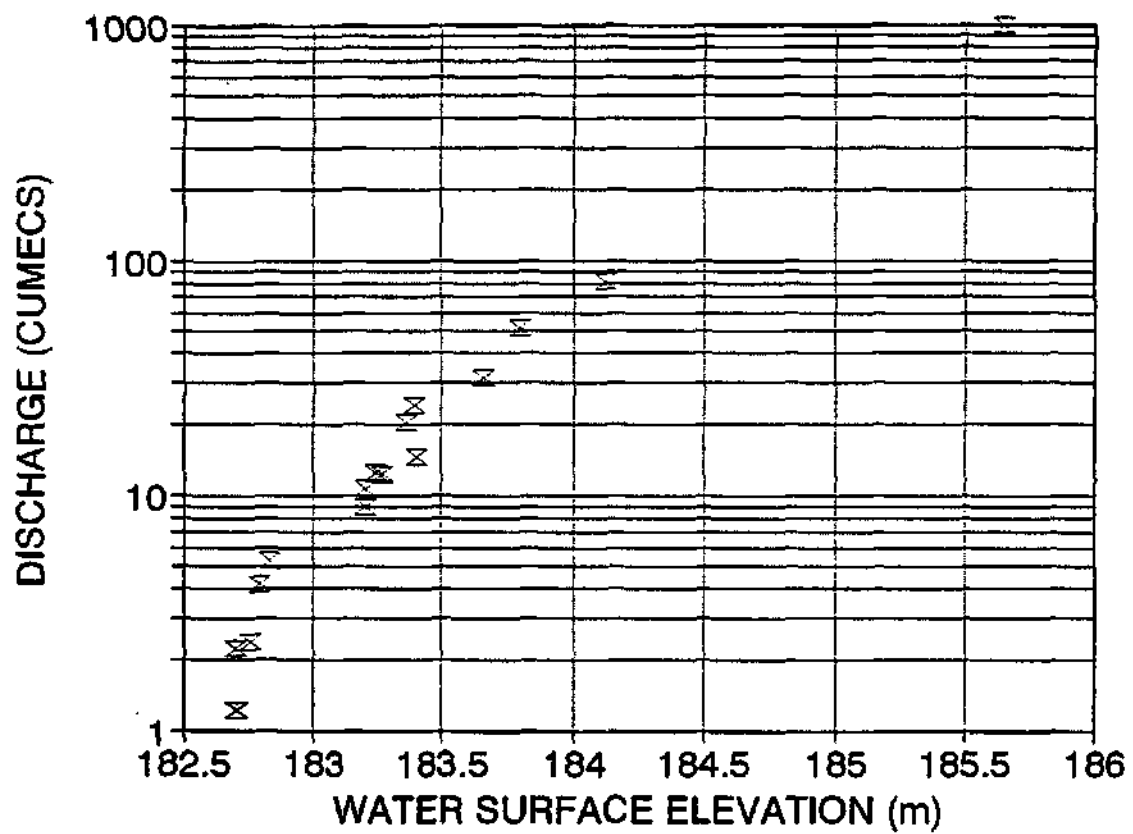
DISCHARGE RATING CURVE

SITE 21.3



DISCHARGE RATING CURVE

SITE 22



APPENDIX 4: SEDIMENTOLOGICAL DATA

"Morcod" refers to the morphological unit code in Appendix 5.

D_{50} and D_{84} are the sediment sizes that 50% and 84% of the sediment sample are less than or equivalent to, respectively.

SEDIMENT SIZE DISTRIBUTIONS

SITE	SAMPLE	MORPH	MORCOD	D50	D84
15.1	A	MCLB	4	323.11	1104.04
15.1	B	SLB	101	294.01	465.04
15.1	C	ACBCB	208	390.67	494.36
15.1	D	SLB	101	593.63	1581.2
15.1	E	SMD	103	439.67	678.91
15.1	F	MCLB	4	412.55	487.49
15.2	A	MCLB	4		350.43
15.2	B	SLB	101	434.18	1086.39
15.2	C	SLB	101	391.93	487.92
15.2	D	SAD	102	481.05	1211.83
15.2	E	SR	113	1302.25	1772.06
15.2	F	ACLB	202	996.2	1476.59
15.2	G	SLB	101	1207.49	1766.14
15.2	H	MCLB	4		438.46
15.3	A	MCLB	4	232.14	1058.78
15.3	B	SAD	102	326.13	1001.78
15.3	C	SLB	101	412.29	485.97
15.3	D	SR	113	555.33	1125.34
15.3	E	ACBB	203	1554.76	1913.88
15.3	F	SAD	102	596.98	1658.05
15.3	G	MCLB	4	124.79	418.61
15.4	A	MCLB	4	188.78	445.33
15.4	B	ACLB	202	739.91	1510.63
15.4	C	ISL		461.32	919.89
15.4	D	ACLB	202	1426.88	1918.75
15.4	E	MCLB	4	260.13	627.53
15.5	A	MCLB	4	424.92	755
15.5	B	SAD	102	437.31	860.24
15.5	C	ACBCB	208	1112.26	1869.52
15.5	D	MCLB	4	291.93	1118.36
15.6	A	MCB	2		423.34
15.6	B	ACBB	203	1716.75	6272.67
15.6	C	ACLB	202	947.37	1530.06
15.6	D	MCB	2		416.53
15.7	A	MCLB	4	291.46	777.66
15.7	B	ACBBW	210	526.73	1310.66
15.7	C	MCLB	4	355.39	1068.24
15.8	A	MCLB	4	255.69	668.21
15.8	B	SR	113	1148.39	5067.53
15.8	C	SMD	103	1252.17	1807.96
15.8	D	MCLB	4	222.19	1357.36

15.8	E	SAD	102	1326.08	8461.99
15.9	A	ACBCB	208	432.38	667.39
15.9	B			1059.18	1727.44
15.9	C	MCI	10	743.45	1325.1
15.9	D	MCRC	6	266.43	1398.38
15.10	A	MCB	2	366.77	1095.85
15.10	B	MCLB	4	1345.03	1827.72
15.10	C	ACLB	202	1072.8	1632.79
15.10	D	MCI	10	261.75	997.08
12.1	A	MCBB	3		460.2
12.1	B	MCEB	5	389.99	474.63
12.1	C	SLB	101	430.51	560.88
12.1	D	SAD	102	1384.06	3127.36
12.1	E	SFB	105	449.66	1082.3
12.1	F	SLB	101	466.04	1339.9
12.2	C	MCLB	4	452.92	869.5
12.2	D	MCB	2	428.26	1777.11
12.3	A	MCLB	4	148.06	256.35
12.3	B	MCLB	4		311.29
12.3	C	ACLB	202	486.08	1336.85
12.3	D	ACBB	203	1159.39	1843.35
12.3	E	SLB	101	365.54	514.76
12.4	A	MCLB	4		1269.71
12.4	B	MCLB	4	409.79	1579.23
12.4	C	SLB	101	903.58	15820.44
12.4	D	SRC	106	368.51	1299.81
12.4	E	MCLB	4	406.75	1693.63
12.5	B	SLB	101	1499.31	2064.51
12.5	C	ACBB	203	820.9	1486.3
12.6	B	SRC	106	1011.12	1690.57
12.6	C	SLB	101	1122.52	1703.797
12.6	D	ACBW	204	659.874	1217.4
12.7	B	ACPB	207	1400.322	1947.589
12.7	C	SBB	109	1462.08	1914.25
12.7	D	ACLB	202	748.75	1245.86
12.8	B	SLB	101	683.63	1549.71
12.8	C	ACBB	203	1099	1675.18
12.9	A	SRC	106	143.44	482.73
12.9	B	SLB	101	463.99	1279.63
12.9	C	ACBB	203	660.46	1409.49
12.9	D	SLB	101	450.02	1054.77
12.10	A	MCLB	4	227.13	498.19
12.10	B	SLB	101	412.25	483.51
12.10	C	MCLB	4	297.24	453.816

12.10	D	MCLB	4	479.81	1212.03
12.11	A	MCLB	4	226.04	959.8
12.11	B	SBD	104	180.61	470.25
12.11	C	SLB	101	670.918	1367.233
12.11	D	MCLB	4	437.65	1082.55
12.11	E	SAD	102	662.37	1258.56
12.11	F	SSS	111	489.58	1211.75
20.1	A	ACSS	214	814.705	1362.004
20.1	C	MCLB	4	1049.134	15553.33
20.1	E	SAD	102	494.254	1208.337
20.1	F	SLB	101	1165.735	1807.47
20.2	A	SBCB	112	127.94	431.22
20.2	B	SMD	103	426.92	882.57
20.2	C	SMD	103	955.728	1626.81
20.2	D	SMBW	108	830.16	1475.4
20.2	E	SMD	103	497.74	1227.49
20.2	F	SBCB	112	274.91	894.41
20.2	G	SMD	103	953.25	1396.53
20.3	A	SBCB	112	1107.743	1765.361
20.3	B	ACLB	202	338.57	468.08
20.3	C	MCBCB	12	463.31	1014.19
20.3	E	SMD	103	1003.284	1546.783
20.3	F	MCLB	4	220.18	1390.42
20.3	G	SMD	103	1173.7	1883.422
20.6	A	SBCB	112	608.235	1287.189
20.6	B	ACLB	202	674.046	1344.572
20.6	C	SBCB	112	499.48	1353.54
20.6	D	SMD	103	745.484	1400.574
20.6	E	MCLB	4	419.06	668.67
20.7	B	ACLB	202	838.181	1350.869
20.7	D	SBCB	112	775.15	1347.39
20.7	E	SMD	103	1145.595	1706.77
20.7	F	SAD	102	1266.103	5538.928
20.7	G	SMD	103	822.6	1418.341
21.1	A	SABW	107	419.782	1438.47
21.1	B	SBCB	112	458.91	1488.93
21.1	C	SABW	107	550.81	1336.57
21.1	D	SBCB	112	756.3	1286.37
21.1	E	ACLB	202	1243.655	2309.661
21.1	F	SBCB	112	828.95	1492.086
21.2	A	SMD	103	752.71	1295.89
21.2	B	SBCB	112	486.644	1120.01
21.2	C	SMD	103	440.08	842.01
21.2	D	SBCB	112	1228.86	1778.426

4.1	B	ACLB	202	1112.669	1319.611
4.1	C	SLB	101	866.779	1471.774
4.1	D	MCB	2	170.552	424.79
4.2	B	MCMP	14	442.004	990.244
4.2	C	MCBCB	12	467.494	868.776
4.2	D	SBP	110	1014.192	1582.785
4.2	F	MCBCB	12	467.377	1037.953
4.2	G	SBCB	112	463.946	1076.927
4.3	A	SBP	110	489.222	1126.084
4.3	B	SBD	104	1269.183	1814.805
4.3	C	ACBD	213	345.759	492.446
4.3	D	SBCB	112	407.891	494.407
4.3	E	ACBCB	208	487.697	1050.267
4.3	G	MCBCB	12	469.4	1475.159
4.4	A	SBP	110	1095.957	1640.045
4.4	B	SMD	103	1455.6	1918.32
4.4	C1	SBCB	112	462.628	950.048
4.4	C2	SBCB	112	474.852	1142.443
4.5	A	MCLB	4	989.481	1568.843
4.5	B	SAD	102	1153.094	1747.562
4.5	C	MCBCB	12	378.71	468.839
4.5	E	ACLB	202	535.391	1240.895
4.5	F	SMD	103	426.008	808.593
4.6	X	ACLB	202	451.179	1058.612
4.6	D	ACLB	202	580.246	1248.342
4.7	B	SAD	102	1224.041	1792.326
4.7	D	ACLB	202	790.659	1360.362
4.7	E	ACBB	203	886.47	1657.795
4.8	A	SAD	102	519.793	16588.69
4.8	B	MCLB	4	437.295	812.512
4.8	C1	ACBB	203	760.423	1351.146
4.8	C2	ACBCB	208	789.113	1343.342
4.9	B	ACLB	202	1417.24	1850.97
4.9	C	SLB	101	426.17	730.11
4.9	D	MCI	10	1084.93	1702.82

APPENDIX 5: MORPHOLOGICAL UNIT GLOSSARY, WITH CODES

MORPHOLOGY GLOSSARY

Macro channel features		
1	MCBT	Bank top
2	MCB	Bank
3	MCBB	Bank bottom
4	MCLB	Lateral bar
5	MCEB	Erosional bench
6	MCRC	River cliff
7	MCAD	Alluvial distributary
8	MCBD	Bedrock distributary
9	MCMD	Mixed distributary
10	MCI	Island
11	MCT	Terrace
12	MCBCB	Bedrock core bar
13	MCBP	Bedrock pavement
14	MCMP	Mixed pavement
Seasonal channel features		
101	SLB	Lateral bar
102	SAD	Alluvial distributary
103	SMD	Mixed distributary
104	SBD	Bedrock distributary
105	SFB	Fringe bar
106	SRC	River cliff
107	SABW	Alluvial backwater
108	SMBW	Mixed backwater
109	SBB	Braid bar
110	SBP	Bedrock pavement
111	SSS	Sand sheet
112	SBCB	Bedrock core bar
113	SR	Rapid
114	SBBW	Bedrock backwater
115	SLEV	Levee

Active channel features		
201	ACB	Bed
202	ACLB	Lateral bar
203	ACBB	Braid bar
204	ACABW	Alluvial backwater
205	ACMBW	Mixed backwater
206	ACRC	River cliff
207	ACPB	Point bar
208	ACBCB	Bedrock core bar
209	ACLEB	Lee bar
210	ACBBW	Bedrock backwater
211	ACAD	Alluvial distributary
212	ACMD	Mixed distributary
213	ACBD	Bedrock distributary
214	ACSS	Sand sheet
215	ACBBB	Bedrock braid bar
216	ACPAN	Pan

APPENDIX 6: PHYSICAL CHARACTERISTICS OF VEGETATION ACROSS CROSS SECTIONS, RELATED TO MORPHOLOGICAL UNITS

"X" refers to the distance across the cross section, from the benchmark.

"Y" refers to the elevation.

"Morph" gives the morphological unit code for individual points, as defined in Appendix 5.

GROUND LAYER COVER:

"Grass/herb/crop" is the % cover, from visual inspection, of the non-reed ground layer, over 3 height classes.

eg. 0.3 = 30% grass groundcover for that point in the cross section.

"Reeds" is the % cover, from visual inspection, of the reeded ground layer, over 3 height classes.

SHRUB LAYER:

"Willow-like" is the % shrub layer cover of shrubs with multiple, thin stems/branches growing from the groundlayer, over 3 height classes.

"Acacia-like" is the % shrub layer cover of acacia shrubs, over 3 height classes.

"Hookthorn-like" is the % shrub layer cover of hookthorn shrubs, over 3 height classes.

"Thick stemmed thorny" is the % shrub layer cover of shrubs with thorn covered, thick stems/branches, over 3 height classes.

"Breonadia" is the % shrub layer cover of Breonadia shrubs, over 3 height classes.

TREE LAYER:

"Dense canopy" is the spacing of dense canopied trees, over 2 height classes.

eg. 0.1 = 1 tree every 10m, upstream and downstream of that point in the cross section.

"Sparse canopy" is the spacing of sparse canopied trees, over 2 height classes.

"Erythrophyllum" is the spacing of trees with horizontally spreading, thick trunks, from the ground and shrub layers, over 2 height classes.

"Willow-like" is the spacing of trees/tall shrubs with multiple, thin trunks, growing from the ground layer, over 2 height classes.

SITE ID	T	GRASS/HERB/CRP			FEEDE			A=WILLOW LIKE APPEARANCE			B=ACACIA LIKE APPEARANCE			C=14X WILLOW LIKE APPEARANCE			D=14X STEMMED 3-4 CM			E=BROKENADA			A=DENR		C=NOFF		E=THYRUS/ELM		D=WILLOW LIKE APPEARANCE	
		MOFFPH	<0.2M	0.2-0.5M	>0.5M	<1M	1-2.5M	>2.5M	<1.5M	1.5-3.5M	>3.5M	<1.5M	1.5-3.5M	>3.5M	<1.5M	1.5-3.5M	>3.5M	<1.5M	1.5-3.5M	>3.5M	5-10M	>10M	5-10M	>10M	5-10M	>10M	5-10M	>10M		
0	402 014	2	0	0.7	0	0	0	0	0	0	0	0	0	0	0	0	0	0	0	0	0	0	0	0	0	0	0	0		
5 19194	408 758	1	0	0.7	0	0	0	0	0	0	0	0	0	0	0	0	0	0	0	0	0	0	0	0	0	0	0	0		
18 55637	404 964	11	0	0.9	0	0.1	0	0	0	0	0	0	0	0	0	0	0	0	0	0	0	0	0	0	0	0	0	0		
26 12507	404 4	11	0	0.8	0	0.1	0	0	0	0	0	0	0	0	0	0	0	0	0	0	0	0	0	0	0	0	0	0		
34 9611	404 1353	11	0	0.8	0	0.1	0	0	0	0	0	0	0	0	0	0	0	0	0	0	0	0	0	0	0	0	0	0		
51 03058	402 8902	206	0	0	0	0	0	0	0	0	0	0	0	0	0.7	0	0	0	0	0	0	0	0	0	0	0	0	0		
54 45553	400 6900	201	0	0	0	0	0	0	0	0	0	0	0	0	0	0	0	0	0	0	0	0	0	0	0	0	0	0		
56 72143	400 2817	201	0	0	0	0	0	0	0	0	0	0	0	0	0	0	0	0	0	0	0	0	0	0	0	0	0	0		
62 74577	400 9649	201	0	0	0	0	0	0	0	0	0	0	0	0	0	0	0	0	0	0	0	0	0	0	0	0	0	0		
69 7182	400 5208	201	0	0	0	0	0	0	0	0	0	0	0	0	0	0	0	0	0	0	0	0	0	0	0	0	0	0		
75 8217	400 4344	287	0	0	0	0	0	0	0	0	0	0	0	0	0	0	0	0	0	0	0	0	0	0	0	0	0	0		
86 94361	400 3684	201	0	0	0	0	0	0	0	0	0	0	0	0	0	0	0	0	0	0	0	0	0	0	0	0	0	0		
94 75707	403 8237	201	0	0	0	0	0	0	0	0	0	0	0	0	0	0	0	0	0	0	0	0	0	0	0	0	0	0		
99 29902	403 5091	208	0	0	0	0	0	0	0	0	0	0	0	0	0	0	0	0	0	0	0	0	0	0	0	0	0	0		
95 78373	404 0087	17	0	0.5	0	0	0	0	0	0	0.1	0	0	0	0	0	0	0	0	0	0	0	0	0	0	0	0	0		
101 0087	404 1717	11	0	0.5	0	0	0	0	0	0	0.1	0	0	0	0	0	0	0	0	0	0	0	0	0	0	0	0	0		
115 1882	407 8081	11	0	0.5	0	0	0	0	0	0	0.1	0	0	0	0	0	0	0	0	0	0	0	0	0	0	0	0	0		
124 798	408 6637	2	0.8	0	0	0	0	0	0	0	0	0	0	0	0	0	0	0	0	0	0	0	0	0	0	0	0	0		
130 837	410 6676	2	0.8	0	0	0	0	0	0	0	0	0.4	0	0	0	0	0	0	0	0	0	0	0	0	0	0	0	0		

SITE 11		GRASS/HERB/POD						REEDS						A= WILLOW LIKE APPEARANCE			P= ACACIA LIKE APPEARANCE			C= LYONNETIUM LIKE APPEARANCE			O= THORN STEMMED BUSH			E= MYRTLEBUSH			A= DENF		C= GUM		B= SPARE		C= GUM		E= BARK		E= WILLOW LIKE APPEARANCE	
K	V	M	0.2M	0.2-0.5M	0.5-1M	1-2M	>2M	<1.5M	1.5-3.5M	>3.5M	<1.5M	1.5-3.5M	>3.5M	<1.5M	1.5-3.5M	>3.5M	<1.5M	1.5-3.5M	>3.5M	<1.5M	1.5-3.5M	>3.5M	<1.5M	1.5-3.5M	>3.5M	<1.5M	1.5-3.5M	>3.5M	<1.5M	1.5-3.5M	>3.5M	<1.5M	1.5-3.5M	>3.5M	<1.5M	1.5-3.5M	>3.5M			
0	400 514	2	0	0.05	0	0	0	0	0	0	0	0	0	0	0	0	0	0	0	0	0	0	0	0	0	0	0	0	0	0	0	0	0	0	0	0	0			
1 12 4074	400 3398	2	0	0.05	0	0	0	0	0	0	0	0	0	0	0	0	0	0	0	0	0	0	0	0	0	0	0	0	0	0	0	0	0	0	0	0	0			
9 407341	407 1082	11	0	0.15	0	0	0	0	0	0	0	0	0	0	0	0	0	0	0	0	0	0	0	0	0	0	0	0	0	0	0	0	0	0	0	0	0			
26 32163	403 1167	14	0	0.15	0	0	0	0	0	0	0	0	0	0	0	0	0	0	0	0	0	0	0	0	0	0	0	0	0	0	0	0	0	0	0	0	0			
33 31566	402 7367	206	0	0	0	0	0	0	0.7	0	0	0	0	0	0	0	0	0	0	0	0	0	0	0	0	0	0	0	0	0	0	0	0	0	0	0	0			
42 41427	399 1640	201	0	0	0	0	0	0	0	0	0	0	0	0	0	0	0	0	0	0	0	0	0	0	0	0	0	0	0	0	0	0	0	0	0	0	0			
44 28109	399 0010	201	0	0	0	0	0	0	0	0	0	0	0	0	0	0	0	0	0	0	0	0	0	0	0	0	0	0	0	0	0	0	0	0	0	0	0			
46 51720	399 0212	201	0	0	0	0	0	0	0	0	0	0	0	0	0	0	0	0	0	0	0	0	0	0	0	0	0	0	0	0	0	0	0	0	0	0	0			
48 35122	399 1826	201	0	0	0	0	0	0	0	0	0	0	0	0	0	0	0	0	0	0	0	0	0	0	0	0	0	0	0	0	0	0	0	0	0	0	0			
50 21224	399 2836	201	0	0	0	0	0	0	0	0	0	0	0	0	0	0	0	0	0	0	0	0	0	0	0	0	0	0	0	0	0	0	0	0	0	0	0			
51 4925	399 8265	203	0	0	0	0	0	0	0	0	0	0	0	0	0	0	0	0	0	0	0	0	0	0	0	0	0	0	0	0	0	0	0	0	0	0	0			
52 13178	399 1980	203	0	0	0	0	0	0	0	0	0	0	0	0	0	0	0	0	0	0	0	0	0	0	0	0	0	0	0	0	0	0	0	0	0	0	0			
53 9852	399 4980	201	0	0	0	0	0	0	0	0	0	0	0	0	0	0	0	0	0	0	0	0	0	0	0	0	0	0	0	0	0	0	0	0	0	0	0			
54 74218	399 4674	201	0	0	0	0	0	0	0	0	0	0	0	0	0	0	0	0	0	0	0	0	0	0	0	0	0	0	0	0	0	0	0	0	0	0	0			
58 17572	405 8670	102	0	0	0	0	0	0.7	0	0	0	0	0	0	0	0	0	0	0	0	0	0	0	0	0	0	0	0	0	0	0	0	0	0	0	0	0			
61 41429	401 3110	202	0	0	0	0	0	0.7	0	0	0	0	0	0	0	0	0	0	0	0	0	0	0	0	0	0	0	0	0	0	0	0	0	0	0	0	0			
63 28341	400 8374	200	0	0	0	0	0	0.3	0	0	0	0	0	0	0	0	0	0	0	0	0	0	0	0	0	0	0	0	0	0	0	0	0	0	0	0	0			
70 21404	402 6306	200	0	0	0	0	0	0.3	0	0	0	0	0	0	0	0	0	0	0	0	0	0	0	0	0	0	0	0	0	0	0	0	0	0	0	0	0			
73 34182	401 1211	200	0	0	0	0	0	0.3	0	0	0	0	0	0	0	0	0	0	0	0	0	0	0	0	0	0	0	0	0	0	0	0	0	0	0	0	0			
77 71104	401 6455	200	0	0	0	0	0	0.3	0	0	0	0	0	0	0	0	0	0	0	0	0	0	0	0	0	0	0	0	0	0	0	0	0	0	0	0	0			
78	398 5370	212	0	0	0	0	0	0	0	0	0	0	0	0	0	0	0	0	0	0	0	0	0	0	0	0	0	0	0	0	0	0	0	0	0	0	0			
80 82078	399 0519	212	0	0	0	0	0	0	0	0	0	0	0	0	0	0	0	0	0	0	0	0	0	0	0	0	0	0	0	0	0	0	0	0	0	0	0			
97 35481	403 463	11	0	0.8	0	0	0	0	0	0	0	0	0	0	0	0	0	0	0	0	0	0	0	0	0	0	0	0	0	0	0	0	0	0	0	0	0			
104 1908	403 8487	11	0	0.8	0	0	0	0	0	0	0	0	0	0	0	0	0	0	0	0	0	0	0	0	0	0	0	0	0	0	0	0	0	0	0	0	0			
111 1825	405 0794	2	0	0.4	0	0	0	0	0	0	0	0	0	0	0	0	0	0	0	0	0	0	0	0	0	0	0	0	0	0	0	0	0	0	0	0	0			
116 2099	409 7287	2	0	0.4	0	0	0	0	0	0	0	0	0	0	0	0	0	0	0	0	0	0	0	0	0	0	0	0	0	0	0	0	0	0	0	0	0			

SITE #	Y	GRASSHERB/COMP			REEDS			AMPHILOXIDINE APPEARANCE			BACILLARIA LINE APPEARANCE			CITRICHLOPHYL APPEARANCE			D-TICHA STELLER THINNY			E-BROW HAIR			A-GRASS		B-SHAPED		E-FLUOROPHYLLUM		D-MULLEUM LINE APPEAR	
		MOVEN	<1M	>1M	<1M	1.2-1M	>1M	<1M	1.1-1M	>1M	<1M	1.1-1M	>1M	<1M	1.1-1M	>1M	<1M	1.1-1M	>1M	<1M	1.1-1M	>1M	<1M	>1M	<1M	>1M	<1M	>1M	<1M	>1M
0	410 5025	2	0	0	0	0	0	0	0	0	0	0	0	0	0	0	0	0	0	0	0	0	0	0	0	0	0	0		
8 904823	410 0420	2	0	0	0	0	0	0	0	0	0	0	0	0	0	0	0	0	0	0	0	0	0	0	0	0	0	0		
8 5246	409 1104	11	0	0	0	0	0	0	0	0	0	0	0	0	0	0	0	0	0	0	0	0	0	0	0	0	0	0		
14 18652	407 7910	11	0	0	0	0	0	0	0	0	0	0	0	0	0	0	0	0	0	0	0	0	0	0	0	0	0	0		
14 1923	407 788	11	0	0	0	0	0	0	0	0	0	0	0	0	0	0	0	0	0	0	0	0	0	0	0	0	0	0		
17 31825	407 4871	11	0	0	0	0	0	0	0	0	0	0	0	0	0	0	0	0	0	0	0	0	0	0	0	0	0	0		
28 3525	406 0432	11	0	0	0	0	0	0	0	0	0	0	0	0	0	0	0	0	0	0	0	0	0	0	0	0	0	0		
28 82057	404 92	11	0	0	0	0	0	0	0	0	0	0	0	0	0	0	0	0	0	0	0	0	0	0	0	0	0	0		
38 47045	402 4734	11	0	0	0	0	0	0	0	0	0	0	0	0	0	0	0	0	0	0	0	0	0	0	0	0	0	0		
43 06591	402 9525	11	0	0	0	0	0	0	0	0	0	0	0	0	0	0	0	0	0	0	0	0	0	0	0	0	0	0		
50 51074	400 4488	202	0	0	0	0	0	0	0	0	0	0	0	0	0	0	0	0	0	0	0	0	0	0	0	0	0	0		
53 31216	398 9311	209	0	0	0	0	0	0	0	0	0	0	0	0	0	0	0	0	0	0	0	0	0	0	0	0	0	0		
54 42533	398 1394	201	0	0	0	0	0	0	0	0	0	0	0	0	0	0	0	0	0	0	0	0	0	0	0	0	0	0		
57 50927	398 6612	201	0	0	0	0	0	0	0	0	0	0	0	0	0	0	0	0	0	0	0	0	0	0	0	0	0	0		
61 83252	398 5051	201	0	0	0	0	0	0	0	0	0	0	0	0	0	0	0	0	0	0	0	0	0	0	0	0	0	0		
64 34375	398 4021	201	0	0	0	0	0	0	0	0	0	0	0	0	0	0	0	0	0	0	0	0	0	0	0	0	0	0		
67 44118	398 4261	201	0	0	0	0	0	0	0	0	0	0	0	0	0	0	0	0	0	0	0	0	0	0	0	0	0	0		
68 48182	388 8078	201	0	0	0	0	0	0	0	0	0	0	0	0	0	0	0	0	0	0	0	0	0	0	0	0	0	0		
77 4616	401 3787	206	0	0	0	0	0	0	0	0	0	0	0	0	0	0	0	0	0	0	0	0	0	0	0	0	0	0		
87 80527	401 8178	11	0	0	0	0	0	0	0	0	0	0	0	0	0	0	0	0	0	0	0	0	0	0	0	0	0	0		
88 78187	402 1186	11	0	0	0	0	0	0	0	0	0	0	0	0	0	0	0	0	0	0	0	0	0	0	0	0	0	0		
104 5724	403 0518	11	0	0	0	0	0	0	0	0	0	0	0	0	0	0	0	0	0	0	0	0	0	0	0	0	0	0		
118 5804	402 4252	11	0	0	0	0	0	0	0	0	0	0	0	0	0	0	0	0	0	0	0	0	0	0	0	0	0	0		
118 7231	404 0628	11	0	0	0	0	0	0	0	0	0	0	0	0	0	0	0	0	0	0	0	0	0	0	0	0	0	0		
128 3647	405 8927	2	0	0	0	0	0	0	0	0	0	0	0	0	0	0	0	0	0	0	0	0	0	0	0	0	0	0		
134 8581	409 9129	2	0	0	0	0	0	0	0	0	0	0	0	0	0	0	0	0	0	0	0	0	0	0	0	0	0	0		

SIF 11

X	Y	OMASSIHERBICIFEM			NEEDS			A-WILLOW LIKE APPEARANCE			B-ACACIA LIKE APPEARANCE			C-FRONT HORN LIKE APPEARANCE			D-THICK STEMMED HORN			E-BROKEN AORN			A-DENSE CANOPY		B-SPARSE CANOPY		ERTH WITH BELLUM		D-MULLOW LIKE APPEAR	
		<0.2M	0.2-0.5M	>0.5M	<1M	1-2DM	>2M	<1.5M	1.5-3.5M	>3.5M	<1.5M	1.5-3.5M	>3.5M	<1.5M	1.5-3.5M	>3.5M	<1.5M	1.5-3.5M	>3.5M	<1.5M	1.5-3.5M	>3.5M	<10M	>10M	<10M	>10M	<10M	>10M	<10M	>10M
0	382.37	1	0	0	0.6	0	0	0	0	0.3	0	0	0	0	0	0.05	0	0	0	0	0	0	0	0	0	0	0	0	0	
7.23	381.83	1	0	0	0.6	0	0	0	0	0.1	0	0	0	0	0	0	0	0	0.7	0	0	0	0	0.04	0	0	0	0	0	
17.72	381.6	1	0.2	0	0	0	0	0	0	0	0	0	0	0	0	0.5	0	0	0	0	0	0	0	0.05	0	0	0	0	0	
18.29	381.14	1	0.2	0	0	0	0	0	0	0	0	0	0	0	0	0	0.5	0	0	0	0	0	0	0.05	0	0	0	0	0	
24.8	380.38	11	0.1	0	0	0	0	0	0	0	0	0	0	0	0	0.8	0.2	0	0	0	0	0	0	0.05	0	0	0	0	0	
29.25	379.48	11	0.1	0	0	0	0	0	0	0	0	0	0	0	0	0.8	0.2	0	0	0	0	0	0	0.05	0	0	0	0	0	
37.15	378.44	206	0	0	0	0	0	0	0	0	0	0	0	0	0	0.7	0	0	0	0	0	0	0	0	0	0	0	0	0	
37.98	378.83	201	0	0	0	0	0	0	0	0	0	0	0	0	0	0	0	0	0	0	0	0	0	0	0	0	0	0	0	
40.1	375.9	201	0	0	0	0	0	0	0	0	0	0	0	0	0	0	0	0	0	0	0	0	0	0	0	0	0	0	0	
45.17	379.03	201	0	0	0	0	0	0	0	0	0	0	0	0	0	0	0	0	0	0	0	0	0	0	0	0	0	0	0	
48.42	376.22	201	0	0	0	0	0	0	0	0	0	0	0	0	0	0	0	0	0	0	0	0	0	0	0	0	0	0	0	
54.88	378.22	201	0	0	0	0	0	0	0	0	0	0	0	0	0	0	0	0	0	0	0	0	0	0	0	0	0	0	0	
60.52	378.4	201	0	0	0	0	0	0	0	0	0	0	0	0	0	0	0	0	0	0	0	0	0	0	0	0	0	0	0	
65.82	378.44	201	0	0	0	0	0	0	0	0	0	0	0	0	0	0	0	0	0	0	0	0	0	0	0	0	0	0	0	
74.78	378.48	201	0	0	0	0	0	0	0	0	0	0	0	0	0	0	0	0	0	0	0	0	0	0	0	0	0	0	0	
83.52	378.87	202	0	0	0	0.5	0	0	0	0	0	0	0	0	0	0.1	0	0	0	0	0	0	0	0	0	0	0	0	0	
87.39	377.22	202	0	0	0	0.6	0	0	0	0	0	0	0	0	0	0.1	0	0	0	0	0	0	0	0	0	0	0	0	0	
93.02	377.26	208	0	0	0	0.5	0	0	0	0	0	0	0	0	0	0.1	0	0	0	0	0	0	0	0	0	0	0	0	0	
100.03	377.18	202	0	0	0	0.5	0	0	0	0	0	0	0	0	0	0.1	0	0	0	0	0	0	0	0	0	0	0	0	0	
108.14	377.11	208	0	0.1	0	0.8	0	0	0	0	0	0	0	0	0	0	0	0	0	0	0	0	0	0	0	0	0	0	0	
108.76	377.81	208	0	0.1	0	0.2	0	0	0	0	0	0	0	0	0	0	0	0	0	0	0	0	0	0	0	0	0	0	0	
108.89	377.59	101	0	0.1	0	0	0	0	0	0	0	0	0	0	0	0	0	0	0	0	0	0	0	0	0	0	0	0	0	
111.28	377.82	101	0	0.1	0	0	0	0	0	0	0	0	0	0	0	0	0	0	0	0	0	0	0	0	0	0	0	0	0	
117.88	377.39	101	0	0.1	0	0	0	0	0	0	0	0	0	0	0	0	0	0	0	0	0	0	0	0	0	0	0	0	0	
128.08	380.84	2	0.1	0	0	0	0	0	0	0	0	0	0	0	0	0	0	0	0.7	0	0	0	0	0	0.0221	0.2	0	0	0	
134.34	381.93	2	0.1	0	0	0	0	0	0	0	0	0	0	0	0	0	0	0	0	0	0	0	0	0	0.0222	0.2	0	0	0	
161.84	382.22	18	0.1	0	0	0	0	0	0	0	0	0	0	0	0	0	0	0	0	0	0	0	0	0	0	0	0	0	0	
168.18	383.15	1	0.1	0	0	0	0	0	0	0	0	0	0	0	0	0	0	0	0	0	0	0	0	0	0	0	0	0	0	

SITE 122

X	Y	MORPH	GRASS/HERB/CROP			WEEDES			A-WILLOW LIKE APPEARANCE			B-ACACIA LIKE APPEARANCE			C-HOOKTHORN LIKE APPEARANCE			D-THICK STEMMED THORNY			A-DENSE CANOPY		B-SPARS CANOPY		ERYTHROPHYLLUM		D-WILLOW LIKE APPE	
			<0.2M	0.2-0.5M	>0.5M	<1M	1.2-2M	>2M	<1M	1.5-3M	>3M	<1M	1.5-3M	>3M	<1M	1.5-3M	>3M	<1M	1.5-3M	>3M	>10M	>10M	>10M	>10M	>10M	>10M	>10M	
14.74	276.57	1	0	0.2	0	0	0	0	0	0	0.5	0	0	0	0	0	0	0	0	0	0	0	0	0	0	0		
22.17	273.4	2	0	0.3	0	0	0	0	0	0	0.1	0	0	0	0	0	0	0	0	0	0	0	0	0	0	0		
31.78	274.04	2	0	0	0.05	0	0	0	0	0	0.03	0	0	0	0	0	0	0	0	0	0	0	0.05	0	0	0		
49.07	272.93	2	0	0	0.05	0	0	0	0	0	0.05	0	0	0	0	0	0	0	0	0	0	0	0	0	0	0		
49.1	272.91	2	0	0	0.3	0	0	0	0	0	0.4	0	0	0	0	0	0	0	0	0	0	0	0	0	0	0		
58.56	272.04	2	0	0	0.3	0	0	0	0	0	0	0.05	0	0	0	0	0	0	0.6	0	0.02	0	0	0	0	0		
73.13	269.83	1	0	0	1	0	0	0	0	0	0	0	0	0	0	0	0	0	0	0	0	0	0	0	0	0		
77.95	269.12	2	0	0	1	0	0	0	0	0	0	0	0	0	0	0	0	0	0.7	0	0	0	0	0	0	0		
83.56	268.67	101	0	0	0.3	0	0	0	0	0	0	0	0	0	0	0	0	0	0.7	0	0	0	0	0	0	0		
82.86	268.09	101	0	0.05	0	0	0	0	0	0	0.05	0	0	0	0	0	0	0	0	0	0	0	0	0	0	0		
86.89	267.87	101	0	0.05	0	0	0	0	0	0	0.05	0	0	0	0	0	0	0	0	0	0	0	0	0	0	0		
103.3	267.29	101	0	0.05	0	0	0	0	0	0	0.05	0	0	0	0	0	0	0	0	0	0	0	0	0	0	0		
112.03	266.45	202	0	0	0	0	0	0	0.5	0	0	0	0	0	0	0	0	0	0	0	0	0	0	0	0	0		
117.86	266.18	202	0	0	0	0	0	0	0.4	0	0	0	0	0	0	0	0	0	0	0	0	0	0	0	0	0		
127.73	265.4	204	0	0	0	0	0	0	0	0	0	0	0	0	0	0	0	0	0	0	0	0	0	0	0	0		
131.57	263.16	204	0	0	0	0	0	0	0	0	0	0	0	0	0	0	0	0	0	0	0	0	0	0	0	0		
133.89	263.16	204	0	0	0	0	0	0	0	0	0	0	0	0	0	0	0	0	0	0	0	0	0	0	0	0		
140.92	264.38	204	0	0	0	0	0	0	0	0	0	0	0	0	0	0	0	0	0	0	0	0	0	0	0	0		
144.11	263.21	204	0	0	0	0	0	0	0	0	0	0	0	0	0	0	0	0	0	0	0	0	0	0	0	0		
145.04	263.33	204	0	0	0	0	0	0	0	0	0	0	0	0	0	0	0	0	0	0	0	0	0	0	0	0		
146.6	262.74	204	0	0	0	0	0	0	0	0	0	0	0	0	0	0	0	0	0	0	0	0	0	0	0	0		
146.42	263.01	204	0	0	0	0	0	0	0	0	0	0	0	0	0	0	0	0	0	0	0	0	0	0	0	0		
143.86	263.11	204	0	0	0	0	0	0	0	0	0	0	0	0	0	0	0	0	0	0	0	0	0	0	0	0		
162.86	264.85	204	0	0	0	0	1	0	0	0	0	0	0	0	0	0	0	0	0	0	0	0	0	0	0	0		
172.46	266.07	2	0	0	0	0	0	0	0	0	0	0	0	0	0.3	0	0	0	0.05	0	0	0	0	0	0	0		
180.96	268.07	2	0	0.3	0	0	0	0	0	0	0	0	0	0	0	0	0	0.23	0	0.0000007	0	0	0	0	0	0		
180.4	270.19	2	0	0.05	0	1	0	0	0	0	0.1	0	0	0	0	0	0	0	0	0.1111111	0	0	0	0	0	0		
201.78	273.83	2	0	0.05	0	0	0	0	0	0	0.1	0	0	0	0	0	0	0	0	0.111	0	0	0	0	0	0		
218.92	277.13	1	0	0.05	0	0	0	0	0	0	0.1	0	0	0	0	0	0	0	0	0.111	0	0	0	0	0	0		

X	Y	MORPH	GRASS/HERB/COF			REEDS			A - WILLOW LIKE APPEARANCE			B - ACACIA LIKE APPEARANCE			C - HOOKTHORN LIKE APPEARANCE			D - THICK STEMMED ENDONY			A - DENSE CANOPY		B - SPARS CANOPY		ERYTHROPHYLLUM		D - WILLOW LIKE APPE	
			<0.2M	0.2-0.5M	>0.5M	<1M	1-2M	>2M	<1.5M	1.5-3M	>3M	<1.5M	1.5-3M	>3M	<1.5M	1.5-3M	>3M	<1.5M	1.5-3M	>3M	5-10M	>10M	5-10M	>10M	5-10M	>10M	5-10M	>10M
4.8	279.03	2	0	0.5	0	0	0	0	0	0	0	0	0	0	0	0	0	0	0	0	0	0	0	0	0	0	0	
13.98	277.36	2	0	0.8	0	0	0	0	0	0	0	0	0	0	0	0	0	0	0	0	0	0.08	0	0	0	0	0	
18.45	273.85	2	0	0.8	0	0	0	0	0	0	0	0	0	0	0	0	0	0	0	0	0	0.05	0	0	0	0	0	
28.56	273.73	2	0	0.8	0	0	0	0	0	0	0	0	0	0	0	0	0	0	0	0	0	0.04	0	0	0	0	0	
28.8	273.47	2	0	0.6	0	0	0	0	0	0	0	0	0	0	0	0	0	0	0	0	0	0.04	0	0	0	0	0	
32.3	272.75	4	0	1	0	0	0	0	0	0	0	0	0	0	0	0	0	0	0	0	0.0571428	0	0	0	0	0	0	
38.57	271.79	4	0	1	0	0	0	0	0	0	0	0	0	0	0	0	0	0	0	0	0.057	0	0	0	0	0	0	
44.12	270.74	4	0	0.5	0	0	0	0	0	0	0	0	0	0	0	0	0	0	0	0	0.20	0.15	0	0	0	0	0	
49.81	269.88	4	0	0.8	0	0	0	0	0	0	0	0	0	0	0	0	0	0	0	0	0	0	0	0	0	0	0	
52.82	268.82	4	0	0.8	0	0	0	0	0	0	0	0	0	0	0	0	0	0	0	0	0	0	0	0	0	0	0	
55.8	270.15	4	0	0.4	0	0	0	0	0	0	0	0	0	0	0	0	0	0	0	0	0	0	0	0	0	0	0	
81.12	268.9	4	0	0.2	0	0	0	0	0	0	0	0	0	0	0	0	0	0	0	0	0	0.0333333	0	0	0	0	0	
84.32	269.99	4	0	0.2	0	0	0	0	0	0	0	0	0	0	0	0	0	0	0	0	0	0.03333	0	0	0	0	0	
87.28	269.48	208	0	0	0	0	0	0	0	0	0	0	0	0	0	0	0	0	0	0	0	0	0	0	0	0	0	
88.18	263.54	201	0	0	0	0	0	0	0	0	0	0	0	0	0	0	0	0	0	0	0	0	0	0	0	0	0	
88.87	263.28	201	0	0	0	0	0	0	0	0	0	0	0	0	0	0	0	0	0	0	0	0	0	0	0	0	0	
89.72	264.82	201	0	0	0	0	0	0	0	0	0	0	0	0	0	0	0	0	0	0	0	0	0	0	0	0	0	
92.05	264.87	201	0	0	0	0	0	0	0	0	0	0	0	0	0	0	0	0	0	0	0	0	0	0	0	0	0	
92.7	265.25	201	0	0	0	0	0	0	0	0	0	0	0	0	0	0	0	0	0	0	0	0	0	0	0	0	0	
93.83	265.27	201	0	0	0	0	0	0	0	0	0	0	0	0	0	0	0	0	0	0	0	0	0	0	0	0	0	0
94.36	264.35	201	0	0	0	0	0	0	0	0	0	0	0	0	0	0	0	0	0	0	0	0	0	0	0	0	0	0
98.22	264.48	201	0	0	0	0	0	0	0	0	0	0	0	0	0	0	0	0	0	0	0	0	0	0	0	0	0	0
82.28	263.04	201	0	0	0	0	0	0	0	0	0	0	0	0	0	0	0	0	0	0	0	0	0	0	0	0	0	0
82.38	265.25	208	0	0	0	0	0	0	0	0	0	0	0	0	0	0	0	0	0	0	0	0	0	0	0	0	0	0
88.1	265.38	208	0	0	0	0	0	0	0	0	0	0	0	0	0	0	0	0	0	0	0	0	0	0	0	0	0	0
93.88	263.27	208	0	0	0	0	0	0	0	0	0	0	0	0	0	0	0	0	0	0	0	0	0	0	0	0	0	0
83.94	264.88	201	0	0	0	0	0	0	0	0	0	0	0	0	0	0	0	0	0	0	0	0	0	0	0	0	0	0
87.12	264.58	201	0	0	0	0	0	0	0	0	0	0	0	0	0	0	0	0	0	0	0	0	0	0	0	0	0	0
88.2	264.72	201	0	0	0	0	0	0	0	0	0	0	0	0	0	0	0	0	0	0	0	0	0	0	0	0	0	0
88.43	264.88	201	0	0	0	0	0	0	0	0	0	0	0	0	0	0	0	0	0	0	0	0	0	0	0	0	0	0
81.48	262.22	201	0	0	0	0	0	0	0	0	0	0	0	0	0	0	0	0	0	0	0	0	0	0	0	0	0	0
82.84	268.77	208	0	0	0	0	1	0	0	0	0	0	0	0	0	0	0	0	0	0	0	0	0	0	0	0	0	0
85.78	268.89	101	0	0	0	0	0	0	0	0	0	0	0	0	0	0	0	0	0	0	0	0	0	0	0	0	0	0
87.48	267.3	101	0	0	0	0	0.7	0	0	0	0	0	0	0	0	0	0	0	0	0	0	0	0	0	0	0	0	0
102.87	267.31	101	0	0	0	0	0.7	0	0	0	0	0	0	0	0	0	0	0	0	0	0	0	0	0	0	0	0	0
105.38	266.8	101	0	0	0	0	0.7	0	0	0	0	0	0	0	0	0	0	0	0	0	0	0	0	0	0	0	0	0
108.07	266.84	101	0	0	0	0	0.7	0	0	0	0	0	0	0	0	0	0	0	0	0	0	0	0	0	0	0	0	0
108.15	266.8	102	0	0	0	0	0	0	0	0	0	0	0	0	0	0	0	0	0	0	0	0	0	0	0	0	0	0
108.92	266.3	102	0	0	0	0	0	0	0	0	0	0	0	0	0	0	0	0	0	0	0	0	0	0	0	0	0	0
111.78	266.87	102	0	0	0	0	0	0	0	0	0	0	0	0	0	0	0	0	0	0	0	0	0	0	0	0	0	0
113.18	267.03	103	0	0	0	0	0.8	0	0	0	0	0	0	0	0	0	0	0	0	0	0	0	0	0	0	0	0	0
114.38	268.81	101	0	0	0	0	0.8	0	0	0	0	0	0	0	0	0	0	0	0	0	0	0	0	0	0	0	0	0
116	267.08	101	0	0	0	0	0.1	0	0	0	0	0	0	0	0	0	0	0	0	0	0	0	0	0	0	0	0	0
117.51	267.28	101	0	0	0	0	0.1	0	0	0	0	0	0	0	0	0	0	0	0	0	0	0	0	0	0	0	0	0
118.67	267.28	108	0	0	0	0	0	0	0	0	0	0	0	0	0	0	0	0	0	0	0	0	0	0	0	0	0	0
120.42	266.38	906	0	0	0	0	0	0	0	0	0	0	0	0	0	0	0	0	0	0	0	0	0	0	0	0	0	0
122.25	266.58	906	0	0	0	0	0	0	0	0	0	0	0	0	0	0	0	0	0	0	0	0	0	0	0	0	0	0
127.35	268.08	4	0	0	0	0	0.8	0	0	0	0	0	0	0	0	0	0	0	0	0	0	0	0	0	0	0	0	0
128.8	267.78	4	0	0	0	0	0.8	0	0	0	0	0	0	0	0	0	0	0	0	0	0	0	0	0	0	0	0	0
131.08	268.01	4	0	0	0	0	0.7	0	0	0	0	0	0	0	0	0	0	0	0	0	0	0	0	0	0	0	0	0
134.11	267.97	4	0	0	0	0	0.7	0	0	0	0	0	0	0	0	0	0	0	0	0	0	0	0	0	0	0	0	0
141.5	268.38	4	0	0	0	0	0.7	0	0	0	0	0	0	0	0	0	0	0	0	0	0	0	0	0	0	0	0	0
148.11	270.01	4	0	0	0	0	0.7	0	0	0	0	0	0	0	0	0	0	0	0	0	0	0	0	0	0	0	0	0
130.88	268.98	4	0	0.8	0	0	0	0	0	0	0	0	0	0	0	0	0	0	0	0	0	0	0	0	0	0	0	0
154.28	268.04	4	0	0.8	0	0	0	0	0	0	0	0	0	0	0	0	0	0	0	0	0	0	0	0	0	0	0	0
157.91	268.82	4	0	0.8	0	0	0	0	0	0	0	0	0	0	0	0	0	0	0	0	0	0	0	0	0	0	0	0
163.6	268.88	3	0	0	0.8	0	0	0	0	0	0	0	0	0	0	0	0	0	0	0	0	0	0	0	0	0	0	0
164.22	268.56	2	0	0	0.8	0	0	0	0	0	0	0	0	0	0	0	0	0	0	0	0	0.2	0	0	0	0	0	0
168.12	270.02	2	0	0	0.8	0	0	0	0	0	0	0	0	0	0	0	0	0	0	0	0	0.1	0	0	0	0	0	0
178.28	271.58	2	0	0	0.8	0	0	0	0	0	0	0	0	0	0	0	0	0	0	0	0	0	0	0	0	0	0	0
188	273.81	2	0	0.7	0	0	0	0	0	0	0	0	0	0	0	0	0	0	0	0	0	0	0	0	0	0	0	0
187.88	273.48	2	0	0.7	0	0	0	0	0	0	0	0	0	0	0	0	0	0	0	0	0	0	0	0	0	0	0	0
208.75	277.2	1	0	0.7	0	0	0	0</																				

SITE 12 #

X	Y	MORPH	GRASS/HERB/CROP			NEEDS			A-WILLOW LIKE APPEARANCE			B-ACACIA LIKE APPEARANCE			C-HOORHORN LIKE APPEARANCE			D-THICK STEMMED THORN			A-DENSE CANOPY		B-SPARS CANOPY		ERYTHROPHYLLUM		D-WILLOW LIKE APPE	
			<0.2M	0.3-0.9M	>0.9M	<1M	1-2.9M	>3M	<1.5M	1.5-3.9M	>3.9M	<1.5M	1.5-3.9M	>3.9M	<1.5M	1.5-3.9M	>3.9M	<1.5M	1.5-3.9M	>3.9M	≤10M	>10M	≤10M	>10M	≤10M	>10M	≤10M	>10M
581	275 22	2	0	0	0	0	0	0	0	0	0.19	0	0	0	0	0	0	0	0	0	0	0	0	0	0	0	0	
12 33	273 50	2	0	0	0	0	0	0	0	0	0	0.15	0	0	0	0	0	0	0	0	0	0	0	0	0	0	0	
18 53	274 79	2	0	0	0	0	0	0	0	0	0	0.13	0	0	0	0	0	0	0	0	0	0	0	0	0	0	0	
24 30	270 01	2	0	0	0	0	0	0	0	0	0	0.2	0	0	0	0	0	0	0	0	0	0	0	0	0	0	0	
28 01	270 42	4	0	0	0	0	0	0	0	0	0	0.2	0	0	0	0	0	0	0	0	0	0	0	0	0	0	0	
28 28	289 94	4	0	0	0	0	0	0	0	0	0	0	0	0	0	0	0	0	0	0	0	0	0	0	0	0	0	
28 73	289 94	6	0	0	0	0	0	0	0	0	0	0	0	0	0	0	0	0	0	0	0	0	0	0	0	0	0	
30 73	287 98	6	0	0	0	0	0	0	0	0	0	0	0	0	0	0	0	0	0	0	0	0	0	0	0	0	0	
32 03	297 39	102	0	0	0	0.5	0	0.3	0	0	0	0	0	0	0	0	0	0	0	0	0	0	0	0	0	0	0	
38 24	297 09	102	0	0	0	0.5	0	0.3	0	0	0	0	0	0	0	0	0	0	0	0	0	0	0	0	0	0	0	
40 77	287 31	101	0	0	0	0	0	0	0	0	0	0	0	0	0	0	0	0	0	0	0	0	0	0	0	0	0	
43 16	286 82	101	0	0	0	0	0	0	0	0	0	0	0	0	0	0	0	0	0	0	0	0	0	0	0	0	0	
45 87	286 53	101	0	0	0	0	0	0	0	0	0	0	0	0	0	0	0	0	0	0	0	0	0	0	0	0	0	
51 21	288 42	101	0	0	0	0	0	0	0	0	0	0	0	0	0	0	0	0	0	0	0	0	0	0	0	0	0	
53 82	288 21	101	0	0	0	0	0	0	0	0	0	0	0	0	0	0	0	0	0	0	0	0	0	0	0	0	0	
54 54	283 89	101	0	0	0	0	0	0	0	0	0	0	0	0	0	0	0	0	0	0	0	0	0	0	0	0	0	
60 67	283 99	101	0	0	0	0	0	0	0	0	0	0	0	0	0	0	0	0	0	0	0	0	0	0	0	0	0	
62 28	284 12	101	0	0	0	0	0	0	0	0	0	0	0	0	0	0	0	0	0	0	0	0	0	0	0	0	0	
62 54	283 89	101	0	0	0	0	0	0	0	0	0	0	0	0	0	0	0	0	0	0	0	0	0	0	0	0	0	
65 93	283 78	101	0	0	0	0	0	0	0	0	0	0	0	0	0	0	0	0	0	0	0	0	0	0	0	0	0	
67 37	283 95	101	0	0	0	0	0	0	0	0	0	0	0	0	0	0	0	0	0	0	0	0	0	0	0	0	0	
68 53	288 94	101	0	0	0	0	0	0	0	0	0	0	0	0	0	0	0	0	0	0	0	0	0	0	0	0	0	
72 18	287 21	101	0	0	0	0	0	0.1	0	0	0	0	0	0	0	0	0	0	0	0	0	0	0	0	0	0	0	
74 87	287 09	101	0	0	0	0	0	0.1	0	0	0	0	0	0	0	0	0	0	0	0	0	0	0	0	0	0	0	
78 8	288 79	101	0	0	0	0	0	0	0	0	0	0	0	0	0	0	0	0	0	0	0	0	0	0	0	0	0	
88 68	284 37	101	0	0	0	0	0	0	0.23	0	0	0	0	0	0	0	0	0	0	0	0	0	0	0	0	0	0	
87 88	284 38	101	0	0	0	0	0	0	0.25	0	0	0	0	0	0	0	0	0	0	0	0	0	0	0	0	0	0	
88 77	288 28	101	0	0	0	0	0	0.75	0	0	0	0	0	0	0	0	0	0	0	0	0	0	0	0	0	0	0	
81 85	288 18	101	0	0	0	0	0	0	1	0	0	0	0	0	0	0	0	0	0	0	0	0	0	0	0	0	0	
82 9	284 77	206	0	0	0	0	0	0	0	0	0	0	0	0	0	0	0	0	0	0	0	0	0	0	0	0	0	
95 87	283 02	204	0	0	0	0	0	0	0	0	0	0	0	0	0	0	0	0	0	0	0	0	0	0	0	0	0	
100 41	283 19	202	0	0	0	0	0.05	0	0	0	0	0	0	0	0	0	0	0	0	0	0	0	0	0	0	0	0	
102 84	283 08	202	0	0	0	0	0	0	0	0	0	0	0	0	0	0	0	0	0	0	0	0	0	0	0	0	0	
107 87	284 88	201	0	0	0	0	0	0	0	0	0	0	0	0	0	0	0	0	0	0	0	0	0	0	0	0	0	
112 53	284 78	201	0	0	0	0	0	0	0	0	0	0	0	0	0	0	0	0	0	0	0	0	0	0	0	0	0	
118 14	284 68	201	0	0	0	0	0	0	0	0	0	0	0	0	0	0	0	0	0	0	0	0	0	0	0	0	0	
120 11	284 77	201	0	0	0	0	0	0	0	0	0	0	0	0	0	0	0	0	0	0	0	0	0	0	0	0	0	
120 3	283 03	201	0	0	0	0	0	0	0	0	0	0	0	0	0	0	0	0	0	0	0	0	0	0	0	0	0	
120 41	283 98	201	0	0	0	0	0	0	0	0	0	0	0	0	0	0	0	0	0	0	0	0	0	0	0	0	0	
121 18	284 48	206	0	0	0	0	0	0	0	0	0	0	0	0	0	0.25	0	0	0	0	0	0	0	0	0	0	0	
123 98	284 42	4	0	0	0	0	0	0	0	0	0	0	0	0	0	0.25	0	0	0	0	0	0	0	0	0	0	0	
130 88	289 34	4	0	0	0	0	0	0	0	0	0	0	0	0	0	0	0	0	0	0	0	0	0	0	0	0	0	
131 32	289 89	4	0	0	0	0	0	0	0	0	0	0	0	0	0	0	0	0	0	0	0	0	0	0	0	0	0	
138 23	289 87	7	0	0	0	1	0	0	0	0	0	0	0	0	0	0	0	0	0	0	0	0	0	0	0	0	0	
143 58	270 83	2	0	0	0	1	0	0	0	0	0	0	0	0	0	0	0	0	0	0	0	0	0	0	0	0	0	
151 2	271 82	2	0	0	0	0.02	0	0	0	0	0	0	0	0	0	0	0	0	0	0	0	0	0	0	0	0	0	
157 08	272 85	2	0	0	0	0.05	0	0	0	0	0	0	0	0	0	0	0	0	0	0	0	0	0	0	0	0	0	
167 7	274 82	1	0	0	0	0	0	0	0	0	0	0	0	0	0	0	0	0	0	0	0	0	0	0	0	0	0	

209

X	Y	MORPH	GRASS/HERB/NOF			PERDS			A-WILLOW LIKE APPEARANCE			B-ACACIA LIKE APPEARANCE			C-HOOKTHORN LIKE APPEARANCE			D-THICK STEMMED THORNY			A-DENSE CANOPY		B-SPARS CANOPY		ERYTHROPHYLLUM		D-WILLOW LIKE APPE	
			<0.2M	0.2-0.5M	>0.5M	<1M	1.0M	>2M	<1.5M	1.5-2.5M	>2.5M	<1.5M	1.5-2.5M	>2.5M	<1.5M	1.5-2.5M	>2.5M	<1.5M	1.5-2.5M	>2.5M	3.10M	>10M	3.10M	>10M	3.10M	>10M	3.10M	>10M
7.13	273.73	2	0	0.75	0	0	0	0	0	0	0	0	0	0	0	0	0	0	0	0	0	0	0	0	0	0	0	
18.35	274.88	2	0	0.75	0	0	0	0	0	0	0	0	0	0	0	0	0	0	0	0	0	0	0	0	0	0	0	
24.08	273.1	2	0	0.75	0	0	0	0	0	0	0	0	0	0	0	0	0	0	0	0	0	0	0	0	0	0	0	
28.22	272.11	2	0	0.75	0	0	0	0	0	0	0	0	0	0	0	0	0	0	0	0	0	0	0	0	0	0	0	
31.04	271.33	2	0	0	0	0	0	0	0	0	0	0	0	0	0	0	0	0	0	0	0	0	0	0	0	0	0	
31.41	270.86	2	0	0	0	0	0	0	0	0	0	0	0	0	0	0	0	0	0	0	0	0	0	0	0	0	0	
38.52	268.87	2	0	0.75	0	0	0	0	0	0	0	0	0	0	0	0	0	0	0	0	0	0	0	0	0	0	0	
42.32	268.72	2	0	0.75	0	0	0	0	0	0	0	0	0	0	0	0	0	0	0	0	0	0	0	0	0	0	0	
44.33	268.28	4	0	1	0	0	0	0	0	0	0	0	0	0	0	0	0	0	0	0	0	0	0	0	0	0	0	
47.37	267.88	4	0	1	0	0	0	0	0	0	0	0	0	0	0	0	0	0	0	0	0	0	0	0	0	0	0	
48.11	267.46	8	0	0.85	0	0	0	0	0.13	0	0	0	0	0	0	0	0	0	0	0	0	0	0	0	0	0	0.1	
50.26	264.85	201	0	0	0	0	0	0	0	0	0	0	0	0	0	0	0	0	0	0	0	0	0	0	0	0	0	
54.8	264.32	201	0	0	0	0	0	0	0	0	0	0	0	0	0	0	0	0	0	0	0	0	0	0	0	0	0	
60.89	264.05	201	0	0	0	0	0	0	0	0	0	0	0	0	0	0	0	0	0	0	0	0	0	0	0	0	0	
72.85	263.88	201	0	0	0	0	0	0	0	0	0	0	0	0	0	0	0	0	0	0	0	0	0	0	0	0	0	
78.18	264.38	201	0	0	0	0	0	0	0	0	0	0	0	0	0	0	0	0	0	0	0	0	0	0	0	0	0	
81.36	264.84	201	0	0	0	0	0	0	0	0	0	0	0	0	0	0	0	0	0	0	0	0	0	0	0	0	0	
88.29	267.18	101	0	0	0	0	0	0	1	0	0	0	0	0	0	0	0	0	0	0	0	0	0	0	0	0	0	
88.28	268.8	101	0	0	0	0	0	0	1	0	0	0	0	0	0	0	0	0	0	0	0	0	0	0	0	0	0	
88.81	268.18	101	0	0	0	0	0	0	1	0	0	0	0	0	0	0	0	0	0	0	0	0	0	0	0	0	0	
93.34	268.42	101	0	0	0	0	0	0	1	0	0	0	0	0	0	0	0	0	0	0	0	0	0	0	0	0	0	
94.33	268	101	0	0	0	0	0	0	0.7	0	0	0	0	0	0	0	0	0	0	0	0	0	0	0	0	0	0	
97.3	268.05	101	0	0	0	0	0	0	0.7	0	0	0	0	0	0	0	0	0	0	0	0	0	0	0	0	0	0	
101.84	268.08	4	0	1	0	0	0	0	0	0	0	0	0	0	0	0	0	0	0	0	0	0	0	0	0	0	0	
104.1	268.47	4	0	1	0	0	0	0	0	0	0	0	0	0	0	0	0	0	0	0	0	0	0	0	0	0	0	
104.81	268.87	4	0	1	0	0	0	0	0	0	0	0	0	0	0	0	0	0	0	0	0	0	0	0	0	0	0	
113.8	268.54	4	0	0.15	0	0	0	0	0	0	0	0	0	0	0	0	0	0	0	0	0	0	0	0	0	0	0	
124.82	268.8	4	0	0.15	0	0	0	0	0	0	0	0	0	0	0	0	0	0	0	0	0	0	0	0	0	0	0	
130.5	268.33	4	0	0.15	0	0	0	0	0	0	0	0	0	0	0	0	0	0	0	0	0	0	0	0	0	0	0	
143.8	267.45	4	0	0	0	0	0	0	0	0	0	0	0	0	0	0	0	0	0	0	0	0	0	0	0	0	0	
150.83	267.18	4	0	0.1	0	0	0	0	0	0	0	0	0	0	0	0	0	0	0	0	0	0	0	0	0	0	0	
158.37	267.07	2	0	0	0.8	0	0	0	0	0	0	0	0.1	0	0	0	0	0	0	0	0	0	0	0	0.02	0	0	
182.21	268.85	2	0	0	0.5	0	0	0	0	0	0	0	0	0.1	0	0	0	0	0	0	0	0	0	0.02	0	0	0	
188.84	270.85	2	0	0	0.5	0	0	0	0	0	0	0	0.5	0	0	0	0	0	0	0	0	0	0	0.1	0	0	0	
178.44	271.89	2	0	0	0.8	0	0	0	0	0	0	0	0	0.3	0	0	0	0	0	0	0	0	0	0.1	0	0	0	
188.86	273.2	2	0	0	0.5	0	0	0	0	0	0	0	0.3	0	0	0	0	0	0	0	0	0	0	0.057	0	0	0	
181.82	273.88	1	0	0	0	0	0	0	0	0	0	0	0	0	0	0	0	0	0	0	0	0	0	0	0	0	0	

X	Y	MORPH	GRASS/HERB/PROF			NEEDS			A-WILLOW LIKE APPEARANCE			B-ACACIA LIKE APPEARANCE			C-MOORTHORN LIKE APPEARANCE			D-THICK STEMMED THORNY			A-DENSE CANOPY		B-SFARS CANOPY		ERYTHROPHYLLUM		D-WILLOW LIKE APPE	
			<0.5M	0.5-0.5M	>0.5M	<1M	1-2.0M	>2M	<1.5M	1.5-3.5M	>3.5M	<1.5M	1.5-3.5M	>3.5M	<1.5M	1.5-3.5M	>3.5M	5.10M	>10M	5.10M	>10M	5.10M	>10M	5.10M	>10M	5.10M	>10M	
10.1	273.87	1	0	0.02	0	0	0	0	0	0	0	0	0	0	0	0	0	0	0	0	0	0	0	0	0	0	0	
13.83	272.88	2	0	0.02	0	0	0	0	0	0	0	0	0	0	0	0	0	0	0	0	0	0	0	0	0	0	0	
17.7	271.07	2	0	0.02	0	0	0	0	0	0	0	0	0	0	0	0	0	0	0	0	0	0	0	0	0	0	0	
23.83	268.34	2	0	0.08	0	0	0	0	0	0	0	0	0	0	0	0	0	0.01	0	0	0	0	0	0.02	0	0	0	
26.44	268.98	2	0	0.04	0	0	0	0	0	0	0	0	0	0	0	0	0	0.01	0	0	0	0	0	0.02	0	0	0	
30.3	267.47	2	0	0.06	0	0	0	0	0	0	0	0	0	0	0	0	0	0.01	0	0	0	0	0	0.02	0	0	0	
32.85	268.35	4	0.08	0	0	0	0	0	0	0	0	0	0	0	0	0	0	0.04	0	0	0	0	0	0.01	0	0	0	
39.3	267.17	4	0	0	0	0	0	0	0	0	0	0	0	0	0	0	0	0.04	0	0	0	0	0	0.01	0	0	0	
39.25	267.84	4	0	0	0	0	0	0	0	0	0	0	0	0	0	0	0	0.04	0	0	0	0	0	0.01	0	0	0	
39.48	264.51	104	0.05	0	0	0	0	0	0	0	0	0	0	0	0	0	0	0.04	0	0	0	0	0	0.01	0	0	0	
38.49	264.68	104	0.05	0	0	0	0	0	0	0	0	0	0	0	0	0	0	0	0	0	0	0	0	0.01	0	0	0	
37.08	265.3	104	0.05	0	0	0	0	0	0	0	0	0	0	0	0	0	0	0	0	0	0	0	0	0.01	0	0	0	
43.51	268.07	110	0.1	0	0	0	0	0	0	0	0	0	0	0	0	0	0	0	0	0	0	0	0	0	0	0	0	
47.56	265.90	110	0.1	0	0	0	0	0	0	0	0	0	0	0	0	0	0	0	0	0	0	0	0	0.025	0	0	0	
48.85	265.72	110	0.1	0	0	0	0	0	0	0	0	0	0	0	0	0	0	0.05	0	0	0	0	0	0.025	0	0	0	
51.02	265.22	110	0.1	0	0	0	0	0	0	0	0	0	0	0	0	0	0	0.05	0	0	0	0	0	0.025	0	0	0	
56.08	264.9	110	0.1	0	0	0	0	0	0	0	0	0	0	0	0	0	0	0.05	0	0	0	0	0	0.025	0	0	0	
56.83	263.31	201	0	0	0	0	0	0	0	0	0	0	0	0	0	0	0	0	0	0	0	0	0	0	0	0	0	
58.28	262.88	201	0	0	0	0	0	0	0	0	0	0	0	0	0	0	0	0	0	0	0	0	0	0	0	0	0	
60.1	263.9	201	0	0	0	0	0	0	0	0	0	0	0	0	0	0	0	0	0	0	0	0	0	0	0	0	0	
60.88	264.14	208	0	0	0	0	0	0	0	0	0	0	0	0	0	0	0	0	0	0	0	0	0	0	0	0	0	
61.45	264.78	208	0	0	0	0	0	0	0	0	0	0	0	0	0	0	0	0	0	0	0	0	0	0	0	0	0	
62.82	264.78	208	0	0	0	0	0	0	0	0	0	0	0	0	0	0	0	0	0	0	0	0	0	0	0	0	0	
64.14	264.72	208	0	0	0	0	0	0	0	0	0	0	0	0	0	0	0	0	0	0	0	0	0	0	0	0	0	
64.82	264.08	201	0	0	0	0	0	0	0	0	0	0	0	0	0	0	0	0	0	0	0	0	0	0	0	0	0	
66.87	263.13	201	0	0	0	0	0	0	0	0	0	0	0	0	0	0	0	0	0	0	0	0	0	0	0	0	0	
68.82	263.47	201	0	0	0	0	0	0	0	0	0	0	0	0	0	0	0	0	0	0	0	0	0	0	0	0	0	
70.22	263.73	201	0	0	0	0	0	0	0	0	0	0	0	0	0	0	0	0	0	0	0	0	0	0	0	0	0	
71.82	264.27	201	0	0	0	0	0	0	0	0	0	0	0	0	0	0	0	0	0	0	0	0	0	0	0	0	0	
72.38	263.94	101	0	0	0	0	0	0	0	0	0	0	0	0	0	0	0	0	0	0	0	0	0	0	0	0	0	
72.82	263.22	101	0	0	0.3	0	0.7	0	0	0	0	0	0	0	0	0	0	0	0	0	0	0	0	0	0	0	0	
77.22	268.26	101	0	0	0	0	0	0	0	0	0	0	0	0	0	0	0	0	0	0	0	0	0	0	0	0	0	
81.44	268.57	101	0	0	0	0	0	0	0	0	0	0	0	0	0	0	0	0	0	0	0	0	0	0	0	0	0	
86.23	268.78	4	0	0	0.4	0	0	0	0	0	0	0	0	0	0	0	0	0	0	0	0	0	0	0	0	0	0	
101.57	268.7	4	0.1	0	0	0	0	0	0	0	0	0	0	0	0	0	0	0	0	0	0	0	0	0	0	0	0	
104.82	268.31	4	0.1	0	0	0	0	0	0	0	0	0	0	0	0	0	0	0	0	0	0	0	0	0	0	0	0	
108.27	267.85	4	0.08	0	0	0	0	0	0	0	0	0	0	0	0	0	0	0	0	0	0	0	0	0	0	0	0	
112.38	268.28	4	0.06	0	0	0	0	0	0	0	0	0	0	0	0	0	0	0	0	0	0	0	0	0	0	0	0	
116.93	268.21	4	0.08	0	0	0	0	0	0	0	0	0	0	0	0	0	0	0	0	0	0	0	0	0	0	0	0	
122.34	268.5	4	0.08	0	0	0	0	0	0	0	0	0	0	0	0	0	0	0	0	0	0	0	0	0	0	0	0	
126.85	268.43	201	0	0.1	0	0	0	0	0	0	0	0	0	0	0	0	0	0	0	0	0	0	0	0	0	0	0	
130.03	268.3	201	0	0.1	0	0	0	0	0	0	0	0	0	0	0	0	0	0	0	0	0	0	0	0	0	0	0	
135.11	268.88	4	0	0.3	0	0	0	0	0	0	0	0	0	0	0	0	0	0	0	0	0	0	0	0	0	0	0	
142.78	268.34	4	0	0.3	0	0	0	0	0	0	0	0	0	0	0	0	0	0	0	0	0	0	0	0	0	0	0	
146.7	267	111	0	0.2	0	0	0	0	0	0	0	0	0	0	0	0	0	0	0	0	0	0	0	0	0	0	0	
152.72	267.1	111	0	0.2	0	0	0	0	0	0	0	0	0	0	0	0	0	0	0	0	0	0	0	0	0	0	0	
158.28	267.24	3	0	0	0.8	0	0	0	0	0	0	0	0	0	0	0	0	0	0	0	0	0	0	0	0	0	0	
164.88	267.7	2	0	0	0.8	0	0	0	0	0	0	0	0	0	0	0	0	0	0	0	0	0	0	0	0	0	0	
171.3	272.45	1	0	0	0.8	0	0	0	0	0	0	0	0	0	0	0	0	0	0	0	0	0	0	0	0	0	0	

X	Y	GRASS/HERB/POP			NEEDS			A= MALLOW LINE APPEARANCE			B= ACORN LINE APPEARANCE			C= HIGH THORN LINE APPEARANCE			D= THICK STEMMED BERRY			E= BIRDENADA			A= DENSE CANOPY		B= SPARSE CANOPY		EMPTY/POPPY/ELM		D= MCKLOW LINE APPEAR	
		<0.2M	0.2-0.5M	>0.5M	<1M	1-2M	>2M	<1.5M	1.5-2.5M	>2.5M	<1.5M	1.5-2.5M	>2.5M	<1.5M	1.5-2.5M	>2.5M	<1.5M	1.5-2.5M	>2.5M	<1.5M	1.5-2.5M	>2.5M	5-10M	>10M	5-10M	>10M	5-10M	>10M	5-10M	>10M
0	207.27	2	0	0.05	0	0	0	0	0	0.3	0	0	0	0	0	0	0	0	0	0	0	0	0.04	0	0	0	0	0	0	
29	207.19	2	0	0.05	0	0	0	0	0	0.3	0	0	0	0	0	0	0	0	0	0	0	0	0.04	0	0	0	0	0	0	
29.33	206.47	2	0	0.06	0	0	0	0	0	0.3	0	0	0	0	0	0	0	0	0	0	0	0	0.04	0	0	0	0	0	0	
32.69	206.08	2	0	0.05	0	0	0	0	0	0.3	0	0	0	0	0	0	0	0	0	0	0	0	0.04	0	0	0	0	0	0	
48.46	202.93	2	0	0.06	0	0	0	0	0	0.2	0	0	0	0	0	0	0	0	0	0	0	0	0.04	0	0	0	0	0	0	
57.26	201.95	101	0	0.2	0	0	0	0	0	0	0	0.1	0	0	0	0	0	0	0	0	0	0	0.2	0	0	0	0	0	0	
75.01	201	100	0	0	0	0	0.2	0	0	0	0	0	0	0	0	0	0	0.25	0	0	0	0.04	0	0	0	0	0	0	0	
81.5	200.86	101	0	0	0	0	0.2	0	0	0	0	0	0	0	0	0	0	0.25	0	0	0	0.04	0	0	0	0	0	0	0	
92.28	200.81	101	0	0.1	0	0	0	0	0	0	0	0	0	0	0	0	0	0.2	0	0	0	0	0	0	0	0.0064	0	0.0064	0	
101.87	200.70	101	0	0.1	0	0	0	0	0	0	0	0	0	0	0	0	0	0.2	0	0	0	0	0	0	0	0.0064	0	0.0064	0	
112.22	200.81	202	0	0	0	0	0.05	0	0	0	0	0	0	0	0	0	0	0	0	0	0	0	0	0	0	0	0	0	0	
121.55	200.54	202	0	0	0	0	0.05	0	0	0	0	0	0	0	0	0	0	0.3	0	0	0	0	0	0	0	0	0	0	0	
128.86	200.47	201	0	0	0	0	0	0	0	0	0	0	0	0	0	0	0	0	0	0	0	0	0	0	0	0	0	0	0	
129.77	200.12	201	0	0	0	0	0	0	0	0	0	0	0	0	0	0	0	0	0	0	0	0	0	0	0	0	0	0	0	
130.62	200.04	201	0	0	0	0	0	0	0	0	0	0	0	0	0	0	0	0	0	0	0	0	0	0	0	0	0	0	0	
132.46	200.95	201	0	0	0	0	0	0	0	0	0	0	0	0	0	0	0	0	0	0	0	0	0	0	0	0	0	0	0	
148.77	207.63	201	0	0	0	0	0	0	0	0	0	0	0	0	0	0	0	0	0	0	0	0	0	0	0	0	0	0	0	
164.31	207.18	201	0	0	0	0	0	0	0	0	0	0	0	0	0	0	0	0	0	0	0	0	0	0	0	0	0	0	0	
164.88	209.41	208	0	0	0	0	0	0.2	0	0	0	0	0	0	0	0	0	0.08	0	0	0	0	0.02	0	0	0	0	0	0	
170.84	200.75	101	0	0	0	0	0	0.2	0	0	0	0	0	0	0	0	0	0.08	0	0	0	0	0	0.02	0	0	0	0	0	
174.58	200.25	105	0	0	0	0	0	0.2	0	0	0	0	0	0	0	0	0	0.08	0	0	0	0	0	0.02	0	0	0	0	0	
178.66	200	102	0	0	0	0	0	0.2	0	0	0	0	0	0	0	0	0	0.08	0	0	0	0	0	0.02	0	0	0	0	0	
182.82	200.17	109	0	0	0	0	0	0.2	0	0	0	0	0	0	0	0	0	0.08	0	0	0	0	0	0.02	0	0	0	0	0	
189.08	200.88	101	0	0	0	0	0	0.2	0	0	0	0	0	0	0	0	0	0.08	0	0	0	0	0	0.02	0	0	0	0	0	
184.4	209.78	102	0	0	0	0	0	0.2	0	0	0	0	0	0	0	0	0	0.08	0	0	0	0	0	0.02	0	0	0	0	0	
188.58	208.83	102	0	0	0	0	0	0.2	0	0	0	0	0	0	0	0	0	0.08	0	0	0	0	0	0.02	0	0	0	0	0	
188.8	201.07	101	0	0	0	0	0	0.2	0	0	0	0	0	0	0	0	0	0.08	0	0	0	0	0	0.02	0	0	0	0	0	
200.71	202.46	4	0	0.5	0	0	0	0	0	0	0	0.25	0	0	0	0	0	0	0	0	0	0	0	0	0	0	0	0	0	
214.16	202.43	4	0	0.5	0	0	0	0	0	0	0	0.25	0	0	0	0	0	0	0	0	0	0	0	0	0	0	0	0	0	
225.26	202.81	4	0	0.5	0	0	0	0	0	0	0	0.25	0	0	0	0	0	0	0	0	0	0	0	0	0	0	0	0	0	
238.43	202.88	4	0	0.5	0	0	0	0	0	0	0	0.25	0	0	0	0	0	0	0	0	0	0	0	0	0	0	0	0	0	
242.2	202.84	4	0	0.5	0	0	0	0	0	0	0	0.25	0	0	0	0	0	0	0	0	0	0	0	0	0	0	0	0	0	
249.8	205.7	2	0	0.2	0	0	0	0	0	0	0	0.2	0	0	0	0	0	0	0	0	0	0	0	0	0	0	0	0	0	
248.88	207.88	2	0	0.2	0	0	0	0	0	0	0	0.2	0	0	0	0	0	0	0	0	0	0	0	0	0	0	0	0	0	
248.16	207.73	2	0	0.2	0	0	0	0	0	0	0	0.2	0	0	0	0	0	0	0	0	0	0	0	0	0	0	0	0	0	

SITE 15 4

X	Y	MORPH	GRASS/HERB/CROP			NEEDLE			A-WILLOW LIKE APPEARANCE			B-ACACIA LIKE APPEARANCE			C-HICKORY LIKE APPEARANCE			D-THICK STEMMED THORNY			A-DENSE CANOPY		B-SPARSE CANOPY		ERYTHROPHYLLUM		D-WILLOW LIKE APPE	
			<0.2M	0.2-0.5M	>0.5M	<1M	1-2.5M	>2.5M	<1.5M	1.5-2.5M	>2.5M	<1.5M	1.5-2.5M	>2.5M	<1.5M	1.5-2.5M	>2.5M	≤ 10M	>10M	≤ 10M	>10M	≤ 10M	>10M	≤ 10M	>10M	≤ 10M	>10M	
2.12	266.53	1	0	0	0	0	0	0	0	0	0	0	0	0	0	0	0	0	0	0	0	0	0	0	0	0	0	
13.56	262.12	3	0	0	0.0	0	0	0	0	0	0	0	0	0	0	0	0	0	0	0	0	0.000	0	0	0	0	0	
24.03	260.86	4	0	0	0	0	0	0	0	0	0	0	0	0	0	0	0	0	0	0	0	0.04	0	0	0	0	0	
32.73	259.39	4	0	0	0	0	0	0	0	0	0	0	0	0	0	0	0	0	0	0	0	0	0	0	0	0	0	
37.49	258.4	4	0	0	0	0	0	0	0	0	0	0	0	0	0	0	0	0	0	0	0	0	0	0	0	0	0	
40.58	258.04	4	0	0	0	0	0	0	0	0	0	0	0	0	0	0	0	0	0	0	0	0	0	0	0	0	0	
42.28	258.86	4	0	0	0	0.02	0	0	0	0	0	0	0	0	0	0	0	0	0	0	0	0.02	0	0	0	0	0	
47.72	258.69	202	0	0	0	0.1	0	0	0	0	0	0	0	0	0	0	0	0	0	0	0	0.02	0	0	0	0	0	
54.03	258.87	202	0	0	0	0	0	0.05	0	0	0	0	0	0	0	0	0	0	0	0	0	0	0	0	0	0	0	
55	258	201	0	0	0	0	0	0	0	0	0	0	0	0	0	0	0	0	0	0	0	0	0	0	0	0	0	
57.24	257.13	201	0	0	0	0	0	0	0	0	0	0	0	0	0	0	0	0	0	0	0	0	0	0	0	0	0	
60.87	257.11	201	0	0	0	0	0	0	0	0	0	0	0	0	0	0	0	0	0	0	0	0	0	0	0	0	0	
64.51	257.53	201	0	0	0	0	0	0	0	0	0	0	0	0	0	0	0	0	0	0	0	0	0	0	0	0	0	
67.65	258.04	201	0	0	0	0	0	0	0	0	0	0	0	0	0	0	0	0	0	0	0	0	0	0	0	0	0	
70.82	257.54	204	0	0	0	0	0	0	1	0	0	0	0	0	0	0	0	0	0	0	0	0	0	0	0	0	0	
76.84	258.05	203	0	0	0	0	0	0	0	0	0	0	0	0	0	0	0	0	0	0	0	0	0	0	0	0	0	
84.26	259.17	202	0	0	0	0	0	0	1	0	0	0	0	0	0	0	0	0	0	0	0	0	0	0	0	0	0	
88.86	257.47	201	0	0	0	0	0	0	0	0	0	0	0	0	0	0	0	0	0	0	0	0	0	0	0	0	0	
89.72	257.19	201	0	0	0	0	0	0	0	0	0	0	0	0	0	0	0	0	0	0	0	0	0	0	0	0	0	
100.17	257.09	201	0	0	0	0	0	0	0	0	0	0	0	0	0	0	0	0	0	0	0	0	0	0	0	0	0	
104.48	257.08	201	0	0	0	0	0	0	0	0	0	0	0	0	0	0	0	0	0	0	0	0	0	0	0	0	0	
108.81	257.48	201	0	0	0	0	0	0	0	0	0	0	0	0	0	0	0	0	0	0	0	0	0	0	0	0	0	
120.42	257.83	201	0	0	0	0	0	0	0	0	0	0	0	0	0	0	0	0	0	0	0	0	0	0	0	0	0	
120.44	258.03	202	0	0	0	0.3	0	0	0	0	0	0	0	0	0	0	0	0	0	0	0	0	0	0	0	0	0	
126.76	258.28	202	0	0	0	0.3	0	0	0	0	0	0	0	0	0	0	0	0	0	0	0	0	0	0	0	0	0	
130.29	258.08	204	0	0	0	0	0	0	0	0	0	0	0	0	0	0	0	0	0	0	0	0	0	0	0	0	0	
137.17	259.81	4	0	0	0	0.05	0	0	0	0	0	0	0	0	0	0	0	0	0	0	0	0.8	0	0	0	0	0	
147.12	260.84	6	0	0	0.1	0	0	0	0	0	0	0	0	0	0	0	0	0	0	0	0	0	0	0	0	0	0	
154.87	261.04	4	0	0	0	0	0	0	0	0	0	0	0	0	0	0	0	0	0	0	0	0	0	0	0	0	0	
172.72	263.21	1	0	0	0	0	0	0	0	0	0	0	0	0	0	0	0	0	0	0	0	0.08	0	0	0	0	0	

SITE 157

X	Y	MORPH	GRASS/HERB CANOP			NEEDS			A-WILLOW LIKE APPEARANCE			B-ACACIA LIKE APPEARANCE			C-HOOKTHORN LIKE APPEARANCE			D-THICK STEMMED THORNY			A-DENSE CANOPY		B-SPARS CANOPY		ERYTHROPHYLLUM		D-WILLOW LIKE APPE	
			<0.2M	0.2-0.5M	>0.5M	<1M	1-2.5M	>2.5M	<1.5M	1.5-3.5M	>3.5M	<1.5M	1.5-3.5M	>3.5M	<1.5M	1.5-3.5M	>3.5M	<1.5M	1.5-3.5M	>3.5M	3-10M	>10M	3-10M	>10M	3-10M	>10M	3-10M	>10M
32	263.06	1	0	0	0	0	0	0	0	0	0	0	0	0	0	0	0	0	0	0	0.000	0	0	0	0	0	0	
73	264	2	0.05	0	0	0	0	0	0	0	0	0.15	0	0	0	0	0	0	0	0	0.000	0	0	0	0	0	0	
1505	262.48	2	0.05	0	0	0	0	0	0	0	0	0.15	0	0	0	0	0	0	0	0	0.000	0	0	0	0	0	0	
1905	261.38	2	0.05	0	0	0	0	0	0	0	0	0.15	0	0	0	0	0	0	0	0	0.000	0	0	0	0	0	0	
21.76	280.8	4	0.05	0	0	0	0	0	0	0	0	0	0	0.25	0	0	0	0	0	0	0.000	0	0	0	0	0	0	
21.2	260.18	4	0.05	0	0	0	0	0	0	0	0	0	0	0	0	0.25	0	0	0	0	0.000	0	0	0	0	0	0	
23.12	258.78	4	0.05	0	0	0	0	0	0	0	0	0	0	0	0	0.25	0	0	0	0	0.000	0	0	0	0	0	0	
32.34	257.81	240	0	0	0	0	0	0.1	0	0	0	0	0	0	0	0	0	0	0	0	0	0	0	0	0	0	0	
33.5	257.89	240	0	0	0	0	0	0.1	0	0	0	0	0	0	0	0	0	0	0	0	0	0	0	0	0	0	0	
34.32	257.6	240	0	0	0	0	0	0.1	0	0	0	0	0	0	0	0	0	0	0	0	0	0	0	0	0	0	0	
37.8	257.78	113	0	0	0	0	0	0	0	0	0	0	0	0	0	0	0	0	0	0	0	0	0	0	0	0	0	
40.31	257.84	113	0	0	0	0	0	0	0	0	0	0	0	0	0	0	0	0	0	0	0	0	0	0	0	0	0	
43.01	258.52	113	0	0	0	0	0	0	0	0	0	0	0	0	0	0	0	0	0	0	0	0	0	0	0	0	0	
46.37	257.47	113	0	0	0	0	0	0	0	0	0	0	0	0	0	0	0	0	0	0	0	0	0	0	0	0	0	
49.99	258.12	113	0	0	0	0	0	0	0	0	0	0	0	0	0	0	0	0	0	0	0	0	0	0	0	0	0	
52.77	257.38	113	0	0	0	0	0	0	0	0	0	0	0	0	0	0	0	0	0	0	0	0	0	0	0	0	0	
56.78	257.83	113	0	0	0	0.4	0.4	0	0	0	0	0	0	0	0	0	0	0	0	0	0	0	0	0	0	0	0	
61.01	257.95	113	0	0	0	0.4	0.4	0	0	0	0	0	0	0	0	0	0	0	0	0	0	0	0	0	0	0	0	
63.08	258.18	113	0	0	0	0.4	0.4	0	0	0	0	0	0	0	0	0	0	0	0	0	0	0	0	0	0	0	0	
68.08	257.73	201	0	0	0	0	0	0	0	0	0	0	0	0	0	0	0	0	0	0	0	0	0	0	0	0	0	
68.42	257.37	201	0	0	0	0	0	0	0	0	0	0	0	0	0	0	0	0	0	0	0	0	0	0	0	0	0	
70.48	258.27	201	0	0	0	0	0	0	0	0	0	0	0	0	0	0	0	0	0	0	0	0	0	0	0	0	0	
71.82	258.81	201	0	0	0	0	0	0	0	0	0	0	0	0	0	0	0	0	0	0	0	0	0	0	0	0	0	
73.18	258.88	201	0	0	0	0	0	0	0	0	0	0	0	0	0	0	0	0	0	0	0	0	0	0	0	0	0	
74.74	258.83	201	0	0	0	0	0	0	0	0	0	0	0	0	0	0	0	0	0	0	0	0	0	0	0	0	0	
76.27	258.83	201	0	0	0	0	0	0	0	0	0	0	0	0	0	0	0	0	0	0	0	0	0	0	0	0	0	
78.35	257.27	201	0	0	0	0	0	0	0	0	0	0	0	0	0	0	0	0	0	0	0	0	0	0	0	0	0	
77.42	257.08	201	0	0	0	0	0	0	0	0	0	0	0	0	0	0	0	0	0	0	0	0	0	0	0	0	0	
78.21	257.42	201	0	0	0	0	0	0	0	0	0	0	0	0	0	0	0	0	0	0	0	0	0	0	0	0	0	
78.73	257.48	208	0	0	0	0	0.7	0	0	0	0	0	0	0	0	0	0	0	0	0	0	0	0	0	0	0	0	
80.32	257.78	208	0	0	0	0	0.7	0	0	0	0	0	0	0	0	0	0	0	0	0	0	0	0	0	0	0	0	
82.87	257.18	210	0	0	0	0	0	0	0	0	0	0	0	0	0	0	0	0	0	0	0	0	0	0	0	0	0	
83.37	258.97	210	0	0	0	0	0	0	0	0	0	0	0	0	0	0	0	0	0	0	0	0	0	0	0	0	0	
83.05	257.2	210	0	0	0	0	0	0	0	0	0	0	0	0	0	0	0	0	0	0	0	0	0	0	0	0	0	
84.82	257.81	208	0	0	0	0	0.7	0	0	0	0	0	0	0	0	0	0	0	0	0	0	0	0	0	0	0	0	
88.03	257.83	208	0	0	0	0	0.7	0	0	0	0	0	0	0	0	0	0	0	0	0	0	0	0	0	0	0	0	
88.88	257.8	208	0	0	0	0	0.7	0	0	0	0	0	0	0	0	0	0	0	0	0	0	0	0	0	0	0	0	
82.82	257.38	210	0	0	0	0	0	0	0	0	0	0	0	0	0	0	0	0	0	0	0	0	0	0	0	0	0	
84.73	258.88	210	0	0	0	0	0	0	0	0	0	0	0	0	0	0	0	0	0	0	0	0	0	0	0	0	0	
85.8	257.28	210	0	0	0	0	0	0	0	0	0	0	0	0	0	0	0	0	0	0	0	0	0	0	0	0	0	
88.29	257.58	107	0	0	0	0	0	0	0	0	0	0	0	0	0	0	0	0	0	0	0	0	0	0	0	0	0	
101.85	257.53	107	0	0.4	0	0	0.3	0	0	0	0	0	0	0	0	0	0	0	0	0	0	0	0	0	0	0	0	
103.38	258.28	112	0	0	0	0.4	0.4	0	0	0	0	0	0	0	0	0	0	0	0	0	0	0	0	0	0	0	0	
105.48	258.28	112	0	0	0	0.4	0.4	0	0	0	0	0	0	0	0	0	0	0	0	0	0	0	0	0	0	0	0	
105.88	257.8	104	0	0	0.1	0	0	0	0	0	0	0	0	0	0	0	0	0	0	0	0	0	0	0	0	0	0	
108.24	257.82	104	0	0	0.1	0	0	0	0	0	0	0	0	0	0	0	0	0	0	0	0	0	0	0	0	0	0	
109.08	257.77	104	0	0	0.1	0	0	0	0	0	0	0	0	0	0	0	0	0	0	0	0	0	0	0	0	0	0	
111.87	258.8	4	0	0	0	0	0	0	0	0	0	0	0	0	0	0	0	0	0	0	0	0	0	0	0	0	0	
118.79	258.43	4	0	0	0	0	0	0	0	0	0	0	0	0	0	0.2	0	0	0.1	0	0	0	0	0	0	0	0	
124.27	258.7	4	0	0	0	0	0	0	0	0	0	0	0	0	0	0	0	0	0	0	0	0	0	0	0	0	0	
127.48	258.48	6	0	0	0	0	0	0	0	0	0	0	0	0	0	0	0	0	0	0	0.025	0	0	0	0	0	0	
137.27	258.34	4	0	0	0	0	0	0	0	0	0	0	0	0	0	0	0	0	0	0	0.025	0	0	0	0	0	0	
147.18	258.88	4	0	0	0.3	0	0	0	0	0	0	0	0	0	0	0	0	0	0	0	0.025	0	0	0	0	0	0	
150.88	259.83	4	0	0	0.3	0	0	0	0	0	0	0	0	0	0	0	0	0	0	0	0.025	0	0	0	0	0	0	
162.27	258.43	3	0	0	0.2	0	0	0	0	0	0	0	0	0	0	0	0	0	0	0	0	0	0	0	0	0	0	
182.58	267.25	1	0	0	0.2	0	0	0	0	0	0	0.2	0	0	0	0	0	0	0	0	0	0	0	0	0	0	0	

217

X	Y	MORPH	GRASS/HERB/CROP			REEDS			A-WILLOW LINE APPEARANCE			B-ACACIA LINE APPEARANCE			C-HOOKTHORN LINE APPEARANCE			D-THICK STEMMED THORPY			A-DENSE CANOPY		B-SPARS CANOPY		ERYTHROPHYLLUM		D-WILLOW LINE APPE	
			<0.2M	0.2-0.5M	>0.5M	<1M	1-2M	>2M	<1.5M	1.5-3.5M	>3.5M	<1.5M	1.5-3.5M	>3.5M	<1.5M	1.5-3.5M	>3.5M	<1.5M	1.5-3.5M	>3.5M	5-10M	>10M	5-10M	>10M	5-10M	>10M	5-10M	>10M
0	281.99	4	0	0	0	0	0	0	0	0	0	0	0	0	0	0	0	0	0	0	0	0	0	0	0	0	0	
4.52	281.33	4	0	0	0	0	0	0	0	0	0	0	0	0	0	0	0	0	0	0	0	0	0	0	0	0	0	
8.29	280.98	4	0	0	0	0	0	0	0	0	0	0	0	0	0	0	0	0	0	0	0	0	0	0	0	0	0	
18.17	279.94	4	0	0	0	0	0	0	0	0	0	0	0	0	0	0	0	0	0	0	0	0	0	0	0	0	0	
20.82	279.32	4	0.0	0	0	0	0	0	0	0	0	0	0	0	0	0	0	0	0	0	0	0	0	0	0	0	0	
24.62	278.33	4	0.0	0	0	0	0	0	0	0	0	0	0	0	0	0	0	0	0	0	0	0	0	0	0	0	0	
27.08	278.44	4	0.0	0	0	0	0	0	0	0	0	0	0	0	0	0	0	0	0	0	0	0	0	0	0	0	0	
32.78	278.88	4	0.0	0	0	0	0	0	0	0	0	0	0	0	0	0	0	0	0	0	0	0	0	0	0	0	0	
37.62	278.57	4	0.0	0	0	0	0	0	0	0	0	0	0	0	0	0	0	0	0	0	0	0	0	0	0	0	0	
41.18	278.11	4	0.0	0	0	0	0	0	0	0	0	0	0	0	0	0	0	0	0	0	0	0	0	0	0	0	0	
44	277.29	4	0.0	0	0	0	0	0	0	0	0	0	0	0	0	0	0	0	0	0	0	0	0	0	0	0	0	
45.4	278.89	201	0	0	0	0	0	0	0	0	0	0	0	0	0	0	0	0	0	0	0	0	0	0	0	0	0	
46.53	278.39	201	0	0	0	0	0	0	0	0	0	0	0	0	0	0	0	0	0	0	0	0	0	0	0	0	0	
47.59	278.83	201	0	0	0	0	0	0	0	0	0	0	0	0	0	0	0	0	0	0	0	0	0	0	0	0	0	
48.45	278.38	201	0	0	0	0	0	0	0	0	0	0	0	0	0	0	0	0	0	0	0	0	0	0	0	0	0	
48.29	278.24	201	0	0	0	0	0	0	0	0	0	0	0	0	0	0	0	0	0	0	0	0	0	0	0	0	0	
50.98	278.5	201	0	0	0	0	0	0	0	0	0	0	0	0	0	0	0	0	0	0	0	0	0	0	0	0	0	
52.88	278.43	201	0	0	0	0	0	0	0	0	0	0	0	0	0	0	0	0	0	0	0	0	0	0	0	0	0	
58.25	278.2	201	0	0	0	0	0	0	0	0	0	0	0	0	0	0	0	0	0	0	0	0	0	0	0	0	0	
58.53	277.08	173	0	0	0	0	0	0	0	0	0	0	0	0	0	0	0	0	0	0	0	0	0	0	0	0	0	
58.85	277.23	173	0	0	0	0	0	0	0	0	0	0	0	0	0	0	0	0	0	0	0	0	0	0	0	0	0	
58.35	277.13	173	0	0	0	0	0	0	0	0	0	0	0	0	0	0	0	0	0	0	0	0	0	0	0	0	0	
62.91	277.27	173	0	0	0	0	0	0	0	0	0	0	0	0	0	0	0	0	0	0	0	0	0	0	0	0	0	
64.82	277.35	173	0	0	0	0	0	0	0	0	0	0	0	0	0	0	0	0	0	0	0	0	0	0	0	0	0	
68.21	277.41	173	0	0	0	0	0	0	0	0	0	0	0	0	0	0	0	0	0	0	0	0	0	0	0	0	0	
72.6	278.88	174	0	0	0	0	0	0	0	0	0	0	0	0	0	0	0	0	0	0	0	0	0	0	0	0	0	
73.51	278.88	174	0	0	0	0	0	0	0	0	0	0	0	0	0	0	0	0	0	0	0	0	0	0	0	0	0	
74.23	277.03	174	0	0	0	0	0	0	0	0	0	0	0	0	0	0	0	0	0	0	0	0	0	0	0	0	0	
75.51	277.72	172	0	0	0	0	0	0	0	0	0	0	0	0	0	0	0	0	0	0	0	0	0	0	0	0	0	
81.35	278.42	172	0	0	0	0	0	0	0	0	0	0	0	0	0	0	0	0	0	0	0	0	0	0	0	0	0	
83.17	278.06	172	0	0	0	0	0	0	0	0	0	0	0	0	0	0	0	0	0	0	0	0	0	0	0	0	0	
83.32	277.3	104	0	0	0	0	0	0	0	0	0	0	0	0	0	0	0	0	0	0	0	0	0	0	0	0	0	
85.72	277.02	104	0	0	0	0	0	0	0	0	0	0	0	0	0	0	0	0	0	0	0	0	0	0	0	0	0	
88.74	278.18	172	0	0	0	0	0	0	0	0	0	0	0	0	0	0	0	0	0	0	0	0	0	0	0	0	0	
88.55	278.27	172	0	0	0	0	0	0	0	0	0	0	0	0	0	0	0	0	0	0	0	0	0	0	0	0	0	
88.85	277.34	104	0	0	0	0	0	0	0	0	0	0	0	0	0	0	0	0	0	0	0	0	0	0	0	0	0	
90.53	277.44	104	0	0	0	0	0	0	0	0	0	0	0	0	0	0	0	0	0	0	0	0	0	0	0	0	0	
92.13	278.18	172	0	0	0	0	0	0	0	0	0	0	0	0	0	0	0	0	0	0	0	0	0	0	0	0	0	
96.88	278.41	172	0	0	0	0	0	0	0	0	0	0	0	0	0	0	0	0	0	0	0	0	0	0	0	0	0	
98.45	277.83	102	0	0	0	0	0	0	0	0	0	0	0	0	0	0	0	0	0	0	0	0	0	0	0	0	0	
100.37	277.41	102	0	0	0	0	0	0	0	0	0	0	0	0	0	0	0	0	0	0	0	0	0	0	0	0	0	
100.97	278.48	4	0	0	0	0	0	0	0	0	0	0	0	0	0	0	0	0	0	0	0	0	0	0	0	0	0	
102.12	277.86	4	0	0	0	0	0	0	0	0	0	0	0	0	0	0	0	0	0	0	0	0	0	0	0	0	0	
111.08	278.1	102	0	0	0	0	0	0	0	0	0	0	0	0	0	0	0	0	0	0	0	0	0	0	0	0	0	
114.47	277.84	102	0	0	0	0	0	0	0	0	0	0	0	0	0	0	0	0	0	0	0	0	0	0	0	0	0	
117.88	278.94	4	0	0	0	0	0	0	0	0	0	0	0	0	0	0	0	0	0	0	0	0	0	0	0	0	0	
118.51	278.85	4	0	0	0	0	0	0	0	0	0	0	0	0	0	0	0	0	0	0	0	0	0	0	0	0	0	
123.24	280.18	4	0	0	0	0	0	0	0	0	0	0	0	0	0	0	0	0	0	0	0	0	0	0	0	0	0	
128.51	278.58	4	0	0	0	0	0	0	0	0	0	0	0	0	0	0	0	0	0	0	0	0	0	0	0	0	0	
133.47	278.86	4	0	0	0	0	0	0	0	0	0	0	0	0	0	0	0	0	0	0	0	0	0	0	0	0	0	
134.88	278.84	102	0	0	0	0	0	0	0	0	0	0	0	0	0	0	0	0	0	0	0	0	0	0	0	0	0	
135.88	278.6	102	0	0	0	0	0	0	0	0	0	0	0	0	0	0	0	0	0	0	0	0	0	0	0	0	0	
137.8	278.28	4	0	0	0	0	0	0	0	0	0	0	0	0	0	0	0	0	0	0	0	0	0	0	0	0	0	
142.65	278.84	4	0	0	0	0	0	0	0	0	0	0	0	0	0	0	0	0	0	0	0	0	0	0	0	0	0	
146.28	278.98	7	0	0	0	0	0	0	0	0	0	0	0	0	0	0	0	0	0	0	0	0	0	0	0	0	0	
148.91	278.41	3	0	0	0	0	0	0	0	0	0	0	0	0	0	0	0	0	0	0	0	0	0	0	0	0	0	
165.24	278.18	3	0	0	0	0	0	0	0	0	0	0	0	0	0	0	0	0	0	0	0	0	0	0	0	0	0	

X	Y	UCORPH	GRASS/HERB/CROP			REEDS			A-WILLOW LIKE APPEARANCE			B-ACACIA LIKE APPEARANCE			C-HODKTHORN LIKE APPEARANCE			D-THICK STEMMED THORNY			A-DENSE CANOPY		B-SPARS CANOPY		ERYTHROPHYLLUM		D-WILLOW LIKE APPE	
			<0.2M	0.2-0.5M	>0.5M	<1M	1-2.9M	>3M	<1.5M	1.5-3.5M	>3.5M	<1.5M	1.5-3.5M	>3.5M	<1.5M	1.5-3.5M	>3.5M	0-10M	>10M	0-10M	>10M	0-10M	>10M	0-10M	>10M	0-10M	>10M	
0	267.72	1	0.0	0	0	0	0	0	0	0	0	0	0	0	0	0	0	0	0	0	0	0	0	0	0	0		
16.62	258.93	2	0.6	0	0	0	0	0	0	0	0	0	0	0	0	0	0	0	0	0	0	0	0	0	0	0		
20.07	258.28	2	0.6	0	0	0	0	0	0	0	0	0	0	0	0	0	0	0	0	0	0	0	0	0	0	0		
27.28	258.42	2	0.6	0	0	0	0	0	0	0	0	0	0	0	0	0	0	0	0	0	0	0	0	0	0	0		
34.41	258	2	0.6	0	0	0	0	0	0	0	0	0	0	0	0	0	0	0	0	0	0	0	0	0	0	0		
38.67	258.28	6	1	0	0	0	0	0	0	0	0	0	0	0	0	0	0	0	0	0	0	0	0	0	0	0		
43.81	257.96	4	?	0	0	0	0	0	0	0	0	0	0	0	0	0	0	0	0	0	0	0	0	0	0	0		
48.22	257.88	4	1	0	0	0	0	0	0	0	0	0	0	0	0	0	0	0	0	0	0	0	0	0	0	0		
47.22	257.58	4	1	0	0	0	0	0	0	0	0	0	0	0	0	0	0	0	0	0	0	0	0	0	0	0		
50.9	257.25	4	0.6	0	0	0	0	0	0	0	0	0	0	0	0	0	0	0	0	0	0	0	0	0	0	0		
54.17	257.24	4	0.6	0	0	0	0	0	0	0	0	0	0	0	0	0	0	0	0	0	0	0	0	0	0	0		
58.81	256.3	4	0	0	0	0	0	1	0	0	0	0	0	0	0	0	0	0	0	0	0	0	0	0	0	0		
60.68	255.48	201	0	0	0	0	0	0	0	0	0	0	0	0	0	0	0	0	0	0	0	0	0	0	0	0		
62.62	255.43	201	0	0	0	0	0	0	0	0	0	0	0	0	0	0	0	0	0	0	0	0	0	0	0	0		
63.9	255.24	201	0	0	0	0	0	0	0	0	0	0	0	0	0	0	0	0	0	0	0	0	0	0	0	0		
66.02	255.24	201	0	0	0	0	0	0	0	0	0	0	0	0	0	0	0	0	0	0	0	0	0	0	0	0		
68.67	255.05	201	0	0	0	0	0	0	0	0	0	0	0	0	0	0	0	0	0	0	0	0	0	0	0	0		
73.48	254.67	201	0	0	0	0	0	0	0	0	0	0	0	0	0	0	0	0	0	0	0	0	0	0	0	0		
74.68	253.73	201	0	0	0	0	0	0	0	0	0	0	0	0	0	0	0	0	0	0	0	0	0	0	0	0		
75.89	255.72	202	0	0	0	0	0	0.7	0	0	0	0	0	0	0	0	0	0	0	0	0	0	0	0	0	0		
76.9	256.28	202	0	0	0	0	0	0.7	0	0	0	0	0	0	0	0	0	0	0	0	0	0	0	0	0	0		
77.85	256.05	205	0	0	0	0	0	0	0	0	0	0	0	0	0	0	0	0	0	0	0	0	0	0	0	0		
79	255.81	200	0	0	0	0	0	0	0	0	0	0	0	0	0	0	0	0	0	0	0	0	0	0	0	0		
79.79	255.73	200	0	0	0	0	0	0	0	0	0	0	0	0	0	0	0	0	0	0	0	0	0	0	0	0		
79.85	256.18	206	0	0	0	0	0	0	0	0	0	0	0	0	0	0	0	0	0	0	0	0	0	0	0	0		
80.8	255.67	208	0	0	0	0	0	0	0	0	0	0	0	0	0	0	0	0	0	0	0	0	0	0	0	0		
81.43	255.88	200	0	0	0	0	0	0	0	0	0	0	0	0	0	0	0	0	0	0	0	0	0	0	0	0		
84.38	256.08	202	0	0	0	0	0	0	0	0	0	0	0	0	0	0	0	0	0	0	0	0	0	0	0	0		
85.83	255.88	202	0	0	0	0	0	0	0	0	0	0	0	0	0	0	0	0	0	0	0	0	0	0	0	0		
86.67	255.71	202	0	0	0	0	0	0	0	0	0	0	0	0	0	0	0	0	0	0	0	0	0	0	0	0		
87.14	255.88	206	0	0	0	0	0	0	0	0	0	0	0	0	0	0	0	0	0	0	0	0	0	0	0	0		
87.86	256.28	10	0.6	0	0	0	0	0.2	0	0	0	0	0	0	0	0	0	0	0	0	0	0	0	0	0	0		
89.24	256.78	10	0.6	0	0	0	0	0.2	0	0	0	0	0	0	0	0	0	0	0	0	0	0	0	0	0	0		
92.13	257.51	10	0	0.2	0	0	0	0	0	0	0	0	0	0	0	0	0	0	0	0.3	0	0	0	0	0	0		
97.98	256.8	10	0	0.2	0	0	0	0	0	0	0	0	0	0	0	0	0	0	0	0.3	0	0	0	0	0	0		
104.05	256.8	10	0	0.2	0	0	0	0	0	0	0	0	0	0	0	0	0	0	0	0.3	0	0	0	0	0	0		
110.12	256.38	16	0	0.3	0	0	0	0	0	0	0	0	0	0	0	0	0	0	0	0.3	0	0	0	0	0	0		
112.12	256.32	10	0	0.5	0	0	0	0	0	0	0	0	0	0	0	0	0	0	0	0.3	0	0	0	0	0	0		
114.21	256.8	10	0	0.5	0	0	0	0	0	0	0	0	0	0	0	0	0	0	0	0.3	0	0	0	0	0	0		
117.47	256.8	102	0.3	0	0	0	0	0	0	0	0	0	0	0	0	0	0	0	0	0.3	0	0	0	0	0	0		
120.21	256.38	10	0.5	0	0	0	0	0	0	0	0	0	0	0	0	0	0	0	0	0.3	0	0	0	0	0	0		
126.26	257.2	8	0	0.05	0	0	0	0	0	0	0	0	0	0	0	0	0	0	0	0	0	0	0	0	0	0		
127.37	255.38	8	0	0.05	0	0	0	0	0	0	0	0	0	0	0	0	0	0	0	0	0	0	0	0	0	0		
130.58	256.71	8	0	0.05	0	0	0	0	0	0	0	0	0	0	0	0	0	0	0	0	0	0	0	0	0	0		
136.37	256.71	2	0.8	0	0	0	0	0	0	0	0	0	0	0	0	0	0	0	0	0	0.3	0	0.05	0	0	0		
141.89	256.73	1	0.8	0	0	0	0	0	0	0	0	0	0	0	0	0	0	0	0	0	0.3	0	0.05	0	0	0		

212

